Eco-friendly functionalisation of cellulose-based textiles with antimicrobial nanoparticles

Qiaoyi Wang

A thesis submitted in partial fulfilment of the requirements of the University of Brighton for the degree of Doctor of Philosophy

July 2021

Abstract

It is estimated that over 4 million patients in the EU acquire a healthcare-associated infection every year, resulting in approximately 37,000 deaths annually and significant financial burden on the healthcare systems. Due to their large surface area, hospital textiles can provide an ideal substrate for microorganisms to grow and may act as vehicles for the transmission of pathogens. The antimicrobial functionalisation of healthcare textiles using nanomaterials offers an alternative approach for infection control. In this study, selenium nanoparticles (SeNPs) were investigated as promising novel antimicrobial agents to functionalise cellulose-based textiles. Additionally, silver nanoparticles (AgNPs) were employed since they are among the most extensively studied and applied antimicrobial inorganic nanoparticles. In the first stage of the study, the nanoparticles were prepared in aqueous suspensions to investigate the influence of synthetic conditions of the nanoparticles on their antimicrobial performance. Based on the literature and findings from this study, it was hypothesised that the presence of chemical stabilisers (polymers, surfactants, etc.) on the surface could hinder the antimicrobial activity of SeNPs against some bacterial species. Therefore, in the second stage, a new method was developed to prepare inorganic nanoparticles *in situ* on the surface of cationized cellulose without the addition of any stabiliser. The method is simple, rapid and environmentally friendly with the employment of ascorbic acid as the mild reducing agent and microwave irradiation as a green and effective source of energy. The results demonstrated that both Se and AgNPs were successfully prepared on the cationized cellulose fabrics and exhibited excellent laundry durability. The antibacterial tests revealed that the cationic groups and the nanoparticles showed combined effects against the bacteria. The presence of Se or AgNPs clearly improved the antibacterial performance of the cationized cellulose. The nanoparticle-functionalised cationic cellulose fabrics demonstrated strong antibacterial activity against all the bacterial species tested (*Staphylococcus aureus, Klebsiella pneumoniae,* and *Escherichia coli*), almost no viable bacteria were detected after 24-h contact when tested using the Absorption Method described by ISO 20743:2013. LIVE/DEAD staining and scanning electron microscopy analysis indicated that bacterial cells were visually damaged through contact with the nanoparticle-functionalised cationic cellulose fabrics. SeNPs prepared *in situ* showed comparable antimicrobial performance to the AgNPs, indicating its potential as an antimicrobial agent to functionalise cellulose materials. Furthermore, the functionalised fabrics showed low cytotoxicity towards human cells when tested *in vitro* using an indirect contact method. In conclusion, this study provides a novel approach to prepare cationic cellulose fabrics functionalised with inorganic nanoparticles. The functionalised cellulose fabrics have excellent antimicrobial performance, low cytotoxicity and good laundry durability, demonstrating great potential to serve as an anti-infective material, especially in healthcare settings.

Table of Contents

Abbreviations

AATCC	American association of textile chemists and colorists
AgNPs	Silver nanoparticles
Ag-C	Silver nanoparticle-modified cationic cotton
ATCC	American Type Culture Collection
AMR	Antimicrobial resistance
ASTM	American society for testing and materials
ATP	Adenosine triphosphate
CC	Cationised cotton
CFU	Colony forming unit
CLSM	Confocal laser scanning microscopy
CS	Chitosan
DLS	Dynamic light scattering
DNA	Deoxyribose nucleic acid
EDS	Energy dispersive X-Ray spectroscopy
FBS	Foetal Bovine Serum
HCAI	Healthcare associated infection
ISO	International Organization for Standardization
JIS	Japanese Industrial Standards
LDH	Lactate dehydrogenase
MHA	Mueller-Hinton Agar

MIC	Minimum inhibitory concentration
MP-AES	Microwave plasma atomic emission spectrometry
MRSA	Methicillin-resistant *Staphylococcus aureus*
NPs	Nanoparticles
NA	Nutrient Agar
NB	Nutrient Broth
OD	Optical density
PBS	Phosphate buffered saline
PCA	Plate Count Agar
PS20	Polysorbate 20
PVA	Polyvinyl alcohol
ppm	parts per million
QAC	Quaternary ammonium compound
qPCR	Quantitative polymerase chain reaction
RCA	Resazurin chromogenic agar
RO	Reverse osmosis
ROS	Reactive oxygen species
Se-C	Selenium nanoparticle-modified cationic cotton
SEM	Scanning electron microscopy
SeNPs	Selenium nanoparticles
TEM	Transmission electron microscopy
TSA	Tryptone soya agar

TSB	Tryptone soya broth
t-Se	Trigonal selenium
XPS	X-ray photoelectron spectroscopy
UV-vis	Ultraviolet–visible
ZoI	Zone of inhibition

List of Figures

List of Tables

Acknowledgement

I would like to sincerely express my gratitude to the many people who have helped and supported me throughout this PhD. Firstly, I would like to wholeheartedly thank my supervisors, Dr Irina Savina, Dr Lara-Marie Barnes, Dr Carol Howell, Dr Matthew Illsley and Dr Patricia Dyer. I would like to thank Carol, Matt and Patricia for the opportunity to do this PhD and for their contribution to the initial stages of the project. I am deeply grateful to Irina and Lara, for your excellent support, guidance, encouragement and understanding. I would also like to formally acknowledge School of Pharmacy and Biomolecular Sciences, University of Brighton for awarding this PhD studentship and for the continued support during the course of the PhD.

I would like to thank all the academic and technical staff who have helped me in the past few years. I would like to thank Dr Pascale Schellenberger at the Electron Microscopy Imaging Centre at University of Sussex for the help with TEM, Dr Jonathan Salvage for his guidance at the Image and Analysis Unit at University of Brighton, and Dr Konstantin I. Maslakov at Lomonosov Moscow State University for conducting the XPS analysis. I am also thankful to the technical support team at PABS for their continued help and support.

I would like to thank my friends, including my lab mates, office mates and house mates, for their support, care and encouragement during this PhD. I really appreciate all the kindness I received from you and the laughter and frustration we shared. A special thank you to Dr Ian Wimpenny. I would not have been able to make this without his support. Thanks also to Dr Yishan Zheng, who has been an inspiration to me and helped me in many ways.

Last and best, I would like to express my biggest thank to my parents and families for the enormous love. Without their support, none of this would have been possible.

Declaration

I declare that the research contained in this thesis, unless otherwise formally indicated within the text, is the original work of the author. The thesis has not been previously submitted to this or any other university for a degree, and does not incorporate any material already submitted for a degree.

Signed

Dated

Thesis structure

A description of each chapter of the thesis is presented as follows:

Chapter 1 Introduction: This chapter explained the background and discussed the need to develop novel nanoparticle-based antimicrobial textiles that exhibit excellent antimicrobial performance, good laundry durability, and low toxicity to humans. Selenium nanoparticles (SeNPs) were identified as a promising but understudied antimicrobial agent for the surface functionalisation of biomedical materials and therefore were chosen as the focus of the study; silver nanoparticles (AgNPs) were chosen to serve as a well-known antimicrobial agent and studied as a comparison.

Chapter 2 Preparation and characterisation of silver and selenium nanoparticles: This chapter focused on the preparation of colloidal SeNPs and AgNPs with controlled sizes. Surface condition (i.e. surface charge and the presence of stabiliser) was hypothesised to be a critical factor influencing the antimicrobial performance of SeNPs and, therefore, a few stabilising agents were chosen for the SeNPs preparation in this study. This was done based on (1) SeNPs have been successfully prepared with the assistance of these stabilisers by the previous studies, and (2) the absence of study or the differing results on the antimicrobial performance of the SeNPs stabilised by these agents from the literature. The physico-chemical properties of the prepared SeNPs and AgNPs were characterised by various techniques.

Chapter 3 Antibacterial activity of colloidal silver and selenium nanoparticles: The antibacterial activities of the SeNPs and AgNPs with different stabilising agents against several Gram-positive and Gram-negative bacterial strains were systematically compared. The following questions were considered: (1) whether the antibacterial performance of SeNPs is related to the Gram-reaction of the bacteria; (2) could the lack of antibacterial activity of the SeNPs against *E. coli* reported by some studies be due to the test methods and conditions; and (3) if the stabilising agent influences on the antibacterial performance of the SeNPs. The feasibility and limitations of the different antibacterial evaluation methods for the study of the nanoparticles were also discussed.

Chapter 4 Functionalisation of cellulose-based textiles by silver or selenium nanoparticles: Based on the findings from the previous chapters and the literature, a new method to functionalise cellulose-based textiles with covalently fixed cationic groups and *in situ* prepared SeNPs or AgNPs was described for the first time in this chapter. The physico-chemical properties of the functionalised textiles and their laundry durability in terms of the loss of nanoparticles after repeated washing were characterised. The results showed that this method can be used to produce uniform inorganic nanoparticles that are securely attached to cellulose surfaces without the aid of stabilising or binding agents.

Chapter 5 Antibacterial evaluation of the functionalised textile materials: The antibacterial activities of the novel functionalised textiles against *S. aureus, E. coli* and *K. pneumoniae* were evaluated using several different methods, including a challenge test method recommended by industry standards, a qualitative test based on chromogenic agar, *in situ* observation of bacteria using Live/dead staining and confocal microscopy, and scanning electron microscopy. The antibacterial performance of the fabric samples after repeated washing was also evaluated using the challenge test method.

Chapter 6 Cytotoxicity evaluation of the functionalised textile materials: The *in vitro* cytotoxicity of the functionalised textiles towards a human keratinocyte cell line (HaCaT) and a human bronchial epithelial cell line (16HBE14o-) was tested using an indirect contact method. The cell activity was determined by measuring the adenosine triphosphate (ATP) and lactate dehydrogenase (LDH) levels of the cells. The influences of the different sample preparation conditions used in the indirect contact method on the test results were discussed.

Chapter 7: Conclusions and future work: This chapter summarised the conclusions arising from the results and discussions from each chapter. The main contributions to knowledge of this study and possible future work were explained.

Chapter 1 Introduction

1.1 Background

The prevention or reduction of infections is an important subject of biomedical research, particularly with the emergence of antimicrobial resistance (AMR). As many strains of microorganisms have become resistant to nearly all of the current antibiotics, antibiotic resistance is now considered to be one of the major global threats to public health.[1] It is of the utmost importance to address the ways of preventing infections as well as the development of new antimicrobial agents. In hospitals, patients with impaired immune systems are more vulnerable to pathogens and are more likely to develop further infections and complications.[2] It is estimated that over 4 million patients are affected by at least one healthcare-associated infection (HCAI) every year in Europe.[3] A report from the National Audit Office in 2000 showed that HCAIs can cost the NHS in the region of £1 billion annually.[4] Moreover, reports from various European and North American countries indicated that the incidence rates have been increasing in the past two decades.[5]

Indirect contact is one of the major routes for the spread of infections within hospital environments; for example, it can occur when an infected patient touches and contaminates a surface, and the contaminated surface is touched by a second person[6]. Hospital soft surfaces such as curtains, beddings and staff uniforms have been reported as possible reservoirs of HCAI pathogens and play an important role in the acquisition and transmission of pathogens in healthcare settings.[7] Textiles can provide ideal substrates for microorganisms to grow on due to their large surface area and the ability to retain oxygen, nutrients, moisture and warmth, especially in contact with the human body.[8] Many published studies have reported that, in healthcare settings, bacterial or fungal organisms are frequently isolated from healthcare textiles. Ohl *et al.*[9] found that over 90% of the hospital privacy curtains in intensive care units and general wards were contaminated within one week with potentially pathogenic bacteria such as methicillin-resistant *Staphylococcus aureus* (MRSA) and vancomycin-resistant *Enterococcus* (VRE). A study conducted at a hospital reported that 60% of physician and nurse clothing carried pathogenic

bacteria, including MRSA.[10] In one study, the survival of *Staphylococcus aureus, Enterococcus faecium*, and *Pseudomonas aeruginosa* on cotton textiles was studied for up to 21 days; the results revealed that at room temperature (25 °C), both *E. faecium* and *S. aureus* survived up to 21 days, and all the challenge bacteria survived for at least 3 days at all the temperatures evaluated (5 °C, 25 °C, and 50 °C).[11] Moreover, unlike some of the environmental textiles such as curtains which remain localised, uniforms worn in healthcare environments move around in the facility quickly and remain in close proximity to human bodies, making them even better substrates for microorganisms to grow on, facilitating spread. The survival of microorganisms on hospital-use fabrics and the transfer between patients and healthcare workers is a possible cause of infections.[7,12]

Healthcare-associated infections and the resulting economic burden could be significantly reduced if the presence of pathogens can be eliminated, or at least controlled, in association with textiles in healthcare settings.[13] The chains of infection can potentially be broken with the presence of antimicrobial textiles. Marcus *et al.*[14] conducted a crossover, double-blind controlled study with patients in two chronic ventilator-dependent wards over a 7-month period; copper oxide-impregnated linens, patient uniforms and towels were used in place of non-treated textiles in the care units and the results indicated that use of copper-impregnated textiles significantly reduced HCAI indicators, including antibiotic treatment initiation events, fever days, and antibiotic usage. Another study conducted in six hospitals in the US involving 1019 beds also supported the notion that the copper oxide-impregnated hospital textiles may help with the reduction of HCAIs.[15] These findings demonstrated the great potential of antimicrobial textiles as a measure aimed to reduce HCAIs in healthcare settings. Although, the number of studies on the clinical use of antimicrobial textiles for the purpose of HCAI control is still very limited and the large-scale applications of these textile products in healthcare facilities need further investigation. For example, there are concerns about the damage to normal skin flora by antimicrobial textiles; so far, there is no evidence that they show significant adverse effects on the ecology of healthy skin.[16,17]

The development of antimicrobial textiles can also address the environmental issues caused by disposable hospital textiles. Currently, hospitals are using large amounts

of disposable textiles including disposable curtains, drapes and uniforms, to reduce the risk of cross-infections. These textiles have to be discarded as bio-hazardous materials immediately after use, which generates an overwhelming amount of waste and environmental concerns.[18] A study conducted in a 2000-bed hospital showed the use of reusable gowns could lead to a waste reduction of approximately 115 tonnes per year, as well as a cost saving of $360,000 (£230,000) annually.[19] Reusable surgical textiles offer substantial sustainability benefits over the same disposable product in energy (200%–300%), water (250%–330%), carbon footprint (200%–300%), volatile organics, and solid wastes (750%).[20] Some of the disposable textiles can potentially be replaced by reusable antimicrobial textiles that exhibit a much longer lifetime as well as better protection from pathogens. Therefore, developing reusable antimicrobial textiles would be of considerable benefit to the population, economy and environment.

With the growing concerns regarding antibiotic resistant microorganisms, a great number of antimicrobial materials have been developed and commercialised. However, many conventional antimicrobial agents on the market suffer from certain disadvantages, including weak antimicrobial potency, potential risk of developing resistance, and potential harmful or toxic effects to the human body and environment.[21] The development of nanotechnology has enabled new approaches in the fight against pathogenic microorganisms.[22] These approaches generally involve the use of nanoparticles (NPs). Nanoparticles are routinely defined as particles in which one dimension is between approximately 1 and 100 nm that show unique properties that are not found in bulk materials due to their exceedingly large specific surface area.[23] The use of nanoparticles as novel antimicrobial agents has been attracting considerable attention. Thanks to their complex modes of action, it is believed that the chance of developing resistance towards nanoparticles is very low.[24,25] Moreover, while hospitals have long been considered as a major source and reservoir of resistant bacteria,[26] extensive evidence has shown that inorganic antimicrobial nanoparticles can be effective against antibiotic-resistant bacteria.[21,27,28] For this reason, nanoparticles provide great potential to serve as an alternative antimicrobial agent and reduce the spread of antibiotic resistance, especially in healthcare settings. In this chapter, the possibilities of developing novel

nanoparticle-based antimicrobial textiles that are effective and long-lasting against pathogens, and safe to use will be explored.

1.2 Bacteria

There are various types of microorganisms, including bacteria, fungi, parasites and viruses. This thesis will focus on bacteria as they play a central role in infections and infectious diseases. Bacteria constitute a large domain of prokaryotic microorganisms and play a vital role in the environment and biosphere. They can be found in almost every habitat on earth, and they establish associations with higher organisms including humans.[29] Most bacteria are harmless or even helpful, but some are pathogenic, causing diseases in humans and other animals; some bacteria that consistently inhabit the bodies of healthy animals are also opportunistic pathogens that can cause infections when suitable conditions arise.[30]

Bacterial cells display a wide variety of shapes and sizes. The most common shapes of bacterial cells include sphere (coccus) and rod (bacillus). A typical bacterial cell is a few micrometres in size. The typical cell structures associated with prokaryotic cells, including bacteria, are depicted in Figure 1.1.

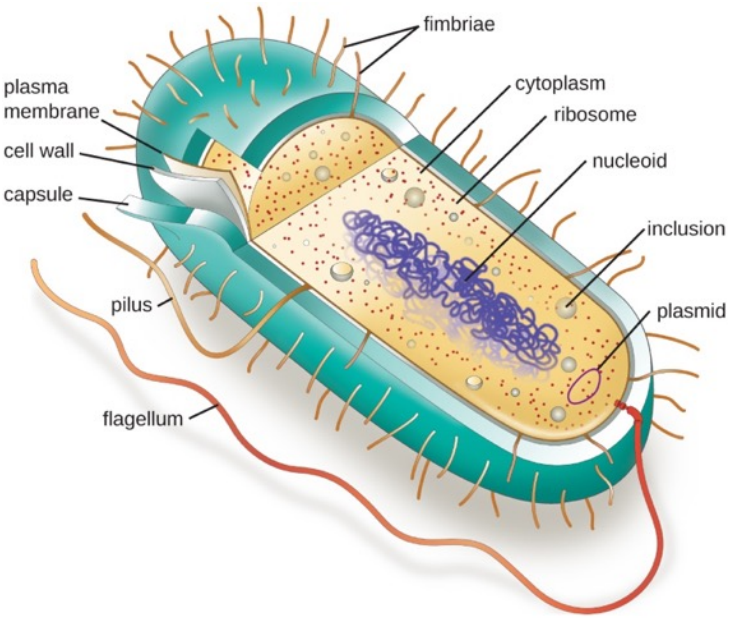

Figure 1.1 Typical cell structures of prokaryotic cells. Image taken from OpenStax Microbiology.

Original in colour

The outer layer of a bacterial cell normally consists of a cell wall and plasma membrane. The semi-rigid cell wall is vital to provide overall strength to the cell and protect the cell from environmental changes. Inside the cell wall, the plasma membrane surrounding the essential components of a bacterial cell exhibits selective permeability, allowing the selective passage of some molecules. Some bacteria also have extra layers such as cell capsules or slime layers external to the cell wall, which help the bacterial cells to adhere to surfaces. These structures enclose the cytoplasm and internal cell components and are known collectively as the cell envelope. The structures inside the cells are analogues to the organs inside a human body, serving specific functions. For example, ribosomes are responsible for protein synthesis, inclusions are able to store extra nutrients, and plasmids carry extrachromosomal genetic materials (deoxyribonucleic acid or DNA). Unlike eukaryotes, the DNA in bacteria and other prokaryotes lack complex nuclear membranes and are localised in an irregular-shaped region known as the nucleoid.[29] Compared with other microorganisms such as fungi and viruses, bacterial cells provide a greater variety of unique targets for selective toxicity due to these cell structures.

1.2.1 Gram-positive and Gram-negative bacteria

Bacteria have conventionally been categorised into two main groups, differentiated by their reaction to a procedure. In 1884, the Danish scientist Hans Christian Gram discovered that certain bacteria retain crystal violet dye when washed with alcohol, whilst in others the dye was washed away.[31] The two types of bacteria are now referred to as Gram-positive and Gram-negative bacteria respectively. The different reactions towards the Gram-staining procedure were due to the different cell wall structures of the two types of bacteria, as shown in Figure 1.2.

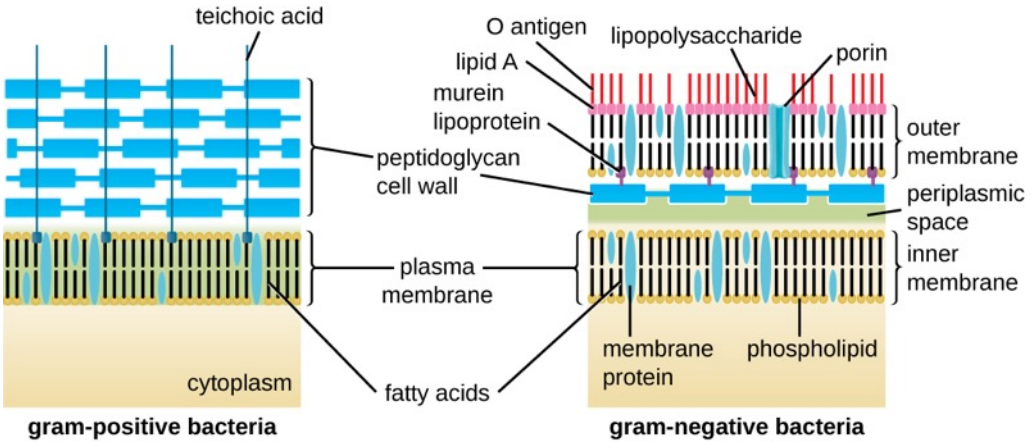

Figure 1.2 Bacterial cell wall structures of Gram-positive (left) and Gram-negative (right) bacteria. Image taken from OpenStax Microbiology.

Gram-positive bacteria have a relatively thick cell wall, which is commonly between 30 nm to 100 nm in thickness. The cell wall is composed of a multilayer of peptidoglycan which protects the plasma membrane located on the inside. The peptidoglycan, which consists of crosslinked polymer network of carbohydrates (N-acetylglucosamine and N-acetylmuramic disaccharide) and peptides, forms a tough, elastic structure which is able to withstand hydrostatic and osmotic pressure differences.[32] In the thick cell walls other cell wall polymers, such as the teichoic acids and polysaccharides, are covalently attached to the peptidoglycan.[33]

The Gram-negative cell wall has a more complex structure than the Gram-positive cell wall. The peptidoglycan layer in Gram-negative bacteria is about only 5 to 10 nm thick. External to this is an outer membrane consisting of proteins, lipopolysaccharides and phospholipids (about 7.5 to 10 nm). For both Gram-positive and Gram-negative bacteria, it is essentially the biomolecules on the cell wall which determine the surface properties of the bacteria, and thus the interactions of the bacterium with the environment.[32]

Due to the different cell wall structure, Gram-positive and Gram-negative bacteria often react differently to antibacterial agents. For example, it is believed that although Gram-negative bacteria have a thinner cell wall, the double layer structure and defences such as efflux pumps make it generally more difficult for drugs to

penetrate.[34] Interestingly, silver-based antimicrobial agents have been found to work better on Gram-negative bacteria. It is believed that the impermeability and clearance ability of the Gram-negative bacterial cell wall can prevent some entry of antibiotics but cannot stop small metal ions effectively, while the peptidoglycan on the thick cell wall of Gram-positive bacteria can successfully limit the penetration of silver ions.[35–38] Therefore, when studying the performance of an antibacterial agent, it is important to investigate both types of the bacteria.

1.2.2 Common bacterial species responsible for HCAIs

The most common bacteria that are monitored by most European HCAIs and/or AMR surveillance systems include Gram-positive bacteria *Staphylococcus aureus* and *Streptococcus pneumoniae,* and Gram-negative bacteria *Escherichia coli, Klebsiella pneumoniae, Acinetobacter baumannii,* and *Pseudomonas aeruginosa*.[39]

Staphylococcus aureus is a Gram-positive coccus (spherical cell) that are up to 1 μm in diameter and appear as grape-like clusters when viewed using a microscope. *S. aureus* is a member of the normal flora. About 20% of the human population are long-term carriers of *S. aureus,* and a large proportion of individuals (approximately 60%) carry *S. aureus* intermittently.[40] It is also an opportunistic pathogen and is a leading cause of bacterial infections in humans. It can cause infections of the skin, heart, lungs and brain. Strains of *S. aureus* have developed resistance to antibiotics such as methicillin and other beta-lactam antibiotics.[41] Methicillin-resistant strains (MRSA) present very challenging problems for treatment, and have been isolated from various surfaces within a hospital environment including floors, air vents, tourniquets, furniture, beddings, and gowns to name but a few.[41,42] MRSA is the leading cause of skin and soft tissue infection in patients reporting to the emergency department, with a rising rate in primary care clinics and intensive care units.[43] In recent years, MRSA has moved outside the hospital and become a major community-acquired pathogen that has enhanced virulence and transmission characteristics.[44]

Another common Gram-positive coccus responsible for HCAIs is *Streptococcus pneumoniae.* They colonise the mucosal surfaces of the human upper respiratory tract. The carriage rates of *S. pneumoniae* can be up to 27% - 65% in children and 10% in adults. It is an opportunistic pathogen that can cause a wide range of infections, including pneumonia, otitis media, sepsis and meningitis.[45]

Escherichia coli is a Gram-negative bacillus measuring approximately 0.5 μm in width and 2 μm in length. They belong to the family *Enterobacteriaceae* and commonly present in the intestines of humans and animals. It is used in water bacteriology as a useful indicator of faecal pollution and thus has become an important marker in food and water hygiene. Most *E. coli* stains are non-pathogenic, but some serotypes are harmful. Multidrug-resistant *E. coli* strains are causing serious HCAIs, including gastroenteritis, urinary tract infections, bloodstream infections, and neonatal meningitis, through direct transmission person to person, environmental contamination, and via vehicles such as contaminated water or food.[46]

Klebsiella pneumoniae, another important member of the family *Enterobacteriaceae,* is also a major cause of HCAIs. *Klebsiella pneumoniae* exists in the normal flora of the intestines, mouth, and skin. However, it is one of the most common hospital-acquired pathogens, causing urinary tract infections, nosocomial pneumonia, and intra-abdominal infections.[47] *Klebsiella pneumoniae* has been identified as a key source for antibiotic resistance; the non-susceptibility rates for the third generation antibiotics including cephalosporins, fluoroquinolones and aminoglycosides can be over 50% to 60% in some European countries.[48]

Pseudomonas aeruginosa is also a Gram-negative rod-shaped bacterium. It is an opportunistic pathogen that plays a leading role in HCAIs caused by Gram-negative rods, responsible for approximately 10% of all HCAIs globally.[49] It can cause various acute infections, including ventilator-associated pneumonia, meningitis, soft tissue infections, urinary tract infections and catheter associated infections. In the United States, *P. aeruginosa* causes about 51,000 HCAIs every year, of which about 6000 (13%) are caused by multidrug-resistant *P. aeruginosa*.[49]

Acinetobacter baumannii is a Gram-negative coccobacillus (very short rod) that are becoming increasingly important in HCAIs. It is an opportunistic pathogen that

primarily infects critically ill patients with compromised immune systems. *A. baumannii* is responsible for approximately 2% HCAIs in the United States and Europe.[50] Alarmingly, it has been found that approximately 45% of all *A. baumannii* isolates are considered multidrug resistant worldwide, and the rates can be as high as 70% in some parts of the world including Latin American and the Middle East.[51]

1.2.3 Antimicrobial agents and antimicrobial resistance

The control of microorganisms can be achieved by physical methods including heat, radiation, and filtration, or chemical methods where antimicrobial agents are involved. An antimicrobial agent is a substance that acts against microorganisms. They can either kill the target organisms, being '-cidal' (e.g. bactericidal and fungicidal); or they can inhibit the microbial growth, being '-static' (e.g. bacteriostatic and fungistatic).[52] Antimicrobial agents have different modes of action and may target different sites of a microbial cell. They may act through oxidations, cross-linking, chemical reactions, or electrostatic interactions with the biomolecules of the microbial cell. Some agents can attack the bacterial cell wall and compromise cell integrity, some can change the permeability or damage the cell membranes, some inhibit the synthesis of proteins, and some have effects on DNA by intercalation or DNA strand breakage.[53] More examples and details will be discussed in the following sections.

In recent decades, the emergence of antimicrobial resistance, especially bacterial resistance to antibiotics, has become a serious threat to public health globally. It is known that any use of antimicrobials contributes to the development of resistance, while the misuse and unnecessary use greatly facilitates the progress.[54] Apart from limiting the inappropriate uses of antimicrobial agents, it is also important to develop novel antimicrobials and alternative means to combat the pathogens. It is believed that multiple modes of action that target different biological pathways in the microbial cells can make it increasingly difficult for microorganisms to develop resistance to the agents as it will require simultaneous mutations to occur.[24]

1.3 Antimicrobial functionalisation of textiles

1.3.1 Requirements for antimicrobial functionalisation of textiles

As mentioned in Section 1.1, antimicrobial textiles can play an important role in maintaining hygienic standards and breaking the chains of infection in healthcare settings.[7,13] The application or incorporation of antimicrobial agents can introduce antimicrobial properties to textile materials. Ideal antimicrobial functionalisation of textiles needs to satisfy the following requirements in order to achieve the greatest benefit:[55]

(1) effective against a broad range of microbial species;
(2) non-toxic to the consumers, not causing toxicity, allergy or irritation;
(3) durable to laundering and cleaning;
(4) cost-effective, safe and environmental-friendly in terms of manufacturing process;
(5) compatible with other textile finishing processes, with no adverse effects on the quality or appearance of the textile.

1.3.2 Antimicrobial agents for textile functionalisation

Various antimicrobial agents with different modes of action have been applied in the textile industry. Most of the commercially available antimicrobial agents for textiles are organic, including triclosan, polyhexamethylene biguanide hydrochloride (PHMB), and quaternary ammonium compounds (QAC).[55] In recent years, inorganic or metal based antimicrobial agents, especially silver, are also attracting increasing attention.[55,56] Some commercially available antimicrobial agents for textiles or antimicrobial fibres are listed in Table 1.1.

Table 1.1 List of some commercially available antimicrobial agents and fibres.

Product name	**Company**	**Description**
AEGIS Microbe Shield®	Microban	Finishing agent based on quaternary ammonium compound (QAC) [64]
Agion®	Agion	Silver-zeolite-based additive[65]
Amicor™	Acordis	Acrylic fibres containing triclosan or combination of triclosan and tolnaftate[66]
Bactekiller®	Fuji Chemical Industries	Silver-based antimicrobial additive[67]
Bioactive®	Trevira	Polyester fibres containing silver[68]
BioCote®	BioCote	A range of antimicrobial additives based on metal ions/compounds (e.g. silver, zinc, or copper) or QAC[69]
Biofresh™	Sterling Fibers	Acrylic fibres containing triclosan[70]
Chitopoly®	Fuji-Spinning	Fibre made by kneading chitosan into polynosic fibre[71]
Crabyon®	SWICOFIL AG	Composite fibre of chitin/chitosan and cellulose viscose[72]

Product name	Company	Description
Cupron®	Cupron	Copper particles incorporated into polymeric fibres[73]
FeelFresh®	Toyobo	Acrylic fibres endowed with antibacterial silver ions[74]
Shieldex®	Statex	Fabrics coated with metal (e.g. silver, copper, nickel or tin)[75]
Reputex 20®	Lonza	Finishing agent based on polyhexamethylene biguanide (PHMB)[62]
Sanigard-Ag	LN Chemicals	Finishing agent based on nano-silver[76]
Sanigard-KC	LN Chemicals	Finishing agent based on QAC with various alkyl chain lengths[76]
Sanigard-nano ZN	LN Chemicals	Finishing agent based on nano-zinc oxide[76]
Silvadur™	Dow Chemicals	Polymer fabrics delivering silver ions as the antimicrobial agent[77]
Silvershield®	Microban	Silver chloride-based textile finishing agent[78]
Swicosilver	Swicofil	Plasma deposited silver coating on filaments[79]
ZPTech®	Microban	Antimicrobial additive to polymer based on zinc pyrithione[78]

1.3.2.1 Triclosan

Triclosan (2,4,4'-trichloro-2'-hydroxydiphenyl ether, structure shown in Figure 1.3) is a synthetic non-ionic halogenated phenol that is widely used in many professional and consumer products such as personal-care products, detergent, plastics and textiles, as an antimicrobial agent. It is effective against a broad range of microorganisms by blocking lipid biosynthesis.

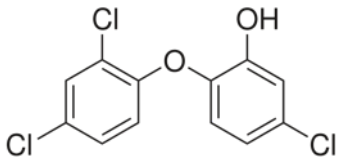

Figure 1.3 Structure of triclosan.

As a small molecule, triclosan has been applied onto commercial textile products at the finishing stage or incorporated into synthetic fibres during manufacturing.[55] However, due to the specific mode of action and widespread use, bacterial resistance to triclosan has been reported.[57] Concerns have also been raised over the accumulation of triclosan in the ecosystem and the related food and water safety issues due to the widespread use of triclosan.[58] Moreover, when exposed to sunlight, triclosan can break down into 2,8-dichlorodibenzo-p-dioxin, which raises concerns about toxic polychlorinated dioxins.[59] Due to these environmental and safety issues, the unnecessary use of triclosan in textiles and some other products have been banned in some countries and areas (not including the UK). A number of companies previously claimed to have used triclosan as the antimicrobial agent to produce antimicrobial fibres (e.g. Amicor™ and Biofresh™). However, this information is no longer to be found on their official website.

1.3.2.2 Polyhexamethylene biguanide hydrochloride

Polyhexamethylene biguanide (PHMB) is a polymer that includes biguanide repeat units separated by hydrocarbon chain linkers (Figure 1.4). PHMB is a potent antimicrobial agent from the polybiguanides family that has over 10 biguanide units and exhibits stronger antimicrobial activity than the corresponding monomer or

dimer. PHMB can damage the cytoplasmic membranes of bacterial cells and cause leakage of low molecular weight components; it can also bind to DNA and interfere with DNA functioning.[60] Due to the low toxicity to humans, PHMB is widely used in antiseptics, hygiene products, the food industry, and the textile industry.[61]

The attachment of PHMB to textiles is mainly through electrostatic and hydrogen bonding and therefore the durability of the PHMB finishing is a challenge. The attachment can be improved by creating or introducing more anionic groups on the fabric surface. For example, Reputex 20® (20% w/w PHMB) developed by Lonza (formerly Arch Chemicals) has an average of 16 biguanide units and is thought to present strong binding ability to the fibre surface due to the long polymer chain.[62] More negatively charged groups on the fabric surface introduced by negatively charged reactive dyes is also thought to be useful for improved binding ability. However, the strong ionic interaction that is useful for improvement of durability of the functionalisation may decrease the antimicrobial efficacy of PHMB.[55,63]

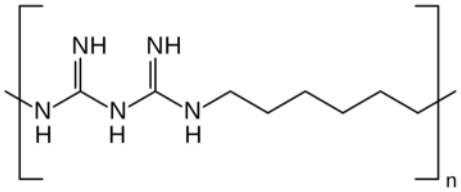

Figure 1.4 Structure of PHMB.

1.3.2.3 Quaternary ammonium compounds

Quaternary ammonium compounds (QACs) are another important group of cationic antimicrobial agents. These compounds have a positive charge at the NR_4^+ structure, R being an alkyl group or an aryl group. QACs can have two types of major interactions with the bacterial cells: the polar interaction between the cationic group and the negatively charged cell membranes, and the non-polar interaction between the hydrocarbon chain on the QAC and the fatty components of the cell membranes.[80] The hydrocarbon chain allows the molecule to penetrate through and rupture the cell membranes to compromise the cell integrity, and the ammonium group causes interruption of the essential functions of the cell.[81] QACs can also

affect the DNA, interfering with the replication process.[82] The antimicrobial activity of QACs depends on the number of cationic ammonium groups and the length of the alkyl chain, as well as the presence of the perfluorinated group. Typically, antimicrobial QACs have a chain length of approximately 12-18 carbon atoms. Figure 1.5 shows the structure of cetrimonium chloride, a typical QAC.

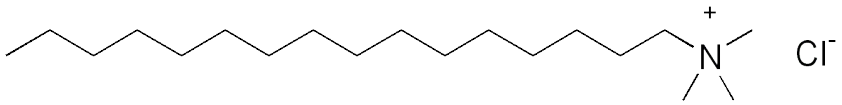

Figure 1.5 Structure of cetrimonium chloride.

QACs have been applied onto textiles as finishing agents to impart antimicrobial properties.[63] One of the issues with QACs is that the attachment onto the fibres is generally through electrostatic interactions, which results in poor durability of the coating, similarly to PHMBs.[81] Different methods have been developed to improve the attachment, including the synthesis of QACs with functional groups to covalently graft the compound to the fibres, and anchoring the QACs onto the backbone of polymers to make polycationic structures, especially polysiloxanes.[83] The company Microban offers a textile finishing agent called AEGIS Microbe Shield® and claims that the agent can "molecularly bond" to the treated surface and form a protective layer. The active ingredient of the product is 3-trimethoxysilylpropyldimethyloctadecyl ammonium chloride, which is a non-volatile silane that can form covalent bonds with the fabrics, offering great durability to the finishing.[64] Unfortunately, although the resistance towards this particular substance has not been reported, the bacterial resistance to QACs has been reported widely.[84,85]

1.3.2.4 Chitosan

Chitosan is made by the deacetylation of chitin, the second most abundant natural polysaccharide after cellulose (shown in Figure 1.6). Chitin exists in the cell wall of some fungi as well as the exoskeleton of insects and crustaceans such as crabs and shrimps. Chitosan is a linear polysaccharide composed of two monomer units, D-Glucosamine and N-acetyl-D-glucosamine, linked by a β(1–4)-glycosidic bond.[86]

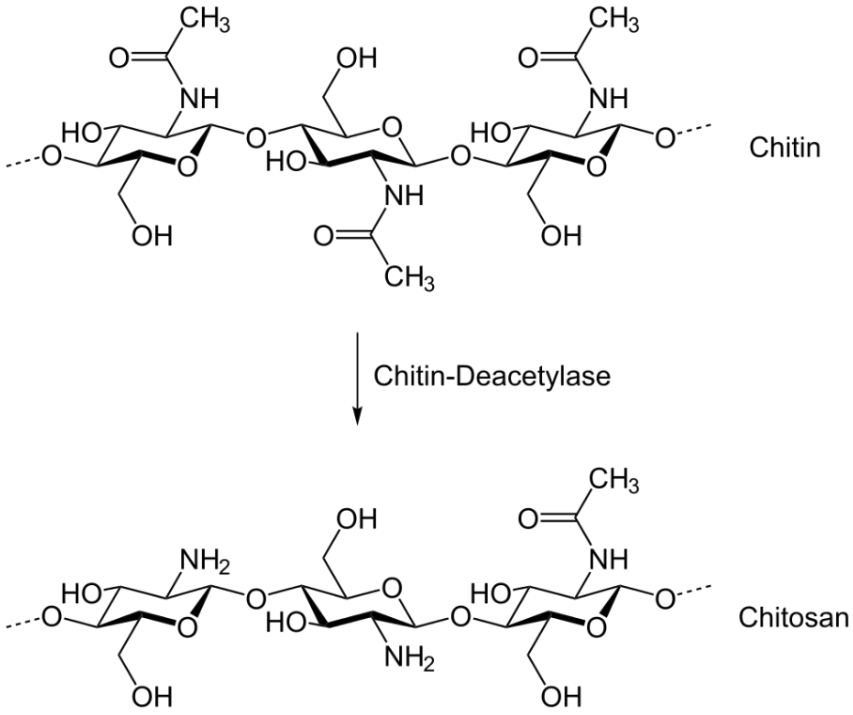

Figure 1.6 Preparation of chitosan from chitin.

Due to good biocompatibility, biodegradability, and antimicrobial activity, chitosan has been widely studied for biomedical applications and textile functionalisation.[63,81] As a natural cationic polymer, chitosan exhibits antimicrobial action against various bacteria and fungi.[87] The antimicrobial activity of chitosan is influenced by several factors including the molecular weight (M_w), polymerisation degree, and degree of deacetylation (DA), as well as the pH of the surrounding environment.[63] The first step of the antimicrobial action is through the electrostatic interaction between the positively charged primary amine and the negatively charged microbial cell wall. For the low M_w water-soluble chitosan, the polymer chain can penetrate through the cell wall, combine with DNA, and prevent protein synthesis. High M_w chitosan presents a higher density of positive amine groups, which may have an impact on the cell membranes, resulting in increased permeability and the leakage of some intracellular substances; or it can form an impermeable layer around the cell, which blocks the transport of substances essential for the cellular activities.[87] The company Swicofil produced fibre product call Crabyon, which is a blend of chitosan/chitin and cellulose viscose with permanent antimicrobial property.[72]

One of the main disadvantages of chitosan as an antimicrobial agent is the performance dependence on environmental pH and temperature. Chitosan is only soluble in an acidic medium and it becomes polycationic when the pH is below the pKa (6.3-6.5), which means the antimicrobial activity of chitosan is highly pH-dependent.[88] Moreover, the properties of chitosan such as M_w and viscosity can alter during the storage and handling of the polymer, which further influence the antimicrobial activity.[89] Another disadvantage is the poor durability of chitosan finishing on textiles. To solve this problem, crosslinking agents such as polycarboxylic acids and derivates of imidazolidinone have been applied to increase the adherence to the fibres.[63]

1.3.2.5 Metal-based antimicrobial agents

Many heavy metals, including silver, copper, zinc, and cobalt, are toxic to microorganisms. There are several possible modes of action of the antimicrobial activity of metals. They commonly bind to proteins and inactivate them to interfere with the cellular functions of the microorganisms;[90] due to their reduction potential, the redox-active metal species can act as catalytic cofactors in cell enzymes to generate or catalyse reactive oxygen species that damage the biomolecules of the cells.[63]

Among all the antimicrobial metals, silver is the most widely used in the textiles industry due to its broad antimicrobial spectrum and non-toxicity to humans at biocidal concentrations.[55] Moreover, it is becoming increasingly popular among all the antimicrobial agents; in 2004, the market share of silver as an antimicrobial agent for textile treatment was estimated to be 9%, while the number increased to 25% in 2011, indicating that silver is replacing the organic compounds for antimicrobial treatment of textiles.[56] There are different forms of silver used to functionalise textiles, including metallic silver, silver ion exchangers (e.g. silver zeolites and silver glass), and silver salts.[56] Metallic silver traditionally mainly includes electrolytically deposited silver on fibre surfaces (e.g. Shieldex®[75] and Swicosilver[79]). In recent years, the use of nano-sized silver (including metallic silver and silver salts) in the textile industry is also emerging, which will be discussed in detail in Section 1.4.

Silver has been used to prevent diseases and food spoilage for thousands of years; the antibacterial property of silver was recognised as early as when bacteria were identified as pathogens, and silver nitrate was used for treatment of infectious diseases such as skin ulcers and suppurating wounds.[91] Silver ions are believed to ultimately provide the antimicrobial actions.[56] Silver ions react with the thiol groups of proteins, resulting in cellular dysfunction, damage of the cell wall and change in permeability of cell membranes; they can also impair DNA replication by disruption of adenosine triphosphate (ATP) production.[36,38,92] Feng *et al.*[38] studied the effects of silver ions on *E. coli* and *S. aureus* using $AgNO_3$. Observations using transmission electron microscopy (TEM) revealed the morphological changes caused by silver ions in both *E. coli* and *S. aureus*. The cell wall became detached from the plasma membrane, and they were both damaged. Unfortunately, on the other hand, due to the extensive usage of silver-based antimicrobial agents in commercial products, there have been concerns regarding the development of bacterial resistance to silver compounds.[91] The first silver-ion resistant bacterium was isolated from a burn wound that was treated with silver nitrate in the 1960s,[93] after which silver resistant microorganisms have been found in many different clinical environments and silver-containing devices, including burn wounds, dental restorations and silver-coated polymer catheters.[94–96]

The metal particles, metal salts or metal-organic complexes can be incorporated into synthetic fibres before fibre extrusion and then diffuse to the fibre surface during use. The main advantage of this method is the simplicity of applying the agents during the manufacturing process; however, the antimicrobial performance can be very limited due to the restricted release of the antimicrobial agent through the polymer matrix as they are trapped inside the fibres and lack interaction with microorganisms.[63] Another approach is to apply the antimicrobial agent at the finishing stage to coat the fibres. For natural plant (e.g. cotton) or protein fibres (e.g. wool), the functionalisation can only be achieved through this method. Pre-treatment of the textiles to create functional groups on the fibre surfaces can be an effective way to increase the uptake and chelating capability towards metal salts.[63] The treatment can be achieved through either chemical (e.g. NaOH[97] and succinic acid[98]) or physical methods (e.g. plasma treatment[99]). For example, Nakashima and coworkers[98] treated cellulosic fabrics with succinic acid to produce carboxyl groups

on the cellulose, which clearly increased the capability of the fabrics to adsorb metal salts ($CuSO_4$ and $ZnSO_4$). When the metal ions are adsorbed to the fabric surface, metal particles, including nanoparticles, can be subsequently synthesised *in situ* on the fabric surface. Sometimes the functional groups created by the pre-treatment are also used to directly attract metal nanoparticles. This will be discussed in detail later in this chapter.

1.3.2.6 Current problems of antimicrobial textiles

There are several major challenges for the antimicrobial functionalisation of textiles. The first is the antimicrobial performance and the concerns of resistance. Some of the antimicrobial agents available for textile functionalisation, including triclosan, QACs and silver compounds, have been used in a wide range of applications for decades. The emergence of bacterial resistance to these agents has been reported.[96] Therefore, it is of value to develop and study novel antimicrobial agents that exhibit complex modes of actions to curb this trend. Another issue is the durability of the functionalisation. Reusable textiles are subject to repeated washing during daily use. When applying the antimicrobial agents at the finishing stage, it is important to make sure that the agents are securely attached to the fabric surfaces because the release of these agents results in the reduction of antimicrobial performance and potential health and environmental impact.

1.4 Antimicrobial inorganic nanoparticles

With the emergence of nanotechnology, many efforts have been made to produce nanoparticles for multiple purposes including antimicrobial applications. Nano-sized materials have unique optical, physicochemical, and biological properties which differ from their corresponding bulk materials due to the extremely large specific surface area. As the material size decreases to the atomic level, the percentage of atoms on the surface increases, resulting in amplified activities and many special properties.[100] Additionally, as biological processes happen on the nanoscale,

nanomaterials have great potential in biomedical applications by their direct involvement in these processes.[101–103] These interesting properties make nanomaterials extremely useful in the areas of biology and biomedicine, where applications include: antimicrobial treatment, anticancer treatment, drug and gene delivery, biosensors, separation of biomolecules and cells, tissue engineering, and bio-imaging.[102]

Many different kinds of nanoparticles have been used as antimicrobial agents. Some have intrinsic antimicrobial properties, while others are made into hybrids and nanocomposites that exhibit synergistic effects or serve as carriers of antimicrobial drugs. Here in this thesis the focus is mainly on inorganic nanoparticles that show inherent antimicrobial properties. As mentioned in Section 1.3.2, many metals and their salts/compounds are toxic to microorganisms. With the development of nanomaterials, their nanoparticles (e.g. Ag, Cu/CuO, ZnO, and TiO_2) are also found to be potent antimicrobial agents. Silver nanoparticles (AgNPs), as the most widely studied and used antimicrobial nanoparticles, have been found to be effective against a broad range of micro-organisms, including both Gram-positive[104] and Gram-negative bacteria,[105] fungi,[24] and viruses.[106] Thanks to their broad-spectrum antimicrobial properties, silver nanoparticles have great potential in a wide range of applications including textile modification, biomedical applications, water and air purification, food production and packaging, and cosmetics; many products have been commercialised and even applied in clinical settings.[107]

1.4.1 Modes of action of antimicrobial metal nanoparticles

Although the exact mechanism by which nanoparticles inhibit or kill microbes is still not fully understood, it is believed that multiple modes of action are involved, which may reduce the risk of developing resistance.[24] Figure 1.7 provides a summary of the possible modes of action by which metal nanoparticles inhibit or kill bacteria.

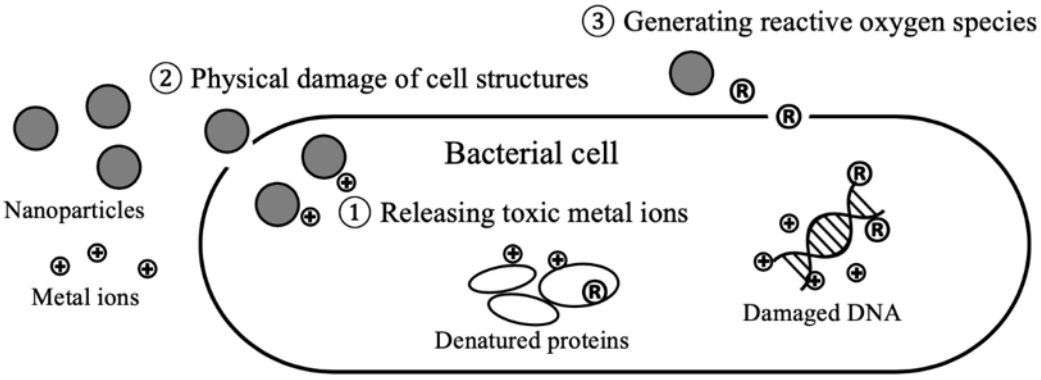

Figure 1.7 A summary of the possible mechanisms associated with the antimicrobial behaviour of metal and metal oxide nanoparticles.

First of all, due to the large surface area, nanoparticles can dissolve faster than larger particles and therefore release an increased quantity of ions. Taking silver nanoparticles as an example, they release silver ions that are toxic to microbial cells, as previously explained in Section 1.3.2.5. Copper nanoparticles and copper ions have been found to show similar toxic effects to that of silver.[108] Secondly, the nanoparticles can physically attach to and damage the microbial cell wall, resulting in membrane disruption and the leakage of intracellular constituents.[105,109] For example, Sondi and Salopek-Sondi[105] prepared surfactant-stabilised AgNPs and investigated their antibacterial activity against *E. coli*; the results of electron microscopy and X-ray microanalysis showed that the AgNPs entered the bacterial cells and accumulated in the cell membranes, and the leakage of cell components coagulated with the AgNPs was also observed. Additionally, studies have shown that some metal/metal oxide nanoparticles have catalytic properties to generate reactive oxygen species (ROS).[110–112] The nanoparticles of some photocatalytic metal oxides such as ZnO and TiO_2 are well known for such effects.[113–115] Silver and copper nanoparticles have also been found to induce the generation of ROS.[116,117] The ROS can oxidise and damage various biomolecules including DNA and the cell membrane and, therefore, is considered as an effective determinant for antimicrobial potency; ROS causes cell death at high concentrations and leads to severe DNA damage and mutation at low concentrations.[118,119] It is believed that since these nanoparticles impact bacteria in so many different ways that it is difficult for bacteria to evolve

resistance to them. Although, laboratory-induced AgNP resistance in *E. coli* after 225 generations of exposure has been reported,[120] which indicated that care should also be taken when developing products based on AgNPs and excessive use of AgNPs should be avoided. The study of novel nanoparticles that exhibit different antimicrobial actions is of value in this regard.

1.4.2 Selenium nanoparticles as novel antimicrobial agents

Apart from the metal and metal oxides, some new inorganic nanoparticles also show promising results in recent research. For example, selenium nanoparticles (SeNPs) have been found to inhibit the growth of several bacterial and fungal species and show low cytotoxicity to mammalian cells.[121–123] Selenium is a trace element and an important micronutrient for animal and human bodies. The normal level of selenium found in adults is approximately 10-20 mg and the daily intake is about 40 μg.[124] However, an excess amount of selenium causes toxicity in humans.[125] Selenium is present in biological systems in amino acids, such as selenocysteine and selenomethionine, usually as part of proteins. The selenoproteins such as glutathione peroxidase are well known for the regulation of redox reactions. The reduction of reactive oxygen metabolites by glutathione peroxidase can help to maintain membrane integrity and reduce the oxidative damage to lipids, lipoproteins, and DNA.[126] Due to the unique role of selenium in biological systems, selenium compounds and elemental SeNPs have been found to be promising antioxidants[127–129] and anticancer agents.[130,131]

Recently, the antimicrobial properties of selenium, especially elemental selenium nanoparticles, have also been investigated. Tran and Webster[132] reported the strong inhibition of *S. aureus* by SeNPs in 2011; subsequently, the antibacterial and antibiofilm activities were reported for different bacterial species including *Escherichia coli*, *Pseudomonas aeruginosa*, *Proteus mirabilis*, *Streptococcus pyogenes*, and *Staphylococcus epidermidis*.[133–137] SeNPs have been coated on the surfaces of polymeric medical devices,[138] hydroxyapatite pegs,[134] paper towels,[139] and textiles,[140] showing great potential for the development of antimicrobial materials to reduce the incidence of infections. However, it is noticeable that there

are some seemingly conflicting results on the antimicrobial properties of SeNPs in the literature. For example, in some studies, little or no inhibitory effect of selenium nanoparticles was found against some bacterial strai ns such as *E. coli* and *Salmonella* species.[122,133,141] The conflicting findings could be due to the different synthetic routes and the resulting difference in morphology, physicochemical and biological properties of the nanoparticles. There are various factors that may influence the antimicrobial performance of nanoparticles, including the particle size, shape, and surface conditions. This will be discussed in Section 1.4.4.

Selenium nanoparticles have been found to exhibit low cytotoxicity towards mammalian cells, making them a unique candidate for biomedical applications.[122] Biswas *et al.*[142] carried out a comparative study of selenium and silver nanoparticles prepared *in situ* on polymeric porous scaffolds (chitosan/polyvinyl alcohol). The study found that the extracts from AgNP-loaded scaffolds reduced bacterial viability significantly when assessed by a colony counting method, while they also exhibited high cytotoxicity towards fibroblast cells; on the other hand, extracts from SeNP-loaded scaffolds resulted in the damage of bacterial cell membranes, and they were non-toxic to fibroblasts. This study demonstrated the good biocompatibility of SeNPs compared with AgNPs, and the potential to be used as antimicrobial agents.

The antimicrobial mechanism of SeNPs has not been extensively studied yet. Although elemental selenium is not normally considered to be soluble in aqueous environments,[143] it is believed that the SeNPs can be transformed into organic forms (e.g. seleno amino acids and selenoproteins) through the interactions with microorganisms.[122,144] Due to the chemical similarity, selenium may be able to displace the sulphur for sulphur-containing amino acids such as cysteine and methionine.[145] Excessive amount of selenoproteins can lead to the generation of ROS, causing DNA damage, structural changes of proteins and enzyme dysfunction.[146] Stolzoff *et al*.[147] treated *S. aureus* with SeNPs and used glutathione, an antioxidant, to “rescue” the bacterial cells. The results showed the addition of antioxidant decreased the antibacterial activity of SeNPs, supporting the hypothesis that ROS might have played a role in the antibacterial actions. Huang *et al.*[148] investigated the potential antimicrobial mechanisms of SeNPs and detected promoted ROS production in the *S. aureus* cells treated with SeNPs compared to the

control cells without SeNPs, which provided evidence for the hypothesis. Additionally, they found that the *S. aureus* treated with SeNPs suffered from depletion of ATP. The depolarisation of bacterial membranes and altered cell morphology (i.e. wrinkled cell wall) were also observed in the study. These findings indicated the SeNPs exhibited multiple modes of action against *S. aureus*, making it more difficult for the bacteria to develop resistance towards the nanoparticles. Moreover, the production of ROS related with SeNPs takes place when the SeNPs are in contact with the bacterial cells and involved in biochemical reactions. Compared with photocatalytic nanoparticles (e.g. TiO_2), which induce ROS production with the presence of light, the use of SeNPs may be safer thanks to the target specificity.

1.4.3 Synthetic Routes to Inorganic Nanoparticles

In recent years, "green" synthesis of nanoparticles has attracted increasing attention to avoid the use of substrates that are hazardous to the human body and environment. Various methods, including chemical reduction with benign reducing agents, physical methods, radiation-chemical reduction and sono-chemical reduction, and even biological synthesis, have been applied to produce inorganic nanoparticles.[149–153] Chemical reduction of silver salt solution by a reducing agent is most commonly used to synthesise AgNPs.[154] Naturally occurring compounds such as ascorbic acid and glucose have been popular reducing agents to produce inorganic nanoparticles. Panáček *et al.*[104] studied the reduction of silver salt to AgNPs by using two monosaccharides (glucose and galactose) and two disaccharides (maltose and lactose). It was found that different saccharides showed different reducing abilities towards silver. By controlling the concentrations of reactants and pH conditions, a wide range of particle sizes (25-450 nm) were obtained. Zhang *et al*.[155] synthesised SeNPs using ascorbic acid and a natural hyperbranched polysaccharide as the reducing agent and stabilising agent respectively. The abundant –OH groups on the polysaccharide had a strong physical adsorption on the Se surface, leading to a well-dispersed, stable particle suspension in water. Amino acids and antioxidant peptides were also used as reducing agents for nanoparticle synthesis. Li *et al.*[156] used L-cysteine as both a reducing and stabilizing agent to prepare SeNPs in aqueous

solution, and the particle size could be adjusted by changing cysteine concentrations. Glutathione, a peptide with antioxidant properties, has been used to prepare various inorganic nanoparticles, including silver,[157] gold,[158] and selenium.[138,142]

To develop eco-friendly techniques for the production of nanoparticles, various organisms including microbes, marine organisms and plants have been employed.[159,160] Living organisms such as fungi, bacteria, and algae can serve as biofactories to produce or treat inorganic nanoparticles. For example, it was reported that the fungus *Fusarium oxysporum* was used to uptake and reduce Ag ions, producing spherical AgNPs with size of 1.6 nm; these AgNPs were then loaded onto cotton fabrics, showing significant antibacterial effect against *S. aureus*.[149] Apart from living biofactories, the use of plant extracts is considered to be a promising approach to synthesise metal nanoparticles. Various plants including *Aloe vera*, *Camellia sinensis* (green tea), *Coriandrum sativum* (coriander), and *Medicago sativa* (alfalfa) have been utilised to produce metal nanoparticles with various sizes and shapes.[160,161] Compared with living organisms, plant extracts are more suitable and cost-effective for mass production of nanoparticles. The rate and stability of biosynthesis by plants are also better than in the case of microorganisms. Plant extracts contain various bioactive compounds that can act as reducing agents or capping agents, or even both at the same time.[160] The limitations of biosynthesis using microorganisms and plant extracts include time-consuming processes, difficulty in the precise control of particle properties, and poor reproducibility.[161,162] Current research is focusing on the investigation of the mechanisms and enzymatic processes that are involved in the biosynthesis to better control and optimise the reaction conditions.

1.4.4 Factors Influencing the Antimicrobial Performance of Nanoparticles

The intrinsic properties of the nanoparticle, such as size, shape, and capping agent, play important roles in determining the antimicrobial activity. It has been found that generally the antimicrobial efficiency of nanoparticles increases with a decrease in size.[104,163] This could be due to the larger specific surface areas of small nanoparticles, which have more active atoms on the surface. A smaller size also

allows particles to penetrate into bacterial cells more easily.[164] The generation of ROS has also been found to be size-dependent with smaller nanoparticles inducing higher level of ROS when interacting with microbial cells.[165]

Many studies have investigated the shape-dependent antimicrobial behaviour of nanoparticles. For example, the nanospheres of ZnO appeared to induce more ROS production than nano-sheets at concentrations of 10 μg/ml and above.[166] It was also reported that truncated triangular silver nanoplates were found to exhibit stronger bactericidal activity against bacteria compared with nanospheres, nanocubes and nanorods.[167,168] Helmlinger *et al*.[167] studied the antimicrobial properties of different shaped AgNPs and found that the AgNPs with higher specific surface area dissolved faster and showed higher antimicrobial activity.

The condition of the surface is another important factor that can significantly influence the antimicrobial activity of nanoparticles. Since bacterial cells are overall negatively charged on the surface, a strong negative charge on the surface of nanoparticles may lead to repulsive effects between the particles and bacteria.[122] Therefore, creating a positive charge on the nanoparticle surface can be a useful way to enhance the electrostatic interaction between particles and bacterial cells and thus improve the antimicrobial activity of nanoparticles.[167,169,170] Apart from surface charge, the presence of some bioactive molecules on the particle surface can also greatly influence the antimicrobial activity of the nanoparticles. Piacenza *et al.*[134] compared the antibacterial efficacy of chemically prepared and biologically synthesised selenium nanoparticles and found that the biogenic SeNPs had better antibacterial performance than the ones prepared by chemical reduction. The authors suggested that the enhanced antibacterial performance of biogenic SeNPs might be due to the biomolecules (e.g. proteins and lipids) on the particle surfaces resulting from the biosynthesis which facilitated the interaction between the SeNPs and bacterial cells. Moreover, as mentioned in Section 1.4.2, there are some differing results from the literature regarding the antimicrobial performance of SeNPs. For example, Guisbiers *et al.*[171] prepared colloidal SeNPs using a laser ablation method without the help of any stabiliser and found antibacterial activity of the SeNPs against *E. coli*. However, it was also reported that the colloidal SeNPs stabilised by polyvinyl alcohol[122] or polysorbate 20[133] effectively inhibited the growth of *S.*

aureus but did not inhibit the growth of *E. coli*. It was hypothesised by Guisbiers *et al*.[171] that the antibacterial activity of SeNPs against some bacterial species can be hindered by the presence of some chemical contaminants on the particle surface (e.g. polymer and surfactant stabilisers). Therefore, it is of value to investigate the influences of different stabilisers on the particle surface so that full antimicrobial potential of the nanoparticles can be achieved.

As discussed in Section 1.4.3, during the synthesis process, a variety of parameters including temperature, heating methods, pH conditions, concentrations of reactants and stabilising agents, can significantly change the properties of particle products as they influence the nucleation and particle growth. Since properties such as size and shape can hugely influence the antimicrobial efficacy and other activities of nanoparticles, the synthetic routes should be carefully designed to prepare nanoparticles with the desired properties.

1.4.5 Methods of applying inorganic nanoparticles onto fabric surfaces

Many textile products available on the market claim to contain nano-sized metals (e.g. nano-silver, nano-ZnO); however, the technical details and product information provided are often very vague. The methods discussed in this section are based on the literature. There are mainly two ways to apply the nanoparticles onto the textiles: (1) *ex situ* synthesis of nanoparticles followed by impregnation of the prepared nanoparticles onto the fabric, and (2) *in situ* synthesis of nanoparticles on the fabric surface directly.

For *ex situ* prepared nanoparticles, conventional textile finishing methods such as exhaustion and pad-dry-cure processes can be used to apply the particles onto the textile surface. Cross-linking or binding agents can be used to increase the attachment of the nanoparticles. Hebeish *et al.*[172] prepared silver nanoparticles (6-8 nm) with hydroxypropyl starch as both the reducing and stabilising agent, and then applied them onto cotton fabrics in the presence/absence of extra binder using the pad-dry-cure method. The results showed that even with the lowest concentration of AgNPs used (50 ppm), the finished textiles showed excellent antibacterial

performance against both *E. coli* and *S. aureus*; the presence of binder significantly increased the washing durability of the fabrics, with great performance even after 20 washing cycles. In another study, the cotton fabrics were pre-treated with a cation-generating agent first to impart cationic quaternary ammonium groups onto the surface, and then the *ex situ* formed AgNPs were adsorbed onto the surface by the conventional exhaustion method; the pre-treated cationic cotton adsorbed more AgNPs than unmodified normal cotton and showed stronger antibacterial activity against *E. coli* compared with the normal cotton treated with AgNPs with the same procedures.[173] One of the advantages of *ex situ* preparation is that the properties of nanoparticles such as size and shape can be better tailored and controlled before applying onto the textiles. For example, as mentioned in Section 1.4.4, different shapes of nano-silver (e.g. silver nanoplates) have been found to have higher antibacterial efficacy than the traditional quasi-spherical silver nanoparticles.[168] Tang *et al*.[174] coated silk fibres with preformed silver nanoparticles and nanoplates, and the treated fibres showed vibrant colours and significant antibacterial abilities against *E. coli*. However, the authors did not make a comparison on the antibacterial performance of the samples functionalised with silver-nanoplates and the ones with regular quasi-spherical AgNPs. Whether the silver-nanoplates still show superior antimicrobial property when fixed onto a surface remains unclear as they will lose approximately half of the specific surface area.

The typical procedure of *in situ* preparation involves the adsorption of the precursor ions onto the fabric surface which are then reduced by wet chemical reducing agents or other methods such as photo-chemical or sono-chemical reduction. *In situ* synthetic methods provide excellent durability as the particles formed on the fibre surface fit the natural morphology of the fibres, and therefore are lodged on the fibres physically.[175,176] Perera *et al*.[177] used both *ex situ* (pad-dry-cure) and *in situ* (UV reduction) approaches to functionalise cotton fabrics with silver nanoparticles and compared the products. The characterisation of the treated fabrics showed that the samples prepared by the *in situ* reduction method had better silver uptake, more uniform particle distribution, stronger antibacterial activity and better washing durability. Moreover, *in situ* synthesis of nanoparticles can be more environmentally friendly due to the simple and facile finishing process, reduced chemical usage and fewer nanoparticles detaching from the fabric.

To the best of our knowledge, so far there are very few published studies using SeNPs as the antimicrobial agents to functionalise textile materials, and an *ex situ* approach was used in those studies. Yip and co-workers[140] prepared colloidal SeNPs with a polysaccharide-protein complex extracted from mushrooms as the stabiliser, and then applied the SeNPs onto polyester fabrics using pad-dry-cure method. The authors tested the antifungal activity of the functionalised fabrics and the results showed that the modified fabrics effectively inhibited the growth of *Trichophyton rubrum* in a 7-day period; unfortunately, due to the unsatisfying antibacterial performance of the colloidal SeNPs against *S. aureus*, the authors did not conduct the antibacterial test on the functionalised fabrics. These results may be in accordance with the hypothesis mentioned in Section 1.4.4 that some stabilisers may hinder the antimicrobial activity of SeNPs, which highlighted the need to study the influence of the stabiliser on the antimicrobial activity of SeNPs so that the SeNP-based antimicrobial materials can be better designed.

1.4.6 Health and environmental concerns surrounding the use of nanoparticles

The incorporation of nanomaterials in productive sectors is growing dramatically. According to the Nanotechnology Consumer Products Inventory, more than 1800 commercial products are claimed to contain or use nanomaterials.[178] The total of over 1800 products in the inventory in 2015 represents a thirty-fold increase over the 54 products originally listed in 2005 (the inventory has stopped updating). The Health and Fitness category (including personal care products such as toothbrush and lotions) accounts for 42% of the total, and nano-silver is the most frequently used nanomaterial, comprising 24% of the total. Nanoparticles have also been used in cosmetics, sunscreens and other personal care products. However, there have been concerns about the potential health and environmental risks associated with nanomaterials. Although some believe that the nanoparticles will soon aggregate or dissolve and subsequently lose the nano size, the fate and impacts of these nanomaterials in natural environments are still poorly understood.[179,180] For the development of nanoparticle-functionalised materials, it is of value to restrict the release of nanoparticles as much as possible in order to avoid the potential hazards.

1.4.6.1 Exposure of the human body to nanoparticles

The main exposure routes of nanoparticles to the human body are dermal, respiratory, and oral.[181] The application of nanoparticles on textiles leads to a direct contact through skin. The primary possible effects of nanoparticles on the skin include local irritation, sensitisation, and skin disease, which can be caused by abrasion resulting from the nanoparticles and the release of irritable ionic species from the nanoparticles.[182] Furthermore, one of the main functions of the skin is to provide protection to the underlying organs. Although theories of transdermal drug delivery suggest that only molecules that are smaller than 600 Da can easily penetrate the skin passively, some studies have investigated the penetration of nano-sized particles into the skin. Larase *et al.*[183] studied the penetration of silver nanoparticles (25 nm) through both intact and damaged full-thickness human skin *in vitro* and found that the penetration occurred at a very low level but was detectable after 24 h exposure. In another study, TiO_2 nanoparticles with a range of different sizes (4 nm to 90 nm) were applied onto an *in vitro* porcine skin model as well as live animals *in vivo*.[184] In the *in vitro* experiments, the TiO_2 nanoparticles were only deposited on the outermost surface of the stratum corneum after 24 h exposure. On the other hand, *in vivo* studies demonstrated that the dermal exposure of live hairless mice for 8 weeks resulted in dermal toxicity, accumulated titanium, and pathological lesions in the major organs. The results also suggested that the penetration of nanoparticles through skin was time and size dependent. Generally, nanoparticles smaller than 4 nm can penetrate and permeate the intact skin; when the size is between 4 – 20 nm, the particles can potentially penetrate and permeate intact and damaged skin; nanoparticles sized 21 – 45 nm can penetrate and permeate damaged skin; for particles larger than 45 nm, no penetration is expected to happen unless the skin is severely damaged.[185] Therefore, although smaller sized nanoparticles can exhibit stronger antibacterial performance, the risks to human body also need to be considered as long-term exposure to nanoparticles can lead to absorption of nanoparticles into the skin.

Inhalation of nanoparticles is also possible in the presence of nanoparticle-incorporating products (including textiles) when the particles are not securely fixed

and become airborne. The human respiratory tract has complicated airways, massive internal surface area, and very thin air-blood tissue interfaces facilitating gas exchange and blood oxygenation functions. Although the respiratory system has a series of structural and functional barriers to deal with the inhaled particulate matters, the prevention system cannot always address the issue adequately.[186] The respiratory tract consists of three sequential regions that assist the filtration effect, including the nasopharyngeal, tracheobronchial and alveolar regions. Depending on the size of the particles, they can be stopped at the different regions. Micron-sized particles can be trapped in the nasopharyngeal and tracheobronchial regions, which can be then removed by mucociliary clearance. However, sub-micron particles and nanoparticles can penetrate deeply into the alveolar region and are difficult to remove, which can lead to inflammation, injury, and other adverse biological responses.[187,188] Moreover, the small particles are able to travel through the blood-air tissue barrier and enter into the blood stream to reach other organs.[189] Gliga *et al*. studied the cytotoxic effects of various AgNPs, with different stabilisers and sizes, on human lung cells.[190] The study suggested that the smallest AgNPs tested (10 nm) showed significant cytotoxicity regardless of the stabiliser; 24 h exposure to the AgNPs (10 nm to 75 nm) resulted in DNA damage in the lung cells; the cytotoxicity was mainly induced by the uptake of nanoparticles and intracellular release of ions.

Considering the penetrating ability and cytotoxicity effects of small nanoparticles (e.g. < 45 nm), although they have stronger antimicrobial performance, it might be worthwhile to avoid the use of these small nanoparticles to reduce the potential harmful effects on human body. Many commercial textile products claimed to have nano-sized silver as an antimicrobial agent; however, the particle characterisation of the nano-silver is poorly documented or reported. From the published scientific studies, the sizes of the nanoparticles used for textile functionalisation range from several nanometres to several hundred nanometres. The release of nanoparticles from the functionalised fabrics and the subsequent effects on animal or human body are rarely reported at the moment.

1.4.6.2 Impact of nanoparticles on the environment

As mentioned earlier, large quantities of products containing nanomaterials are now available on the market, which is likely to result in the release of nanomaterials into the environmenta.[191] There are concerns about the environmental impacts caused by engineered and manufactured nanomaterials; however, reports on the damage to animal health, ecological risk and food chain risks for humans are still limited. The nanomaterials that enter natural water systems can be harmful to many organisms such as phytoplankton and fish.[192] In one study, the effects of metallic nanoparticles (silver, copper, aluminium, nickel, and cobalt) on aquatic organisms including zebrafish, daphnids, and an algal species were studied.[193] The results suggested that silver and copper nanoparticles caused toxicity in all the organisms tested, with 48 h median lethal concentrations as low as 40 and 60 μg/L respectively. The toxicity was dependent on the metal type, the transformation of particles by aggregation and dissolution, as well as the organism species. Reed *et al.*[194] studied the release of silver from nano-silver treated textiles during washing and found that the toxicity of the effluent to zebrafish embryos was negligible unless the silver content reached 1 mg/L, which was the highest level of silver detected. However, the study suggested that the silver is likely to continue leaching from the fabrics after disposal in the landfill which may cause other problems.

In conclusion, when developing NP-based antimicrobial materials, including textiles, not only the antimicrobial performance but also the potential hazards need to be considered. Although smaller particles have higher antimicrobial efficacy compared to larger ones, the toxicity to humans and other organisms is also higher as the size decreases. It may be worthwhile avoiding small nanoparticles (e.g. < 45 nm) to reduce the potential risks. The release of nanoparticles from the functionalised textiles should also be minimised by secure attachment to the textile substrate.

1.5 Aims and Objectives

The current antimicrobial functionalisation of textiles has the limitations of insufficient antimicrobial performance, poor durability, potential harmful effects to humans and the environment, as well as the possibility of resistance to them developing. In order to address these issues, inorganic nanoparticles have been employed to functionalise textile materials. Some inorganic NPs have been found to exhibit excellent antimicrobial activity and multiple modes of action, which makes it very difficult for the microorganisms to develop resistance. With suitable methods, the NPs can be securely attached to the textile surface, resulting in good laundry durability. The overall aim of this thesis is to develop novel NP-based antimicrobial textile materials to address the shortcomings.

Selenium nanoparticles (SeNPs) have recently been identified as a promising antimicrobial agent that exhibits relatively low toxicity to humans, making them a unique candidate for the development of novel antimicrobial materials, especially in healthcare settings.[122] This study aims to develop antimicrobial healthcare textiles using SeNPs as a novel antimicrobial agent. Since SeNPs are a relatively new antimicrobial agent that has not been extensively studied, there are some seemingly conflicting results on the antimicrobial performance of SeNPs from the literature. For example, in some studies, the SeNPs effectively inhibited the growth of some bacterial species (e.g. *E. coli*),[171] whereas there are also some reports showing the SeNPs did not affect the growth of these bacteria.[122,133] As we know, the antimicrobial performance of nanoparticles is largely dependent on the particle properties such as size, shape, and surface conditions. It is important to understand what factors led to the different results from different studies, so that the antimicrobial textile materials based on SeNPs and the preparation method thereof can be better designed. It has been hypothesised that the presence of some stabilisers may adversely affect the antimicrobial performance of the SeNPs.[163] However, there had not been a systematic study to investigate the influences of different stabilisers on the antimicrobial performance of SeNPs (by the time this work was conducted). Moreover, very few studies have been reported using SeNPs as the antimicrobial agent for textile functionalisation. Yip *et al.*[140] used a natural protein-polysaccharide complex as the stabiliser to prepared SeNPs *ex situ* and then padded the SeNPs onto

the fabrics; the functionalised fabrics showed good antifungal activity; however, the authors did not conduct the antibacterial test on the functionalised fabrics due to the unsatisfying results on the *ex situ* prepared colloidal SeNPs. There are many different ways to immobilise NPs onto textile materials, and in order to obtain the desired performance, the methods need to be carefully designed based on the understanding of the NPs. Therefore, the thesis can be mainly divided into two parts, of which the first one was focused on colloidal nanoparticles and the second one was to immobilise nanoparticles onto textile surfaces and characterise the functionalised materials. Silver nanoparticles, being the most extensively studied and used antimicrobial inorganic nanoparticles, were studied in parallel as a comparison for the less-studied SeNPs.

The major objectives are as follows:

- To study the feasibility of using SeNPs as a novel antimicrobial agent for the functionalisation of healthcare textiles by conducting a systematic comparison of the antibacterial activities of the colloidal SeNPs with different types of stabilisers, addressing the confounding results from the literature.
- To employ AgNPs as a type of widely investigated antimicrobial inorganic nanoparticle in comparison with SeNPs to aid the study.
- To develop a rapid, simple and eco-friendly method to functionalise the textile materials with antimicrobial inorganic nanoparticles (SeNPs and AgNPs).
- To evaluate the antimicrobial performance, the durability to repeated washing, and the toxicity to mammalian cells of the functionalised textiles.

Chapter 2 Preparation and Characterisation of Silver and Selenium Nanoparticles

2.1 Introduction

In order to develop nanoparticle-based antimicrobial textile materials, the first part of this study aimed to prepare nanoparticles using methods that are simple, controllable and environmentally friendly. Although biosynthesis, which involves the use of living micro-organisms or plant extracts, has been receiving increasing attention in recent years, there are currently some major challenges in this field, including the time-consuming process, difficulty in the precise control of particle properties and poor reproducibility.[162,195] In this thesis, conventional wet chemical approaches were the focus, where the precursor salt is reduced into elemental nanoparticles by a reducing agent chemically. In order to avoid harsh chemicals and toxic products, environmentally safe reducing agents that work in aqueous solution are favourable in the process.

As mentioned in Chapter 1, selenium nanoparticles (SeNPs) were identified as a novel antimicrobial agent that requires further exploration, while silver nanoparticles, (AgNPs) as the most extensively studied inorganic nanoparticles, would be used as a comparison. A goal of this chapter was to prepare SeNPs and AgNPs with similar methods so that they could be used for antimicrobial tests in the following chapters. Selenous acid (H_2SeO_3) and sodium selenite (Na_2SeO_3) are the most frequently used precursors; several reducing agents including ascorbic acid,[122,155,196–198] glutathione,[141,142] and sodium thiosulphate[199,200] have been used, among which ascorbic acid is probably the most widely used one because it is easily accessible, inexpensive, and environmentally benign. As a naturally occurring organic compound, it has also been identified as one of the reducing agents in the biosynthesis of various inorganic nanoparticles using plant extracts.[201,202] Ascorbic acid is a highly water soluble vinylogous carboxylic acid in which the electrons in the double bond, the hydroxyl group lone pair, and the lactone ring carbonyl double bond form a conjugated system. It serves as an electron and proton donor and is converted into dehydroascorbic acid when oxidised, as shown in Figure 2.1.

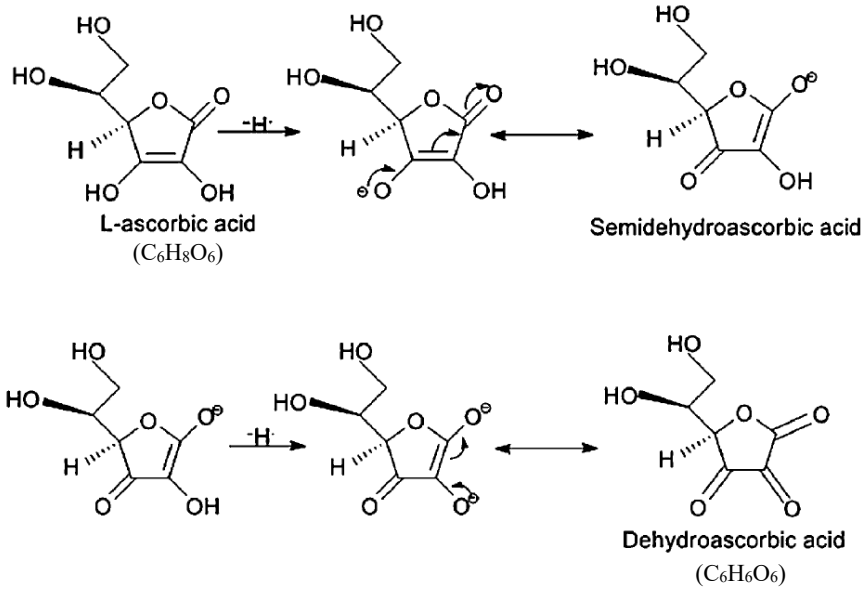

Figure 2.1 Conversion between ascorbic acid and dehydroascorbic acid[203]

Ascorbic acid ($C_6H_8O_6$) and dehydroascorbic acid ($C_6H_6O_6$) together constitute a redox system. The reduction of selenite or silver ions by ascorbic acid can be described by the following reactions:

$$SeO_3^{2-} + 2H^+ + 2C_6H_8O_6 = Se + 3H_2O + 2C_6H_6O_6 \qquad \text{Equation } \mathbf{2.1}$$

$$2Ag^+ + 2OH^- + C_6H_8O_6 = 2Ag + 2H_2O + C_6H_6O_6 \qquad \text{Equation } \mathbf{2.2}$$

It is known that the characteristics of nanoparticles, including the size, shape and surface conditions, can significantly influence the properties of the nanoparticles. Individual studies have shown some seemingly confounding results on the antimicrobial performance of SeNPs with different stabilisers; however, there had not been a reported study that investigated the influences of different stabilisers on the antimicrobial performance of the SeNPs when this work was conducted. Tran *et al.*[122] reported an antibacterial study on polyvinyl alcohol (PVA) stabilised SeNPs and found that the nanoparticles inhibited the growth of *Staphylococcus aureus* at a very low concentration (2 ppm) but showed no effect on *E. coli* at any of the concentrations tested (up to 64 ppm). The authors speculated that the differing results could be due to the different repulsive forces between the negatively charged

SeNPs and Gram-positive and Gram-negative bacteria, as Gram-negative bacteria usually have stronger negative surface charge. Bartůněk *et al.*[133] prepared polysorbate 20 (PS20) stabilised SeNPs and carried out a disk diffusion study of the SeNPs on different bacterial strains. They also observed that SeNPs inhibited the growth of Gram-positive bacteria (*Staphylococcus epidermidis* and *S. aureus*) but not Gram-negative bacteria (*E. coli*); however, only one concentration (2 ppm) was tested. In contrast, several other reports have demonstrated that the SeNPs produced by different methods successfully inhibited the growth of Gram-negative species including *E. coli* and *P. aeruginosa*.[136,137,171,204] For example, bare SeNPs prepared by the laser ablation method were found to effectively inhibit the growth of *E. coli* at 50 ppm.[171] Such varied findings could be due to the different surface conditions of the nanoparticles prepared by different synthetic routes. Guisbiers *et al*.[171] hypothesised that the presence of chemical contaminants (e.g. polymer or surfactant stabilisers) might hinder the antimicrobial property of SeNPs. It is also noticeable that the test strains of bacteria, for example strains of *E. coli* or *S. aureus,* used in these published studies are different. Different strains of the same species may react differently to antimicrobial agents as well. Therefore, it is of value to systematically investigate and compare the antibacterial performance of SeNPs with different stabilising agents using the same test strains and testing methods, which had not been reported by the time this work was conducted.

Four different stabilisers, including PVA, PS20, chitosan, and potassium iodide (KI), were chosen to prepare SeNPs in this thesis. SeNPs stabilised by PVA and PS20 were prepared using sodium selenite and ascorbic acid as it was in the original reports by Tran *et al.*[122] and Bartůněk *et al.*[133] to rule out the possibility that the lack of antimicrobial action against *E. coli* mentioned above was due to low test concentrations or the test methods. Additionally, since bacterial cells normally have negative net charges on the surface, it is believed that a positive charge on the nanoparticle surface can enhance the physical interactions between the particles and bacteria,[170] and thus a cationic polymer of natural origin, chitosan, was employed as a stabiliser to prepare SeNPs in this chapter as well. Several studies have prepared and studied chitosan-stabilised SeNPs;[127,198,205] however, the antimicrobial evaluation of these nanoparticles was rarely reported. Moreover, attempts were made to prepare bare SeNPs stabilised by purely electrostatic forces without steric

stabilisation to test the hypothesis that the steric hindrance might have negative effects on the antibacterial performance of SeNPs against some bacterial strains. It has been reported that potassium iodide (KI) can be used as an electrostatic stabiliser for the synthesis of SeNPs with ascorbic acid and sodium selenite; no antimicrobial study was performed on these SeNPs stabilised by KI.

The aim of this chapter was to synthesise SeNPs and AgNPs using suitable methods for subsequent assessment of their antimicrobial properties (Chapter 3). To address the question raised from the seemingly conflicting results on the antibacterial performance of SeNPs reported by different studies, the focus was placed on SeNPs with different stabilisers which determines the presence of steric stabilisation and particle surface charge; the sizes of these nanoparticles should be similar considering the fact that size is also a critical factor that influences the antimicrobial property of the nanoparticles. The research questions are:

(1) Is it possible to prepare SeNPs with different stabilisers (i.e. PVA, PS20, chitosan and KI) and similar sizes using Na_2SeO_3 as the precursor and ascorbic acid as the reducing agent?
(2) Is it possible to prepare AgNPs that have controllable sizes to match with the SeNPs using ascorbic acid as the reducing agent?

2.2 Materials

Sodium selenite (Na_2SeO_3, ≥98%), silver nitrate ($AgNO_3$, ≥99%), trisodium citrate dihydrate ($C_6H_5O_7Na_3.2H_2O$, TSC, ≥99%), L-ascorbic acid ($C_6H_8O_6$, ≥99%), polyvinyl alcohol (PVA, Mowiol® 18-88), Tween® 20 (polysorbate 20) and chitosan (medium molecular weight) were purchased from Sigma Aldrich (UK). Potassium iodide (KI, ≥99%), sodium hydroxide (NaOH, analytical grade), and acetic acid (CH_3COOH, pure) were purchased from Thermo Fisher Scientific (UK). Reverse osmosis (RO water) with a resistance of 18 mΩ was used in all the experiments. All glassware was cleaned with aqua regia ($HCl:HNO_3$ in a 3:1 ratio by volume) and rinsed thoroughly with RO water prior to the experiments.

2.3 Methods

2.3.1 Preparation of Nanoparticles

2.3.1.1 Preparation of Chemical Solutions

All nanoparticles were prepared in aqueous solutions. Chemicals were dissolved in RO water to prepare stock solutions with concentrations described in the following sections. Ascorbic acid solutions were prepared freshly prior to use. Chitosan stock solution (1% w/v) was prepared by dissolving chitosan in 1% (v/v) acetic acid and left for 3 days at room temperature to allow to fully dissolve. The chitosan stock solution was then diluted in RO water where necessary and filtered with filter paper (Whatman, Grade 1) before being used.

2.3.1.2 Preparation of Selenium nanoparticles (SeNPs)

Sodium selenite (100 mM, 0.2 mL) was added to 8.8 mL of aqueous solution containing one of the several different kinds of stabilising agent: 8 mM KI, 0.2% PVA, 0.25% polysorbate 20, or 0.05% chitosan (w/v), after which 1 mL of ascorbic acid (100 mM) was injected at room temperature (about 20 °C), with vigorous stirring. After several minutes, the solution turned to yellowish-orange, indicating the formation of SeNPs. The reaction finished in approximately 2 h, after which the colour of the suspension no longer changed. The products were named KI-SeNPs, PVA-SeNPs, PS20-SeNPs and CS-SeNPs respectively.

2.3.1.3 Preparation of Silver Nanoparticles (AgNPs)

For the preparation of AgNPs, the method was modified according to a previous report by Qin *et al*.[206] In a typical procedure, at room temperature (about 20 °C), ascorbic acid (100 mM, 0.1 mL) and TSC (100 mM, 0.3 mL) were added to 9.5 mL RO water, and the pH was adjusted to the alkaline range (pH 9.5, 10.2 and 10.8) by the addition of NaOH (1 M) with constant magnetic stirring. Silver nitrate (100 mM, 0.1 mL) was then added to the solution, by either rapid injection or dropwise. The

solution immediately changed from colourless to yellowish-brown with the addition of silver salt, indicating the formation of silver nanoparticles. The total reaction time was approximately 3 mins.

Subsequently, the nanoparticles were aged in a water bath at 100 °C for 2 h in order to improve the particle uniformity. The TSC stabilised nanoparticles were named TSC-AgNPs. A range of TSC-AgNPs with different sizes were obtained by varying the synthetic conditions as described above and they were labelled as sample A-E (Table 2.1).

Table 2.1 TSC-AgNPs sample names and synthetic conditions

Sample name	Synthetic condition*
TSC-AgNPs-A	pH 10.8, $AgNO_3$ added by quick drop
TSC-AgNPs-B	pH 10.2, $AgNO_3$ added by quick drop
TSC-AgNPs-C	pH 9.5, $AgNO_3$ added by rapid injection
TSC-AgNPs-D	pH 9.5, $AgNO_3$ added by quick drop
TSC-AgNPs-E	pH 9.5, $AgNO_3$ added by slow drop

* Quick drop = 1 drop/second, slow drop = 1 drop/5 seconds.

2.3.2 Characterisation of Nanoparticles

Prior to characterisation, nanoparticles were washed by centrifugation to remove the residues of reactants and stabilising agent. The centrifuge was chilled to 4 °C prior to the procedure considering the fact that the nanoparticles can be sensitive to heat. The centrifugal conditions were optimised for each type of the nanoparticles with repeated attempts to suit their size, weight and continuous phase. The resulting pellet was dispersed in RO water thoroughly for washing. AgNPs were treated in an ultra-sonication bath (Fisher Scientific, 40 kHz) for approximately 1 min to break any agglomeration; SeNPs were vortexed vigorously for thorough dispersion because

sonication treatment was found to induce the irreversible aggregation of SeNPs. The process was repeated three times to remove the reactant residues and loose stabilisers. The nanoparticles were stored in RO water at 4 °C for future applications. Centrifugation conditions are listed in Table 2.2.

Table 2.2 Centrifugal conditions to wash the nanoparticles

Nanoparticles	Centrifugal force (g)	Time (min)
PVA-SeNPs	10000	45
PS20-SeNPs	10000	15
CS-SeNPs	10000	60
TSC-AgNPs-A&B	15000	30
TSC-AgNPs-C&D	11000	30
TSC-AgNPs-E	8000	15

2.3.2.1 UV-vis Spectrophotometer

UV-vis absorption spectra of nanoparticle suspensions between 350 nm – 700 nm were determined by UV-vis spectrophotometer (Jenway 7315) with disposable semi-micro polystyrene cuvettes (Fisher Scientific).

2.3.2.2 Hydrodynamic Particle Size and Zeta Potential

The hydrodynamic particle size and zeta potential of the nanoparticles were measured using a Zetasizer Nano-ZS90 instrument (Malvern, UK) using dynamic light scattering (DLS) technique. Disposable cuvettes (Fisher Scientific) and disposable surface zeta potential cells (Malvern, UK) were used for the measurements.

2.3.2.3 Transmission Electron Microscopy (TEM)

A JEOL JEM1400-Plau (120kV, LaB6) equipped with a Gatan OneView 4k camera was used to observe the nanoparticles. Samples were prepared by dropping 10 μL of nanoparticle colloids onto 300-mesh copper grids covered with carbon film (Agar Scientific) and air-drying in a fume hood. The sizes of the nanoparticles were measured manually with ImageJ software package. At least 100 particles from 5 images were analysed for each type of nanoparticle.

2.4 Results and Discussion

2.4.1 Preparation and Characterisation of Selenium Nanoparticles

Four stabilisers were employed in this chapter, including potassium iodide, PVA, polysorbate 20 and chitosan. They were expected to create the following surface conditions:

(1) Potassium iodide: salt providing solely electrostatic repulsions with negative surface charge; the nanoparticles with solely electrostatic stabilisation (i.e. without steric hindrance) will be called bare nanoparticles in the following discussion.
(2) PVA: polymer stabiliser providing steric hindrance and electrostatic repulsions with negative surface charge;
(3) Polysorbate 20: surfactant stabiliser providing steric hindrance and electrostatic repulsions with negative surface charge;
(4) Chitosan: polymer stabiliser providing steric hindrance and electrostatic repulsions with positive surface charge;

2.4.2.1 The stability of Bare Selenium Nanoparticles in Suspension

Selenium is a non-metal element, and sometimes considered as metalloid. Elemental selenium has three allotropes: red amorphous selenium, red monoclinic selenium and black/grey trigonal selenium. Spherical selenium nanoparticles can be either

amorphous (a-Se) or monoclinic, which have an orange/red colour in colloids depending on the size of the nanoparticles (shown in Figure 2.2). Trigonal nano-selenium (t-Se) usually has a 2-dimentional structure, i.e. nanorods and nanowires. Trigonal selenium is the most thermodynamically stable form of selenium but is often considered a bioinert material.[198,205,207] Most of the research on the biological application of nano-selenium used red selenium, while the antibacterial aspects of black/grey nano-selenium are rarely reported.

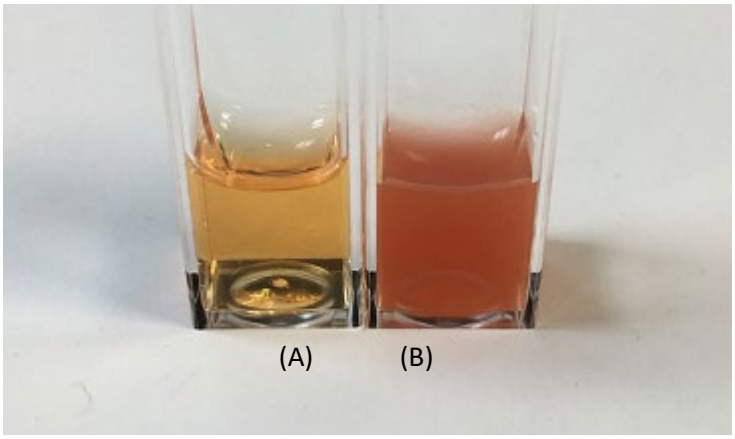

Figure 2.2 Aqueous suspensions of KI-SeNPs indicating that the colour is dependent upon nanoparticle size; the sizes of the SeNPs are (A) 50 nm and (B) 220 nm (determined by DLS technique).

To prepare bare selenium nanoparticles, potassium iodide was used as a stabiliser. It is believed that the I^- ions can be adsorbed onto particle surface and form a double layer with Na^+ and K^+ ions, which provide electrostatic stabilisation.[208] Initially, the synthesis protocol reported by Ng and Fan[208] was followed. However, the concentration of SeNPs prepared using this protocol is very low (0.3 mM according to the amounts of reactants used). For future studies, the nanoparticles will need to be concentrated. The most commonly used method to increase the concentration of nanoparticles in suspension is by centrifugation and resuspending in a smaller volume. It was observed in this study that the bare SeNPs stabilised by KI tended to stick to the wall of the centrifuge tubes. Several different types of tubes, including different brands of microcentrifuge tubes, 15 mL and 50 mL centrifuge tubes, were trialled. The particles attached to all the tubes and even in the tubes where the least

Original in colour

attachment occurred, only a very small portion of the nanoparticles could be collected from the pellets, resulting in very low product yield and further disposal of potentially hazardous substances.

The clustering of nanoparticles is a common problem when dealing with colloidal nanoparticles. The two terms, agglomeration and aggregation, both refer to the clustering of nanoparticles and the difference is that the first one is reversible and the other is irreversible. A common way to disperse and homogenise metal nanoparticles is by ultra-sonication treatment. However, as selenium is a non-metal material, it responds differently to metal nanoparticles when subject to sonication treatment. Many reports have discussed the changes to morphology and structure of SeNPs caused by sonication.[208–211] In sonochemistry, the sound waves migrate through a medium, inducing pressure variations and cavitation, and transforming the sound waves into mechanical energy. Cavitation is referred to as the formation, growth and subsequent implosion of microbubbles during sonication. It gives rise to acoustic streaming and turbulent fluid movement in the medium, causing high local temperatures in the hot-spot interfacial regions.[212] For metal nanoparticles, the energy brought by ultrasonic waves can be used to break the agglomerated particles apart and loosen particles adhering to surfaces. However, selenium is a non-metal material with low phase transformation energy (6.63 kJ/mol);[211] the ultra-sonication can induce aggregation and recrystallization of SeNPs. Figure 2.3 demonstrates the change that occurs as a result of sonication treatment. Dimers and trimers were formed after 10 s of sonication in an ultrasonic bath (40 kHz), which is in accordance with the observation reported by Ng and Fan.[208] If the ultra-sonic treatment was prolonged, the selenium nanoparticles could recrystallize and grow into 2-dimentional nanorods or nanowires of t-Se.

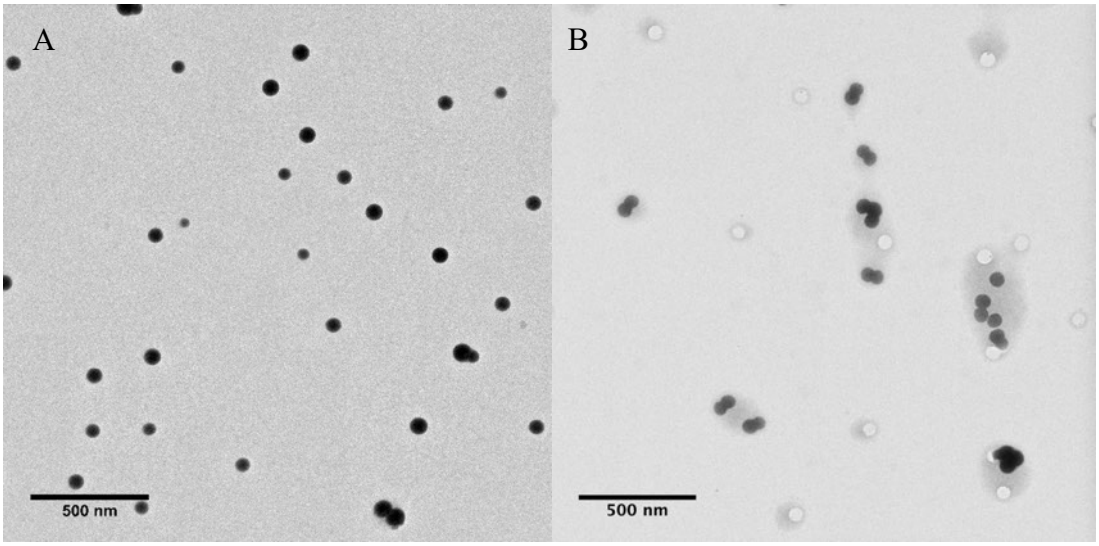

Figure 2.3 TEM images of (A) crude and well dispersed KI-SeNPs and (B) the small aggregations formed after being treated in an ultra-sonic bath for 10s (TEM samples prepared immediately after sonication).

Efforts were made to adjust and increase the concentrations of reactants, in order to (1) improve product yield and (2) make it easier to prepare moderate concentrations of SeNPs. Multiple reaction conditions were trialled, but because of the weak stabilisation capability of KI, the reaction often resulted in visible red precipitated aggregations of selenium (Figure 2.4 A) and a stable and homogeneous suspension could not be formed.

When the initial concentration of Na_2SeO_3 was 2 mM as described in Section 2.3.1.2, during the synthesis process, it was observed that the colour first changed to light orange within a couple of minutes, and then gradually became darker and stopped changing after approximately 1 h (Figure 2.4 B). After 1 h reaction, some visible red solids were precipitated into the suspension. A TEM image of the resulting cloudy suspension obtained after an hour is shown in Figure 2.4 C. It can be seen large aggregations of Se with irregular morphologies were formed. TEM images showing very similar irregular selenium structures were reported by Kong *et al.*[197] when the authors prepared SeNPs using H_2SeO_3 and ascorbic acid with the absence of a- stabiliser. It seemed that with the limited stabilising ability of potassium iodide, stable monodispersed SeNPs could only be obtained at low concentration of Se. Selected area electron diffraction (SAED) technique was used to

determine the crystallinity of the SeNPs. When the sample has a crystal structure, the atoms act as a diffraction grating and the high speed electrons pass through will be diffracted, forming a series of bright spots constituting a diffraction pattern. The SAED pattern of the SeNPs (Figure 2.4 D) shows that the SAED image of the reduced selenium only had diffused halo rings but no patterned bright spot, indicating it was of amorphous nature.

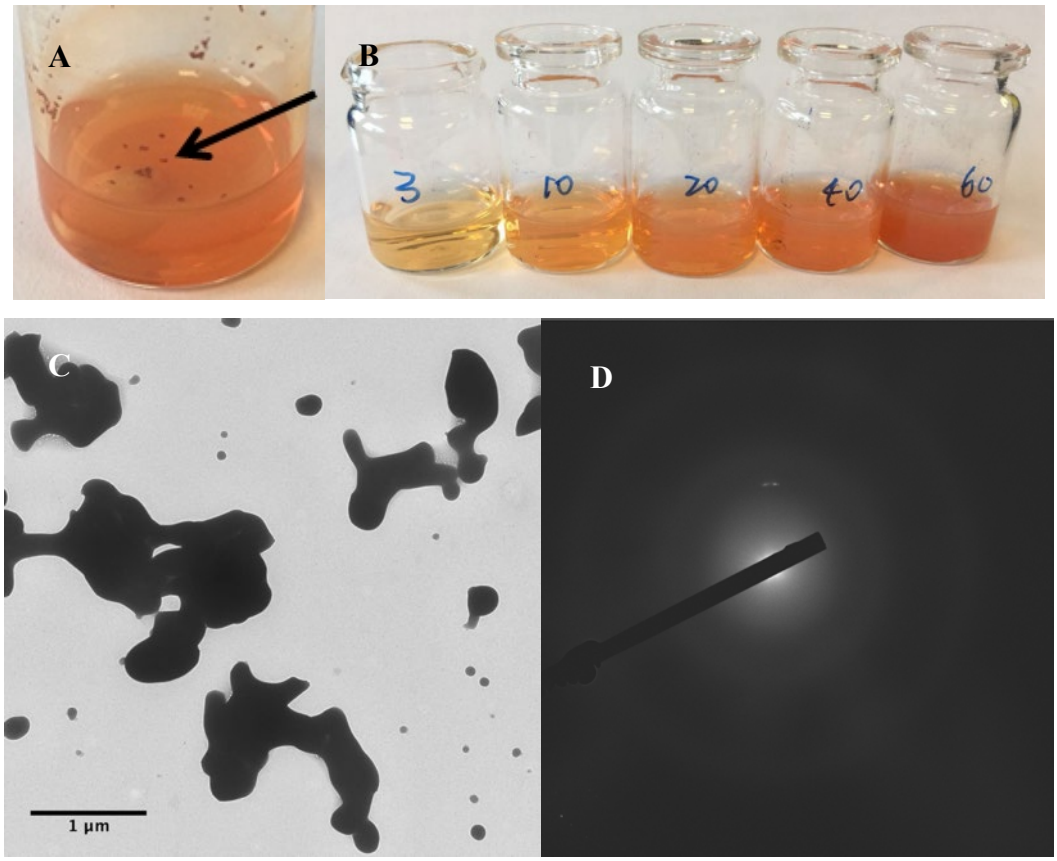

Figure 2.4 (A) Large aggregations of selenium formed during synthesis due to the lack of sufficient stabilisation; (B) change in appearance of KI-SeNP suspension (2 mM) during synthesis (from 3 min to 60 min); (C) TEM image of aggregations formed after an hour of reaction (sample from the last vial in image B, crude); (D) SAED pattern confirming the amorphous nature of the nano-selenium.

Another issue with SeNPs is that they tend to aggregate irreversibly over time without sufficient stabilisation. When evaluating the stability of colloidal suspensions, zeta potential as a function of the surface charge of the particles is often measured. Suspensions with zeta potential values of 0 ± 10 mV, ± 10-20 mV, ± 20-30 mV, and > ± 30 mV are usually considered as unstable, relatively stable, moderately stable, and highly stable respectively.[213,214] Nanoparticles with a zeta potential between 0 ± 10 mV are considered approximately neutral, and the particles tend to agglomerate. With highly negative or positive values (more than +30 mV or less than -30mV), particles in dispersion tend to repel each other which makes the suspension stable. The zeta potential of crude KI-SeNPs was -27.7 ± 0.2 mV, which should be moderately stable. The KI-SeNPs can stay stable at low concentration (0.3 mM) without washing for a week. However, when concentrated by centrifugation, the particles tend to aggregate quickly. An easy way to tell if the SeNPs are aggregated is looking at the transparency of the suspension. Suspensions of freshly prepared SeNPs (less than 100 nm) are clear and orange in colour. The corresponding TEM image is shown in Figure 2.3 A, where well dispersed spherical SeNPs can be seen. As time goes by, the suspension becomes cloudy, layered, and finally red solids are precipitated in the vial. The speed of this process differs with different stability and concentration of the suspension. Figure 2.5 is the TEM image of the aggregated KI-SeNPs exhibiting cloudiness after a week. It can clearly be seen that the particles deformed, and boundaries of particles almost disappeared, indicating that the particles were fusing or merging into each other irreversibly and large clusters of micro-sized selenium were formed. In the paper by Guisbiers *et al*.[171] where bare SeNPs were prepared by laser ablation technique from bulk selenium pallets, no stabiliser was employed and the zeta potential was as low as -45.6 mV, indicating the high stability of the colloidal SeNPs. However, the concentration of the SeNPs was low (50 ppm or 0.633 mM). The authors did not describe any long-term storage and centrifugation for further use. Instead of concentrating the SeNPs and finding the actual minimal inhibition concentration (MIC) of the SeNPs against the bacteria, the MIC was estimated by plotting a SeNPs concentration – inhibition rate curve using the data obtained at low concentrations. It is possible that the same stability problem would occur with the bare SeNPs prepared by laser ablation even though the zeta potential was very negative.

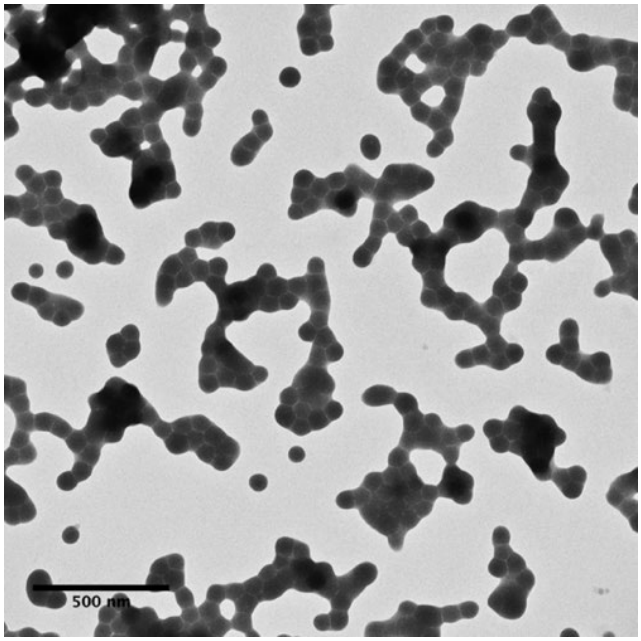

Figure 2.5 A TEM image of the aggregations of SeNPs from a suspension that appeared to be cloudy after 1 week of storage at room temperature.

In summary, there are two issues leading to failure to prepare bare KI-SeNPs for the future antibacterial tests: (1) difficulties in scaling up the preparation process to obtain sufficient quantity and concentration of KI-SeNPs; (2) KI-SeNPs in aqueous suspensions are very unstable. Centrifugation or ultrasonic treatment can quickly lead to the irreversible aggregation of the bare SeNPs. These behaviours indicate that bare SeNPs are not suitable for further investigation in the colloidal state. Therefore, stabilisers with better performance are needed to study colloidal nano-selenium.

2.4.2.2 Selenium Nanoparticles Stabilised by Different Capping Agents

As mentioned in Chapter 1, particle size is one of the important factors which determines the antimicrobial performance of the nanoparticles. Therefore, when comparing the effects of different stabilisers, it is important to keep the particle size the same or as similar as possible. When the influence of different stabilisers on the antimicrobial performance of AgNPs was investigated by Kvítek *et al*.,[215] the AgNPs were prepared with only electrostatic stabilisation at first, and then coated with different stabilisers. This is probably the ideal approach since it made sure that the only difference between each group was the stabilising agent, and the nanoparticle cores were identical. However, as discussed above, KI could not provide sufficient stabilisation for the synthesis of SeNPs with sufficient amount and concentration for further antimicrobial investigation. The method used by Kvítek *et al.*[214] could not be applied to SeNPs successfully. Therefore, efforts were made to prepare different SeNPs with similar sizes by altering the concentration of the different stabilising agents.

When talking about the size of inorganic nanoparticles, there are a few different measurements that need clarification before further discussion. One of the most commonly used and direct method is with microscope, for example, TEM, as shown previously in Figure 2.3 – 2.5. TEM images reveal the actual sizes of the nanoparticles. When an inorganic nanoparticle is coated by a polymer, normally it is difficult to see the polymer layer in TEM images due to the lack of contrast and sensitivity of the polymer.[216] It means that usually only the contrast related to the inorganic core can be observed, and the size determined through TEM images are considered the actual size of the nanoparticle. On the other hand, dynamic light scattering (DLS) analysis is a technique commonly used for the analysis of nanoparticles which reveals the hydrodynamic particle size. The hydrodynamic size reported by DLS analysis is determined through the measurement of Brownian motion of the particles and is defined as "the size of a hypothetical hard sphere that diffuses in the same fashion as that of the particle being measured".[217] The average sizes calculated by TEM analysis are normally smaller than those reported by DLS analysis, which is due to the fact that DLS technique determines the hydrodynamic size that includes the particle itself as well as the surrounding diffusive layer. The electric double layers surrounding the charged particles in an aqueous solution affect

the diffusion speed of the particles and consequently affect the hydrodynamic sizes determined by DLS.[218] Moreover, the DLS technique also gives the polydispersity index (PDI) of a sample, which indicates the width of the particle size distribution. When the PDI is lower than 0.1, the sample can be considered a highly monodisperse sample with a very narrow size distrubtion.[219] The z-average size reported from DLS cumulant analysis is an intensity-weighted average size, which should not be confused with number mean value produced by TEM analysis. It means the DLS technique can be sensitive to the presence of large nanoparticles that have stronger scattering intensity and give more weight to the calculation.[217]

Based on the data from the literature, some preliminary experiments were performed to optimise the concentrations of the stabilisers. For example, Bartůněk *et al*.[133] reported that the size of SeNPs increased as the concentration of polysorbate 20 increased; the average sizes of the SeNPs prepared with 0.17% and 0.4% of polysorbate 20 were 48 nm and 59 nm (by DLS) respectively. In order to prepare PS20-SeNPs with average sizes of approximately 50 nm, 0.25% was chosen as the concentration of polysorbate 20. It is worth noting that with the surfactant as the stabiliser, the sizes of SeNPs increased as the concentration of surfactant increased, which is a unique observation. Normally when using polymer or surfactant as stabilisers, the sizes of metal NPs decrease as the concentration of the stabiliser increases, which leads to stronger steric hindrance and prevents the particle growth. Bartůněk *et al.*[133] explained the unique phenomenon by the shift of reaction kinetics that the higher concentration of surfactant slowed down the reaction. At the initial stage, fewer particles were formed, but as the particle grew, the stabilisation was not strong enough to stop the growth, resulting in fewer and larger particles. Bartůněk *et al.*[220] later also conducted the study on the synthesis of SeNPs using anionic surfactant sodium dodecyl sulphate (SDS) as the stabiliser. Similar observations that the size of SeNPs increased as the concentration of SDS increased were reported. For the PVA-SeNPs and CS-SeNPs, the suitable concentrations of the polymer stabiliser were also determined according to the literature.[122,196,205]

TEM images and size distribution of the SeNPs are shown in Figure 2.6. Table 2.3 summarises the DLS analysis results for selenium nanoparticles synthesised in the presence of PVA, polysorbate 20, and chitosan. The obtained SeNPs with different stabilisers were all approximately 50 nm in size, which was similar to those synthesised in the other studies.[122,127,133] As can be seen from the table, both PVA and polysorbate 20 capped selenium nanoparticles were highly monodispersed, with PDI values of 0.09 and 0.04 which fall below the 0.1 threshold. However, the SeNPs prepared with chitosan as the stabiliser had a higher PDI of 0.22. This may be a result of the heterogeneous nature of chitosan which leads to heterogeneous nucleation and growth of nanoparticles. On the other hand, the DLS z-average size of PS20-SeNPs were similar to the size obtained by TEM analysis, while the sizes determined by TEM were much smaller than DLS z-average sizes for PVA-SeNPs and CS-SeNPs. This can be attributed to the presence of polymer on the surface of the nanoparticles, which significantly increased the hydrodynamic size of the nanoparticles but were invisible in the TEM images with the resolution used. The actual average sizes of the selenium nanoparticles obtained from TEM analysis were very similar. Since many reports have discussed the influence of particle size on the properties of nanoparticles, similar sizes (i.e. the actual size of the SeNPs determined by TEM) are favourable for future study when comparing the different coatings.

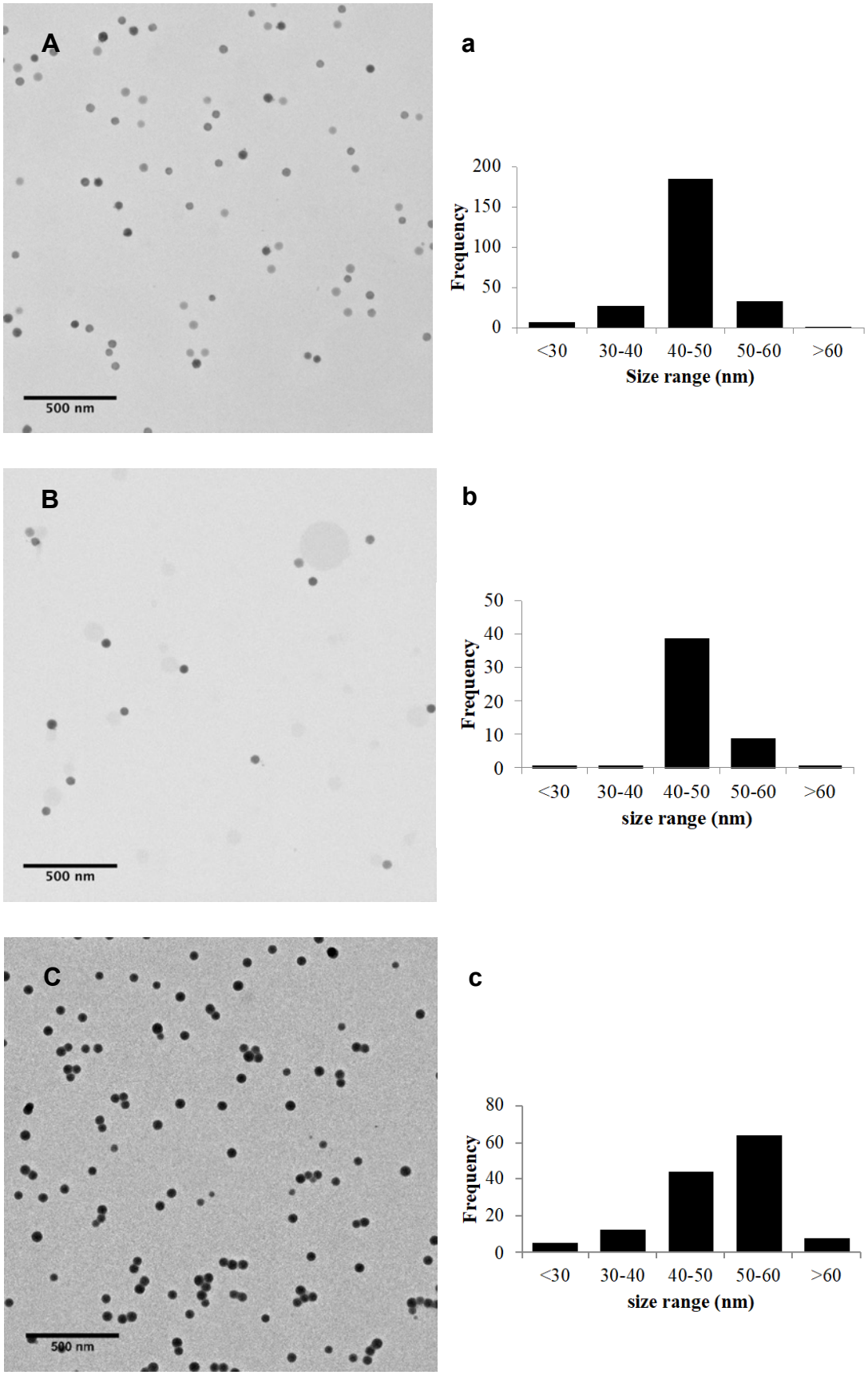

Figure 2.6 TEM images and size distributions of (A) PVA-SeNPs; (B) PS20-SeNPs; and (C) CS-SeNPs and corresponding histograms of size distribution (a, b, c).

Table 2.3 DLS analysis results for selenium nanoparticles synthesised in the presence of PVA, polysorbate 20, and chitosan.

Nanoparticles	DLS z-average size (nm)	PDI	Size by TEM (nm)
PVA-SeNPs	119 ± 7	0.09±0.04	45 ± 6
PS20-SeNPs	56 ± 1	0.04±0.01	48 ± 5
CS-SeNPs	150 ± 4	0.22±0.02	50 ± 9

* Data presented as mean ± SD, n=3.

The zeta potential values of the SeNPs with different capping agents are shown in Table 2.4. The zeta potential of PVA-SeNPs described here is lower than the value reported by Tran *et al*.[122] It is possibly due to the different degree of hydrolysis of the PVA used, as details of the polymer were not provided by Tran *et al*. Since the zeta potential of PVA-SeNPs was only around -8.2 mV, the nanoparticles were mainly stabilised by the steric hindrance provided by the polymer. Both polysorbate 20 and chitosan coated nanoparticles have moderate electrostatic repulsion as well as steric hindrance. It does not necessarily mean that polysorbate 20 and chitosan have better stabilisation ability than PVA, since the PVA used here has a much larger molecular weight and the steric hindrance may be stronger. Actually, all of these three types of SeNPs can stay stable for several weeks at room temperature with a clear transparent look without showing cloudiness.

Table 2.4 Zeta potential of SeNPs stabilised by different capping agents.

Nanoparticles	**Zeta potential (mV)**
PVA-SeNPs	-8.2 ± 2.5
PS20-SeNPs	-24.6 ± 4.6
CS-SeNPs	+23.8 ± 3.7

* Data presented as mean ± SD, n=3.

2.4.2 Preparation and Characterisation of silver nanoparticles

At the initial stage of this study, attempts were made to prepare different shapes of AgNPs, as studies have indicated that the antimicrobial activity of colloidal AgNPs is influenced by the particle shape; for example, silver nanoprisms (triangular nanoplates) were found to have better antimicrobial performance than conventional AgNPs.[167] However, it is unclear if this difference remains when the nano-silver is fixed onto a surface. Therefore, one of the original goals of this study was to prepare different shaped nano-silver *ex situ* and then fix them onto fabric surface. Unfortunately, from the preliminary studies, it was found that the reproducibility of the shaped nano-silver was poor. The properties of the products varied between different batches. More importantly, the shaped nano-silver lost their special shape easily with external stimuli such as heat and electrostatic disturbance, which is not desirable for applying them onto fabrics. Subsequently, the experiment was terminated. The details of the preparation and characterisation of the silver nanoprisms can be found in the Appendix A.

Subsequently, silver nanoparticles, as a type of well-studied antimicrobial nanoparticles, were investigated as a comparison for SeNPs. Studies have shown that the presence of polymer or surfactant stabilisers on the particle surface generally has no significant adverse effect on the antimicrobial properties of AgNPs.[215,221] Therefore, the aim here was to produce AgNPs with comparable sizes to that of SeNPs other than creating different surface conditions for the AgNPs. A method reported by Qin *et al.*[206] was followed to prepare quasi-spherical silver nanoparticles with controlled sizes using ascorbic acid as the reducing agent; in the original report, the authors discussed the influences of pH on the reaction and the AgNP products. In this thesis, poor reproducibility was a major problem when the method was followed initially. After repeated trials, factors other than the temperature, reactant concentrations, and pH of the reaction system were identified to be crucial to the synthesis as well since the synthesis is highly sensitive to the reaction conditions. For example, when mixing the precursor salt with the reducing agent and stabiliser, it is often described simply as “added to” or “by dropwise” in many reports, while it is actually a critical condition that affects the nanoparticle synthesis. It is rarely mentioned in published studies that other factors such as the size and shape of the

reaction vessels and magnetic stir bars also play their roles in the process, and therefore need to be controlled to improve the repeatability of the reactions.[222] In this section, apart from the pH values which were discussed as a critical condition in the original report, the mixing of reactants (e.g. by drop wise or injection) is also studied as a supplement to the synthetic method.

2.4.2.1 Influence of the pH of the Reaction System on the Silver Nanoparticle Products

The AgNPs prepared at different pH possess distinct colours as shown in Figure 2.7. In metal nanoparticles such as silver, electrons move freely, which gives rise to a surface plasmon resonance (SPR) absorption band. This band occurs when the frequency of the electromagnetic field of an incoming light wave becomes resonant with the coherent electron motion, which is the origin of the observed colour and the absorption peak on the UV-vis spectrum.

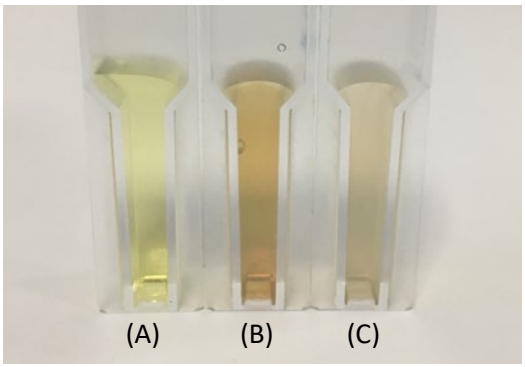

Figure 2.7 Silver nanoparticle colloids prepared with different pH: (A) pH 10.8, (B) pH 10.2, and (C) pH 9.5.

The absorption peak strongly depends on the particle size, shape and dielectric medium. In a UV-Vis spectrum of AgNPs, the average particle size is associated with the maximum absorption wavelength, while the particle size distribution is related to the full width at half maximum (FWHM).[223] The UV-vis spectra of the TSC-AgNPs prepared at different pH are shown in Figure 2.8 (correlated to Figure 2.7). The as-prepared fresh silver nanoparticles synthesised at pH of 9.5, 10.2, and

Original in colour

10.8 presented absorption peaks at 454, 404, and 396 nm respectively. The absorption peak red shifted as the pH value decreased, indicating larger particle sizes were generated as the pH value decreased. This was because the reactivity of ascorbic acid as a reducing agent was increased with the increase of pH and, consequently, the number of nuclei formed at the initial stage was higher, which resulted in a smaller amount of silver ions for particle growth and smaller particle sizes.[206] The values of FWHM for these samples were 55, 64, and 224 nm respectively. It is noticeable that all of the peaks became narrower and sharper after ripening. The FWHM values decreased to 50, 57, 96 nm respectively, indicating an improvement of size distribution.

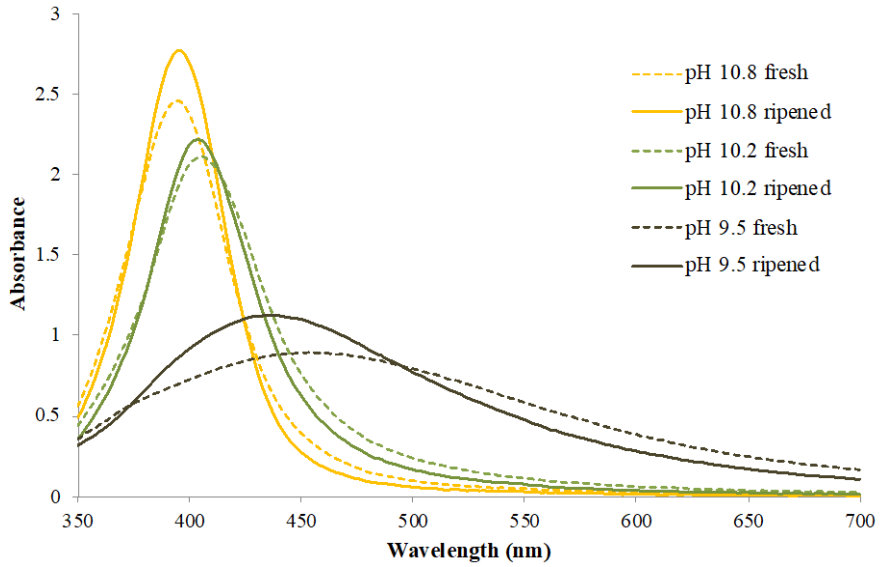

Figure 2.8 UV-vis spectra of the AgNPs synthesised at pH 9.5, 10.2, and 10.8 by adding silver nitrate dropwise (1 drop/sec).

The results obtained from DLS analysis are summarised in Table 2.5. There is a clear trend that the average particle size increased with the decrease of pH value of the system before the addition of silver salt, which is in accordance with the UV-vis spectra results. Additionally, the decrease of pH value resulted in a lower PDI value, which indicates better uniformity of particle size. This can be explained by the different reactivity of the reducing agent as well. For example, at pH 9.5, the reactivity of ascorbic acid was not as high as at pH 10.8, which gave time for the silver ions to be homogenised by the magnetic stirrer when added to the reaction

Original in colour

system before being reduced to metallic silver. On the other hand, when the reactivity of the reducing agent was very high at a higher pH value, there was little time for the silver ions to be properly dispersed in the reaction system, resulting in a heterogeneous growth of particles. From the DLS analysis it can also be seen that the ripening process effectively improved the monodispersity, while slightly increasing the average hydrodynamic sizes. This might be due to the intraparticle ripening accelerated by the high temperature of the ripening process. After all the monomers are consumed, nanoparticles will undergo intraparticle ripening, where the aggregations of nuclei become more spherical-like.[206] The irregular shapes of the particles might have been an additional contribution to the hydrodynamic size measurements by DLS. Therefore, during the ripening process, the small particles were consumed, and the irregular shapes of particles disappeared, which led to a better size distribution. This can be evidenced by Figure 2.9, an example size distribution graph of AgNPs synthesised at pH 10.2 obtained from DLS analysis. After the ripening process, the peak of small particles with sizes around 10 nm disappeared, and the main peak became taller and shifted to a slightly smaller size, from 79 nm to 68 nm.

Table 2.5 DLS analysis results for TSC-AgNPs synthesised at different pH conditions, silver nitrate added by quick drop (1 drop/sec).

pH condition	Fresh or ripened	DLS z-average (nm)	PDI	Size by TEM (nm)
10.8	Fresh	33 ± 3	0.47 ± 0.03	14 ± 5
10.8	Ripened	39 ± 4	0.18 ± 0.03	13 ± 5
10.2	Fresh	47 ± 4	0.53 ± 0.07	32 ± 11
10.2	Ripened	57 ± 1	0.31 ± 0.01	31 ± 7
9.5	Fresh	86 ± 2	0.30 ± 0.01	53 ± 21
9.5	Ripened	96 ± 3	0.29 ± 0.01	55 ± 17

* Data represent mean ± SD, n=3.

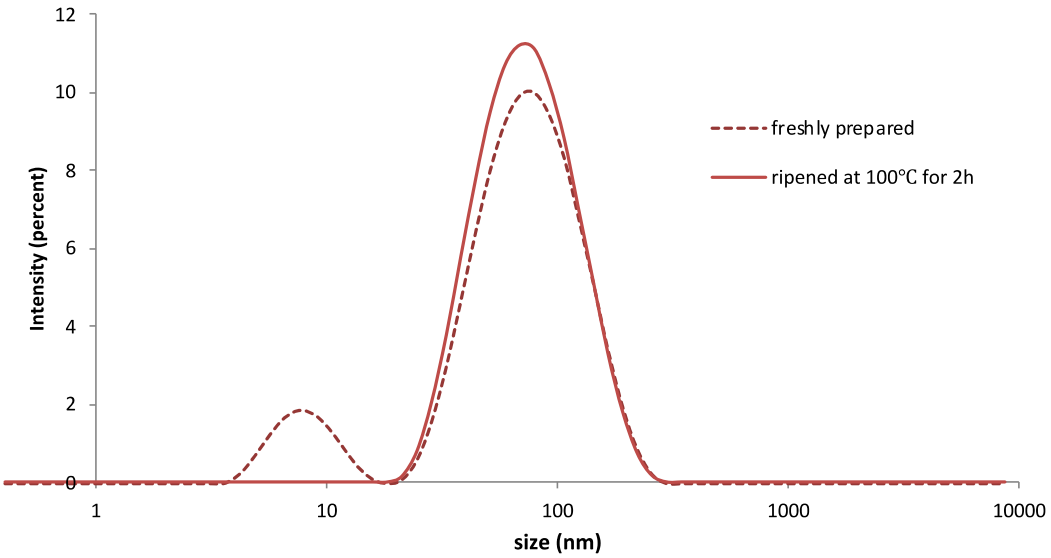

Figure 2.9 Size distribution by intensity obtained by DLS analysis before and after accelerated ripening, sample prepared at pH 10.2.

The analysis above can be further confirmed by the TEM images of the silver nanoparticles (Figure 2.10 – 2.12). As can be seen, the size of nanoparticles increased significantly as the pH value decreased, which was consistent with the results from the UV-vis spectra and DLS analysis. No major differences in the sizes before and after the ripening process can be seen, but it is noted that the morphologies of the particles become more smooth and spherical-like after the ripening process. The average sizes obtained from TEM image analysis for the AgNPs prepared at pH 10.8, 10.2 and 9.5 are 13 ± 5 nm, 31 ± 7 nm, and 55 ± 17 nm respectively. These sizes are smaller than those determined by DLS. As mentioned earlier, the hydrodynamic size is usually larger than the actual particle size because it includes the diffusive layer around the particles. The size distribution of ripened nanoparticles determined by TEM images are also shown in Figure 2.10. It can be seen that size distributions of all the samples, especially at pH 10.2 and 9.5, were clearly improved after the accelerated ripening process and became single-peaked with the peak value close to the calculated mean size.

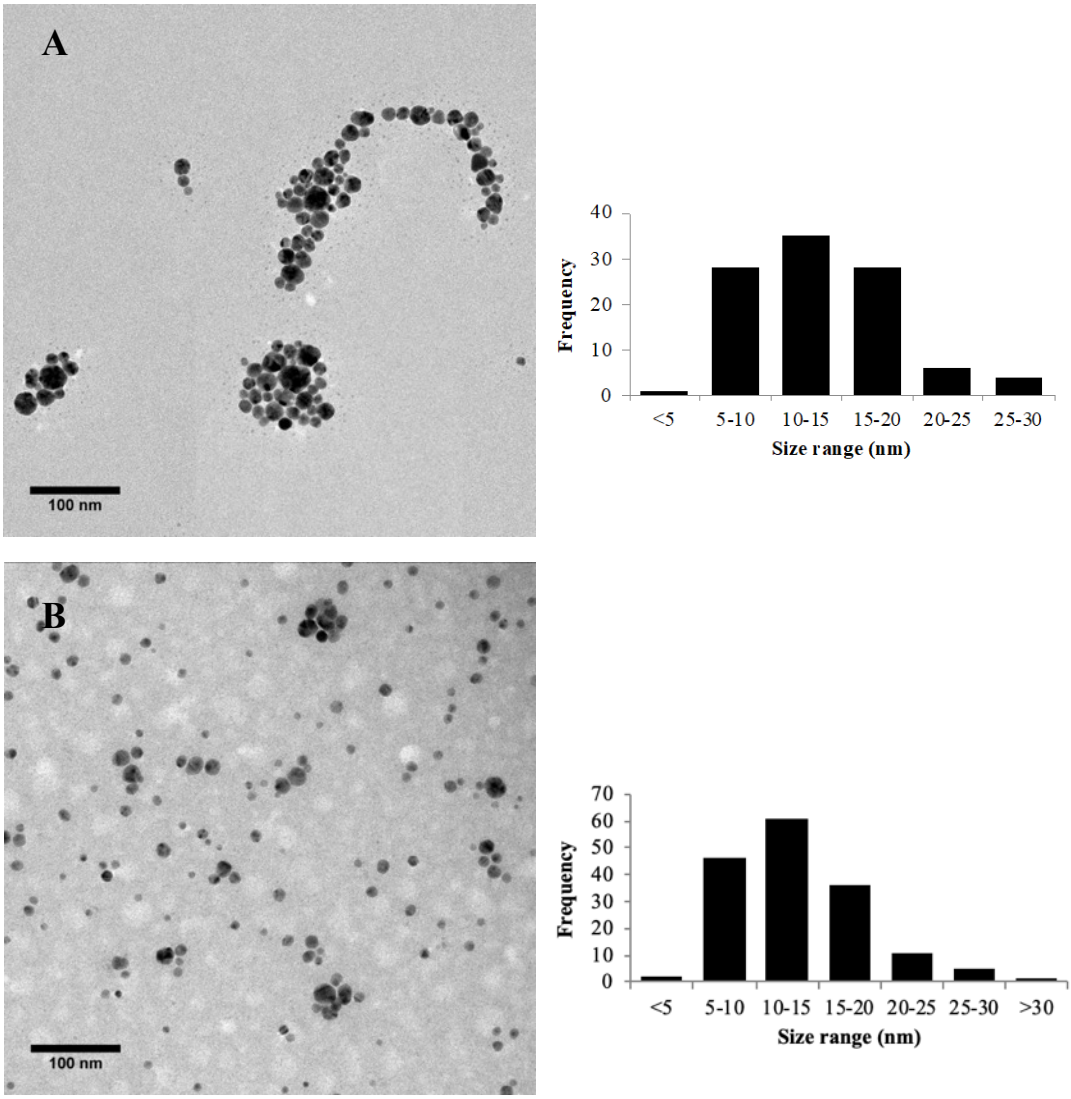

Figure 2.10 TEM images of AgNPs synthesised at pH 10.8: (A) freshly prepared and (B) ripened in 100 °C water bath for 2 h, and the corresponding particle size distribution.

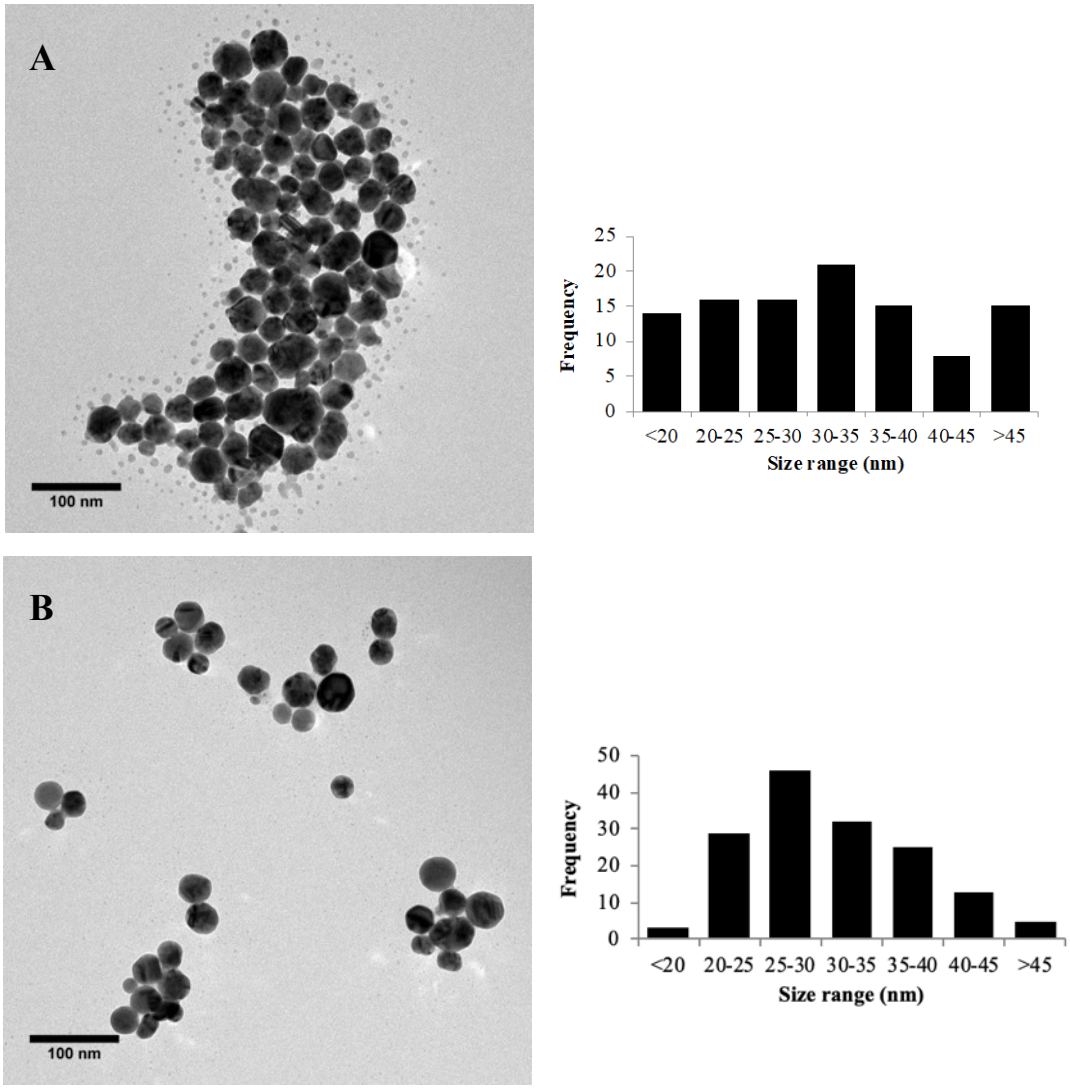

Figure 2.11 TEM images of AgNPs synthesised at pH 10.2: (A) freshly prepared and (B) ripened in 100 °C water bath for 2 h, and the corresponding particle size distribution.

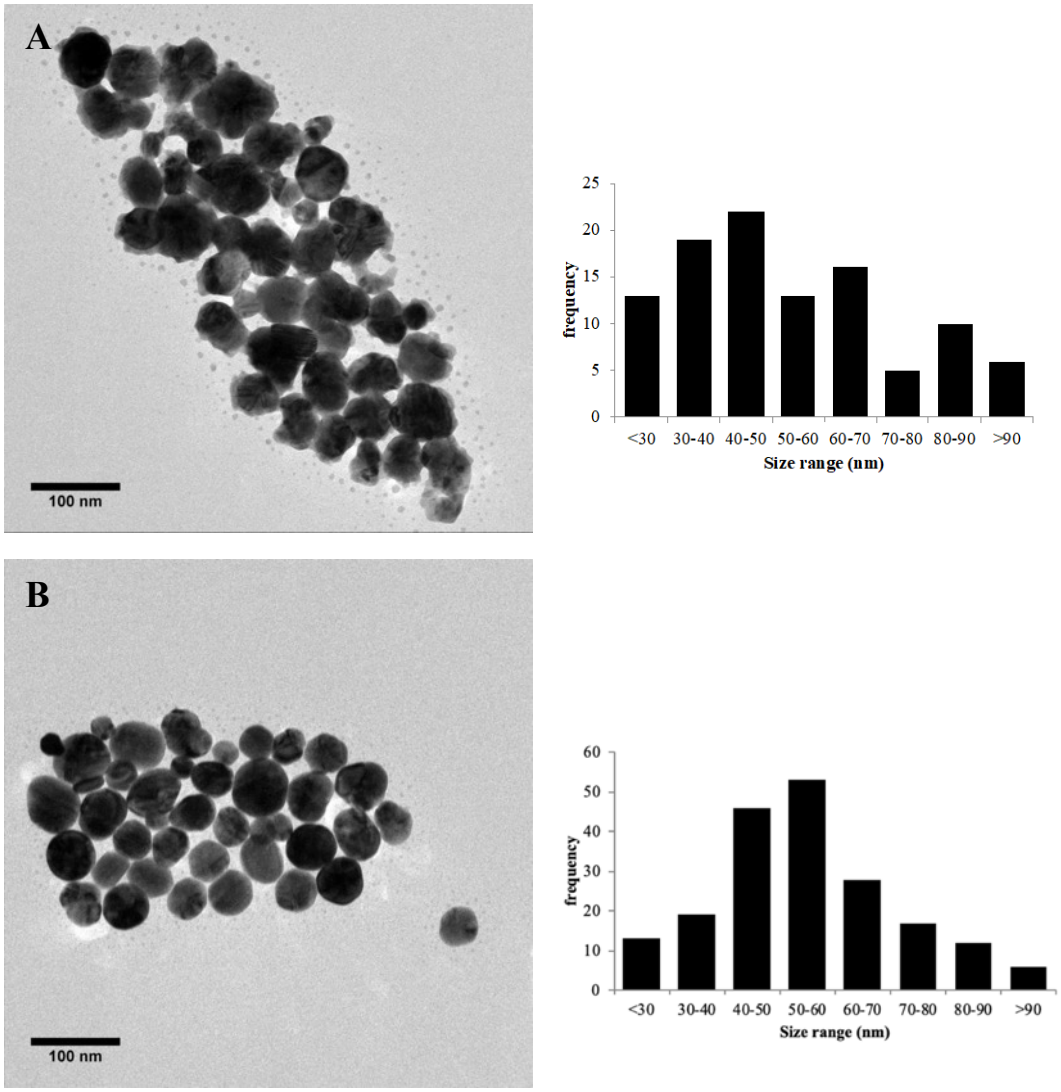

Figure 2.12 TEM images of AgNPs synthesised at pH 9.5: (A) freshly prepared and (B) Ripened in 100 °C water bath for 2 h, and the corresponding particle size distribution.

2.4.2.2 Influence of the Precursor Addition Speed on the Silver Nanoparticle Products

As discussed earlier, there are many factors in the synthetic conditions that can influence the properties of the nanoparticle product. Apart from the pH value of the reaction system, another factor is how the reactants are mixed. This information is often omitted from published reports. When mixing the precursor salt with the reducing agent and stabiliser, “added to” or “added by dropwise” is often given in the methodology section; however, the speed of addition can also make a significant difference to the product. In order to study the influence caused by the different ways to mix reactants, in this section, the silver nitrate was added to the system by rapid injection, quick drop (1 drop/sec), or slow drop (1 drop/5 secs). The pH of the system was fixed at 9.5 for this investigation because the AgNPs synthesised at pH 10.2 and 10.8 by quick drop were already very small.

Figure 2.13 shows the UV-vis spectra of the silver nanoparticles synthesised by different mixing speed of reactants at pH 9.5. Table 2.6 is the summary of DLS analysis on the particles. TEM images and size distribution of the AgNPs are shown in Figure 2.12, Figure 2.14 and Figure 2.15. Some findings are similar with the study on the effects of pH. It can be seen that the increase of mixing speed caused similar changes on the nanoparticles as the increase of pH (i.e. reducing agent reactivity). When the silver salt was rapidly injected to the system, the nanoparticles obtained were even smaller than those nanoparticles synthesised at pH 10.2 and the addition of silver salt by dropwise. This was because when the silver precursor was injected rapidly into the reaction system, a large number of nuclei were formed immediately, and the monomers remaining for particle growth were limited. On the contrary, when $AgNO_3$ was added slowly, the number of nuclei formed at the initial stage was limited and therefore there were more monomers added later for the particles to grow larger. It is also noticeable that the AgNPs prepared by rapid injection of silver precursor have the narrowest size distribution. When the $AgNO_3$ was injected into the reaction system, the silver ions could be more easily and rapidly homogenised, and thus the formation of nuclei and nanoparticles could be more uniform across the reaction system.

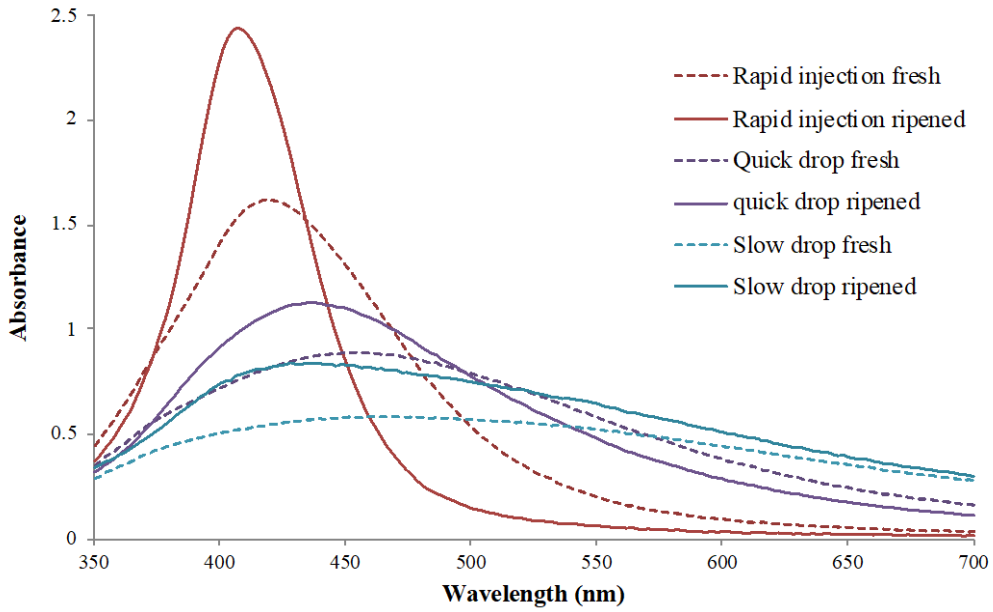

Figure 2.13 UV-vis spectra of the AgNPs synthesised by adding silver nitrate by rapid injection, quick drop (1 drop/sec), or slow drop (1 drop/5 secs) at pH 9.5.

Table 2.6 DLS analysis results for TSC-AgNPs synthesised at pH 9.5.

Addition of $AgNO_3$	Fresh or ripened	DLS z-average (nm)	PDI	Size by TEM (nm)
Rapid injection	Fresh	43 ± 2	0.19 ± 0.02	37 ± 6
Rapid injection	Ripened	49 ± 3	0.11 ± 0.01	42 ± 5
Quick drop	Fresh	86 ± 2	0.30 ± 0.01	53 ± 21
Quick drop	Ripened	96 ± 3	0.29 ± 0.01	55 ± 17
Slow drop	Fresh	123 ± 6	0.24 ± 0.01	90 ± 36
Slow drop	Ripened	127 ± 6	0.22 ± 0.02	100 ± 26

* Data represent mean ± SD, n=3.

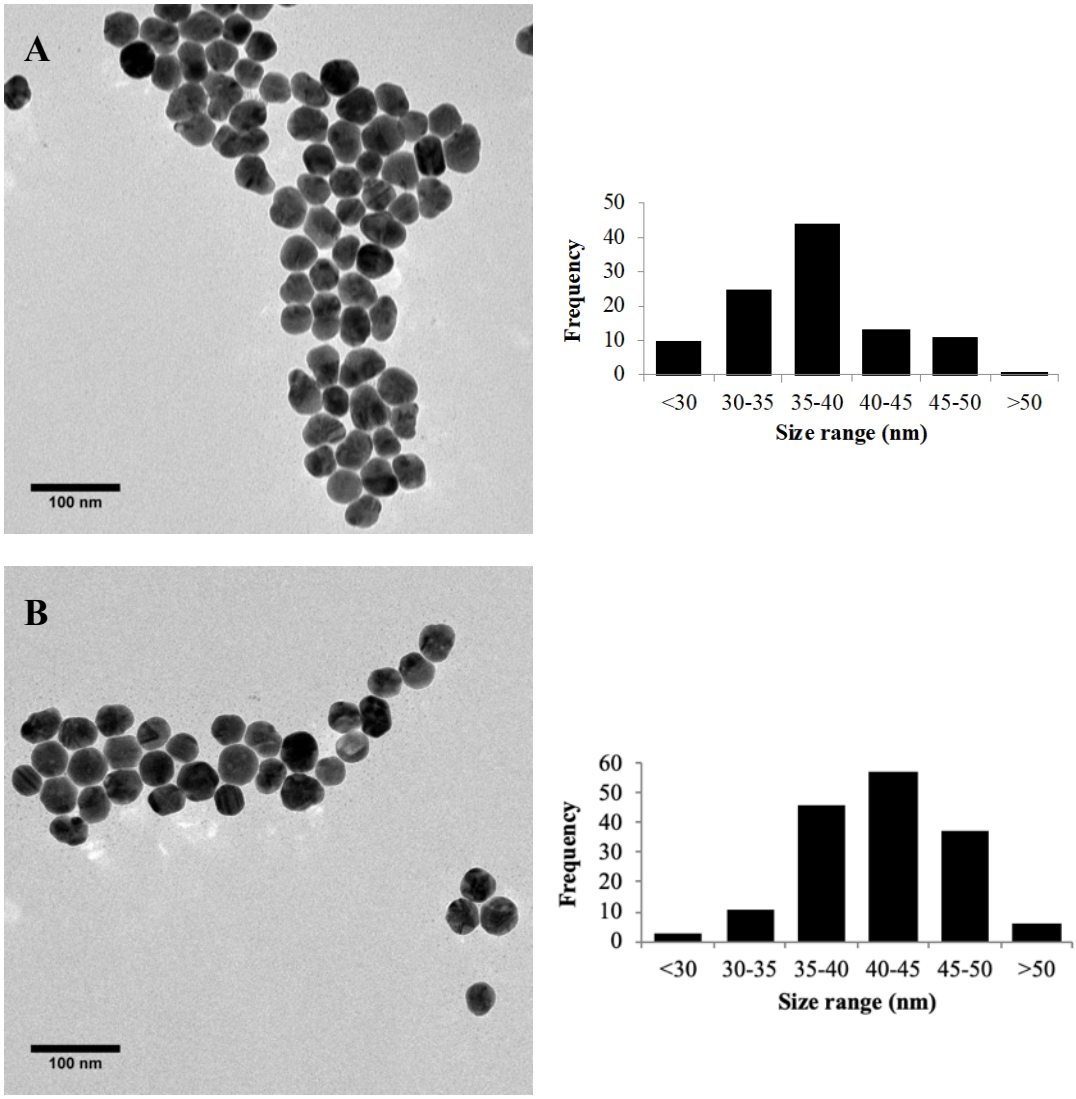

Figure 2.14 TEM images of AgNPs synthesised at pH 9.5 by rapid injection of silver salt: (A) freshly prepared and (B) ripened in 100 °C water bath for 2 h and the corresponding particle size distribution.

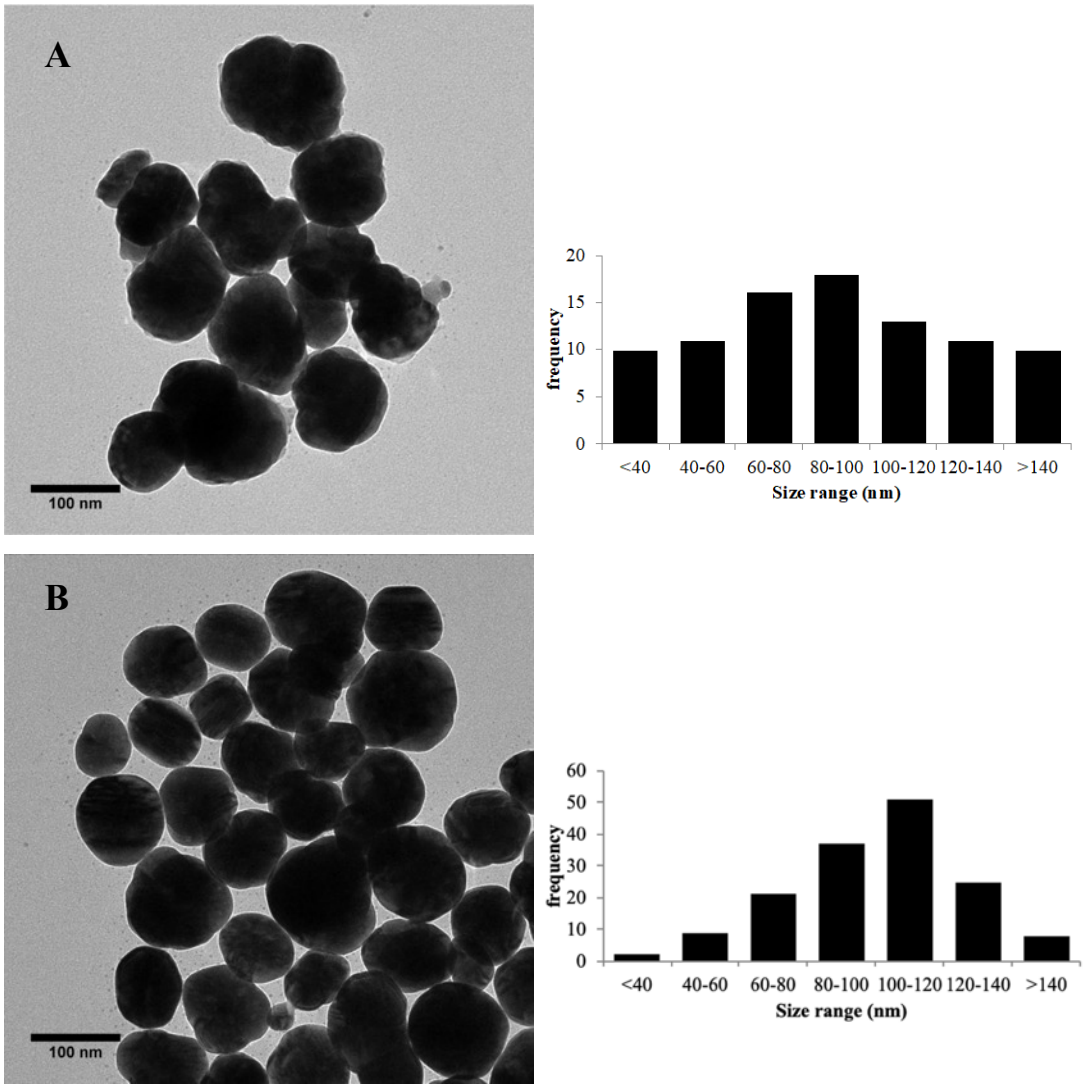

Figure 2.15 TEM images of AgNPs synthesised at pH 9.5 by slow drop of silver salt: (A) freshly prepared and (B) ripened in 100 °C water bath for 2 h and the corresponding particle size distribution.

The average sizes of AgNPs determined by TEM for the three different samples are 42 ± 5 nm, 55 ± 17 nm, and 100 ± 26 nm respectively (Table 2.6). The average sizes by TEM analysis are smaller than the results reported by DLS technique as expected, due to the reasons previously discussed. It is worth noticing that the average sizes of the AgNPs prepared by rapid injection of silver salt obtained from the two different techniques are quite close, with 49 nm and 42 nm from DLS and TEM respectively, while this sample also has significantly lower PDI compared with other samples.

This could lead to the observation that when the nanoparticles have a narrow size distribution, the z-average size calculated by DLS is closer to the actual average size. As mentioned previously, z-average size is sensitive to the presence of large nanoparticles which contribute more weight to the calculation due to the stronger scattering intensity. Therefore, the more uniform the nanoparticles are, the more accurate the z-average size can be.

Table 2.7 Zeta potential of silver nanoparticles prepared at different conditions.

Nanoparticle synthetic condition	Zeta potential (mV)
pH 10.8, quick drop	-47.5±1.3
pH 10.2, quick drop	-52.3±0.1
pH 9.5, quick drop	-49.1±0.6
pH 9.5, rapid injection	-56.9±1.0
pH 9.5, slow drop	-52.3±0.7

* Data represent mean ± SD, n=3.

Table 2.7 summarises the zeta potentials of TSC stabilised silver nanoparticles. The zeta potential values for all the silver nanoparticles were at around -50 mV. Neither the different pH conditions nor reagent mixing speeds had a major influence on the zeta potential and the stability of the AgNP suspensions. These results indicated highly stable electrostatic stabilisation for the AgNPs, which is favourable for the storage and further evaluation of the nanoparticles.

2.5 Chapter summary

In this chapter, both selenium and silver nanoparticles were successfully prepared by a facile chemical reduction method at room temperature. Ascorbic acid was

employed as a nontoxic and mild reducing agent to achieve environmentally friendly synthesis. The sizes and surface conditions of the nanoparticles were controlled and characterised as these properties are known to influence the antimicrobial performance of the nanoparticles.

Spherical selenium nanoparticles with similar sizes but different stabilisers were successfully prepared using the same method. Since the aim here was to investigate the influences of stabilisers on the antimicrobial performance of SeNPs, the sizes of the different SeNPs should be similar. The electrostatic stabilisation with KI alone failed to provide stable suspensions of SeNPs. The monodispersed bare selenium nanoparticles could be prepared at low concentration (approximately 0.5 mM) but the process could not be scaled up to obtain stable nanoparticle suspension with sufficient quantity of nanoparticles for future application in antibacterial assessment. When increasing the concentration of selenium, the nanoparticles tended to aggregate irreversibly. The SeNPs with different stabilisers, including PVA, polysorbate 20, and chitosan all had excellent stability and similar sizes (40 – 50 nm), which are favourable for the investigation to be conducted in the next chapter.

For quasi-spherical silver nanoparticles, a synthetic method based on Qin and colleagues' report[206] was employed, and AgNPs with a range of diameters were obtained by altering the pH of the synthesis reaction and the mixing speed of the reactants. It was found that increased pH value could lead to increased reactivity of ascorbic acid as a reducing agent, and thus smaller AgNPs with narrower size distribution could be obtained, which is in accordance with the original report. Apart from the pH value, how the reactants are mixed was identified in this thesis as another factor that can greatly affect the synthesis reaction. It was found that mixing the reactants quickly, i.e. adding $AgNO_3$ by rapid injection, could result in smaller particles sizes and improved size distribution comparing with adding the silver precursor drop by drop. With the controlled synthetic conditions, silver nanoparticles with averages sizes from approximately 10 to 100 nm were obtained. These results also demonstrated that the properties of nanoparticles were sensitive to the conditions during the synthesis process, thus great care needs to be taken when preparing nanoparticles.

Chapter 3 Antibacterial Activity of Colloidal Silver and Selenium Nanoparticles

3.1 Introduction

The overall aim of this chapter was to test the antibacterial performance of the different nanoparticles prepared in Chapter 2, which could provide valuable insights for the development of nanoparticle-based antimicrobial textiles. Numerous methods have been developed to evaluate the antibacterial performance of nanoparticles in suspension, however many are flawed and as yet there is no standard method for the antibacterial assessment of nanoparticles. When applying the antimicrobial susceptibility test methods of antibiotics to nanoparticles, modification is often needed since nanoparticles, as nano-scale solid materials, act differently from soluble antibiotic compounds, thus more than one method is often necessary.[224] Some commonly used antibacterial assessment methods for colloidal nanoparticles are summarised Table 3.1.

Disk diffusion is one of the oldest methods for antimicrobial susceptibility testing and still remains one of the most widely used standardised methods now due to its simplicity and good applicability to a wide range of microorganisms.[225] This method involves inoculating the whole surface of agar plates to achieve confluent bacterial growth, and then disks impregnated with antimicrobials are plated onto the surface. With the diffusion of antibiotic from the disk, a clear zone without bacterial growth can be observed after incubation. By comparing the zone of inhibition (ZoI) formed with a database, the extent to which microbes are affected by the antimicrobial agent can be determined.

Table 3.1 Commonly used antibacterial assessment methods for nanoparticles.

Method	Advantages	Disadvantages	References
Agar diffusion method (disk diffusion or well diffusion)	Simple qualitative/semi-quantitative method	Not applicable for many nanoparticles that do not diffuse on agar plates; cannot distinguish bactericidal and bacteriostatic effects	[163,226,227]
Optical density reading	Simple	Low accuracy; the presence of nanoparticles interfering with the optical density	[105,163,168,228]
Viable counts on agar plates	No special reagent and equipment required	Determines colony forming unit (CFU) but not total cell population; time consuming; large amount of disposable materials needed	[229–231]
Colorimetric viability assays such as MTS/MTT/XTT and AlamarBlue	Applicable to both planktonic cells and cells on surfaces	Costly reagents; quantifies metabolic activity rather than viable cell population; uncertainty of the interaction between reagents and nanomaterials	[114,232,233]
Live/dead staining	Accuracy; visualisation of sample	Costly reagents; special equipment needed	[122,234]

Conventionally, the antimicrobial agents, including antibiotics and antimicrobial plant/microorganism extracts, are normally soluble and therefore can diffuse in the agar. However, for nanoparticles, the size of nanoparticles may not allow them to diffuse in the semi-solid agar. Agnihotri *et al*.[163] prepared a range of silver nanoparticles with different sizes (from 5 nm – 100 nm) and performed the disk diffusion test against *E. coli*. The results showed that only particles smaller than 15 nm formed ZoI on the nutrient agar plates and the ZoI decreased with increased size of nanoparticles. For larger nanoparticles, no ZoI was observed, showing inferior antibacterial efficacy compared with tests carried out in liquid culture. There are two possible reasons that could explain the difference between the small (<15 nm) and large nanoparticles. Firstly, the mobility of nanoparticles might be strictly related to the size of the nanoparticles. Small particles might be able to penetrate through the agar, but larger ones may not. Secondly, it is believed that the release of silver ions is one of the main mechanisms of antibacterial activity of AgNPs. The release of silver ions from large nanoparticles is slower than smaller ones due to the larger specific surface area of the latter.[235]

Due to the limited applicability of disc diffusion method for nanoparticles, the well diffusion method has also been commonly used to test the antibacterial efficacy of metal nanoparticles. It is a modification of the disk diffusion method, and the procedure is similar but instead of using an impregnated disk, a well is cut out of the agar plate and the liquid antibacterial agent is placed directly into the well. The presence of liquid may facilitate the release of ions and therefore could be applicable to a wider range of particle sizes. Dong *et al*.[226] used the well diffusion method to test the antibacterial performance of nano-silver against *E. coli*. AgNPs with average sizes of 4 nm, 21 nm, and 40 nm, and silver nano-prisms (triangular plates) with a wide size distribution (from 25 nm to 400 nm) were tested. In this study, even the largest AgNPs (40 nm) formed a clear ZoI. Surprisingly, it was found that the ZoI of silver nano-prisms was even larger than the smallest AgNPs (4 nm). From the perspective of size, the nano-prisms would not be able to diffuse better in the agar than the smallest AgNPs. Therefore, the increased antibacterial efficacy might have resulted from the distinct crystal structure and altered ability to release silver ions. However, as discussed in Section 1.4, different nanoparticles have different antimicrobial modes of action. For those nanoparticles whose main mechanism is not

the release of toxic ions but requiring direct contact with the cells, the agar diffusion method may not be suitable. Moreover, this method cannot distinguish whether the effect is bactericidal or bacteriostatic.

The monitoring of turbidity/optical density is a commonly used method to estimate the density and proliferation of planktonic bacterial cells. Bacterial cells block and scatter light just like other particles do. Within a suitable range, the absorbance reading is proportional to the number of cells present in the suspension. The advantage of this technique is the simplicity. Once a standard curve of optical density – cell density is established, the bacterial viability can be estimated by measuring the turbidity of the test suspension. The method is also used to determine the effect of nanoparticles on the bacterial growth. However, one complication associated with this technique is that nanoparticles also contribute to the optical density reading of the sample which may interfere with the optical density reading. Moreover, when in contact with the culture media, biomolecules and bacterial cells, the nanoparticles may agglomerate/aggregate and the optical properties of the nanoparticles may change significantly. The change is not necessarily the same as when nanoparticles are suspended in culture media alone and thus it is difficult to prepare a control of the turbidity contributed by the nanoparticles. Therefore, the accuracy of this method is questionable.[224]

The viability of bacteria after exposure to nanoparticles can also be determined by spreading the bacterial suspension on agar plates and performing colony counts. When comparing the viable counts from control groups incubated without nanoparticles, the reduction rate of colony forming units (CFU) can be determined. This method is cheap and easy to perform; however, it is also time consuming and labour-intensive. One intrinsic limitation of this method is that a colony on an agar plate may have arisen from a single bacterium or from a large cluster of many bacteria.[224] Additionally, the present of viable but non-culturable (VBNC) cells may increase the uncertainty of the results. VBNC cells have intact membranes and genomic materials, but they are in a state of very low metabolic activity and cannot grow on standard media. Some bacterial cells can enter this state when under stress, including exposure to an antimicrobial agent.[236] When assessing the performance of an antimicrobial agent using a plate count method, the inactivation or removal of the

agent from the suspension is normally carried out by adding an inactivation agent or by filtration, to ensure that there is no carryover of the antimicrobial agent onto the agar plate which could impede the growth of the test microorganism, so that the killing efficacy can be determined. However, there is no effective method to inactivate or remove the nanoparticles from the mixture so far. It is possible that the nanoparticles adhere to the bacteria and thus continuously inhibit the growth of the bacteria preventing them from developing into a visible colony on the agar plates. This can increase the uncertainty of the experimental results.

A variety of colorimetric or fluorometric assays estimate the cell viability through the measurement of a biochemical marker that is related to cell metabolic activity. Examples of this type of assay include tetrazolium salt-based assay (e.g. MTT and XTT), resazurin salt-based assay (e.g. AlamarBlue) and ATP assay. These assays are easy to use and are applicable for both planktonic cells and cells attached to a surface. However, the cell metabolic activity may not always accurately represent the cell viability. For example, as discussed above, bacterial cells may enter a state of low metabolism but remain viable under stress; bacterial cells in a biofilm may also have reduced metabolic activity, resulting in artificially low numbers of viable cells.[237] Similar to the optical density reading method, the presence of NPs in the suspension may also cause interference of the colorimetric reading. Another dye-based assay is Live/Dead staining, which can offer better accuracy and more detailed analysis when determining the cell viability. The assay uses a combination of two fluorescent nucleic acid dyes, of which one (SYTO 9) stains all cells living or dead, and the other (propidium iodide) stains dead or dying cells with compromised membranes. When used together, red propidium iodide causes reduced fluorescence of green SYTO 9 when both dyes are present such that the dead cells would present as red in colour. The assay results can be analysed by fluorescent plate reader or flow cytometry or visualised by confocal microscopy. The limitations of Live/Dead staining include the need of special equipment and costly reagents.

When assessing the performance of an antimicrobial agent, in particular antimicrobial nanoparticles, the methods should be carefully selected according to the characteristics and applications of the test material. More than one assay may be required to avoid skewed results. Bankier *et al.*[234] compared three different methods, including plate count, flow cytometry Live/Dead staining assay and quantitative

polymerase chain reaction (qPCR), to evaluate the antibacterial performance of metal NPs in suspension. The results indicated that the plate count method and Live/Dead staining assay provided consistent results; however, the viability qPCR analysis seemed to be hindered by the NPs as they bind to the DNA and interfere with the qPCR amplification. An increasing number of studies have also generated confounding or even conflicting data when evaluating the toxicity of NPs. The unique physicochemical properties of nanoparticles may interfere with assay components, biomarkers or detection systems, introducing artefacts into the studies. Therefore, it is of value to evaluate the antimicrobial property of nanoparticles using more than one method to avoid distorting and misleading results.

In this chapter, both qualitative and quantitative methods were employed to study the antibacterial performance of the nanoparticles prepared in Chapter 2. It is believed that the surface charge and the presence of polymer or other capping agents can significantly influence the activity of nanoparticles.[170] For selenium nanoparticles, the antibacterial ability remains controversial. For example, some studies have suggested that the SeNPs showed no effect on Gram-negative strains such as *E. coli*,[122,133] while other reports showed good antibacterial effect of the SeNPs on *E. coli*.[171,204] This might be due to the different surface properties of the SeNPs. Guisbiers *et al.*[171] prepared bare SeNPs using a laser ablation method and reported inhibition of *E. coli* by the bare SeNPs; the authors also hypothesised that the seemingly conflicting results were due to the presence of chemical contaminants (e.g. polymer or surfactant stabiliser) on the SeNPs. The influences of stabilising agents on the antimicrobial performance of SeNPs had not been systematically studied by the time this work was conducted. In the previous chapter, attempts were made to prepare bare SeNPs using KI as the stabiliser, but the bare SeNPs were unstable and went through rapid, irreversible aggregation. Sufficient colloidal bare SeNPs were not able to be obtained. This is probably why the antibacterial activity of bare SeNPs has rarely been reported. It is worth noting that in the report of Guisbiers and colleagues', the concentrations of SeNPs they used were also very low (up to 50 ppm).[171]

SeNPs with different capping agents, including PVA, polysorbate 20, and chitosan, were used to study the influence of surface properties of nanoparticles on their antibacterial performance. Reports on PVA-SeNPs[122] and PS20-SeNPs[133] showed

that these two types of SeNPs did not inhibit the growth of *E. coli*, while they significantly inhibited the growth of *S. aureus*, exhibiting species-dependent effects. Several methods and concentrations from the two reports were utilised in this chapter to assess the antibacterial activity of the SeNPs to determine whether the negative results from the literature could be due to the low concentrations tested or unsuitable assessment methods used. Chitosan was employed to prepare selenium nanoparticles with a positive surface charge and to enhance the interaction between the nanoparticles and bacterial cells. It has been reported that chitosan and SeNPs exhibited synergistic effects against *Candida albicans*.[238]

The research questions are:

(1) Do SeNPs have antibacterial effects towards Gram-negative bacteria such as *E. coli*?
(2) If SeNPs do have antibacterial effects towards *E. coli*, what may have led to the negative results reported in the literature?
(3) Do the surface conditions, including a coating of polymer or surfactant, and surface charge influence the antibacterial activity of SeNPs significantly?

Since particle size is known to be another important factor that can influence the antibacterial activity of nanoparticles, the sizes of SeNPs capped with different agents were controlled to be in a similar range (40 – 50 nm). In addition, AgNPs were studied as a well-established antimicrobial nanoparticle model. Four types of AgNPs were employed, with two sizes (approximately 35 nm and 60 nm) and two surface conditions (bare TSC-AgNPs with strong negative charge and chitosan-coated AgNPs with positive charge). It has been reported that the positive surface charge imparted by cationic polymer can improve the antimicrobial of the nanoparticles.[169,170] However, in most of the published studies, when studying the influence of surface conditions on the antibacterial performance of AgNPs, the nanoparticles were prepared in the presence of different stabilisers, which usually resulted in AgNPs with different surface conditions as well as slightly different sizes and shapes. Here in this study, the pre-prepared bare TSC-AgNPs as described in Chapter 2 were coated with chitosan and their performance was compared. In this way, it was made sure that the presence of chitosan was the only difference between the two types of the nanoparticles.

3.2 Materials

3.2.1 Preparation of nanoparticle suspensions

Bare TSC-AgNPs prepared at pH 10.2 and 9.5 with quick drop addition of $AgNO_3$, as described in Section 2.3.1, were chosen to prepare chitosan-coated AgNPs. A 19 mL aliquot of the bare TSC-AgNPs suspension after ripening was added to 1 mL of 0.5% chitosan solution drop by drop with vigorous stirring, resulting in AgNPs capped and dispersed in 0.025% chitosan solution. The product was named CS-AgNPs. All types of chosen nanoparticles (listed in Table 3.2) were washed and sterilised prior to being used in biological experiments. Briefly, the as-prepared nanoparticle colloids were filtered through sterile cellulose acetate syringe filters (0.2 μm, Sartorius), after which the nanoparticles were handled aseptically. Centrifugation was used to wash the nanoparticles as described in Section 2.3.2 (Table 3.2), as well as to concentrate nanoparticles by resuspending the nanoparticles in smaller volumes. After washing, the concentration of nanoparticles was determined by Microwave Plasma Atomic Emission Spectroscopy (4100 MP-AES, Agilent), which uses a microwave-induced nitrogen plasma. The samples were digested using concentrated nitric acid by mixing washed nanoparticles with concentrated HNO_3 in a glass vial. The vial was kept at 80 °C in an oven for 1 h and left at room temperature overnight, after which the colour of the nanoparticle suspension disappeared. The solution was then diluted in volumetric flasks and the concentration of Ag or Se was analysed by MP-AES. The washed nanoparticles were then adjusted to desired concentrations accordingly with sterile RO water (15 mΩ), and then stored at 4 °C. The characteristics of the nanoparticles used in biological experiments are summarised in Table 3.2.

Table 3.2 Nanoparticles used for antibacterial tests

Nanoparticles	Size by TEM (nm)	Size by DLS (nm)	Zeta potential (mV)
TSC-AgNPs (35 nm)	33 ± 7	48 ± 5	-47.6 ± 2.1
CS-AgNPs (35 nm)	33 ± 7	100 ± 4	+13.4 ± 1.3
TSC-AgNPs (60 nm)	59 ± 15	85 ± 4	-46.8 ± 0.9
CS-AgNPs (60 nm)	59 ± 15	128 ± 6	+14.2 ± 0.7
PVA-SeNPs	45 ± 6	119 ± 7	-8.2 ± 2.5
PS20-SeNPs	48 ± 5	56 ± 1	-24.6 ± 4.6
CS-SeNPs	50 ± 9	150 ± 4	+18.4 ± 5.6

* Data represented as mean ± SD.

3.2.2 Bacterial culture media and diluent

Nutrient Agar (NA, Oxoid), Nutrient Broth (NB, Oxoid), Tryptone Soya Agar (TSA, Oxoid), Tryptone Soya Broth (TSB, Oxoid), and Mueller-Hinton Agar (MHA, Oxoid) were prepared according to the manufacturer's instructions with RO water. Normal saline solution (0.85% NaCl) was prepared by dissolving NaCl (Thermo Fisher Scientific) in RO water. Phosphate buffered saline (PBS) tablets (Oxoid) were used to prepare the buffered saline solution according to the manufacturer's instruction. All the culture media, and saline solution, were sterilised by autoclaving at 121°C for 15 minutes.

3.2.3 Bacterial strains

Gram-positive bacteria *Staphylococcus aureus* (NCTC 10788), *Streptococcus pyogenes* (NCIMB 13285), and *Enterococcus faecalis* (NCIMB 13280); Gram-negative bacteria *Escherichia coli* (NCTC 10418), *Pseudomonas aeruginosa* (NCTC 10662), and *Klebsiella pneumoniae* (NCTC 11228) were obtained from the University of Brighton culture collection and used for testing of antibacterial activities of nanoparticles. Stock cultures of all microorganisms were stored in TSB containing 10% (v/v) glycerol at -20°C. Subcultures were prepared from frozen isolates by streaking onto fresh NA plates. All streaked plates were incubated at 37°C for 24 hours and stored in a refrigerator at 4°C prior to use. These streaked plates were replaced every four weeks, with fresh cultures being made before each experiment.

3.3 Methods

3.3.1 Antibacterial assessment of nanoparticles by direct contact on agar plates

The method for the preparation of the bacterial inoculum was adapted from the European Committee on Antimicrobial Susceptibility Testing (EUCAST) antimicrobial susceptibility methodology[225] and British Standard BS EN 1040:2005 (Chemical disinfectants and antiseptics — Quantitative suspension test for the evaluation of basic bactericidal activity of chemical disinfectants and antiseptics).[239] All of the six bacterial strains mentioned above were used in this method. Individual bacterial species were inoculated onto TSA plates by streak plating and incubated overnight at 37°C, from which a few individual colonies were removed aseptically and suspended in 2 mL sterile PBS in a glass vial containing 0.2 g glass beads (diameter 2 mm). The vial was shaken for a few minutes until the bacterial cells were thoroughly suspended. The optical density at 600 nm (OD600) of the bacterial suspension was measured using a spectrophotometer (Jenway 6305) and adjusted to approximately 0.1 by diluting with PBS. The bacterial suspension was then inoculated evenly onto MHA (or MHA supplemented with 5% mechanically

defibrinated horse blood for fastidious *S. pyogenes*) using a sterile cotton swab. Within 15 mins after inoculation, nanoparticle suspensions with a silver or selenium concentration of 200 ppm were dropped onto the surface. A drop of 25 µL could make a circle with a diameter of approximately 1 cm. The agar plates were left at room temperature for about 10 mins to allow the liquid to absorb and then incubated at 37°C for 24 h.

For the well diffusion method, holes (6.5 mm) were made on MHA using a sterile glass Pasteur pipette, after which the bacterial suspension was inoculated onto the agar surface as described above. Nanoparticle suspensions (50 µL, 200 ppm) were then added to the wells and agar plates were incubated at 37°C for 24 h before being examined. A spread plate method adapted from Pal *et al.*[168] was also carried out by spreading nanoparticle suspensions (50 µL) using a L-shaped spreader onto inoculated agar surface (NA and MHA).

3.3.2 Antibacterial assessment of nanoparticles using a viable count method

The viable count method was modified from a report by Rasool *et al.*[231] *E. coli* and *S. aureus* were used as representatives of Gram-negative and Gram-positive bacteria respectively. Bacterial suspensions in PBS were prepared as described in Section 3.3.1.

To estimate the cell density in liquid culture, optical density – bacterial concentration standard curves were constructed for *S. aureus* or *E. coli.* An overnight culture was prepared by inoculating a colony of *S. aureus* or *E. coli* from stock plates into TSB (10 mL) and incubating at 37 °C and 120 rpm. Subsequently, the cultures were washed by centrifugation (5000 g, 10 min) twice and the pellet was resuspended thoroughly in 5 mL of sterile PBS. The OD600 of the bacterial suspension was adjusted to approximately 1. This suspension was designated as 100%, and dilutions to 80%, 60%, 40% and 20% were prepared using the PBS as diluent. The OD600 of each dilution was measured. Viable counts were performed using the 100% suspension by serial dilution and spread plates on NA in triplicate. The process was repeated twice more. The plate colonies were counted after 24 h incubation at 37 °C.

A calibration plot of optical density versus viable count was constructed for *S. aureus* and *E. coli* respectively (shown in Appendix B).

The density of bacteria was adjusted to approximately $1\times10^7 – 5\times10^7$ CFU/ml using the optical density standard curve. Nanoparticles at varying concentrations were mixed with bacterial suspensions in 96-well plates. To achieve this, 100 μL of nanoparticle suspension (200 ppm) was added into each well by doubling dilution in RO water, and subsequently 100 μL bacterial suspension was added to each well. The final concentrations of nanoparticles were 100, 50, and 25 ppm. Bacterial suspension mixed with sterile PBS without nanoparticles was used as a negative control. The 96-well plate was incubated at 37°C on an orbital shaker at 150 rpm for 4 h. The suspensions were then plated onto TSA plates following 10-fold serial dilution in PBS, and colonies were counted after 24h incubation at 37°C. The experiments were repeated for 3 times on different individual occasions.

The reduction rate was calculated by using the viable count of the control group, incubated with sterile PBS and without nanoparticles, as 100% viable. The following equation was used:

$$\textbf{Relative bacterial reduction}\ (\%) = \left[\mathbf{1} - \frac{\mathbf{Nt}}{\mathbf{Nc}}\right] \times \mathbf{100} \qquad \textbf{Equation 3.1}$$

where Nt is the bacterial colony count of samples treated with nanoparticles, and Nc is bacterial colony count of control samples.

3.4 Results and Discussion

3.4.1 Qualitative methods for antibacterial assessment

S. aureus and *E. coli* were chosen as the representatives of Gram-positive and Gram-negative bacteria respectively as they are among the most common bacteria responsible for healthcare-associated infections and, moreover, there are many published reports on the antibacterial evaluation of AgNPs and SeNPs against these two species, enabling a comparison with the results from this study.

Initially, the antibacterial activities of the nanoparticles were assessed qualitatively. The well diffusion method, as discussed in Section 3.1, was attempted, but the nanoparticles tested did not form any zone of inhibition. It could clearly be seen that the particles deposited on the inner wall of the wells. Subsequently, a spread plate method adopted from Pal *et al*.[168] was used. However, no noticeable effect was found for most of the samples. The only significant inhibition effect was found on *S. aureus* treated with SeNPs of all the three types (PVA-SeNPs, PS20-SeNPs and CS-SeNPs). Figure 3.1 shows *E. coli* and *S. aureus* (from a suspension of around 10^6 – 10^7 CFU/mL) grown on TSA plates and treated with PVA-SeNPs (500 ppm, 50 µL). The selenium nanoparticles showed strong inhibition towards *S. aureus*, while all the other groups tested, including PVA-SeNPs and PS20-SeNPs against *E. coli*, as well as TSC-AgNPs (60 nm) against *E. coli* and *S. aureus*, exhibited no noticeable difference to the untreated controls.

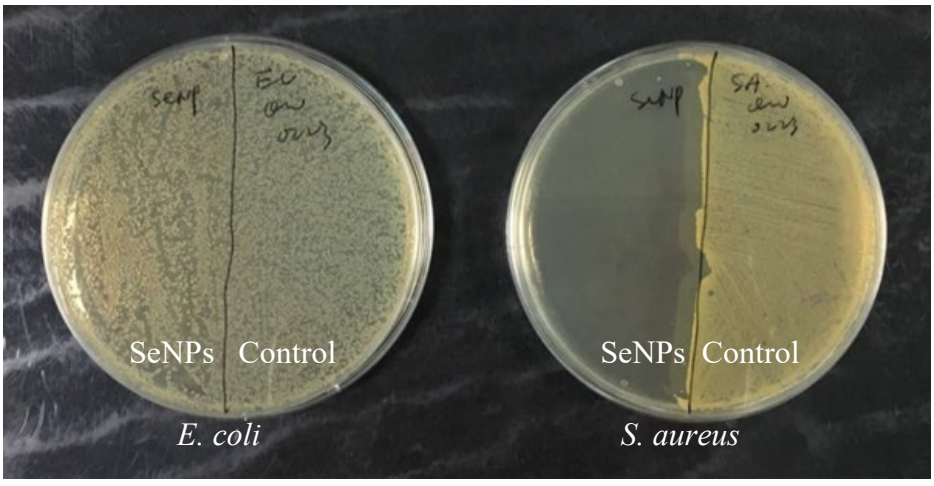

Figure 3.1 *E. coli* and *S. aureus* treated with PVA-SeNPs.

Original in colour

The antibacterial performance of SeNPs reported in the literature is limited and controversial. It is possible that the activity is selective. However, AgNPs, as the most extensively studied antibacterial nanoparticles, have demonstrated good antibacterial activity with agar diffusion methods in many published reports.[163,168,169,226] For example, in the study from which this spread plate method was adapted, Pal *et al*.[168] reported strong inhibition of *E. coli* by AgNPs using this method on NA plates. Considering the fact that the ingredients in the culture media could possibly influence the efficacy of AgNPs, different media, including NA and MHA plates, were also trialled. NA is often used for the antibacterial study of AgNPs probably because it contains little protein that can interfere with the activity of silver; MHA is also often used as it is the recommended medium by microbiology standards.[225] However, the use of different culture media did not make a significant difference.

Since the effects of SeNPs on *E. coli* and *S. aureus* were so distinct, and this difference agreed with some of the published reports, it was hypothesised that there could be a Gram-negative/Gram-positive dependent effect. Therefore, a greater range of bacterial strains were tested, including three Gram-positive bacteria *S. aureus*, *S. pyogenes*, and *E. faecalis*; and three Gram-negative bacteria *E. coli*, *P. aeruginosa*, and *K. pneumoniae*.

At the initial stage of the antibacterial evaluation, an important factor, the size of the silver nanoparticles, was overlooked. Only TSC-AgNPs (60 nm) were used in the preliminary spread plate test (as discussed at the beginning of this section). The particle size is a critical factor that influences the results of the agar diffusion method. In the literature, most of the chemically prepared AgNPs that successfully showed inhibition directly on an agar surface had average sizes of about 40 nm or less.[163,168,169,226] Another possible reason for the negative results observed here might be due to the insufficient ratio between the number of nanoparticles and bacterial cells. Therefore, a method in which the nanoparticle suspensions were directly dropped onto an inoculated agar surface was used. In this way, the contact between bacterial cells and nanoparticles, as well as the number of nanoparticles presented, could be ensured. With this new method, some clear inhibition zones were obtained

from AgNPs (60 nm), but the effect was still not as pronounced as expected with some of the strains tested. Subsequently, the test was repeated with AgNPs of smaller size (35 nm), after recognising the critical influence particle size can have on the test outcome.

In the new direct drop method, five different zone appearances were observed in the presence of the NPs (Figure 3.2): (1) the best outcome, the zone (approximately 1 cm) on which the drop of suspension was set on was totally clear, and a 1-2 mm diffusion ring was also found; (2) for many other samples, the 1 cm zone was clear, but no diffusion was observed; (3) there are also some zones in which the density of bacterial colonies was significantly reduced but some individual tiny colonies could still be seen; (4) the bacteria in the zone were still confluent, but the thickness of layer was apparently reduced, indicating some very weak effect, if there was any; and (5) no effect was shown at all. The five different results described above are labelled as 1-5 respectively. The results are summarised in Table 3.3 and Table 3.4, and some of the representative images of the effects are shown in Figure 3.2.

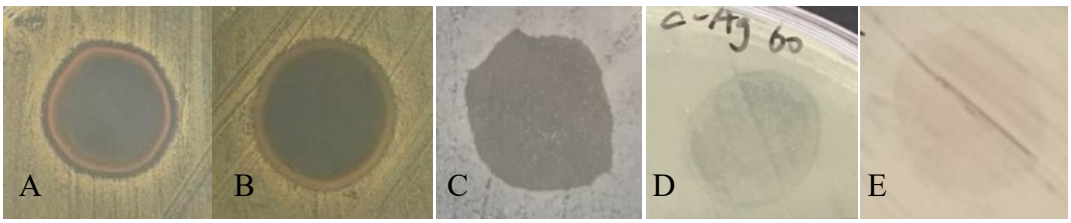

Figure 3.2 Images of the inhibition effects corresponding to Table 3.2: (A) inhibition level 1 - *S. aureus* treated with PS20-SeNPs; (B) inhibition level 2 - *S. aureus* treated with PVA-SeNPs; (C) inhibition level 3 - *E. coli* treated with CS-AgNPs (60); (D) inhibition level 4 - *P. aeruginosa* treated with CS-AgNPs (60); and (E) inhibition level 5 - *K. pneumoniae* treated with CS-SeNPs.

Table 3.3 Antibacterial effect of AgNPs directly dropped on agar surface

Bacterial strain	Antibacterial effect of nanoparticles			
	TSC-AgNPs (35 nm)	CS-AgNPs (35 nm)	TSC-AgNPs (60 nm)	CS-AgNPs (60 nm)
S. aureus	2	1	4	4
E. faecalis	5	5	5	5
S. pyogenes	5	5	5	5
E. coli	2	1	3	3
P. aeruginosa	4	3	4	4
K. pneumoniae	2	1	2	2

Table 3.4 Antibacterial effect of SeNPs directly dropped on agar surface

Bacterial strain	Antibacterial effect of nanoparticles		
	PVA-SeNPs	PS20-SeNPs	CS-SeNPs
S. aureus	2	1	2
E. faecalis	5	5	4
S. pyogenes	3	3	3
E. coli	4	4	4
P. aeruginosa	5	5	5
K. pneumoniae	5	5	5

*1 = best antibacterial effect, forming a clear inhibition zone as well as a diffusion ring; 2= forming a clear inhibition zone but no diffusion; 3= forming a zone of inhibition but individual colonies can still be seen; 4= forming a zone with thinner layer of bacteria but still confluent; 5 = no antibacterial effect.

Overall, it can be seen from Table 3.3 that for AgNPs, CS- AgNPs demonstrated better inhibition than the bare TSC-AgNPs with this method; small AgNPs (35 nm) showed better results than large AgNPs (60 nm); AgNPs showed better inhibition on Gram-negative strains than Gram-positive strains. These findings are in accordance with many other reports in the literature.[101,163,170,240] The size-dependent effect has been discussed in Section 1.4.4 and earlier in this section. It is believed that the different cell wall structures of Gram-positive and Gram-negative bacteria have different abilities to defend the effects of silver ions.[36,38] Due to the thick layer of peptidoglycan, it is more difficult for Ag^+ ions to penetrate into the Gram-positive bacterial cell wall. On the other hand, although Gram-negative bacteria have a double-layered cell wall structure and are generally more resistant to antibiotic drugs, the relatively thin cell wall is not sufficient to defend against Ag^+ ions which are much smaller than the drugs.[36] Moreover, nanoparticles can cause the deconstruction of bacterial cell wall, and the relatively thick cell wall of Gram-positive bacteria may be less susceptible to this and more effective at defending such damage from the nanoparticles.[241]

Selenium nanoparticles on the other hand showed different antibacterial activities (Table 3.4). The SeNPs with different capping agents did not show obviously different results with this method. It seems that *S. aureus* was particularly sensitive to SeNPs; however, SeNPs were not equally effective against all Gram-positive strains and the antibacterial effect on *E. faecalis* was limited. The inhibition of Gram-negative strains was minimal. The results are in accordance with the reports from Tran *et al*.[122] and Bartůněk *et al*.,[133] from which the synthesis of PVA-SeNPs and PS20-SeNPs were adapted respectively. Bartůněk *et al.*[133] reported diffusion rings when PS20-SeNPs (43 nm) were tested against *Staphylococcus epidermidis* and *S. aureus* at Se concentration of as low as 2 ppm, indicating strong inhibition effects of SeNPs against the *Staphylococcus* species; no zone of inhibition was observed on *E. coli* treated with the SeNPs at 2 ppm. In 2019, Boroumand *et al.*[242] reported a study very similar to that that was conducted in this chapter; the authors prepared PVA-SeNPs and CS-SeNPs using ascorbic acid as the reducing agent and tested the antibacterial performance of the nanoparticles using disc diffusion and microdilution MIC determination methods. Interestingly, they were able to determine the zone of inhibition and MIC of the SeNPs against both *E. coli* and *S.*

aureus. However, the authors did not report the amounts of reactants used in the preparation of the nanoparticles, and they did not mention the washing of the nanoparticles after the synthesis to remove the leftover reactants either, which might have interfered with the antibacterial tests. Sodium selenite, as the precursor of the nanoparticles, is also known to be toxic to bacteria,[204] and as an oxyanion, the selenite can diffuse in the agar to form a zone of inhibition.

In the literature, many of the SeNPs that showed inhibition towards Gram-negative bacteria, such as *E. coli* and *P. aeruginosa,* were biogenic.[123,135,136,204] It is possible that the biomolecules resulting from the biosynthesis process on the surface of the SeNPs helped with the antibacterial activities of the nanoparticles. Estavam *et al*.[123] used water and ethanol to wash the biogenic SeNPs respectively. The particles still had bacterial proteins attached to the surface after being washed thrice with ethanol, but the presence was significantly reduced compared with particles washed with water. The SeNPs washed with water seemed to be more active in the antibacterial tests, indicating that the bacterial proteins attached to the SeNPs played an important role in the antibacterial activities. They also used the proteins separated from the process as a control, yet no significant inhibition was observed at concentrations tested. This suggested that the bacterial proteins remaining on the particle surface were not toxic to the tested bacteria strain, but the presence helped with the antibacterial activities of the SeNPs. Apart from biogenic SeNPs, other studies reported antibacterial effects of SeNPs chemically synthesised *in situ* on different surfaces towards Gram-negative strains.[137,138] Hegerova *et al.*[243] reported a study on SeNPs with Na_2SeO_3, carboxymethyl cellulose, and mercaptopropionic acid as the selenium precursor, stabiliser, and reducing agent, respectively. The authors studied the antimicrobial activity of the SeNPs towards 69 clinically isolated bacterial strains using a disc diffusion method and found that the SeNPs formed ZoIs of at least 5 mm with all of the strains tested. It was found that the antimicrobial performance of the SeNPs varied between different strains, but overall, the antimicrobial activity towards Gram-positive strains was higher than towards Gram-negative strains. The data are of great significance as it was the first time that the antimicrobial activity of SeNPs towards so many clinically isolated bacterial strains was investigated, and the study showed promising results. However, unfortunately, the authors did not describe any washing steps of the prepared colloidal SeNPs either. If no washing was

performed, the presence of unfinished reactants might have contributed to the results as both Na_2SeO_3 and mercaptopropionic acid[244] can inhibit the growth of bacteria. If the effect of the reactant residues was negligent, the ZoIs created by the SeNPs might be due to the enhanced interactions between the bacterial cells and the presence of thiol containing compound mercaptopropionic acid on the surface of the SeNPs.[245]

Moreover, the interaction between nanoparticles and bacterial cells can be different when in suspension and on solid surfaces. Additionally, when fixed on surfaces, the instability and aggregation issues may be removed. Therefore, although the SeNPs did not show significant inhibition towards all the strains tested in this qualitative test, it is still worth investigating the possibility of employing SeNPs for antibacterial functionalisation of textile materials.

3.4.2 Quantitative Methods for the Antibacterial Assessment of Nanoparticles

For quantitative methods, the initial attempts started with the conventional broth dilution method which is often used to determine the minimal inhibition concentration (MIC) of drugs. However, although SeNPs showed excellent antibacterial effect towards *S. aureus* on the agar plates, the determination of MIC was not successful. The concentration was raised to up to 1000 ppm by concentrating through centrifugation, but whether the bacterial activity was fully inhibited was still not clear. It can be seen that due to the interaction between nanoparticles and bacteria, the selenium aggregated in the Nutrient Broth (Figure 3.3); and *E. coli* and *S. aureus* apparently had different interactions with the SeNPs. The suspension containing *E. coli* was still relatively homogeneous after overnight incubation, while some red precipitates were formed with the presence of *S. aureus*. Moreover, the precipitations formed were also different with different capping agents. The precipitation of PVA-SeNPs was a loose red solid at the corner of the wells, while the PS20-SeNPs formed a dense red pellet in the centre of the wells. The plates were not shaken during incubation, so the precipitation patterns were not the result of shaking. This also indicated that the capping agents had a significant influence on the interaction between the nanoparticles and the bacteria cells. According to this

method, the results above (Figure 3.4) suggest an MIC of in excess of 1000 ppm for the SeNPs tested.

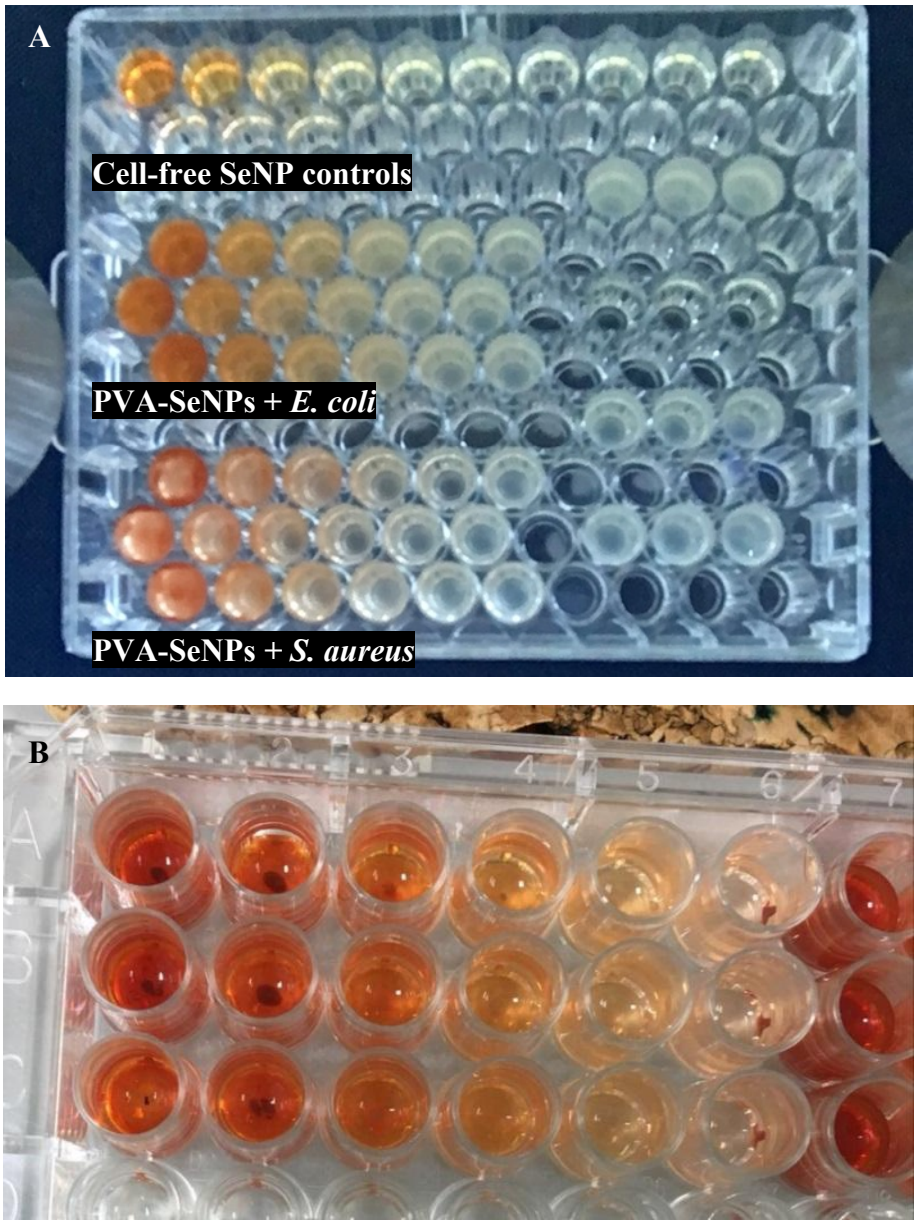

Figure 3.3 Suspensions containing bacteria and SeNPs after incubation at 37 °C overnight in NB. (A) *E. coli* and *S. aureus* treated with PVA-SeNPs; highest concentration of SeNPs was 250 ppm, with a dilution factor of 2; (B) PS20-SeNPs with *S. aureus*; highest concentration from the left-hand side was 1000 ppm.

Original in colour

Guisbiers *et al*.[171] prepared bare SeNPs using a laser ablation method and determined the MIC of SeNPs against both *E. coli* and *S. aureus*. However, the MIC values they reported were predicted by plotting a concentration-inhibition rate curve, rather than finding the actual MIC by experiments demonstrating total inhibition. The author did not mention the reason why it was performed this way, but it is speculated that it may be due to the instability of the bare SeNPs at higher concentrations. Most of the studies were testing only the inhibition of growth by comparing SeNPs-treated bacteria with controls without nanoparticles. Considering the proposed future application where the SeNPs will be immobilised on a fibre surface, the determination of MIC may not be very relevant as the concentration (μg/mL) of the nanoparticles in suspension is not applicable on solid surface.

Consequently, the viable count method was adopted to assess the antibacterial performance of the nanoparticles quantitatively. Briefly, the nanoparticle suspension was mixed with bacterial suspension in PBS, and after a period of incubation, the bacteria were plated onto agar plates for colony enumeration. When mixing the nanoparticles and bacterial suspensions, it was observed that bare TSC-AgNPs immediately changed colour from yellow to grey, indicating the agglomeration of the nanoparticles. The change did not happen as quickly for CS-AgNPs, but grey precipitation was also found after 4h incubation. The immediate agglomeration of bare TSC-AgNPs might be a result of the disturbed electrostatic forces between nanoparticles when mixing with the buffer. Since the bare TSC-AgNPs were stabilised only by electrostatic force without any additional steric hindrance, the agglomeration happened instantly. Additionally, the interaction between nanoparticles and bacterial cells as well as the biomolecules released from the cells can also lead to agglomeration/aggregation of nanoparticles in suspension. The CS-AgNPs did not change colour immediately as the nanoparticles were protected by the chitosan polymer. Even though the electrostatic stabilisation could be disturbed by the buffer, the steric hindrance provided by chitosan still kept the nanoparticles separated from each other. However, as the interaction between nanoparticles and bacteria took place gradually, the nanoparticles eventually aggregated and precipitated. The relative reductions in the viability of bacteria treated with AgNPs are shown in Figure 3.4.

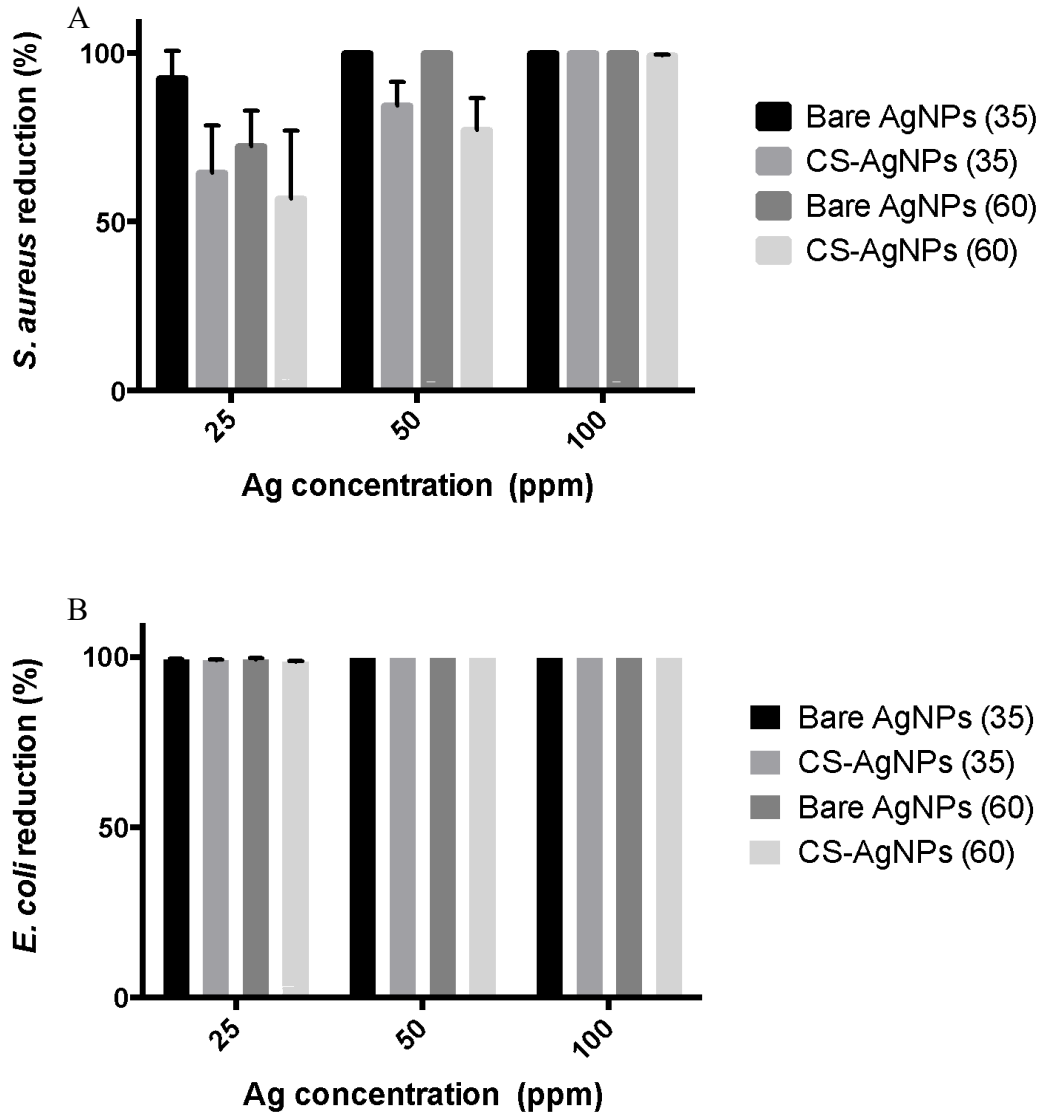

Figure 3.4 Relative reduction in viability of (A) *S. aureus* and (B) *E. coli* treated with different AgNPs in aqueous suspension. Data presented as mean ± SD (n=3). Bars without an error bar means the reduction was higher than 99.5%.

In Figure 3.4, some of the sample groups do not have error bars, indicating that the viable count was below detection limitation. Different countable ranges are recommended by different standards. For example, the American Section of the International Association for Testing Materials (ASTM) provides countable ranges of 20 – 200 CFU/plate; the US Food and Drug Administration recommends 25 – 250 CFU/plate as a countable range. It has been shown that when the upper limit is exceeded, the colonies begin to compete for space and nutrients, skewing the count.

When the CFU/plate count drops below the countable range, the error as a percent of the mean can increase rapidly. When doing the viable count, in some groups, all of the counts from plates of different dilution factors dropped below the countable range. In some cases, the 10^{-1} plate even had fewer colonies than the 10^{-2} plates. An example of this condition could be that the counts for 10^{-1}, 10^{-2} and10^{-3} plates were 10, 15, and 1 respectively. In normal conditions, the count from 10^{-1} dilution should be approximately 10 times of the count from 10^{-2} dilution, but here it was even lower. It might be because a considerable amount of silver (2.5 – 10 ppm) was still in contact with the bacteria on the agar plates after the 10^{-1} dilution, and it continuously inhibited the bacteria to grow into colonies. Such a situation was not found when the dilution factor was higher than 10^{2}. Consequently, it was assumed that the counts from the 10^{-1} plates with silver concentration of 2.5 – 10 ppm were unreliable and were not suitable for further calculation; on the plates of higher dilutions factors, the effect of silver carried over was limited and could be neglected. Since the initial concentration of the bacteria was around 10^{7} CFU/mL, a count from the 10^{-2} plate that was lower than 20 is reported as ">99.5%" here, and in Figure 3.4, the ">99.5%" sample groups do not have error bars.

From Figure 3.4, it can be seen that the AgNPs almost eliminated the *E. coli* at all the concentrations tested, while it showed some size- and dose-dependent effect on *S. aureus*. All the AgNPs tested showed over 99% *S. aureus* reduction at 100 ppm. The bare TSC-AgNPs (35) demonstrated the best efficacy, with still around 90% reduction at the lowest concentration tested (25 ppm); while for the CS-AgNP (60), the reduction dropped to around 50% at 25 ppm. These results demonstrated that the AgNPs tested had better antibacterial effects on *E. coli* than on *S. aureus,* which is in accordance with the findings discussed previously (Section 3.4.1) and also with the literature.[101,163,170,240] One noticeable finding here is that the bare TSC-AgNPs showed better antibacterial effects than the CS-AgNPs against *S. aureus*, which is different from the results of the previous section where CS-AgNPs exhibited a diffusing ring of inhibition (Table 3.3). It has been shown in the literature that positive surface charge can be used to enhance the interaction between NPs and bacterial cells, resulting in higher antibacterial properties of AgNPs.[240,246] The lower antibacterial activity of CS-AgNPs found in this test might be a result of the delayed or prolonged release of silver ions due to presence of chitosan on the nanoparticle

surface. The polymer coating could hinder the release of silver ions, so after the relatively short exposure time (4 hours), the CS-AgNPs showed a reduced antibacterial activity compared with the bare TSC-AgNPs. Similar results were reported by Wu *et al*.[247] In their study, the positively charged AgNPs coated with amine-silica were found to have released the least amount of Ag^+ ions and showed the lowest antimicrobial activity. The authors explained this phenomenon by the more significant Ag^+ ion release from other types of AgNPs with neutral or negative surface charge, which predominantly determined the antimicrobial activity of the colloidal AgNPs. Similarly, in this chapter, when the AgNPs were mixed with bacterial cells in PBS, the quick release of Ag^+ ion from the bare TSC-AgNPs might have determined the antimicrobial performance. The Ag dissolution dynamic was different from on agar surface where the positively charge CS-AgNPs showed higher antimicrobial activity.

The relative reductions in bacterial viability effected by the SeNPs are shown in Figure 3.5. It can be seen that all SeNPs showed excellent antibacterial activity against *S. aureus*, while only CS-SeNPs reduced the viability of *E. coli* for over 50%. In the case of *S. aureus*, CS-SeNPs did not show significant dose-dependent behaviour. Even with the lowest concentration tested (25 ppm), the reduction was higher than 95%. PVA-SeNPs and PS20-SeNPs exhibited variable dose-dependent effects. At 25 ppm, the *S. aureus* reduction of PVA-SeNPs was still higher than 85%, while the reduction of PS20-SeNPs dropped to around 50%. This difference might be due to the different zeta potential of the nanoparticles.[122] The PS20-SeNPs had moderate negative surface charge (around -25 mV), and the PVA-SeNPs had weak negative surface charge of only about -8 mV. The negative surface charge could lead to repulsion effects between the nanoparticles and the bacterial cells. The repulsion effect may be more pronounced when the nanoparticle concentration is low (i.e. 25 ppm) and there is more space in the system.

An observation from this assay performed in aqueous suspension was that the CS-SeNPs went through similar changes to that of the CS-AgNPs. The CS-SeNPs did not change colour immediately when mixed with the bacterial suspension in PBS. However, after being incubated for 4 h, red precipitation of selenium nanoparticles was found at the bottom of the wells. As with the CS-AgNPs, this may also be a result of the interactions between the positively charged nanoparticles and the

bacterial cells. On the contrary, no change of appearance was found with PVA-SeNPs and PS20-SeNPs. The suspensions looked clear and orange in colour before the exposure with bacterial suspensions and maintained their transparent appearance until the end of the 4h incubation, which indicated high stability of the nanoparticle suspensions. However, this might also suggest that the protection for the SeNPs from the PVA polymer and the polysorbate 20 surfactant was too strong and that the interaction between the nanoparticles and bacterial cells were hindered.

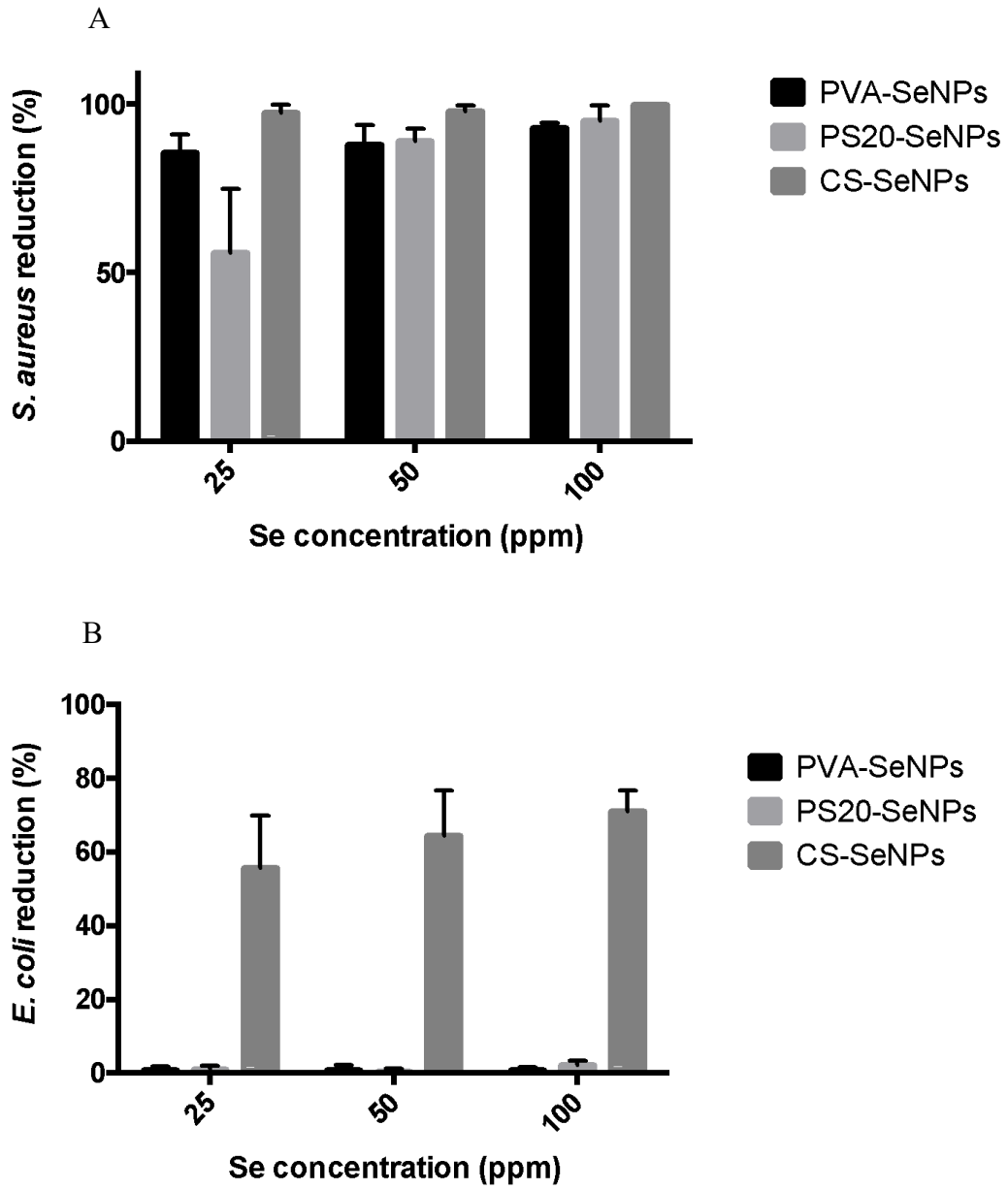

Figure 3.5 Relative bacteria reduction of (A) *S. aureus* and (B) *E. coli* treated with different SeNPs in aqueous suspension. Data presented as mean ± SD (n=3). Bars without an error bar means the reduction was higher than 99.5%.

With all of the SeNPs tested, only CS-SeNPs showed significant antibacterial effect against *E. coli*. A concern was that chitosan itself is also considered to be antibacterial, so whether the antibacterial efficacy towards *E. coli* arose from the chitosan or the selenium core is questionable. In other words, how much did the selenium core contribute to the antimicrobial activity against the *E. coli* cells? Based on the findings in this chapter and the evidence from the literature, it seems like the presence of polymer or surfactant can hinder the interaction of the SeNPs with *E. coli*; if this applies to chitosan as well, then the antibacterial effects of CS-SeNPs against *E. coli* might be mainly attributed to the chitosan. On the other hand, it is also possible that the presence of chitosan facilitated the interactions between the nanoparticles and the bacterial cells through the positive charge at the initial stage, and eventually the selenium was able to be exposed and carry out its role. Lara *et al*.[238] reported the synergistic antifungal effects of chitosan and SeNPs against *Candida albicans*. Although the details of the chitosan sample used in the antifungal study were not reported, their study indicated that the presence of chitosan on the surface of SeNPs allowed the nanoparticles to adhere to the fungal cells and made the fungal cells more permeable.

3.5 Chapter summary

In this chapter, the antibacterial activities of different colloidal silver and selenium nanoparticles were studied. Various methods of studying this activity were attempted and two were employed to assess the antibacterial activities qualitatively and quantitatively. The potential limitations of different methods for the antibacterial evaluation of nanoparticles were discussed. For example, when using the agar diffusion method, the particle size and solubility of the nanoparticles may affect the diffusion of the nanoparticles and therefore influence the results; in other words, negative results in an agar diffusion assay does not necessarily mean that the test substance has no antibacterial property against the test bacteria.

For silver nanoparticles, as a type of widely studied antimicrobial metal nanoparticle, there are plenty of data and results available from the literature. The major findings on the antibacterial activities of the silver nanoparticles here are in accordance with those from the literature. It was found that smaller AgNPs had stronger antibacterial performance than the larger ones, Gram-negative bacteria were more susceptible to AgNPs, and antibacterial activity was dose-dependent. Moreover, in this study, for the first time the antibacterial performance of CS-AgNPs and the bare TSC-AgNPs that were used to prepare the CS-AgNPs were compared. In this way, it was ensured that the surface condition was the only difference between the two types of test AgNPs. It was found that when using the qualitative direct contact on agar method, the presence of chitosan enhanced the antibacterial activity of silver; however, the effect could be delayed and therefore show lower activity in a short period of exposure time (4 hours) in the quantitative plate count assay.

Some confounding results were found from the literature and this chapter aimed to find the reasons behind it; however, the antibacterial activities of selenium nanoparticles remain obscure. It would be ideal to test the bare SeNPs, but, as previously discussed, a major issue was that adequate amount of stable colloidal bare SeNPs for the test were not obtained. Consequently, the SeNPs studied in this chapter were stabilised with polymer or surfactant. For the first time a systematic comparative study on the antibacterial performance of SeNPs capped by PVA, PS20 and CS was conducted. The antibacterial activities of PVA-SeNPs and PS20-SeNPs were reported by Tran *et al.*[122] and Bartunek *et al.*[133] respectively, showing these selenium nanoparticles had no inhibition effect on *E. coli* while significantly inhibiting the growth of *S. aureus*. Different methods and particle concentrations of these two types of SeNPs from the original reports were used in this chapter and similar results were obtained. It is worth noting that when mixing the bacterial suspension with the colloidal SeNPs, different precipitations were observed with different species, indicating the different interactions between different species of bacteria and the SeNPs. The inadequate interactions between *E. coli* and the SeNPs may be an important reason of the poor performance. The antimicrobial activity of CS-SeNPs had not been reported by the time the work described in this chapter was conducted. Although in this chapter the inhibition effects against *E. coli* were significantly enhanced with the presence of chitosan as the capping agent, the

contribution of the Se core in the antibacterial performance was not determinable since chitosan itself is also antimicrobial. However, it is promising that the cationic charge on the nanoparticles may facilitate the interaction between the particle and bacterial cells.

In order to determine if the antibacterial activity of SeNPs is dependent on the Gram-type of the bacterial species, three Gram-positive and three-Gram negative strains were tested together for the first time. It was clear that *S. aureus* was particularly sensitive to the SeNPs, regardless of the surface conditions, which is in accordance with the literature. Overall, it seems that the SeNPs were more effective against Gram-positive strains, however, not all Gram-positive strains are sensitive to the SeNPs. This is an interesting finding because AgNPs are believed to be less effective against Gram-positive species and,[35] therefore, SeNPs might be a good alternative to cover the gap.

Overall, the findings in this chapter are in accordance with the literature. Guisbiers *et al*.[169] prepared bare SeNPs using a laser ablation method and found that the SeNPs were able to inhibit the growth of both *S. aureus* and *E. coli.* The authors hypothesised that the presence of capping agent may hinder the antimicrobial activity of SeNPs. Unfortunately, stable bare SeNPs in aqueous solution that can be used for antimicrobial evaluation was not successfully prepared. Considering the fact that the overall aim of this work is to develop antimicrobial textile materials, the instability issue of SeNPs could potentially be addressed in the future work where nanoparticles are immobilised on fibre surfaces. Moreover, the antibacterial activity of these colloidal nanoparticles may be different from their activity when they are fixed onto a solid surface, where contact will be forced between the bacterial cells and the nanoparticles. Therefore, the next stage of study will address the issues from a different perspective and in order to gain a better understanding.

Chapter 4 Functionalisation of Cellulose-based Textiles by Selenium and Silver Nanoparticles

4.1 Introduction

This chapter focused on developing a simple, effective and environmentally friendly method to functionalise textile materials with selenium or silver nanoparticles. There are very few published reports using SeNPs as the antimicrobial agent for textile functionalisation. Yip *et al.*[140] prepared colloidal SeNPs using a polysaccharide-protein complex extracted from mushrooms as the stabiliser; the SeNPs were applied onto polyester fabrics using a padding machine. The authors found that the functionalised fabrics had good antifungal activity against *Trichophyton rubrum*; however, they did not test the antibacterial activity of the fabrics due to the poor antibacterial performance of the SeNPs in suspensions. Based on the findings from the previous chapters, and the analysis of the literature, it is hypothesised that the presence of steric stabilisation agents which provide negative surface charge may hinder the antimicrobial activity of the SeNPs against some species (e.g. *E. coli*). A list of representative studies using non-biogenic SeNPs as the antimicrobial agent can be seen in Table 4.1. As can be seen, the negative results indicating that SeNPs failed to inhibit *E. coli* were mainly reported by studies on colloidal SeNPs. When using SeNPs as the antimicrobial agent to functionalise other materials, the SeNPs showed antibacterial activity against both Gram-positive and Gram-negative bacterial, including *E. coli*. This is probably because when the SeNPs are fixed onto a surface, the bacteria inoculated would be forced to get into contact with the SeNPs, whereas in a suspension, the interactions between the NPs and the bacterial cells can be minimised due to the repulsion.

Table 4.1 A list of representative studies using non-biogenic SeNPs as the antimicrobial agent

Type of SeNPs	**Antimicrobial property**
Colloidal PVA-SeNPs[122]	Inhibited *S. aureus* but NOT *E. coli*
Colloidal bare SeNPs[171]	Inhibited both *S. aureus* and *E. coli*
Colloidal PS20-SeNPs[133]	Inhibited *S. aureus* and *S. epidermidis* but NOT *E. coli*
Colloidal CS-SeNPs[238]	Inhibited *Candida albicans*
Colloidal SeNPs capped with quercetin and acetylcholine[148]	Inhibited reference and resistant strains of *S. aureus, E. coli, P. aeruginosa, K. pneumoniae* and *Acinetobacter baumannii*
Colloidal bare SeNPs or stabilised with various surfactants[248]	Bare SeNPs showed the strongest antibacterial activity against *S. aureus, E. coli, P. aeruginosa* and *Salmonella typhi*
Ex situ prepared SeNPs capped by polysaccharide-protein complex, on polyester[140]	Colloidal SeNPs showed moderate inhibition against *S. aureus*, functionalised fabrics inhibited *Trichophyton rubrum* fungus
In situ prepared SeNPs on polymeric substrates[138]	Inhibited *P. aeruginosa*
Ex situ prepared laser induced SeNPs deposited by printing on glass substrates[249]	Inhibited *S. aureus* and *P. aeruginosa*
In situ prepared SeNPs on paper towels[137]	Inhibited *S. aureus* and *P. aeruginosa*
Ex situ prepared SeNPs stabilised by polyvinylpyrrolidone printed onto wool[250]	Inhibited *S. aureus, Bacillus cereus, E. coli,* and *Candida utilis*

In this chapter, it was decided to conduct *in situ* synthesis of the nanoparticles on fabric surfaces. With *in situ* synthesis, no stabiliser is needed for the SeNPs as the particles are generated on the surface directly. Moreover, as mentioned in Section 1.3.2, durability is one of the major challenges of nanoparticle-based textile functionalisation. Reusable textiles are subject to repeated washing, and the loss of nanoparticles during the process can result in decreased antimicrobial performance of the fabrics and potential health and environmental hazards. It has been shown that *in situ* synthesis can provide secure attachment of nanoparticles to the fabric surface as the nanoparticles formed *in situ* fit the natural morphology of the fibres and became physically lodged.[175,176] Additionally, the *in situ* approach can be easily adapted and used for the functionalisation of other materials, for which the impregnation of *ex situ* prepared NPs can be difficult, for example, 3-dimensional porous materials.

In the work presented here, cellulose-based fabrics were used as the substrate for the functionalisation. With the increasing concerns over plastic waste, sustainable materials are highly desirable to reduce the pollution caused by non-degradable synthetic polymers.[251] Cellulose can be harvested from many plants and is the most abundant and easily renewable organic resource on the planet.[252] Many natural cellulose-based fibres including cotton, flax and jute have been used to produce yarns and fabrics since ancient times. Although the development of synthetic fibres has provided many attractive characteristics in the last century, natural fibres still play an important role in textile manufacturing today. Moreover, the development of regenerated cellulose materials for various applications such as food packaging, wound care, and filtration systems has also been attracting increasing attention. This method reported here may be used to functionalise other cellulosic materials as well. In this chapter, cotton was used as a cellulosic substrate for antibacterial functionalisation as it is the most widely used plant fibre in the textile industry.

Cellulose is a natural linear polysaccharide comprising many glucose monosaccharides with the chemical formula $(C_6H_{10}O_5)_n$ as shown in Figure 4.1. There are three alcohol groups on the polysaccharide chain, two secondary and one primary alcohol. The primary alcohol is more prominent and easily neutralised in chemical reactions of cellulose.[253]

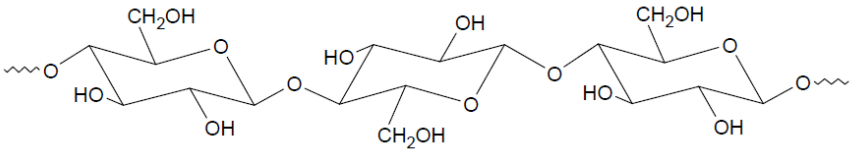

Figure 4.1 Chemical Structure of Cellulose

One of the most important chemical intermediate forms of cellulose is known as alkali cellulose (shown in Figure 4.2). Alkali cellulose is the product of cellulose treated with an alkali. The alkali treatment neutralises the acidic alcohol groups on cellulose and prepares cellulose as a nucleophile for chemical reactions.[254] The degree of deprotonation depends on the type and amount of base used as well as other parameters such as temperature and time. Alkali cellulose is important as it allows cellulose to readily react with many types of reagents, making cellulose, or more importantly cotton, a commercially important textile fibre.[255]

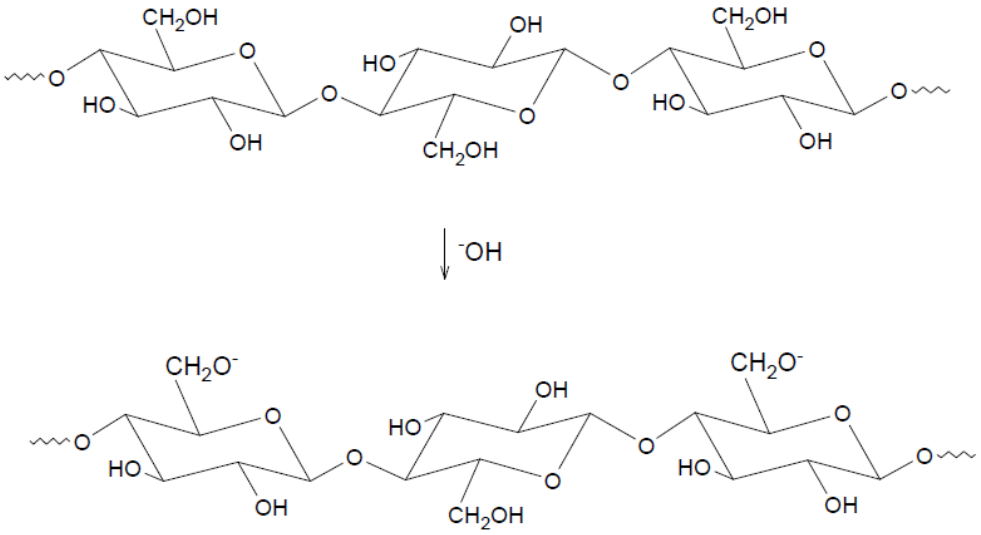

Figure 4.2 Conversion of cellulose into alkali cellulose

Cationized cotton is another important cotton derivative. The cationization of cotton is especially useful for sustainable dyeing processes, as it can significantly reduce the amounts of dye, time, water, and energy required for the dyeing processes.[256] Many cationization agents have been investigated for the treatment of cotton, among which 3-chloro-2-hydroxypropyl trimethyl ammonium chloride (CHPTAC) is a

promising candidate considering the obtainable volume for global consumption, cost, and ease of application. The utilisation of CHPTAC as the cationization agent for cotton is well documented in the literature.[173,255,257] CHPTAC and its derivatives are the only family of compounds that can be synthesised economically and in pure and stable forms for cellulose cationization. Currently, the most important application of CHPTAC is the cationization of starch, which has nearly identical chemical structure with cellulose. The cationic starch is used in producing triple layer board for food packaging of dry goods such as pasta and corn flakes, which speaks to its acceptable safety.[258]

CHPTAC itself is not reactive with starch or cellulose. It first needs to be converted into the reactive epoxide form, 2,3-epoxypropyltrimethylammonium chloride (EPTAC) in the presence of alkali as shown in Figure 4.3 (A). Once EPTAC is formed from CHPTAC, EPTAC is reacted with cellulose under alkaline conditions as shown in Figure 4.3 (B) to form stable ether linkages. However, as also shown in Figure 4.3 (B), hydrolysis of EPTAC is also possible under alkaline conditions resulting in an unreactive diol. Various application methods of CHPTAC including cold pad batch, pad-steam, pad-dry-cure, and exhaustion have been used to cationize cotton goods, and all of them have their advantages and disadvantages; among all the techniques, cold pad batch has been shown to result in the highest fixation rate of applied CHPTAC, although it requires a 16 – 24 h batch time which makes the throughput very low.[255]

In this chapter, the cationized cotton was used as the substrate for the *in situ* synthesis of silver or selenium nanoparticles. The functional groups (i.e. activated alkali cellulose and cationic quaternary groups) can attract the precursor ions (i.e. Ag^{+} or SeO_3^{2-}) onto the fabric surfaces. Moreover, the presence of cationic groups on the cellulose surface may provide additional antimicrobial activity and combined effects with the nanoparticles. The antibacterial effects of CHPTAC-modified cellulose materials have been reported by several recent studies.[259–261]

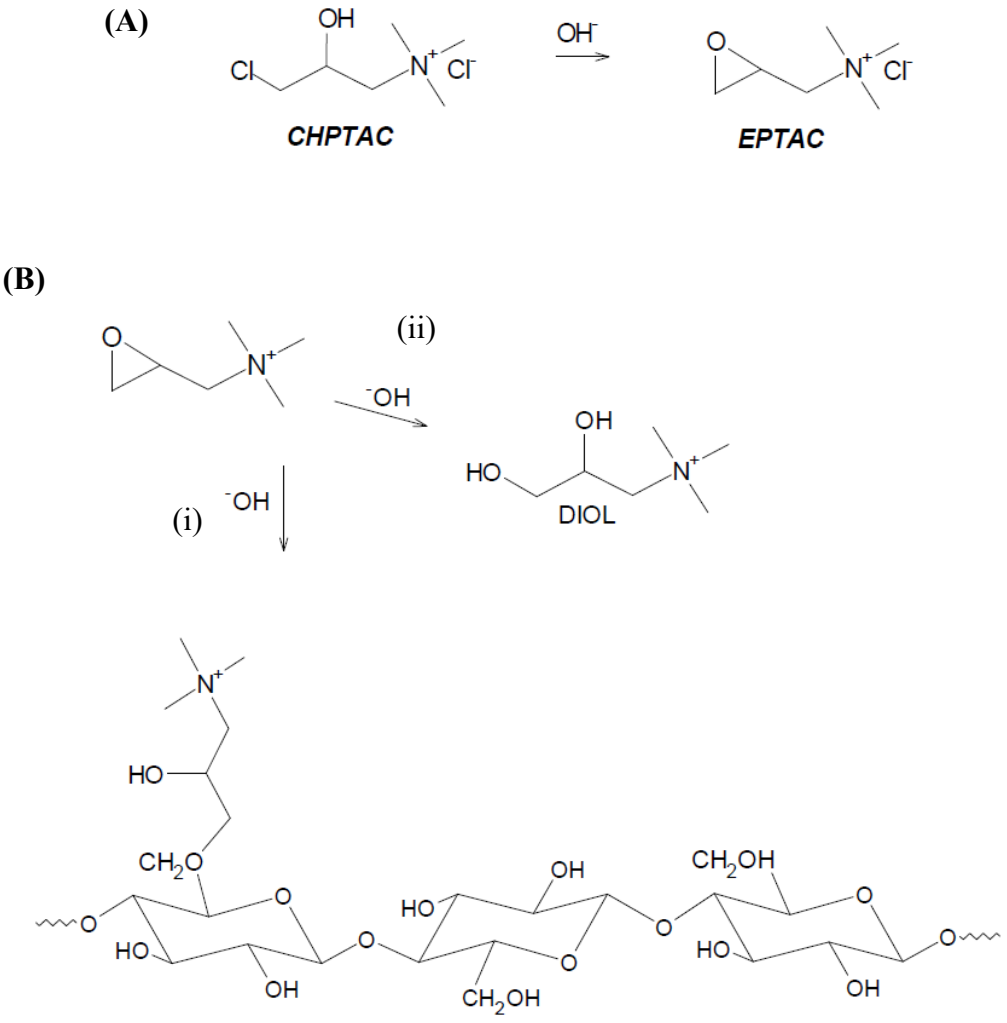

Figure 4.3 (A) Formation of EPTAC from CHPTAC; (B) Reactions of EPTAC with (i) cellulose and (ii) hydrolysis

Some researchers have reported the employment of this cationization process for the preparation of nanoparticle-functionalised cellulose-based fabrics. Khalil-Abad *et al.*[173] used CHPTAC to functionalise cotton fabrics and found that the cationzation improved the adsorption of pre-formed colloidal silver nanoparticles (stabiliser not reported). There are other studies on the assembly of pre-formed metal nanoparticles onto cationized fabrics.[262,263] Dong and Hinestroza[264] used both *ex situ* and *in situ* methods to prepare metal nanoparticles (Au, Pd and Pt) on the surface of CHPTAC-functionalised cellulose fibres. With the *ex situ* method, citrate-capped gold and

platinum nanoparticles were adsorbed onto the positively charged fibres. For the *in situ* preparation, negative metal complex ions ($AuCl^{4-}$, $PdCl_4^{2-}$ and $PtCl_6^{2-}$) were employed for adsorption onto the cationic quaternary groups; $NaBH_4$ was used to reduce the metal complexes at room temperature. In this chapter, it will be shown that not only anions (e.g. metal complex ions and SeO_3^{2-}) but also free metal ions (e.g. Ag^+) can be attracted onto the surface of cationized cotton and used as the precursor for the *in situ* synthesis of nanoparticles. Microwave irradiation is employed to assist the generation of SeNPs and AgNPs with ascorbic acid as the reducing agent. Many studies have successfully prepared inorganic nanoparticles using microwave irradiation, which offers significantly increased rate of reaction compared to the traditional thermal heating, lower energy consumption, and homogeneous heating that results in fairly good particle size distributions.[265–268] Microwave irradiation has also been used in textile functionalisation to increase the dyeability or fixation rate of the functional agents.[41,175,269,270] It has been shown that microwave irradiation can be used to assist the synthesis of AgNPs using ascorbic acid as the reducing agent in acidic solution.[267]

The aim of this chapter was to develop a simple, effective and environmentally friendly method to functionalise cellulose fabrics with cationic charge and *in situ* prepared SeNPs and AgNPs. The nanoparticles should be securely attached to the fabric and provide a good coverage over the surface. The chapter objectives include:

(1) To prepare cotton fabrics with cationic quaternary ammonium groups using cationization agent CHPTAC.
(2) To prepare the nanoparticles (e.g. SeNPs and AgNPs) *in situ* on the surface of cationized cotton by a chemical reduction method, using ascorbic acid as the reducing agent with the assistance of microwave irradiation.
(3) To characterise the functionalised fabrics to confirm the presence of cationic groups and nanoparticles on the fabric surface.
(4) To study the laundry durability of the functionalised fabric samples in terms of the loss of nanoparticles after repeated washes.

4.2 Materials

Bleached woven cotton fabric (250 g/m^2) was purchased from a local fabric store. 3-chloro-2-hydroxypropyl trimethyl ammonium chloride (CHPTAC) aqueous solution (wt 60%), sodium selenite (Na_2SeO_3, 99%), silver nitrate ($AgNO_3$, ≥99%), and L-ascorbic acid (99%) were purchased from Sigma Aldrich. NaOH solution (10 M), potassium chloride (KCl, ≥99%) and Tween® 80 (Polysorbate 80) was purchased from Fisher Scientific. Reverse osmosis water (RO water) with a resistance of 15 mΩ cm was used throughout the experiments.

4.3 Methods

4.3.1 Cationization of cotton fabrics

In some preliminary experiments, it was found that the as-purchased cotton might have some chemical impurities on the surface, assumed to result from the cotton processing and manufacturing, which were toxic to human bronchial epithelial cells (16HBE14o-) *in vitro*. Consequently, the as-purchased cotton was purified first before any functionalisation was conducted. The cotton was soaked in RO water at a material-to-liquor ratio of 20:1 until it was brought to a boil. This procedure was carried out three times with fresh RO water. The cotton was then soaked in 50% ethanol overnight with 100 rpm agitation and rinsed thoroughly with RO water. This purified cotton was designated as unmodified cotton (UC).

The methods to cationize cotton fabric with CHPTAC have been described in several reports.[173,255,257] In this study, the cationization method was based on a cold pad batch protocol,[255] (in textile industry, cold pad batch method is used for reactive dyeing, where fabrics are immersed in dye bath, run through padders to remove excessive dye, and then left for the reaction to be finished) with a molar ratio of NaOH and CHPTAC of approximately 2:1, and batching time of 24 h. The reaction solution containing NaOH (1 M) and CHPTAC (100 g/L, 0.53 M) was prepared with 10 M NaOH solution and CHPTAC aqueous solution (wt 60%). Unmodified cotton

(UC) was immersed into the solution at a material-to-liquor ratio of 1:20. The reaction bath was shaken constantly at 150 rpm for 1 h at room temperature. Subsequently, the samples were removed from the bath, dried briefly by squeezing to remove excess liquid (wet pick-up approximately 120%), placed into polypropylene sample bags, and sealed for 24 h at room temperature. After 24 h, the samples were neutralized using 1% acetic acid (material-to-liquor ratio of 1:20) and washed thoroughly with RO water. Finally, the air-dried cationized cotton (CC) was autoclaved at 121 °C for 15 minutes, after which the *in situ* preparation of nanoparticles was performed, as described in Section 4.3.2, using aseptic technique to avoid contamination.

4.3.2 In situ synthesis of Ag and Se nanoparticles on cationic cotton fabrics

Prior to the *in situ* preparation of nanoparticles, chemical solutions including silver nitrate, sodium selenite, and ascorbic acid, were sterilised by filtration through sterile cellulose acetate filters with pore size of 0.2 μm (Minisart). Surfactant solution, RO water and glassware were sterilised by autoclaving at 121 °C for 15 min. After preparation, the functionalised samples were dried in laminar air flow cabinets and kept in sterile sample tubes.

The CC samples (4.8 g) were immersed in different concentrations of silver nitrate or sodium selenite solutions (0.2, 0.5, and 1 mM) at a material-to-liquor ratio of 1:20 in 200 mL beakers. The beakers were shaken at 150 rpm for 1 h in the dark at room temperature to allow the precursor ions to be adsorbed onto the fabric surfaces. Subsequently, ascorbic acid (100 mM) was added to the beakers resulting in concentrations of 2, 5, and 10 mM respectively. The reactants and fabrics were mixed thoroughly with a glass rod and then microwaved using a domestic microwave oven at 700 w for 90 s and taken out to cool down and age for 2 h at room temperature. The cotton fabrics turned from white to beige or orange colours, indicating the formation of silver or selenium nanoparticles respectively. The samples were rinsed with RO water, soaked in 0.1% non-ionized surfactant, Tween 80, for 30 min while shaken at 150 rpm, and finally washed thoroughly with sterile RO water again to wash off unattached NPs before drying in a laminar air flow hood.

The products were designated AgNPs modified cotton (Ag-C) and SeNPs modified cotton (Se-C).

4.3.3 Characterisation of modified cotton fabrics

4.3.3.1 Zeta potential of cotton fibres

The measurement of cotton fibre zeta potential was modified from Zhang *et al*.[271] and Rashidi *et al*.[272] The cotton samples were carefully shredded and ground into cotton powders. The powder (0.05 g) was dispersed in 50 mL KCl solution (1 mM). Firstly, the suspension was sonicated in a sonication bath for 30 mins and stirred vigorously with a magnetic stirrer for 30 mins, and then left still to settle for 1 hour. Subsequently, the supernatant was loaded into a Malvern DTS 1070 folded capillary cell and the zeta potential was measured by Zetasizer Nano ZS90 (Malvern, UK).

4.3.3.2 Electron scanning microscopy (SEM)

Microscopic investigations of the fabric samples were carried out using a Zeiss SIGMA Field Emission Gun Scanning Electron Microscopy (FEG-SEM) at an accelerating voltage of 2 kV. The samples were coated with 4 nm platinum by sputtering coating, to increase the conductivity, using a Quorum Q150T ES Turbo-Pumped Coater. The sizes of the NPs were determined manually with ImageJ software. Three batches of samples prepared on individual occasions and approximately 300 particles in total from 10 – 15 images were analysed for each type of sample. The energy-dispersive X-ray spectroscopy (EDS) spectra of the samples were acquired using the EDS detector of the SEM by scanning different areas of the samples.

4.3.3.3 X-ray Photoelectron Spectroscopy (XPS)

The XPS spectra were acquired on an Axis Ultra DLD spectrometer (Kratos Analytical) using a monochromatic AlKα source (hν = 1486.7 eV, 180 W) by Dr Konstantin I. Maslakov at Lomonosov Moscow State University. The pass energies of the analyzer were 160 eV for survey spectra and 40 eV for high resolution scans. The Kratos charge neutralization system was used and the position of the low energy component in C1s spectra was referenced to 284.8 eV, which corresponded to C−C bonds of hydrocarbon contamination.

4.3.3.4 Determination of Ag and Se loadings on cationized cotton

To determine the total amounts of Ag or Se nanoparticles loaded onto the cationized cotton fabrics, the cotton samples were digested in acid and the solutions were analysed with Microwave Plasma-Atomic Emission Spectroscopy (4100 MP-AES, Agilent Technologies). The cotton samples were carefully disassembled and shredded into short loose fibres. Piranha solution was prepared in Pyrex test tubes by slowly adding one portion of H_2O_2 (30% wt) to three portions of concentrated H_2SO_4. Approximately 100 mg of the loose fibres were weighed accurately and then wet oxidised by 2 mL of the Piranha solution. After the fibres were fully dissolved, the solution was slowly added to 18 mL of cold RO water to dilute and prepare for MP-AES analysis. Three batches of samples prepared on individual occasions were analysed.

4.3.3.5 Laundry durability of the nanoparticles

In this study, the washing durability was evaluated by a method based on the accelerated laundering test method recommended by AATCC (American Association of Textile Chemists and Colorists) Test 61-2013 Colorfastness to Laundering: Accelerated.[273] The washing apparatus comprised 300 mL polypropylene wide-mouth bottles (Thermo Fisher Scientific), stainless steel balls (6 mm), and a TURBULA T2F Shaker Mixer (WAB, Switzerland). The laundry detergent Persil Colour Care Biological Washing Powder (containing 5-15% anionic

surfactants, <5% Enzymes, nonionic surfactants, optical brighteners, perfume, phosphonates, polycarboxylates, soap, zeolites, butylphenyl methylpropional, geraniol, and hexyl cinnamal) was purchased from a local supermarket. The washing temperature was controlled to be above 65 °C for at least 10 mins, according to the Department of Health guidelines.[274] Bottles were filled with 150 mL RO water along with 50 stainless steel balls and 0.225 g washing powder (0.15% w/v), which was then heated in a water bath to 75 °C, and a 2.5 g fabric sample (5 cm × 20 cm) added. The bottle was wrapped in oven gloves, to insulate for heat loss, and then shaken (96 rpm) for 30 mins (one accelerated washing cycle). The samples were then rinsed in 150 mL sterile RO water in the bottles for 3 times, after which no bubble was seen with the rinse. According to AATCC 61-2013,[273] one washing cycle with this accelerated method is equivalent to 5 typical home launderings. Four accelerated washing cycles were performed for each type of sample. After each accelerated washing cycle, a small piece (approximately 5 cm × 2 cm) was cut from the fabric for MP-AES elemental analysis using the method described in Section 4.3.3.4 The washing procedure was carried out three times using samples prepared on three individual occasions for the analysis.

4.4 Results and discussion

4.4.1 Cationization of cotton fabrics

As mentioned earlier, the cold pad batch method has been found to routinely provide the highest fixation rate of CHPTAC (i.e the percentage of CHPTAC that has been fixed successfully onto the fabric surface).[275] Farrell[255] found that using this method, the fixation rate decreased as the CHPTAC concentration increased; and the fixation of CHPTAC almost plateaued at 100 g/L, that is, the number of fixed quaternary groups would not be effectively increased further when the concentration of CHPTAC was higher than 100 g/L. In this chapter, based on the apparatus available in the laboratory, an adapted method based on the cold pad batch protocol described by Farrell[255] was used. In order to provide sufficient quaternary groups on the cotton surface, 100 g/L was chosen as the concentration of CHPTAC used to cationize the cotton samples. With the data reported by Farrell[255], that the fixation rate of

CHPTAC was approximately 30% with the reaction conditions used in the chapter, it is estimated that the number of fixed cationic quaternary groups was approximately 0.1 mmol per gram of cotton, which in theory is sufficient for the highest concentration of Na_2SeO_3 (1 mM) used in this chapter for the preparation of SeNPs on the cotton surface.

The measurement of zeta potential is one of the most straightforward ways to confirm the effect of the cationization process. As can be seen from Figure 4.4 (A), after the cationization treatment, the zeta potential of the cotton fibres increased dramatically from -26.27 ± 2.53 mV to +13.33 ± 0.48 mV. Cotton is naturally electronegative in aqueous suspension due to the presence of hydrophilic groups, and the cationization process changed the surface charge of cotton from a negative to a positive range. The difference between the unmodified control cotton and cationized cotton could also be seen macroscopically. The photographic image of Figure 4.4 (B) shows the cotton powder suspensions used for the zeta potential measurement. There is a clear difference between the two vials in that the cationized cotton fibres tended to adhere to the inner wall of the glass vial, which was a result of the electrostatic interaction between the negatively charged glass and the positively charged cationized cotton fibres. These results confirmed the successful fixing of cationic groups onto the cotton fabrics.

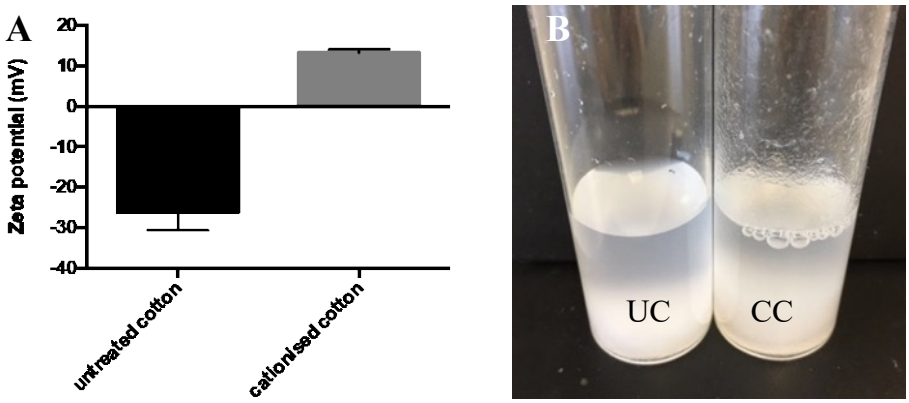

Figure 4.4 (A) zeta potential results of unmodified control cotton and cationized cotton; (B) photographic image of the suspensions of unmodified control cotton (left) and cationized cotton (right).

4.4.2 *In situ* synthesis of nanoparticles

Based on the literature and findings described in the previous chapters, a method that can be used to prepare both silver and selenium nanoparticles *in situ* on cotton fabrics (Figure 4.5) was developed. In the first step, CHPTAC, is used to functionalize the cotton fabrics prior to the preparation of nanoparticles. During the cationization, NaOH is used to transform the CHPTAC into EPTAC to react with cellulose, while the excessive NaOH activates the primary –OH groups on the cellulose chain into alkali cellulose (Cell–O^-Na^+). This results in a fabric surface with both cationic quaternary ammonium groups (-$N^+(CH_3)_3$) and activated –O^-Na^+ groups. The –O^-Na^+ groups on activated alkali cellulose can attract silver ions. Yazdanshenas and Shateri-Khalilabad[97] prepared silver nanoparticles *in situ* on the surface of alkali cellulose. They suggested that the sodium salt of Cell–O^-Na^+ was exchanged to the silver salt of Cell–O^-Ag^+ due to the higher electronegativity (Pauling's scale) of silver (1.93) towards sodium (0.93) in the aqueous solution of $AgNO_3$.[41] In the method described in this chapter, due to the presence of Cl^- ions as the counter-ion of the quaternary ammonium groups, some AgCl may precipitate in the solution when the $AgNO_3$ is added. There may also be a small amount of AgCl generated on the fabric surface and reduced by ascorbic acid into elemental AgNPs later. On the other hand, the cationic quaternary ammonium groups can attract the anionic selenite groups (SeO_3^{2-}) onto the fabric surface and, subsequently, SeNPs can be generated by *in situ* reduction using ascorbic acid.

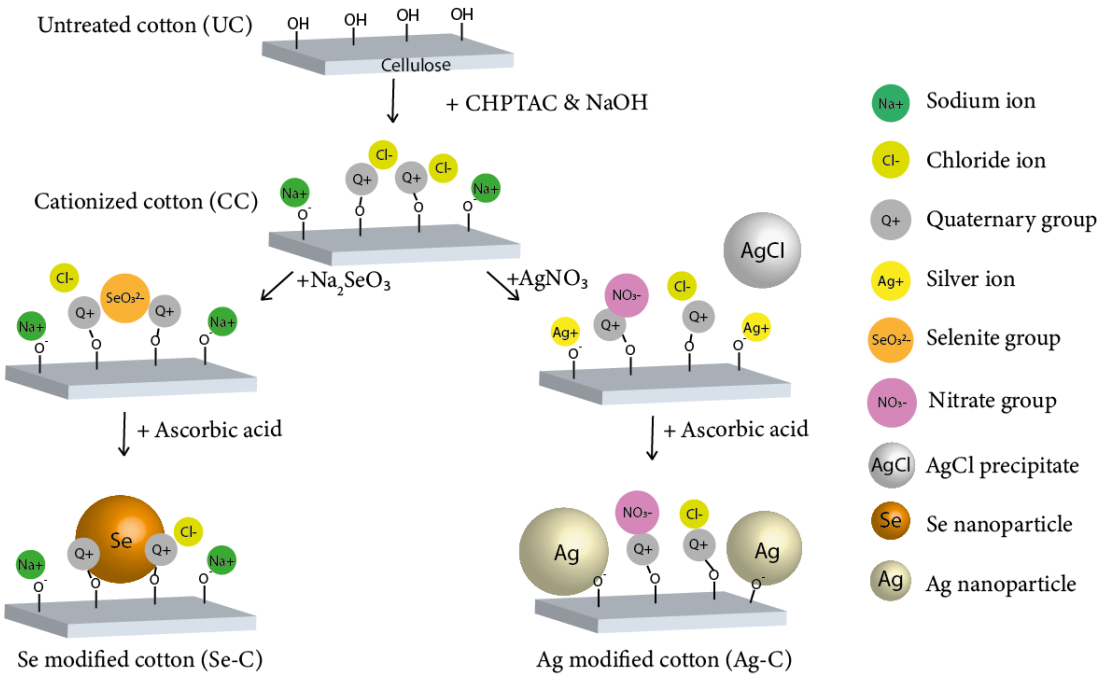

Figure 4.5 Preparation of Se or Ag nanoparticles *in situ* on a cellulose surface.

The photographic image of the control (UC) and modified (CC, Ag-C and Se-C) cotton fabrics are shown in Figure 4.6 (A). As can be seen, the cationization process did not result in colour change of the cotton fabric, while the formation of Se or Ag nanoparticles changed the colour of the fabrics from white to orange or beige respectively, with the intensity of the colour dependent on the concentration of precursor salt. Several reports have described the orange colour of SeNPs[137,142,199]; and the colours of AgNPs ranging from yellow to beige/grey, depending on the size of the particles, are also well documented.[163,276] Figure 4.6 (B) shows the colours of the functionalised fabrics when UC and CC were placed in the same pot to act as the substrates for *in situ* synthesis of SeNPs. It can clearly be seen that, in comparison with the cationized samples, the colour of the unmodified cotton barely changed as it failed to actively attract the SeO_3^{2-} ions onto the fabric surface. Similar results were observed with AgNPs as well. The difference demonstrated that the cationization process successfully prepared the cotton surface for the *in situ* synthesis of the nanoparticles.

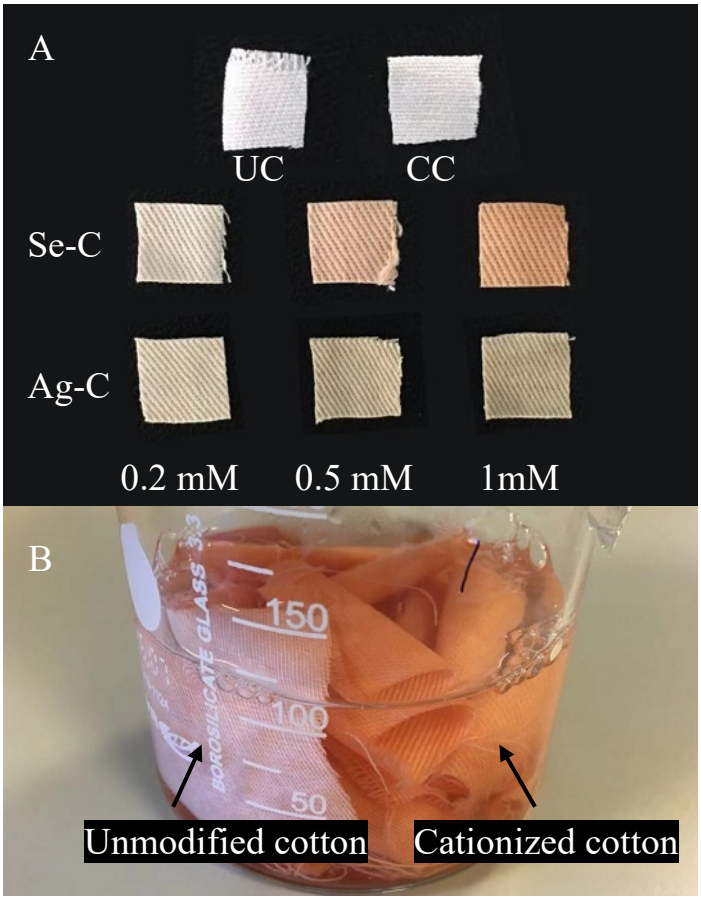

Figure 4.6 Photographic images of (A) cotton fabric samples (UC, CC, Se-C and Ag-C) showing different colours and colour intensities; and (B) one-pot *in situ* synthesis of SeNPs with different UC and CC as the substrates.

4.4.3 SEM analysis

The SEM images of the control (UC) and modified (CC, Ag-C and Se-C) cotton fabrics are shown in Figure 4.7 - 4.9. As a plant material, cotton fibres have a natural surface roughness (Figure 4.7 A). No significant morphological change was observed on the cationized fibres from the SEM images (Figure 4.7 B), which is in accordance with the previous reports on the cationization of cellulose using CHPTAC.[277–279] The presence of SeNPs (Figure 4.8) or AgNPs (Figure 4.9) can be clearly seen from the images. Both types of nanoparticles were observed to have formed over the surface of the fibres. The particles were predominantly quasi-spherical in shape, although small numbers of silver nanorods can also be seen. Compared with the AgNPs, the shapes of the SeNPs were more spherical and

Original in colour

smoother, which is in accordance with the observations described in Chapter 2. The AgNPs and SeNPs were evident at all initial concentrations of precursors (0.2, 0.5 and 1 mM) and numbers of nanoparticles increased with increasing precursor concentrations, which is in agreement with the colour changes shown in Figure 4.6 (A). The nanoparticles had relatively narrow size distributions, falling predominantly into the range of 40 nm – 140 nm. The average sizes of SeNPs prepared with different concentrations of Na_2SeO_3 were relatively similar, at around 100 nm. It can also be seen from the size distributions of SeNPs that the peaks of the histograms were also relatively stable, at around 100 nm. On the other hand, when looking at the average sizes and size distributions of the AgNPs, the particle sizes seemed to increase as the concentration of $AgNO_3$ increased. The different trends can be due to various reasons including the different nucleation and particle growth mechanisms between the metal and non-metal elements.

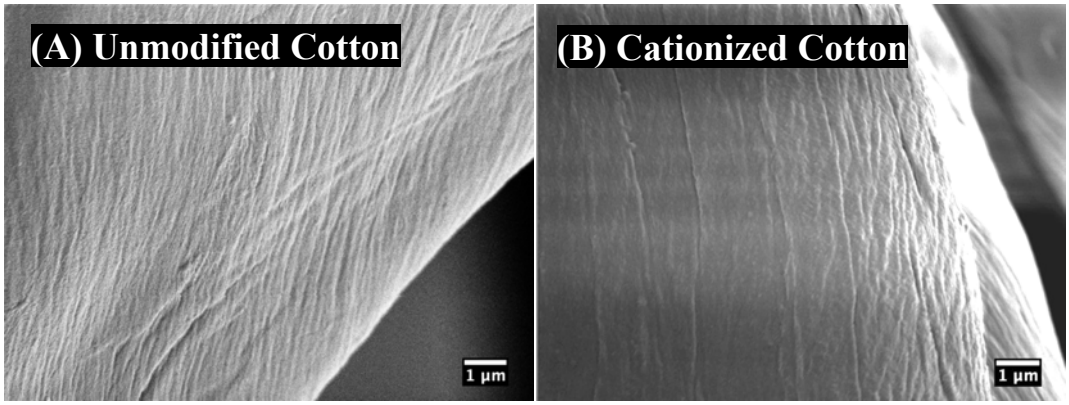

Figure 4.7 SEM images of (A) unmodified cotton and (B) cationized cotton.

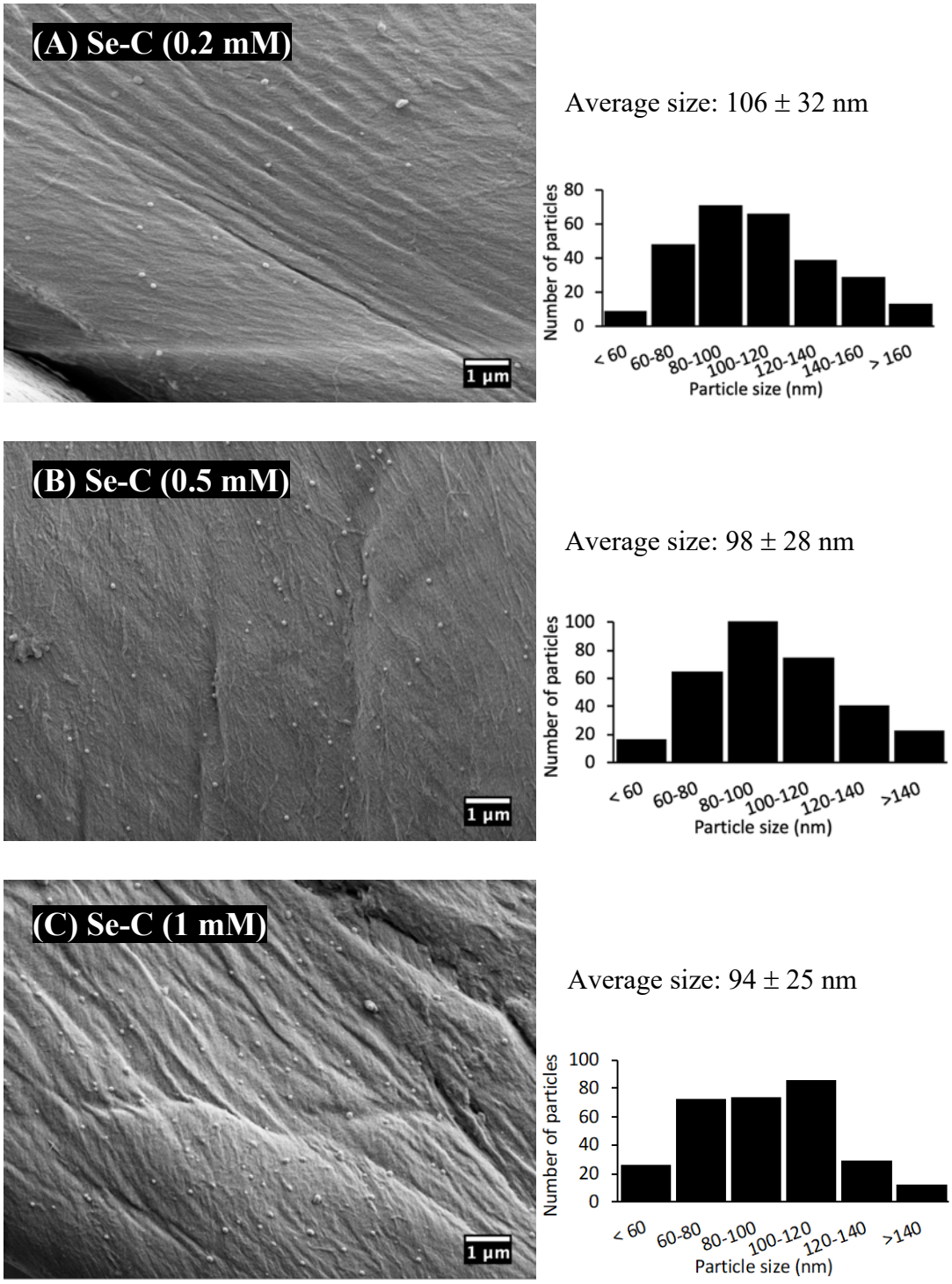

Figure 4.8 SEM images and particle size distributions of cotton samples: (A) 0.2 mM Se-Cotton; (B) 0.5 mM Se-Cotton; and (C) 1 mM Se-Cotton.

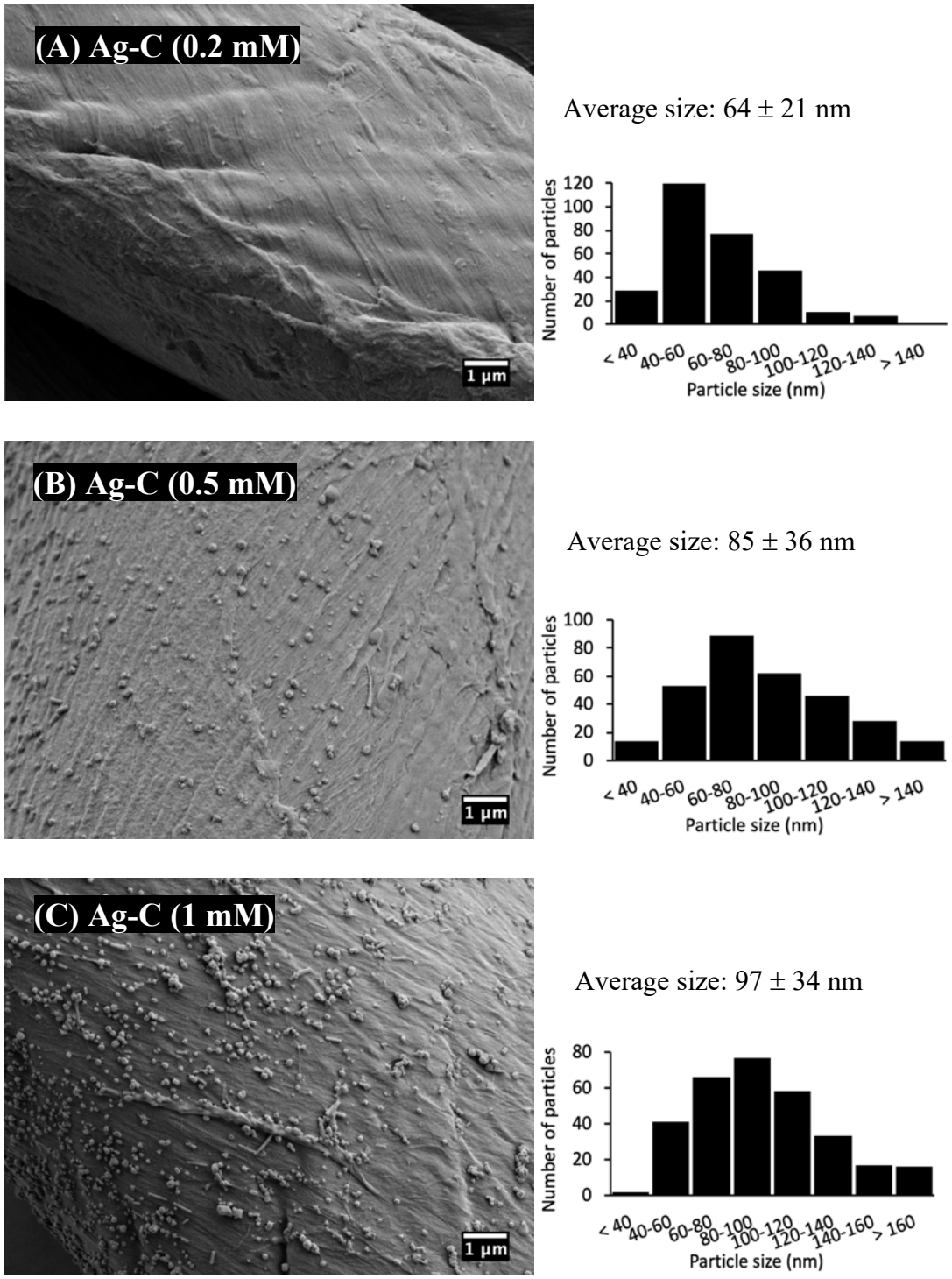

Figure 4.9 SEM images and particle size distributions of cotton samples: (A) 0.2 mM Ag-Cotton; (B) 0.5 mM Ag-Cotton and (C) 1 mM Ag-Cotton.

4.4.4 Surface chemistry analysis

Energy-dispersive X-ray spectroscopy (EDS) was used to characterise the chemical compositions of the cotton fabric surface before and after the functionalisation, as shown in Figure 4.10. For the unmodified control cotton (Figure 4.10 A), the two strong peaks corresponding to carbon and oxygen can be seen as the main composition of cotton is cellulose. The peaks for platinum are from the platinum coating that was used to increase the conductivity of the samples. After the cationization (Figure 4.10 B - D), new peaks of chlorine emerged which were attributed to the chloride ions as the counter ions of the quaternary groups.[280] The peak for nitrogen was expected between the peaks for carbon and oxygen but is not visible and might have been masked by the two major peaks of C and O. The new peaks corresponding to silver and selenium on Figure 4.10 (C) and (D) respectively confirmed the presence of silver or selenium on the fabric after the *in situ* synthesis of the nanoparticles.

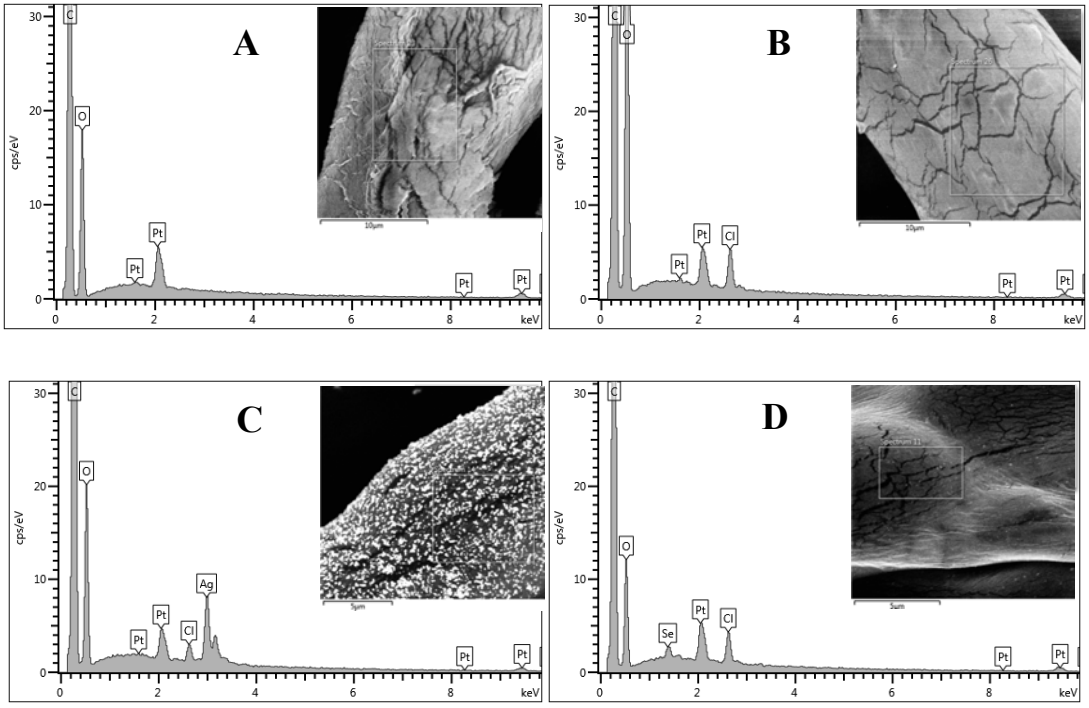

Figure 4.10 EDS spectra and corresponding scanning areas of the fabric samples (A) unmodified control cotton, (B) cationized cotton, (C) Ag-cotton (1 mM) and (D) Se-cotton (1 mM).

For more detailed surface chemical compositions, XPS was used to analyse the fabric samples. The XPS spectra for the samples are shown in Figure 4.11. The binding energies of XPS lines, kinetic energy of Ag $M_4N_{45}N_{45}$ line and silver Auger parameter (AP) are summarised in Table 4.2. As can be seen from Figure 4.11 (B) and Table 4.2, the peak at about 399.8 eV observed in the N1s spectra of all samples can be attributed to NR_3 species, which exist naturally in cotton fibres. The additional peak at 402.6 eV in the spectra of cationized cotton, Ag-C and Se-C corresponds to quaternary nitrogen species (NR_4^+). No chlorine was detected on the surface of unmodified cotton, while the binding energy of Cl $2p_{3/2}$ peak at about 197.6 eV observed in other samples is typical for Cl^- ions as the counter-ions of the fixed quaternary ammonium groups, which is in accordance with the EDS results. These new peaks on the modified samples demonstrated the successful fixing of quaternary ammonium groups onto the cotton fabrics. On Ag-C, the binding energy of the $Ag3d_{5/2}$ line (Figure 4.11D) and the Auger parameter calculated for Ag $M_4N_{45}N_{45}$ transition (Figure 4.11E) are close to that for non-oxidized silver,[281] indicating the silver on the surface of Ag-C was mostly metallic silver. The $Se3d_{5/2}$ line for Se-C is centred at 55.3 eV, which is typical for non-oxidized elemental selenium (Figure 4.11F).[282] These results confirmed that the AgNPs and SeNPs formed *in situ* on the surface of cationized cotton were non-oxidized elemental nanoparticles, which is as expected.

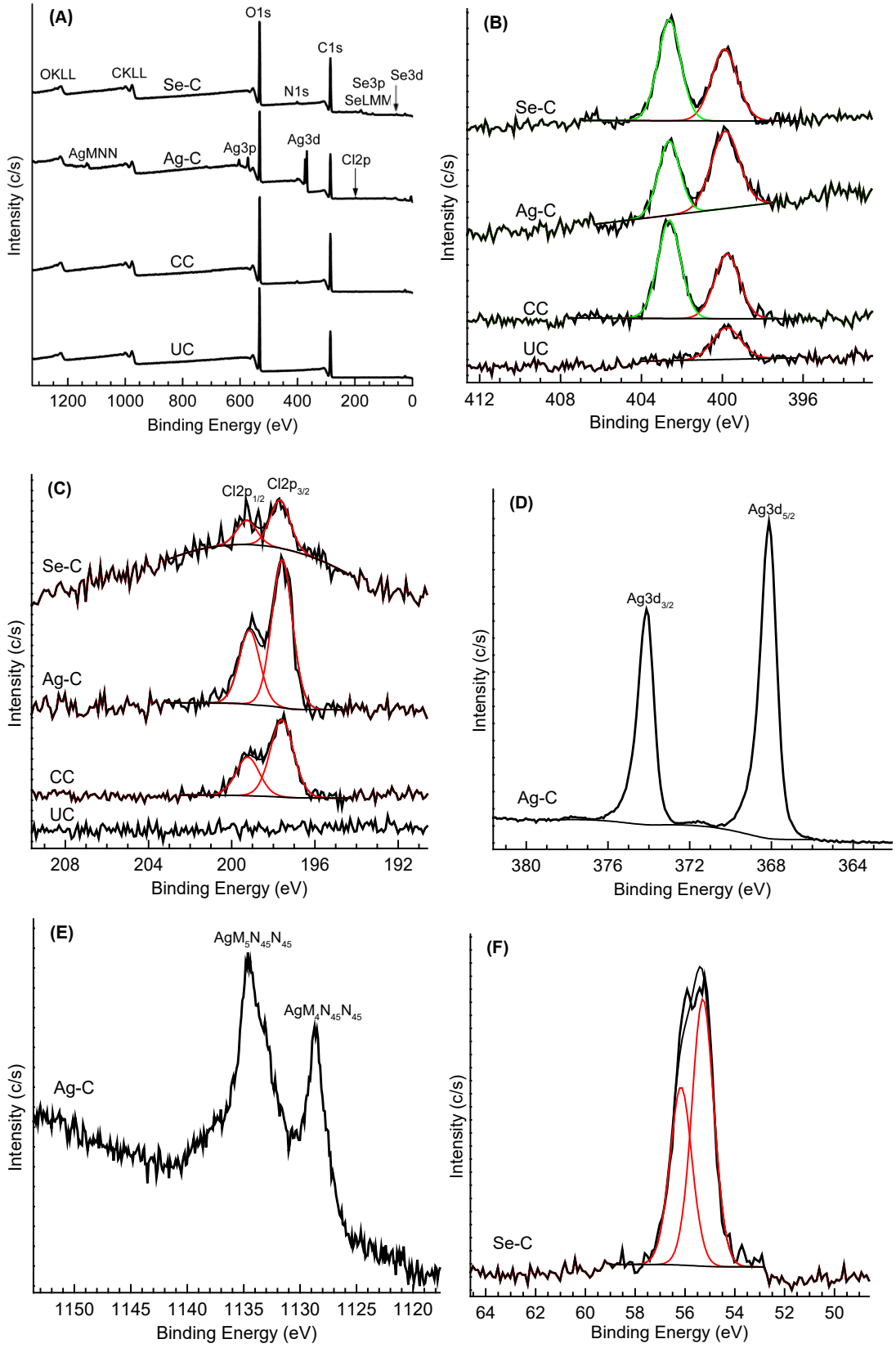

Figure 4.11 (A) Survey XPS spectra; (B) N1s XPS spectra; (C) Cl2p XPS spectra; (D) Ag3d XPS spectrum of sample Ag-C; (E) AgLMM Auger spectrum of Sample Ag-C; (F) Se3d XPS spectrum of Sample Se-C.

Table 4.2 Binding energies of XPS lines, kinetic energy of Ag $M_4N_{45}N_{45}$ line and silver Auger parameter (AP) for samples (eV).

Line	Sample				Species
	UC	CC	Ag-C	Se-C	
N 1s	399.8	399.8	399.9	399.9	NR_3
	–	402.6	402.6	402.6	NR_4^+
Cl $2p_{3/2}$	–	197.6	197.6	197.7	Cl^-
Ag $3d_{5/2}$	–	–	368.1	–	Ag^0
Ag $M_4N_{45}N_{45}$	–	–	358.1	–	
AP ($3d_{5/2}$, $M_4N_{45}N_{45}$)	–	–	726.2	–	Ag^0
Se $3d_{5/2}$	–	–	–	55.3	Se^0

4.4.5 Loadings and washing durability of Se or Ag on the functionalised fabrics

One of the major challenges of textile functionalisation with nanoparticles is the durability of the modification. For reusable textiles, one of the most important factors is the laundry durability. In order to address this issue, the amounts of Se or Ag on the samples before and after repeated laundering were analysed. The contents of Se or Ag per gram of cotton was determined by digesting the fabrics in acid and analysing the solution using atomic emission spectroscopy. The washing method was based on both the accelerated laundry method described in AATCC Test 61-2013 (Colorfastness to Laundering: Accelerated)[273] and the elevated washing temperature for healthcare linens recommended by the Department of Health.[274] As can be seen from Table 4.3, the amount of Se or Ag per gram of cotton was dependent on the concentration of the precursor salt used, which is in agreement with the observations from the colour intensities of the modified samples as well as the SEM images (Figure 4.6 – 4.9). All of the samples retained over 80% of the Se or Ag after 4 accelerated laundry cycles (equivalent to 20 typical home laundry cycles), indicating excellent washing durability of the nanoparticle-fabric interaction. AgNPs reduced *in situ* on cotton fabrics have been found to be more securely attached to the fibres

compared to AgNPs prepared *ex situ* and applied onto the fabrics using pad-dry cure method.[177] This may be due to the fact that particles formed *in situ* on the fibre surface fit the natural topography and therefore were physically lodged on the fibre. Moreover, the microwave treatment for the synthesis of nanoparticles may have resulted in the swelling of cotton fibres, which facilitated the penetration of nanoparticles into the intramolecular structure of the fibres.[175,176]

Another interesting observation is that thermal treatment, including autoclaving or washing in hot water (>70 °C), resulted in the colour change of Se-C, from bright orange to darker colours. Figure 4.12 shows the photographic images of Se-C before and after being autoclaved or washed in hot water. Considering the observations described in Chapter 2, the colour changes might indicate some change to the SeNPs on the fabric surfaces.

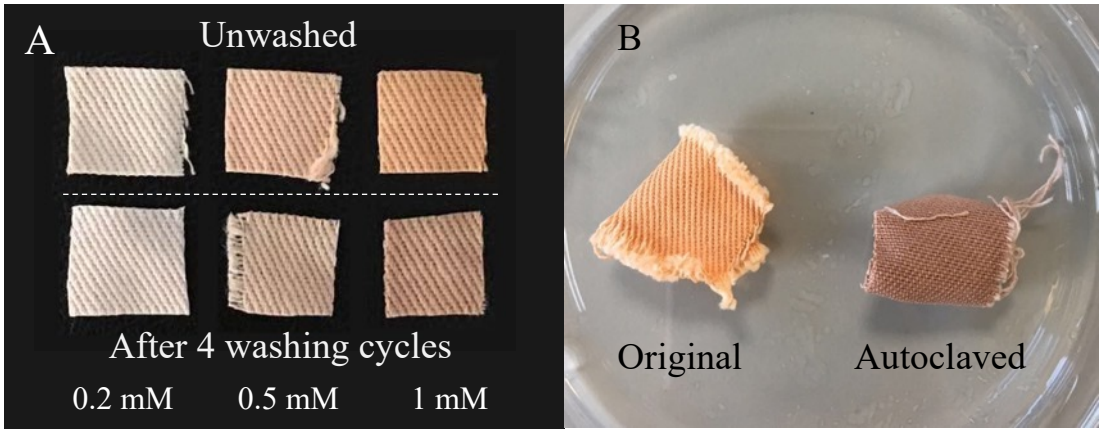

Figure 4.12 Photographic images of Se-C (A) before and after being washed in hot water and (B) Se-C prepared with 1 mM Na_2SeO_3 before and after being autoclaved.

Original in colour

Table 4.3 Amount of Se or Ag per gram of cotton before and after being washed

Sample	unwashed	1 cycle		2 cycles		3 cycles		4 cycles	
	mg/g	mg/g	%	mg/g	%	mg/g	%	mg/g	%
Se-C (0.2 mM)	0.327 ± 0.027	0.308 ± 0.006	94.2	0.293 ± 0.016	89.4	0.294 ± 0.026	89.7	0.285 ± 0.028	87.1
Se-C (0.5 mM)	0.658 ± 0.023	0.532 ± 0.065	80.9	0.542 ± 0.020	82.3	0.560 ± 0.013	85.1	0.547 ± 0.042	83.1
Se-C (1 mM)	1.069 ± 0.122	1.014 ± 0.049	94.8	0.983 ± 0.136	91.9	1.020 ± 0.021	95.4	1.013 ± 0.009	94.7
Ag-C (0.2 mM)	0.167 ± 0.016	0.162 ± 0.044	97.0	0.151 ± 0.027	90.6	0.157 ± 0.007	94.4	0.153 ± 0.017	91.7
Ag-C (0.5 mM)	0.481 ± 0.119	0.425 ± 0.060	88.4	0.400 ± 0.052	83.2	0.435 ± 0.045	90.5	0.423 ± 0.045	87.9
Ag-C (1 mM)	1.383 ± 0.179	1.315 ± 0.185	95.1	1.342 ± 0.164	97.1	1.236 ± 0.063	89.4	1.227 ± 0.095	88.7

* % represents the retention rate of silver or selenium after being washed. Retention % = (amount of Ag or Se before being washed/amount of Ag or Se after being washed) × 100. Data represented as mean ± SD, n=3.

As discussed in Chapter 2, the colloidal spherical SeNPs were amorphous and would recrystallize to become trigonal selenium (t-Se) upon heating or sonication. The SEM images of heat treated Se-C are shown in Figure 4.13 – 4.16. It was noticeable that after repeated washing in hot water, the SeNPs lost the smooth and spherical shape and became irregular and pointed (Figure 4.13). With the autoclaved samples (Figure 4.14), it can clearly be seen that the spherical SeNPs merged into each other and became nanorods. The diameters of the nanorods were similar to the nanoparticles, which were mostly around 100 nm. The length could be up to several micrometres. In addition to the long nanorods, some urchin-shaped nanoclusters could also be seen (Figure 4.15). On the Se-C prepared with 0.2 mM Na_2SeO_3 (Figure 4.16), the particles did not grow into nanorods, probably because the particles were too far apart from each other. However, it is still noticeable that the particles were not as spherical as they were before the autoclave process, indicating they have recrystallised and become t-Se. Whether the nanoparticles simply become non-spherical or grow into nanorods/nanoclusters might be dependent on the size and distribution of the original SeNPs, as well as the heat applied.

The antimicrobial activity of t-Se is rarely reported.[207] Wang *et al.*[283] prepared red amorphous SeNPs on the surface of polymer sheet by a chemical reduction method and heat treated the sheet in an oven to turn the red SeNPs into grey crystallised Se nanorods; the anti-biofilm tests against *P. aeruginosa* on the two types of Se nanostructures showed that both types of nano-selenium inhibited the bacterial growth but did not result in significantly different inhibition rates. Therefore, even though the loss of nanoparticles after repeated washing was very limited, any effect on the antimicrobial performance of the washed fabric samples must be investigated. This will be discussed in Chapter 5.

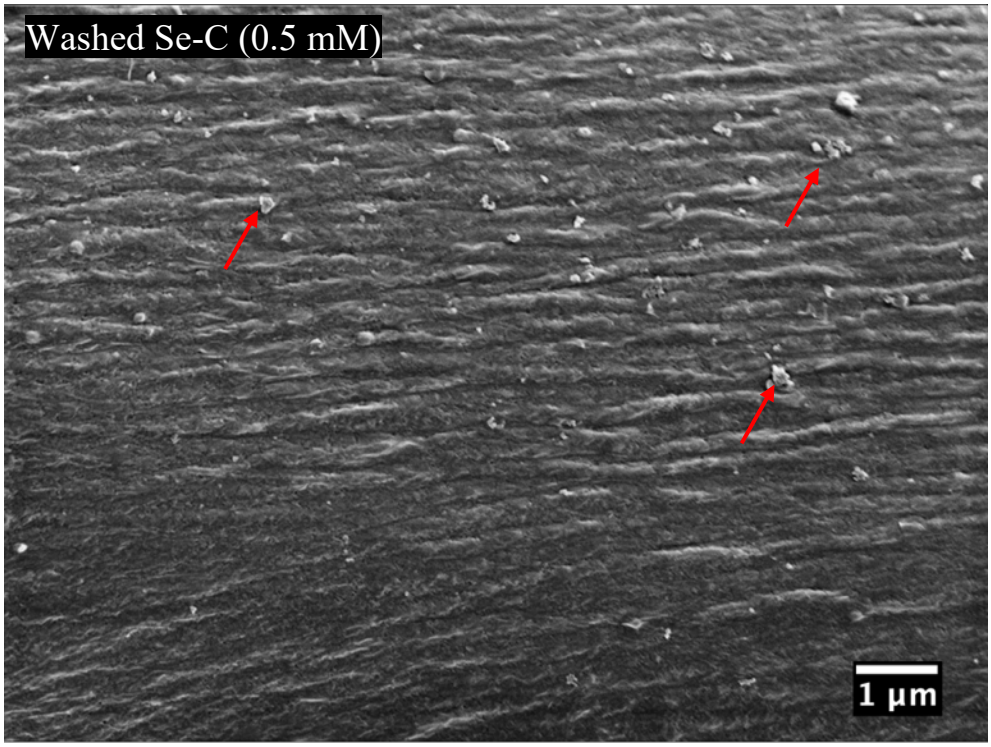

Figure 4.13 SEM image of washed Se-C (0.5 mM) showing non-spherical shapes; red arrows highlight the irregular shaped particles.

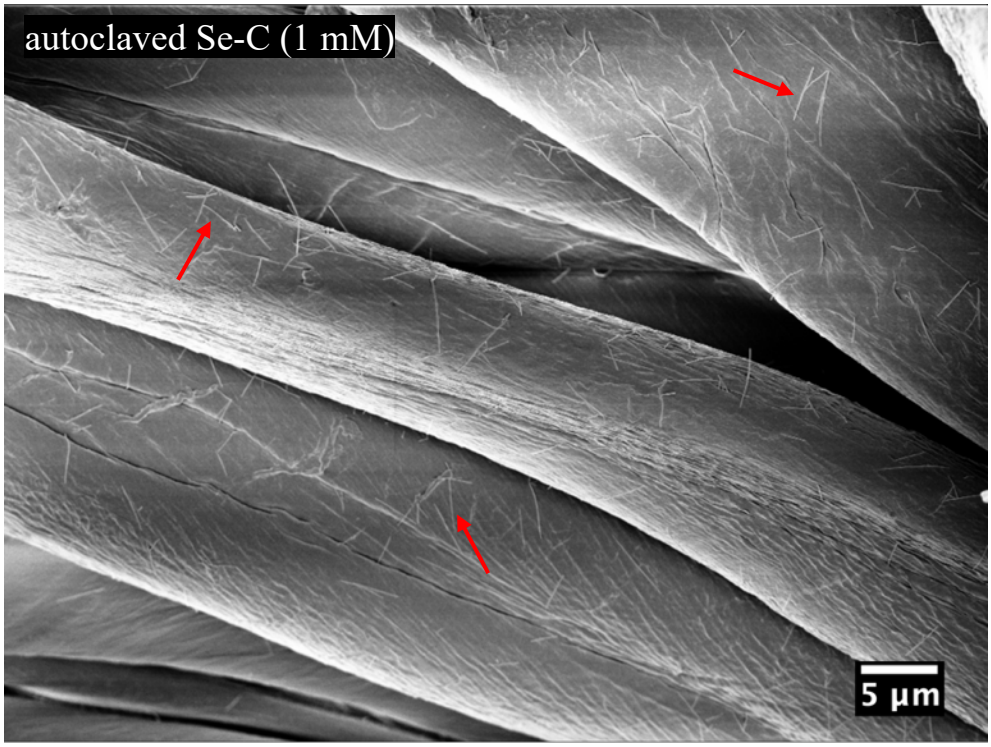

Figure 4.14 SEM image showing Se nanorods on autoclaved Se-C (1 mM); red arrows highlight the nanorods.

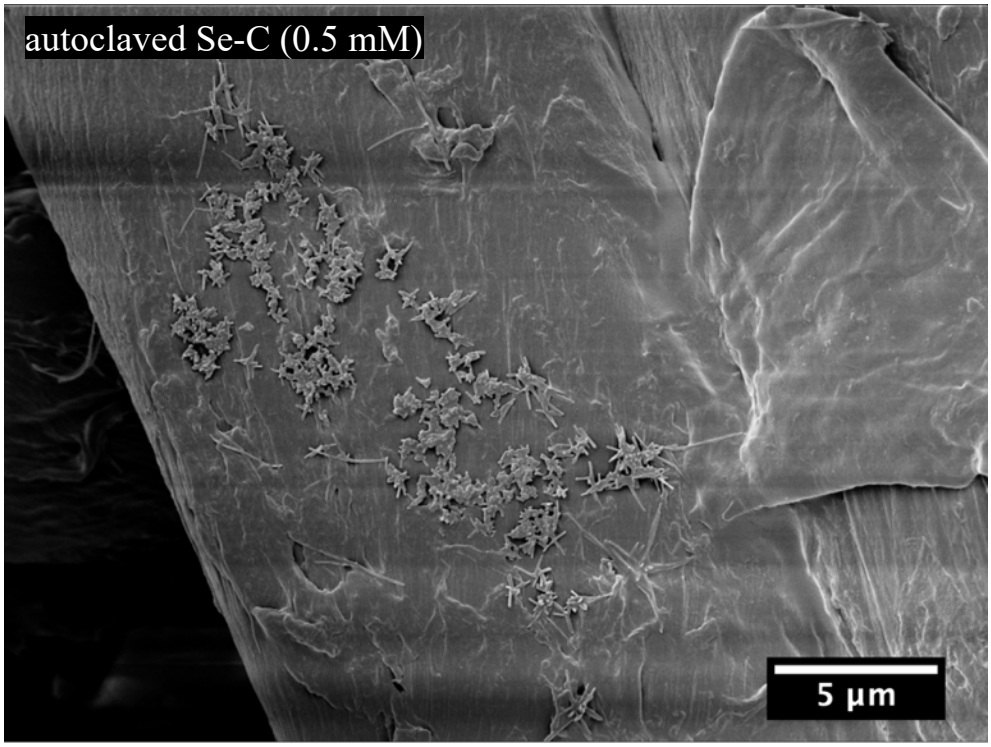

Figure 4.15 SEM image showing urchin-shaped Se nanostructures on autoclaved Se-C (0.5 mM)

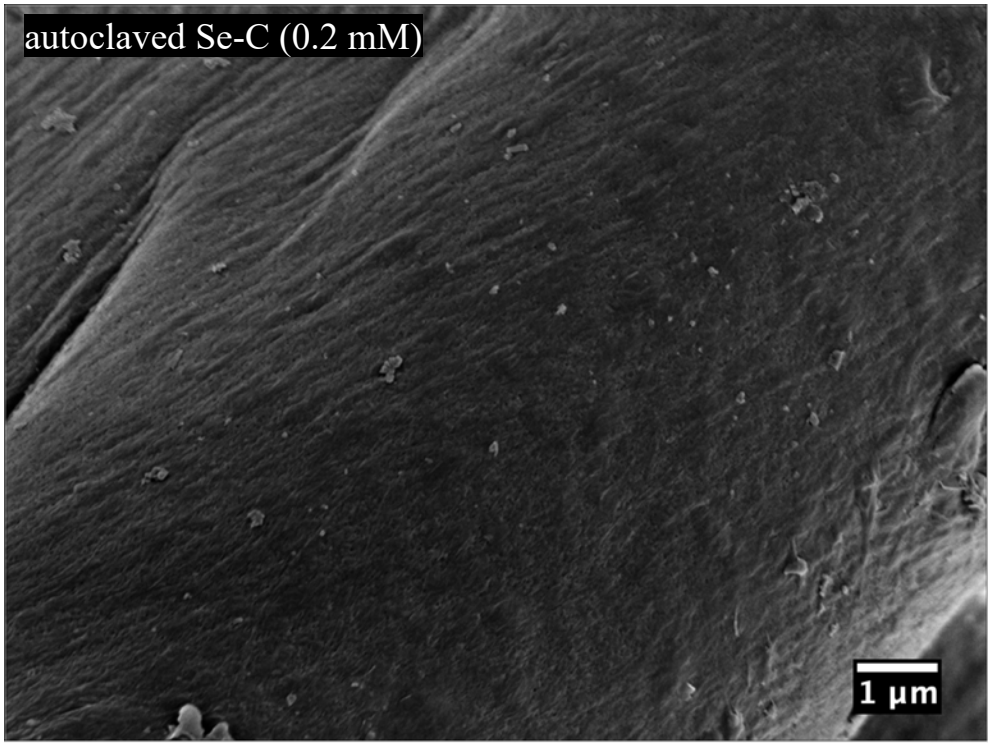

Figure 4.16 SEM image showing irregular shaped SeNPs on autoclaved Se-C (0.2 mM)

4.5 Chapter summary

Based on the results from the previous chapters, and the analysis of the literature, a novel method to functionalise cellulose-based textiles using a cationization agent, CHPTAC, and inorganic nanoparticles (AgNPs or SeNPs) was described in this chapter. The *in situ* synthesis of AgNPs and SeNPs on cationized cotton has not been reported before. The advantages of *in situ* preparation of nanoparticles with the assistance of microwave irradiation include quick and effective synthesis, even particle distribution compared to *ex situ* method, and secure attachment of nanoparticles to the fabric surface. Moreover, *in situ* preparation can be more versatile than *ex situ* approaches. *In situ* methods can be easily adapted and used to treat 3-dimensional porous materials that are difficult for the fixation of *ex situ* prepared NPs. The cationic groups and antimicrobial nanoparticles together may offer combined antimicrobial activities, which lead to excellent antimicrobial performance and increased difficulty for the development of resistance.

The characterisation of the functionalised fabrics showed that the cationic quaternary groups were successfully fixed onto the surface of cotton, which changed the zeta potential of the cotton fibres to the positive range. After the cationization, Ag or Se nanoparticles were prepared *in situ* on the cotton surfaces using ascorbic acid as the reducing agent with the help of microwave irradiation, which makes the nanoparticle synthesis quick, facile and environmentally friendly. Cationized cotton fabrics with a range of different concentrations of AgNPs or SeNPs were obtained by using different concentrations of precursor salts. The formation of the AgNPs or SeNPs were confirmed by visible colour changes and supporting techniques including SEM, EDS, and XPS. The nanoparticles formed *in situ* had relatively narrow size distributions, with most of the AgNPs and SeNPs measured between 40 nm to 140 nm in size. In order to determine the laundry durability of the nanoparticles fixed onto the fabric surface, the Ag or Se concentration per gram of cotton was determined before and after repeated washes in hot water. Prior to the laundering, the amounts of nanoparticles (per gram of cotton) prepared with different concentrations of precursors (0.2 – 1 mM) ranged 0.327 – 1.069 mg/g for SeNPs and 0.167 – 1.383 mg/g for AgNPs. It was found that after 4 accelerated washing cycles, all of the fabric samples retained over 80% of the original nanoparticles formed *in situ*,

indicating excellent laundry durability of the functionalisation. It was also found that the SeNPs would crystallise when subjected to heat treatment (i.e. autoclaving or washing in hot water). The antimicrobial performance of the functionalised fabrics before and after washing would be studied and reported in the next chapter.

Chapter 5 Antibacterial Evaluation of Functionalised Fabrics

5.1 Introduction

The aim of the chapter was to evaluate the antibacterial performance of the cellulose fabrics functionalised with cationic quaternary groups and nanoparticles prepared as described in Chapter 4. A number of standard methods have been established to evaluate the antibacterial efficacy of functionalised textiles. However, there is no consensus on the best method to be used as they all have different advantages and disadvantages. The methods can be divided into two groups: qualitative assessment and quantitative assessment.[284]

Qualitative methods are mainly based on agar diffusion. The test samples are placed onto agar plates that have been inoculated with bacterial cells and the formation of a zone of inhibition is used to determine the antibacterial performance. The advantages of qualitative methods are that they are simple to perform, quick, and suitable for when a large number of samples need to be tested. The most commonly used standards with qualitative methods include American Association of Textile Chemists and Colorists (AATCC) AATCC TM147-2016 (Antibacterial Activity of Textile Materials: Parallel Streak),[285] ISO 20645:2004 (Textile fabrics — Determination of antibacterial activity: Agar diffusion plate test),[286] and Japanese Industrial Standards (JIS) JIS L 1902:2015 (Testing Antibacterial Activity and Efficacy on Textile Products — Halo method).[287] In the AATCC TM147 method, a bacterial inoculum is streaked onto a Nutrient Agar (NA) surface and the textile sample is placed over the streaks, making intimate contact with the bacterial cells and agar surface. The ISO 20645 method involves putting the test sample between two agar layers, with the upper layer containing a bacterial inoculum in it and the lower one being NA only. For the JIS L 1902-Halo method, the bacteria are inoculated into warm molten agar and the test sample is placed onto the agar once it has solidified. The evaluation of results for these 3 methods is based on the size of the halo/zone of inhibition (ZoI) formed around the edge of the samples and the

bacteria growth under the samples. The analysis of positive results from tested samples with diffusible antibacterial agents is shown in Figure 5.1.

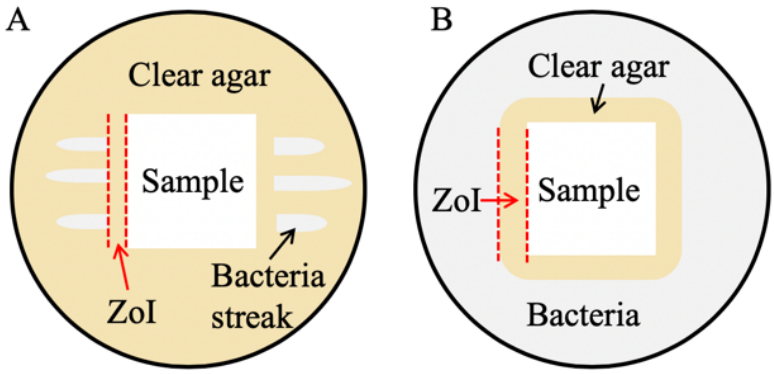

Figure 5.1 Analysis of positive results from (A) AATCC TM147 method and (B) ISO 20645 or JIS L 1902-Halo method.

As discussed in Section 3.1, the zone of inhibition will only be observed when the antibacterial agent is diffusible. The fabrics can show antimicrobial activity when in direct contact with microbes but may not exhibit the effect when assessed via a diffusion assay. Pinho *et al.*[284] compared three standard qualitative evaluation methods (AATCC 147, ISO 20645, JIS L 1902-Halo method). The results demonstrated that only the positive control which was treated with diffusible triclosan formed clear halos, while the tested samples treated with silver ions did not result in any halo; however, with the AATCC 147 and JIS L 1902-Halo methods, the inhibition of bacterial growth could be seen when the fabrics were removed from the agar plate, whereas since with ISO 20645 the sample was placed between two layers of agar and could not be removed, the determination of clear zone under the sample could not be achieved. Therefore, the author concluded that the AATCC 147 and JIS L 1902-Halo methods could be used for both diffusible and non-diffusible fabrics, while ISO 20645 could only be used for samples with diffusible antimicrobial agents. However, it should be noted that even though the test samples with silver ions as the antibacterial agent did not create halos around the sample, silver ions should be a diffusible antimicrobial agent. Many reports have demonstrated the inhibition zones created by silver ions and silver nanoparticles with agar diffusion

Original in colour

methods, as discussed in Section 3.1. The information about how the sample was prepared was not presented in the paper by Pinho *et al*.[284]; it is possible that the silver ions were incorporated into the synthetic fibre before spinning so that the release of ions was very slow. In the JIS L 1902-Halo method, the bacterial cells were mixed with molten agar rather than presented on the surface of agar, and the small clear zones were found under the test specimens, which proved that the silver ions were released into the agar, but not sufficient to form a halo around the fabrics. Therefore, the ability of JIS L 1902-Halo method to test fabrics with non-diffusible antibacterial agent may be questionable. Moreover, when using the AATCC 147 method for samples with non-diffusible antibacterial agents, the bacterial cells under the fabric sample may be carried away together with the fabric during the removal, making it difficult to tell whether the lower bacterial density left on the agar is due to the antimicrobial activity of the fabric. In conclusion, the qualitative methods based on agar diffusion may not be the suitable methods for testing fabrics with non-diffusible antibacterial agents, in which case the quantitative methods can be used to more accurately evaluate the performance of the samples.

Most of the quantitative tests use a method called the "challenge test" (Figure 5.2). The basic procedure of the challenge test involves inoculating the test sample surface with a small volume of bacterial suspension, incubating the sample for a period of time, and then washing the bacterial cells off the sample surface and plating them onto agar plates to determine viable counts. Control samples are used to determine the bacterial growth without the presence of antibacterial agent. The bacterial concentrations at two different time points, "0" contact time and after incubation, are compared to determine the bacterial growth. The typical procedure of a challenge test is illustrated in Figure 5.2. Commonly used standard methods employing a challenge test include AATCC TM100-2019 (Test Method for Antibacterial Finishes on Textile Materials),[288] ISO 20743:2013 (Textiles — Determination of antibacterial activity of textile product: Absorption method),[289] and JIS L 1902:2015 (Testing Antibacterial Activity and Efficacy on Textile Products — Absorption method).[287] Although the procedures are similar, the standards recommend different parameters to evaluate the performance. For example, AATCC 100 requires the calculation of percent reduction of bacteria by the specimen treatments, the ISO 20743-Absorption method provides an equation to calculate the antibacterial activity value. The

parameters to judge the antibacterial performance will be discussed in further detail later in this chapter.

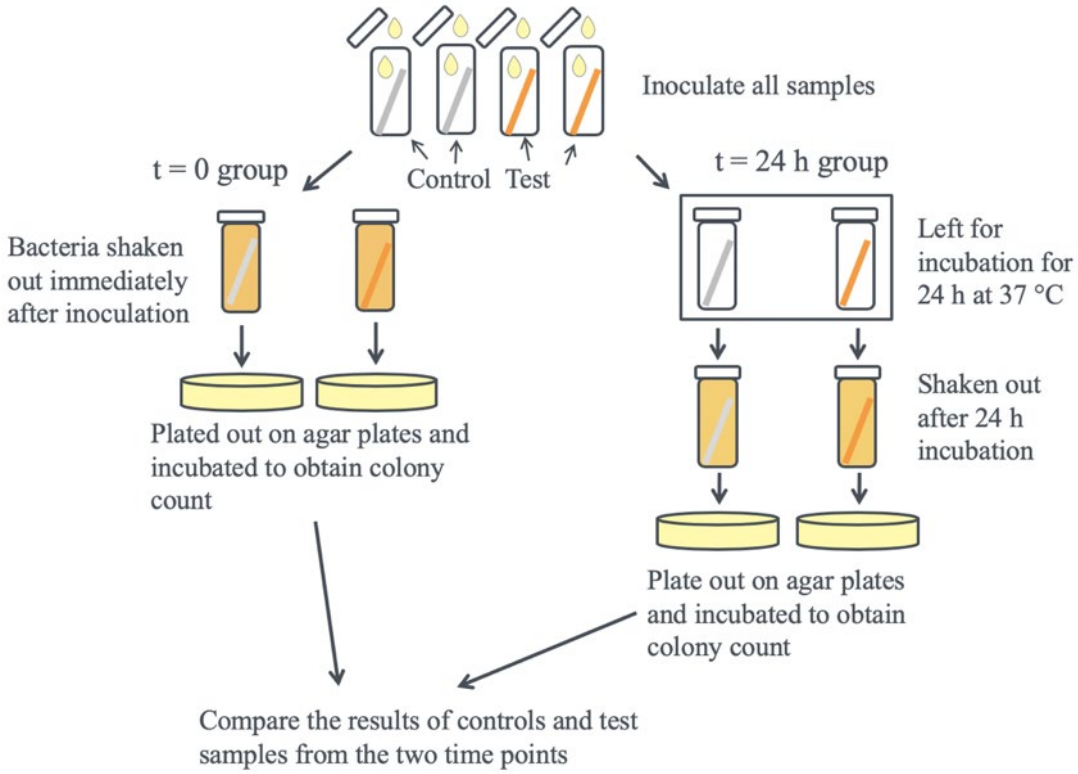

Figure 5.2 Scheme of challenge test for antibacterial textiles.

Another quantitative/semi-quantitative method that can be used to evaluate fabrics with non-diffusible antibacterial agent is the dynamic shake flask method. Standard methods based on the shake flask method have been published by the American Society of Testing and Materials (ASTM E2149)[290] and the International Bureau for Standardisation of Man-made Fibres (BIFSA).[291] In this method, the test samples are immersed in a large amount of liquid bacterial culture in a flask, which is constantly shaken to ensure dynamic contact with the fabric and the bacterial cells even if the antibacterial agent is not diffusible. The standards recommend quantitative analysis by removing samples of the liquid culture at different time points and plating onto agar plates to determine the viable count. Alternatively, a quicker and simpler semi-quantitative test can be performed by removing samples of the liquid culture for optical density measurement instead of viable colony count. However, one of the

issues of this method is the culture condition, where the samples are immersed in liquid culture, can be distinct from real life applications of the fabrics as the fabrics are unlikely to be immersed in nutrient-rich liquid for a long time.

Apart from the standard methods discussed above, many of the assays listed in Table 3.1 can also be applied to textile materials. Haase *et al.*[292] compared 5 different methods to evaluate the antibacterial activities of fabrics modified with silver and copper pigments, including the MTT assay, optical density assay, disk diffusion assay, and plate count method with fabric sample either immersed in bacterial suspension statically or inoculated with a small volume of bacterial suspension. The results showed that the different methods yielded results that were generally comparable. However, it was worth noting that some tests produced some unusual results. For example, the copper-containing samples resulted in the discoloration of bacterial culture media, which affected the OD reading. Moreover, the copper-based agent was not able to diffuse in agar and resulted in no zone of inhibition. Therefore, multiple methods should be employed to avoid misleading or skewed results.

In this chapter, the antibacterial performance of the novel functionalised fabrics prepared in Chapter 4 was evaluated. With the experience from Chapter 3 and the analysis of the literature, several methods were chosen for this chapter. The specific chapter objectives included:

(1) To test the antibacterial performance of the fabric samples quantitatively using a challenge test method with the test conditions recommended by an industry standard ISO 20743:2013-Absorption Method.
(2) To observe the bacterial cells *in situ* on the functionalised fabric surface using LIVE/DEAD staining and confocal microscopy.
(3) To study the effects of the functionalised fabrics on bacterial morphology using scanning electron microscopy (SEM).
(4) To test the antimicrobial performance of the fabric samples after repeated washes using the standard challenge test method to determine the laundry durability of the functionalisation.

5.2 Materials

Nutrient Agar (NA), Nutrient Broth (NB), and Standard Plate Count Agar (PCA) were purchased from Oxoid (UK) and prepared according to the manufacturer's instruction.

Soyabean-Casein Digest broth with Lecithin and Polysorbate 80 medium (SCDLP) was used as the shaking-out medium. To prepare SCDLP medium, 30 g Tryptone Soya Broth powder (TSB, Oxoid), 1 g Lecithin (Fisher Scientific), and 7 g Tween® 80 (Fisher Scientific) were dissolved in 1 L RO water. Peptone salt solution was prepared by dissolving 8.5 g NaCl and 1 g peptone (Fisher Scientific) in 1 L RO water and used as a diluent. All the RO water, culture media, diluents, and saline solutions used in microbiology experiments were sterilised by autoclaving at 121°C for 15 minutes.

Resazurin chromogenic agar (RCA) was used in a supplementary test for the challenge test. RCA was prepared according to a report by Sener *et al.*,[293] by mixing 1 mL of resazurin solution with 100 mL of molten NA; to prepare resazurin solution, resazurin sodium salt (Fisher Scientific) was dissolved in RO water to prepare a solution of 2.5 mg/mL and sterilised by filtration through a 0.2 µm sterilisation filter (Cellulose acetate, Minisart).

The antibacterial activities of the samples were evaluated against *Staphylococcus aureus* (NCTC 10788) and *Klebsiella pneumoniae* (NCTC 11228), as recommended by ISO 20743-2013. *Escherichia coli* (NCTC 10418) was also tested as an additional Gram-negative species to be consistent with the study conducted in Chapter 3. The bacteria were recovered from frozen stock as described in Section 2.2 and inoculated onto PCA plates using the streak plate method. The PCA plates were stored at 4 °C and used within one week. Optical density at 600 nm was used to estimate the bacterial concentration in broth culture, based on the standard curves shown in Figure 3.1.

5.3 Methods

5.3.1 Challenge test

This method was based on the Absorption Method from ISO 20743:2013 (Textiles — Determination of antibacterial activity of textile products).[289] A diagram of this method is shown in Figure 5.2. Briefly, bacterial suspension in dilute broth was inoculated onto the control and test samples, and the bacterial cells were removed from the fabric surfaces at different time points to compare the number of viable bacteria by the plate count method.

5.3.1.1 Preparation of test inoculum

To prepare the test inoculum, single colonies were picked off the PCA plate and inoculated into 10 mL fresh TSB using an inoculating loop. The inoculated broth was incubated at 37 °C at 120 rpm overnight. Subsequently, 0.2 mL of this culture was inoculated into 10 mL of fresh TSB. This inoculum was incubated for a further 2 – 3 h at 37 °C at 110 rpm, after which the expected bacterial concentration reached approximately 1×10^9 CFU/mL (log phase). The concentration was then adjusted to 1×10^5 to 3×10^5 CFU/mL by serial dilution in 1/20 dilute NB (0.65 g/L), which was confirmed by spread plate method.

5.3.1.2 Test procedure

The fabric samples were prepared aseptically, as described in Section 4.3.2. Six specimens were prepared for each type of sample (control sample UC and test samples CC, Se-C and Ag-C), by cutting the samples into 4 cm × 4 cm swatches (0.4 ± 0.05 g). As mentioned in Chapter 4, the SeNPs on the cotton fabrics could turn into t-Se nanorods when subject to heat treatment. In order to investigate if the Se nanorods also exhibit antibacterial activity, autoclaved Se-cotton (1 mM tSe-C) was also tested. Aliquots of the bacterial inoculum (0.2 mL) were pipetted over the surface of all the specimens in individual universal containers. Care was taken not to touch the inner wall of the vial. Immediately after the inoculation, 20 mL of SCDLP

was added to 3 specimens of each type of sample. The vials were shaken vigorously on a vortex mixer for 5 s × 5 cycles to remove the bacterial cells from the specimens. The bacteria in SCDLP were then serially diluted and plated into PCA in duplicate using the pour plate method to determine the number of viable bacteria. These specimens are referred to as the time zero (t_0) group. The remaining 3 specimens of each type of sample were incubated at 37 °C for 24 ± 3 hours after the inoculation. After incubation, the specimens were treated in the same way with SCDLP as the t_0 group and referred to as time 24 h (t_{24}) group. When there were no viable colonies found in the plate, the number was recorded as 1 colony, as indicated by the standard. The whole experiment was repeated on individual occasions until 3 sets of valid data (according to the criteria in Section 5.3.3.3) were obtained.

5.3.1.3 Judgement of test effectiveness

The ISO 20743:2013 standard includes guidelines for judging the effectiveness of the test. These are outlined below:

i. The concentration of the test inoculum falls within the range of 1 – 3 x 10^5 CFU/ml.

ii. Differences in extremes for the three control fabrics immediately after inoculation and after incubation respectively should be < 1 log.

iii. The growth value (explained in Section 5.3.1.4) calculated according to the formula below should be ≥ 1.0 by the plate count method.

5.3.1.4 Calculation of antibacterial activity

When the test had been judged effective, the antibacterial activity was obtained using the following formula:

Equation 5.1: $A = (\log_{10} C_{24} – \log_{10} C_0) – (\log_{10} T_{24} – \log_{10} T_0) = F – G$

Where

A is the antibacterial activity value;

F is the growth value on the control fabric ($F = \log_{10} C_{24} – \log_{10} C_0$);

G is the growth value on the coated/impregnated fabric ($G = \log_{10} T_{24} – \log_{10} T_0$);

$\log_{10} C_{24}$ is the average common logarithm for the number of bacteria (CFU) obtained from three control samples after 24 ± 3 h incubation;

$\log_{10} C_0$ is the average common logarithm for the number of bacteria (CFU) obtained from three control samples immediately after inoculation;

$\log_{10} T_{24}$ is the average common logarithm for the number of bacteria (CFU) obtained from three antibacterial functionalised samples after 24 ± 3 h incubation;

$\log_{10} T_0$ is the average common logarithm for the number of bacteria (CFU) obtained from three functionalised samples immediately after inoculation.

In case of $C_0 > T_0$, substitute C_0 for T_0. According to Annex F of ISO 20743:2013, the antibacterial efficacy of the test fabric can be considered as “significant” when $2 \leq A < 3$ and “strong” when $A \geq 3$.

Apart from the antibacterial activity value, the growth reduction (R%) in the numbers of viable/live bacteria after incubation was calculated using the following equation:

Equation 5.2: $R\ (\%) = (C_{24} – T_{24})/C_{24} \times 100$

5.3.2 Resazurin chromogenic agar

Resazurin chromogenic agar (RCA) was use in a supplementary test conducted alongside the challenge test. Control and test specimens were cut into 2 cm × 2 cm squares and used for RCA supplement tests; 2 specimens were prepared for each type of sample and were used for the t_0 and t_{24} groups respectively. The specimens were inoculated in the same way as described in Section 5.3.1.2. For the t_0 group, immediately after inoculation, the specimens were taken out of the test tubes, rinsed gently in 10 mL sterile physiological saline, and then placed onto RCA plates. For the t_{24} group, the same procedure was carried out after the samples were incubated for 24 ± 3 hours after the inoculation. The RCA plates were incubated at 37 °C for 18 – 24 h and the colour change was observed.

5.3.3 *In situ* observation of bacteria using confocal laser scanning microscopy

The viability of the bacteria after incubation with the fabric samples was visualised by LIVE/DEAD™ Baclight™ Bacterial Viability Kit and confocal laser scanning microscopy (CLSM). Since the fabrics have a complex 3-dimensional structures which makes it difficult to locate the bacterial cells under the microscope with high magnification, a high inoculum concentration was used for microscopic examination to ensure bacterial coverage on the fibres. Moreover, the inoculum was prepared in saline to avoid broth constituents interfering with components of the LIVE/DEAD stain, as indicated by the manufacturer's instructions.[294] A liquid culture in TSB (OD_{600nm} approximately 1), prepared as described above, was centrifuged in Eppendorf tubes at 5,000 g for 5 mins. The supernatant was discarded, and the cells were re-suspended in 0.85% physiological saline. The washing procedure was carried out twice.

Sterile fabric samples were cut into square swatches of 0.5 cm × 0.5 cm and placed into Eppendorf tubes individually. Bacterial suspension (10 µL) was then inoculated onto the fabric surfaces and incubated at 37 °C for 24 ± 3 h. After the incubation, the fabric samples were disassembled carefully with sterile forceps into loose yarns and

fibres and placed onto microscope slides. The staining reagent containing SYTO 9 and propidium iodide (PI) was prepared according to the manufacturer's instructions and dropped (10 µL) onto the samples. Glass cover slips (22 mm × 22 mm) and DPX mountant (SureChem) were used to seal the samples. The samples were incubated at room temperature for at least 15 mins before being examined using a Leica SP5 Confocal Laser Scanning Microscope. Excitation was performed using an Argon laser (488 nm) for both dyes with power set to 25%. SYTO 9 emission was measured at 510 to 550 nm and PI emission at 610 to 650 nm. Z-stack images were acquired at 1 µm intervals (20 – 30 µm thick) and orthogonal projections were constructed.

5.3.4 Effect of functionalised fabrics on bacterial morphology

Control (UC) and test (CC, Se-C and Ag-C) fabric samples were inoculated with a bacterial suspension as described above. After 24 h incubation, the samples were washed twice with 1 mL sterile PBS and fixed with 2.5% glutaraldehyde (in PBS) for 2 h at room temperature. After the fixation, the samples were washed with PBS twice and then dehydrated with a series of graded ethanol solutions (35%, 50%, 75%, 95%, 100%, for 15 mins each and twice for 100%). Finally, the samples were air dried for two days and left in a desiccator overnight. Prior to the SEM examination, the samples were coated with 4 nm platinum by sputter coating and examined as previously described in Section 4.3.3.2.

5.4 Results and discussion

5.4.1 Challenge test

The principle of the challenge test is to inoculate the antibacterial fabric with bacterial suspension and compare the numbers of viable bacterial cells before and after the incubation. In addition to the antibacterial activity value ('A' value) introduced by the ISO 20743 standard, another value growth reduction (R%) was also calculated. They both describe the difference in the number of viable bacteria on

the test samples compared to the control samples after incubation. On the control fabrics, the number of viable bacteria should increase during the incubation. If the test fabrics have antibacterial activity, then the number of viable bacteria on the test samples of t_{24} group should be less than the number of viable bacteria on the control fabrics. An 'A' value of 2 represents a 2 $\log_{10}$ reduction, which is equivalent to 99% of growth reduction R%. The interactions between the bacteria and the various fabric samples are summarised in Figure 5.3 and Table 5.1.

It is noticeable from Figure 5.3 that even at time zero, the numbers of bacteria recovered from the fabric samples were significantly smaller than the inoculum, which indicated that not all of the bacteria were successfully eluted from the fabric surfaces, especially from the functionalised samples with cationic charge (i.e. CC, Ag-C and Se-C). The three bacterial species reacted differently in terms of the removal from the cotton fabrics. Compared to *K. pneumoniae* (Figure 5.3 B) and *E. coli* (Figure 5.3 C), it was easier to remove *S. aureus* (Figure 5.3 A). It was particularly difficult to remove *K. pneumoniae* from the fabric surfaces, probably because *K. pneumoniae* is capsulated with viscous extracellular layers mainly composed of polysaccharides, which protect the cells and facilitate attachment to surfaces.[295] The negative charge on the polysaccharides makes it even more difficult to remove the cells from cationic surfaces. The numbers of *K. pneumoniae* recovered from the control samples immediately after inoculation (1.8×10^4 CFU) were smaller than the number of bacteria inoculated onto the surface (2.9×10^4 CFU), and the differences between the numbers of bacteria recovered from the control samples and the functionalised samples could be as large as 10 to 30-fold. The observation that it was more difficult to remove *K. pneumoniae* and *E. coli* than *S. aureus* from the fabrics was probably because these cells are rod shaped, which resulted in larger contact area between the bacterial cells and the fabric surfaces than with *S. aureus* which are cocci. In summary, from the viable count results at time zero, it could be seen that not all bacterial cells were successfully removed from the fabrics, and the ease with which they could be removed varied between species.

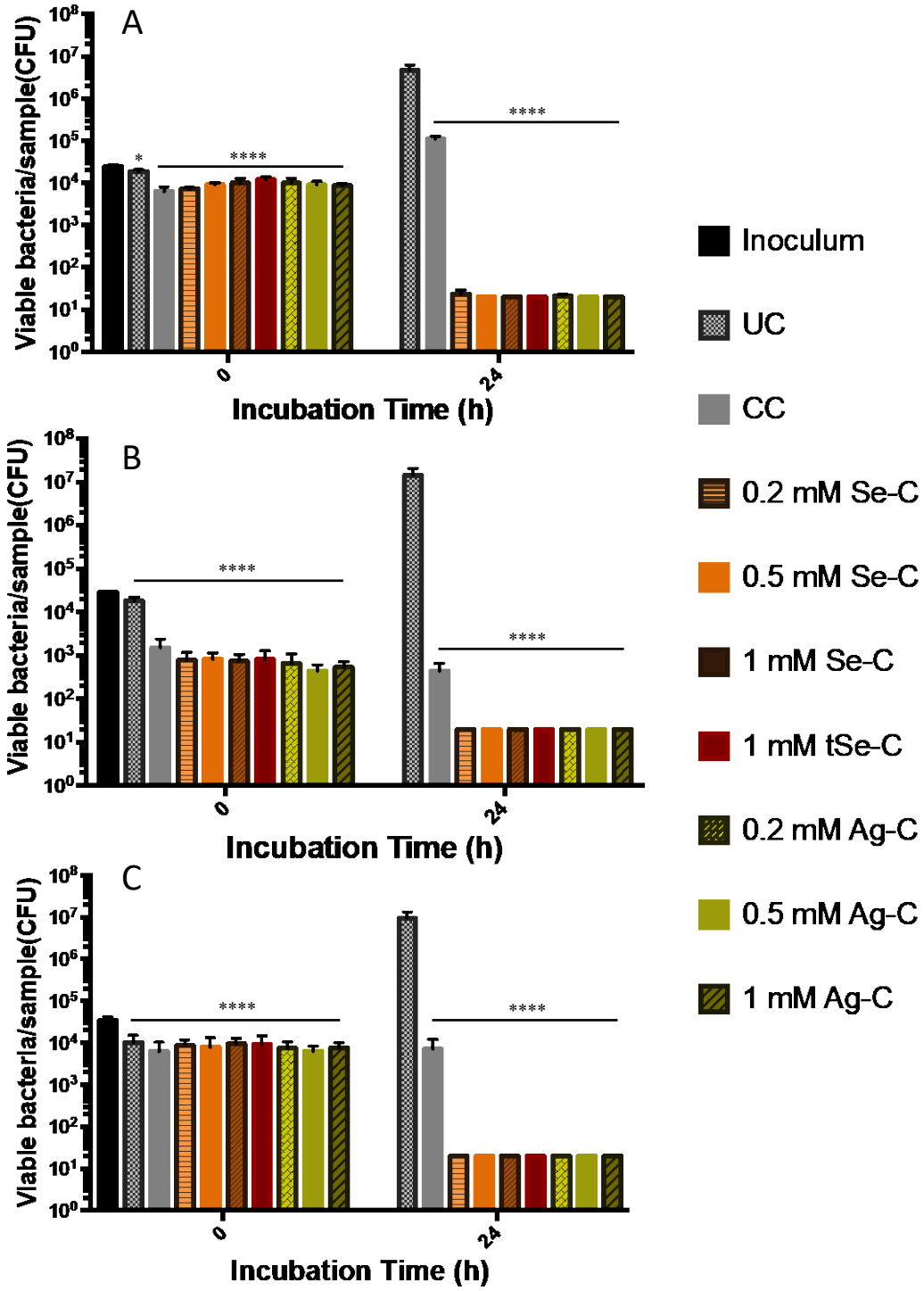

Figure 5.3 Viable counts of bacteria recovered from the cotton samples at time zero (sampled immediately after inoculation) and after 24-h contact; (A) *S. aureus*, (B) *K. pneumoniae* and (C) *E. coli.* Data represent mean ± SD, n=3.

As discussed in Section 1.3, the electrostatic interaction between bacterial cells and the antibacterial agent is one of the important modes of actions of antibacterial agents. The antibacterial effects of CHPTAC-modified cellulose materials have been reported by several recent studies.[259–261] It is believed that the negatively charged bacterial cells could be adsorbed onto the cationic surface and the cell membranes could be physically damaged due to the electrostatic interactions and the penetration of lipophilic alkyl groups, causing the leakage of cell constituents.[296,297] The cationic groups could also lead to the uneven distribution of moisture and nutrients.[298] Eventually, the bacteria could die from altered osmotic pressure, membrane damage and lack of nutrients.[296–299] As can be seen from Table 5.1, it was found that the antibacterial efficacy of the cationized cotton against *S. aureus* was lower than against the two Gram-negative strains, although the growth reduction rate against *S. aureus* was still as high as 97.51%. *S. aureus* may be less susceptible to the cationic cellulose due to the fact that the Gram-positive bacterial cell wall has a comparatively thicker and more rigid peptidoglycan layer than Gram-negative strains.[300] The net negative surface charge of Gram-positive bacteria is also less negative than Gram-negative strains due to the different chemical composition of the bacterial cell walls.[122] Furthermore, as mentioned above, the contact area between the spherical *S. aureus* cells and the cellulose surface is likely to be less than between the rod-shaped *K. pneumoniae* and *E. coli* cells and the surface. Therefore, the cationized cotton showed stronger antibacterial efficacies against *K. pneumoniae* and *E. coli* than against *S. aureus*.

Table 5.1 Growth reduction rate (R %) and antibacterial value 'A' of the modified cotton samples after 24 h contact time

Sample	*S. aureus*		*K. pneumoniae*		*E. coli*	
	R (%)	'A'	R (%)	'A'	R (%)	'A'
C-C	97.51	1.61	>99.99	4.52	>99.99	3.24
Se-C (0.2 mM)	>99.99	5.30	>99.99	5.83	>99.99	5.66
Se-C (0.5 mM)	>99.99	5.36	>99.99	5.83	>99.99	5.66
Se-C (1 mM)	>99.99	5.36	>99.99	5.83	>99.99	5.66
tSe-C (1 mM)	>99.99	5.36	>99.99	5.83	>99.99	5.66
Ag-C (0.2 mM)	>99.99	5.33	>99.99	5.83	>99.99	5.66
Ag-C (0.5 mM)	>99.99	5.36	>99.99	5.83	>99.99	5.66
Ag-C (1 mM)	>99.99	5.36	>99.99	5.83	>99.99	5.66

In contrast, it was found that both Se-C (including tSe-C) and Ag-C prepared with all of the three different concentrations of precursor salts (0.2, 0.5 and 1 mM) showed strong antibacterial performance, with growth reduction rates all above 99.99% and 'A' values all above 5 for both Gram-positive and Gram-negative strains. The autoclaving and transformation of SeNPs into selenium nanorods did not result in the loss of antibacterial activity. The numbers of viable bacteria recovered from almost all of the NP-functionalised fabrics, with the exception of 0.2 mM Se-C and Ag-C against *S. aureus*, after 24 h contact time, were lower than the limit of detection (LOD, 100 CFU/ml or 20 CFU/sample). Therefore, under the test conditions recommended by ISO 20743:2013, the actual antibacterial performance of the Se-C and Ag-C with different concentrations of SeNPs and AgNPs could not be differentiated. Overall, it can be seen that the cationized cotton alone had already demonstrated moderate antibacterial activity against *S. aureus* and strong

antibacterial activity against *K. pneumoniae* and *E. coli*; the incorporation of SeNPs or AgNPs, even at a low concentration, further improved the antibacterial efficacies of the fabrics. It has been widely reported that the positive surface charge of nanoparticles can enhance their antibacterial performance by facilitating the interaction between the negatively-charged bacterial cells and nanoparticles.[169,301] In this chapter, although the positive charge was not directly applied onto the nanoparticle surface, the presence of cationic groups on the cotton surface, as the substrate for the nanoparticles, could also force contact between the bacterial cells and the nanoparticles.

5.4.2 Supplementary tests with resazurin chromogenic agar

As discussed above, not all of the bacterial cells could be removed from the fabrics even immediately after inoculation, and the effect was especially noticeable with *K. pneumoniae*. Although after 24-h incubation, from the NP-functionalised fabrics, the number of bacteria recovered from the samples was lower than the LOD, the difficulty of eluting bacteria from the samples made it possible that the <LOD results were an artefact of failing to remove the viable bacteria from the sample surfaces. Therefore, a supplementary test was designed in addition to the Absorption Method to further confirm the results. Resazurin chromogenic agar (RCA, Nutrient Agar supplemented with resazurin) was used to provide a direct indication as to whether there was viable cell activity from the fabric surface. Resazurin (7-hydroxy-10-oxidophenoxazin-10-ium-3-one, sodium) is a blue dye, itself weakly fluorescent until it is irreversibly reduced to the pink coloured and highly red fluorescent resorufin. It is used as an oxidation-reduction indicator in cell viability assays for both aerobic and anaerobic respiration. Figure 5.4 shows the colour change of RCA plate when *K. pneumoniae* was inoculated using the streak plate method. It can be seen that the agar changed from purple to pink around the bacterial colonies.

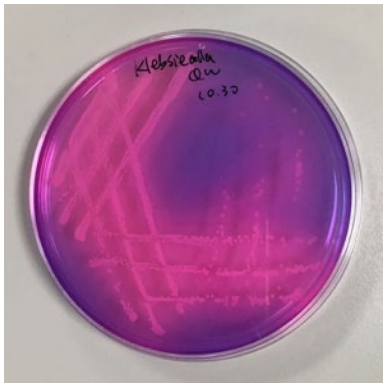

Figure 5.4 Colour change of RCA plates inoculated with *K. pneumoniae.*

The bacterial growth and inhibition/killing are dynamic processes. When placed in an environment that is more favourable for the bacterial growth, the growth and inhibition dynamics can change. The idea of the RCA test was to place the fabric samples along with the inoculated bacteria onto the chromogenic agar at different time points to compare the colour changes. The fabric sample on RCA plates turning pink indicates there was viable bacterial activity during the period when the inoculated sample was in contact with the RCA; no colour change on the sample indicates there was no viable bacteria on the sample by the time it was placed on the RCA. For the t_0 group, immediately after inoculation, the fabric samples were placed onto the RCA plates. The RCA is relatively nutrient-rich compared to the 1/20 dilute NB which was used to prepare the inoculum and, therefore, the bacteria might be able to grow on the samples on RCA and the colour changes were expected as a control. On the other hand, after the inoculated samples were incubated in universal containers for 24 h, as the results of the challenge test suggested, there should be no or very few viable cells left on the functionalised fabric samples, and consequently, no colour change on RCA was expected with these samples.

Figure 5.5 shows the colour changes of RCA plates incubated with the fabric samples inoculated with *S. aureus*. It can be seen that all the samples in the t_0 group showed some colour change, which indicated that when in contact with RCA, the antibacterial performance of these fabric samples was not strong enough to totally inhibit the cell metabolism activity. However, it is also noticeable that the samples prepared with 1 mM selenium precursor (with both spherical SeNPs and autoclaved

Se nanorods) only turned pink very slightly compared with other samples. The colour change was so weak that the pink colour was almost covered by the original colours of the samples. This difference might indicate that the Se-C prepared with 1 mM Na_2SeO_3 had the strongest inhibition effects against the *S. aureus* among all the samples. It might also indicate that the 1 mM tSe-C with was still more effective against *S. aureus* than the other samples after the SeNPs were turned into Se nanorods by autoclaving. For the t_{24} group, all the NP-functionalised samples did not change colour, which is in accordance with the results from the challenge test where the numbers of viable bacteria recovered from the NP-functionalised samples after 24-h contact were below LOD.

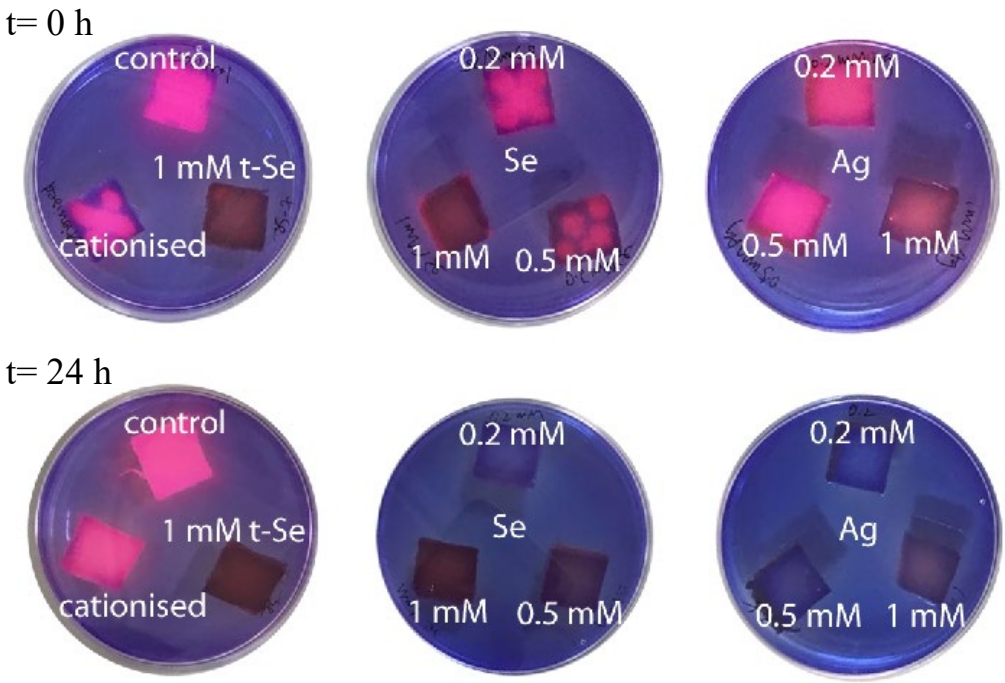

Figure 5.5 Colour changes of the samples on RCA plates incubated with *S. aureus*.

The RCA plates with samples inoculated with *K. pneumoniae* and *E. coli* are shown in Figure 5.6 and Figure 5.7 respectively. With the t_{24} group, the colours of all the NP-functionalised samples remained unchanged, which again confirmed the results obtained from the Absorption method that after 24-h contact time with the dilute NB as the inoculum media, no viable bacteria could be detected from the NP-functionalised samples. When comparing with the t_0 group in Figure 5.5, it can be

Original in colour

seen that the Se-C inoculated with *K. pneumoniae* and *E. coli* are visibly pinker than when inoculated with *S. aureus*, which is in accordance with the findings from Chapter 3, that SeNPs showed better antibacterial performance against *S. aureus* than against Gram-negative strains including *K. pneumoniae* and *E. coli*. On the other hand, the colour changes on the Ag-C inoculated with *K. pneumoniae* and *E. coli* were less significant than the colour changes with *S. aureus*. This is also in accordance with the findings from Chapter 3 that AgNPs were more effective at inhibiting Gram-negative bacteria than Gram-positive bacteria. Another noticeable thing is that even in the t_0 group, the Ag-C prepared with 0.2 mM $AgNO_3$ barely changed colour when incubated with *K. pneumoniae* and *E. coli*. This is a strange result which seemed unreasonable because the antibacterial performance of the nanoparticles should be concentration dependent. On the other hand, as mentioned in Section 4.4.3 (Figure 4.9), the size of the AgNPs on the 0.2 mM Ag-C was the smallest. It is known that the antibacterial performance of AgNPs is also dependent on the particle size. Therefore, it is possible that the although the number of AgNPs on the 0.2 mM Ag-C was the smallest, the size-dependent effect was more significant than the concentration-dependent effect in this case. However, it does not mean that the 0.2 mM Ag-C has the best performance against *K. pneumoniae* and *E. coli*, because the result of the antibacterial test can be dependent on the test conditions including inoculum concentration, incubation length and culture medium. For example, if the inoculum concentration was increased, the number of AgNPs might not be sufficient on the 0.2 mM Ag-C to inhibit the bacterial growth; in other words, the chance that a bacterium landing on the fabric but not in contact with a nanoparticle would be increased. Another point to consider is that in the RCA test, the fabrics were placed onto semi-solid agar and the small AgNPs might quickly release Ag ions which diffused to adjacent area and killed the bacteria before they had time to grow, while in the challenge test, only a small volume of liquid was applied onto the fabrics and the environment was dryer than when in contact with the agar and, therefore, the diffusion of Ag ions was limited. From the practical point of view, the challenge test may better mimic the real-life situation. Moreover, the durability and safety issues will also need to be considered for the overall performance of the fabric. In conclusion, this issue will need further investigation.

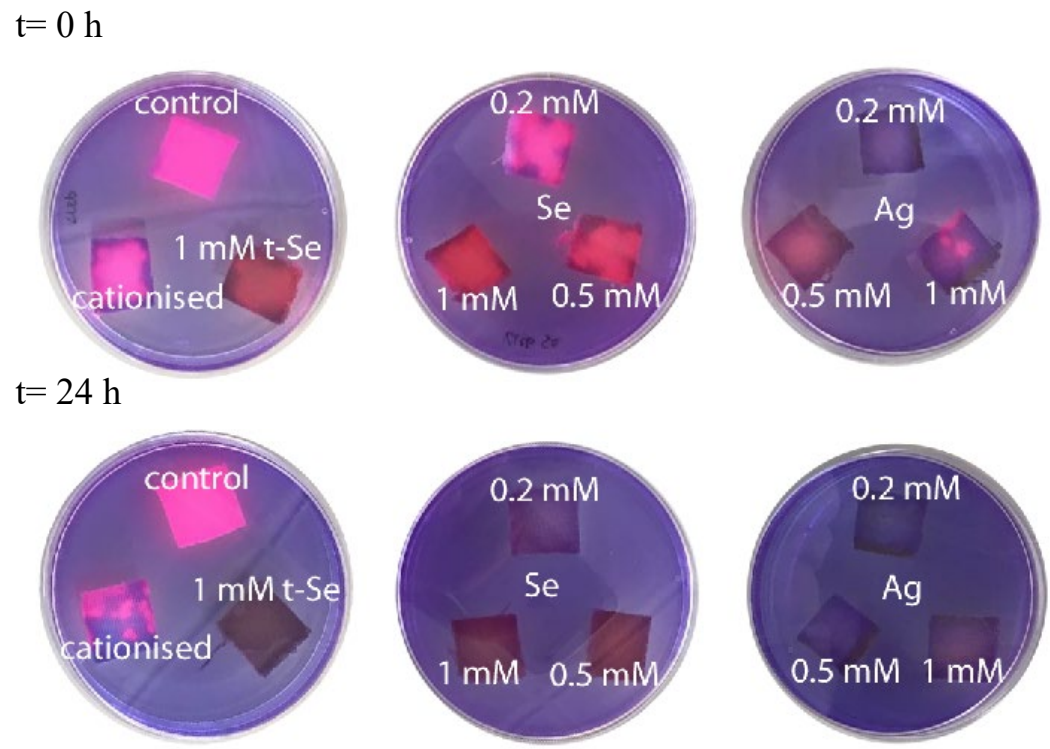

Figure 5.6 Colour changes of the samples on RCA plates incubated with *K. pneumoniae*.

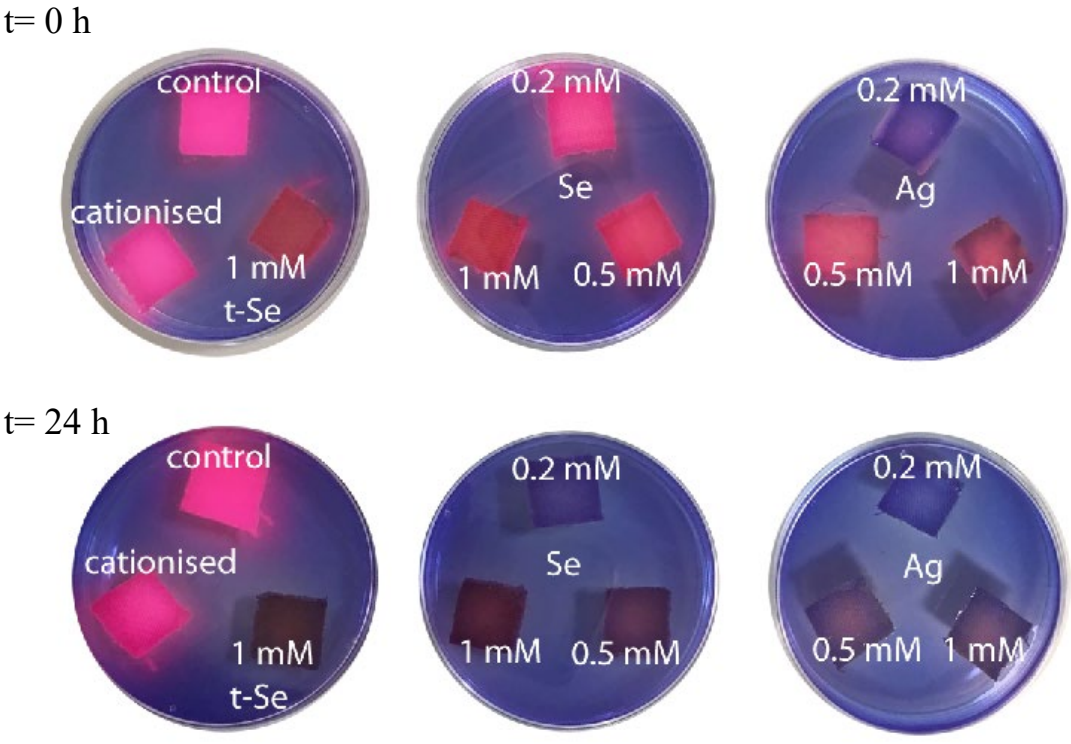

Figure 5.7 Colour changes of the samples on RCA plates incubated with *E. coli*.

Original in colour

5.4.3 *In situ* observation of bacteria using confocal laser scanning microscopy

Confocal laser scanning microscopy and LIVE/DEAD staining was used to directly observe the status of the bacterial cells in contact with the fabric samples (Figure 5.8 – Figure 5.10). Using confocal microscopy to conduct *in situ* observation avoids the uncertainty inherent in a bacterial removal procedure; for example, when conducting an *ex situ* observation, the dead cells may be removed more easily from the fabrics than the live cells, which may lead to erroneous results. Since the inoculum was prepared in physiological saline rather than broth, this assay determined cell death only, without cell growth effects.

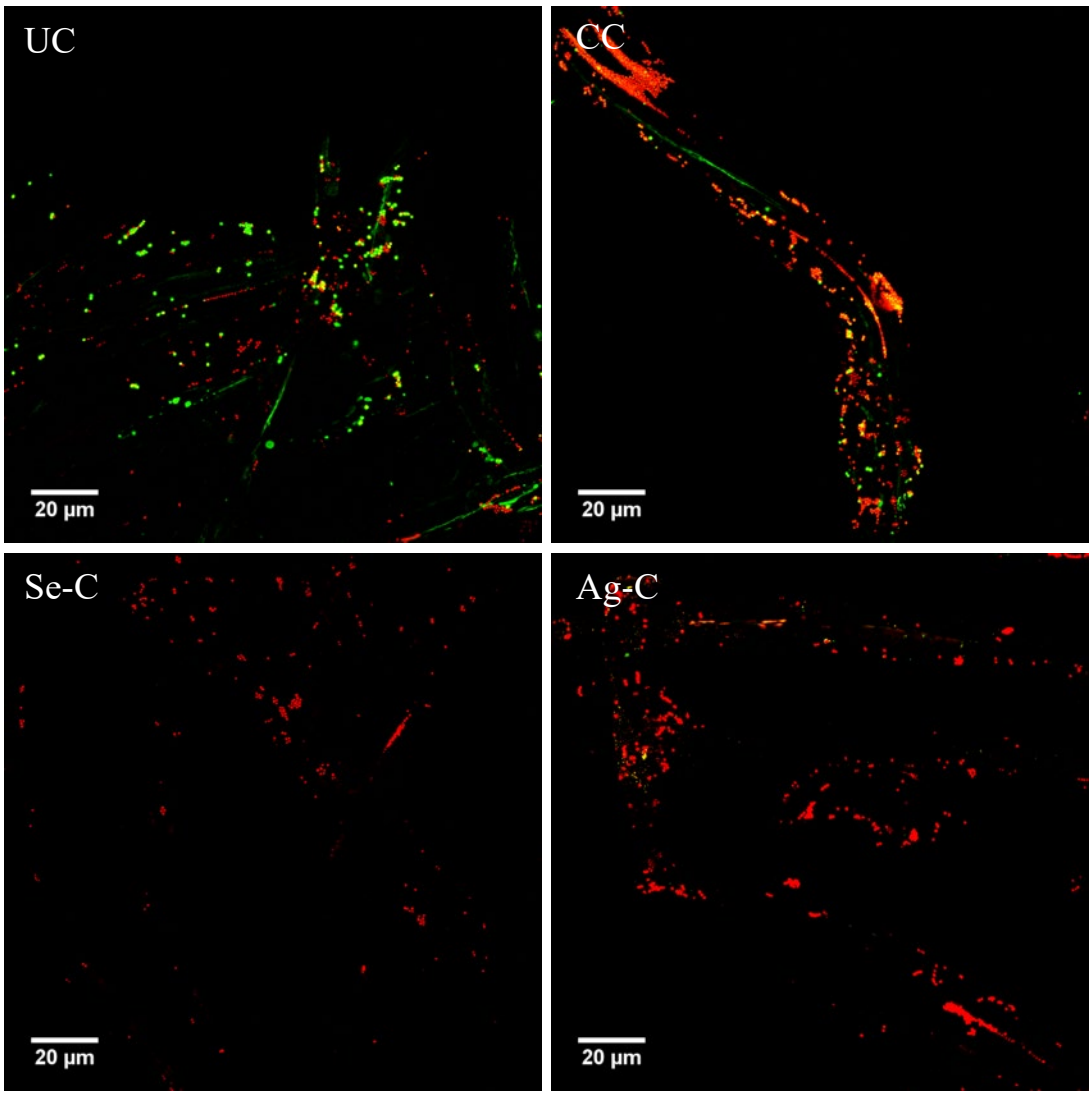

Figure 5.8 Confocal microscopy images of *S. aureus* cells in contact with the fabric samples for 24 h; green=live, red=dead.

Original in colour

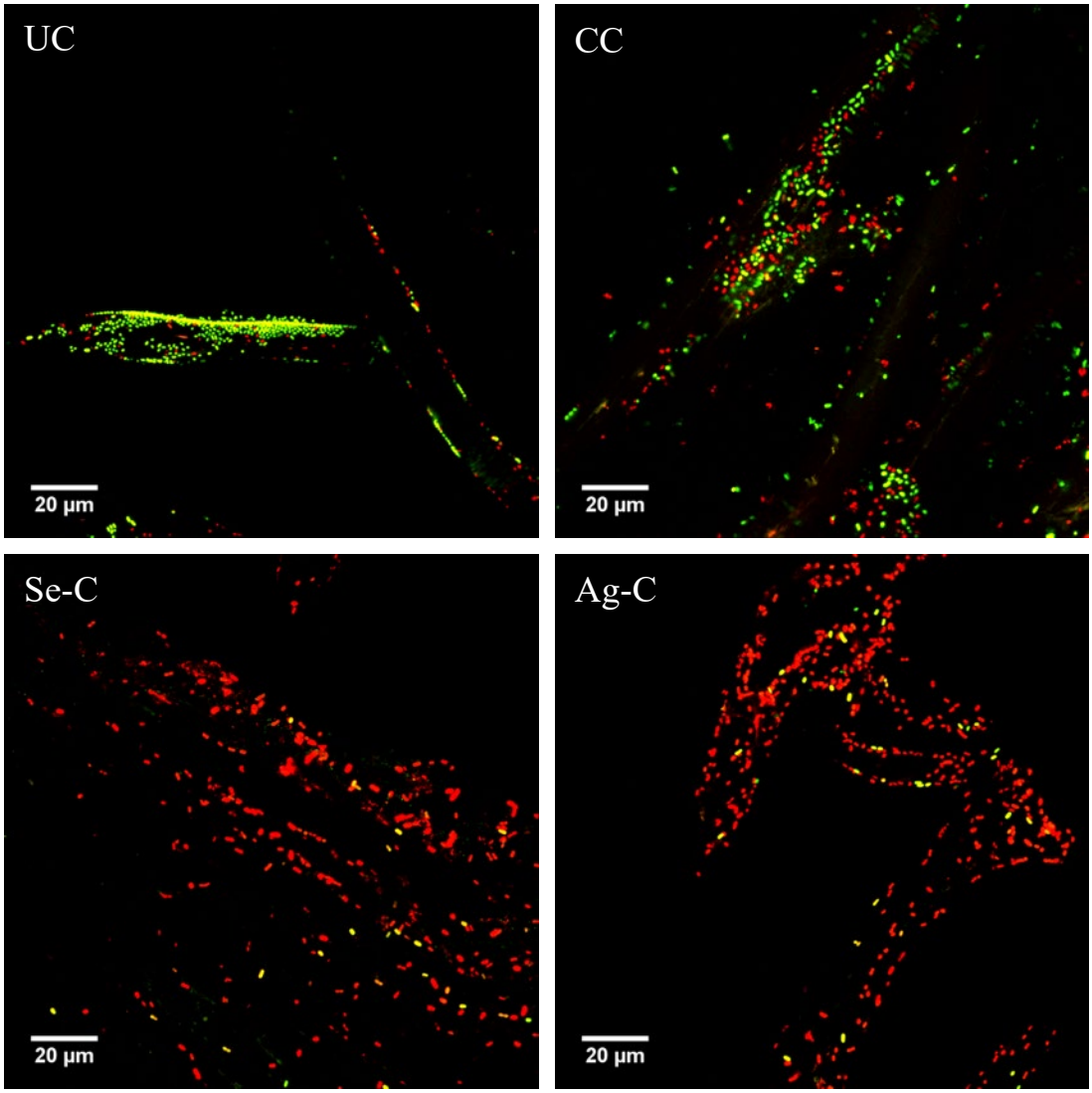

Figure 5.9 Confocal microscopy images of *K. pneumoniae* cells in contact with the fabric samples for 24 h; green=live, red=dead.

Original in colour

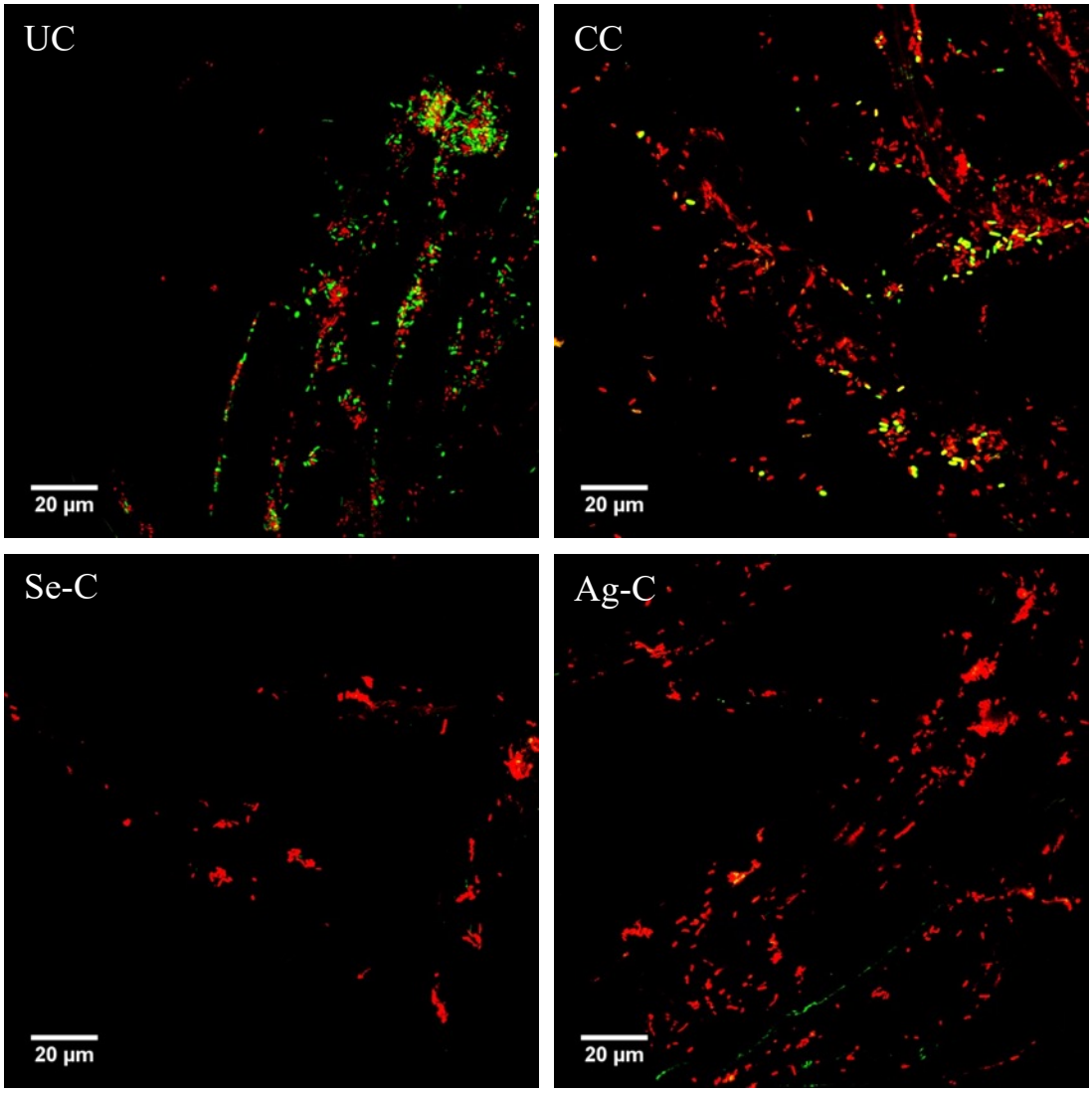

Figure 5.10 Confocal microscopy images of *E. coli* cells in contact with the fabric samples; green=live, red=dead.

The bacterial LIVE/DEAD staining kit contains SYTO 9 green-fluorescent nucleic acid stain, which labels both intact live cells and membrane-damaged cells, and propidium iodide (PI), the red-fluorescent nucleic acid stain, which can only penetrate damaged cell membranes of dead or dying cells with compromised membrane integrity. PI causes reduced fluorescence of green SYTO 9 when both dyes are present such that the dead cells would present as red in colour.[294] As can be seen from Figure 5.8 – 5.10, on the UC, there were considerable numbers of live cells (green) of all the three bacterial strains, while there were also dead cells (red). Some cells will die naturally due to nutrient limitation on the untreated cotton

Original in colour

samples. When examining the cationized cotton, it is noticeable that the number of dead cells increased for all three of the strains compared with the UC. It is also evident that there were many yellow/orange coloured cells, especially of *S. aureus* (Figure 5.8). The intermediate colours (yellow and orange) of the cells are due to the varying amounts of PI entering the cells, indicating different degrees of damage to the cell membrane, and thus these cells are often considered to be sub-lethally injured.[302,303] The results of the Absorption Method showed an increase in the number of *S. aureus* cells over the 24 h incubation period (Figure 5.3). Therefore, it can be postulated that the cationic quaternary groups of the cationized cotton can compromise the membrane integrity of the *S. aureus* cells, but the effects may not always be lethal. Furthermore, in the Absorption Method, the bacterial inoculum was prepared in dilute broth, and therefore, the dynamics between bacterial cell growth and antibacterial effects would be different from the LIVE/DEAD assay where the inoculum was prepared in saline. In dilute broth, overall cell growth could occur when the damage was not significant or not as fast as the cell reproduction.

It is clear that almost all of the bacterial cells on the Se-C and Ag-C samples were dead after 24 h contact time. Small numbers of *K. pneumoniae* cells appeared to be yellow on the Se-C and Ag-C samples, indicating that the integrity of these cells was compromised at least (Figure 5.9). As discussed above, it is difficult to make direct comparisons between the Absorption Method and the LIVE/DEAD assay. It must be taken into consideration that the initial concentration of the inoculum used in the Absorption Method was between $1 – 3 \times 10^5$ CFU/mL and, even after 24 h incubation, the highest final concentration on the untreated cotton was approximately 10^8 CFU/mL (Figure 5.3). In contrast, the inoculum concentration used in the LIVE/DEAD assay was over 10^9 CFU/mL, in order to obtain a suitable number of bacteria to observe under the microscope. When the concentration of antibacterial agents remains the same on the sample, but the bacterial concentration is increased, this may result in an insufficient antibacterial effect towards some of the cells. However, in this LIVE/DEAD assay, it can be seen that the Se-C and Ag-C killed the majority of bacteria despite such a high inoculum level, demonstrating excellent antibacterial performance of the NP-modified fabrics.

5.4.4 Effect of functionalised fabrics on bacterial morphology

The morphologies of the bacterial cells in contact with the fabric samples were observed with SEM (Figure 5.11 – 5.13). It can be seen that on the control UC, most of the cells display their expected morphologies; *S. aureus* being spherical, *K. pneumoniae* being short rods and *E. coli* being long rods respectively. Although the LIVE/DEAD assay showed that many cells died naturally on the untreated cotton control sample, in the SEM images it can be seen that most of the control cells did not exhibit significant morphological changes, with a small number of cells appearing shrunken slightly. This may indicate that natural death of the cells does not result in significantly altered morphology.

In contrast, morphological abnormalities can be seen in all three bacterial species incubated on the modified cotton surfaces. The *S. aureus* cells on the CC and the Ag-C were observed to have some indentations on the surface and were not as rounded as the control cells on the untreated cotton (Figure 5.11). The effects seemed to be more pronounced on the Se-C where some cells were clearly shrunken and wrinkled. *K. pneumoniae* cells on the CC and the Ag-C had similar morphologies, appearing collapsed (Figure 5.12). Interestingly, the *K. pneumoniae* cells on the Se-C were not flattened in the same manner, but deep holes were visible, which might indicate that the damage caused by the SeNPs occurred faster than the effects caused by the cationic quaternary groups, as such features were not visible on the *K. pneumoniae* – CC sample. The *E. coli* cells were also observed to be collapsed on all the modified cotton samples, with the effects more significant on Se-C and Ag-C than on the CC (Figure 5.13). Similar morphological changes including collapsing, shrinking, and dents/holes in the cells, have been observed in other studies where bacterial cells have been treated with antimicrobials such as silver nanoparticles,[304] selenium nanoparticles,[305] copper nanoparticles,[306] and cationic antimicrobial peptides.[307]

S. aureus

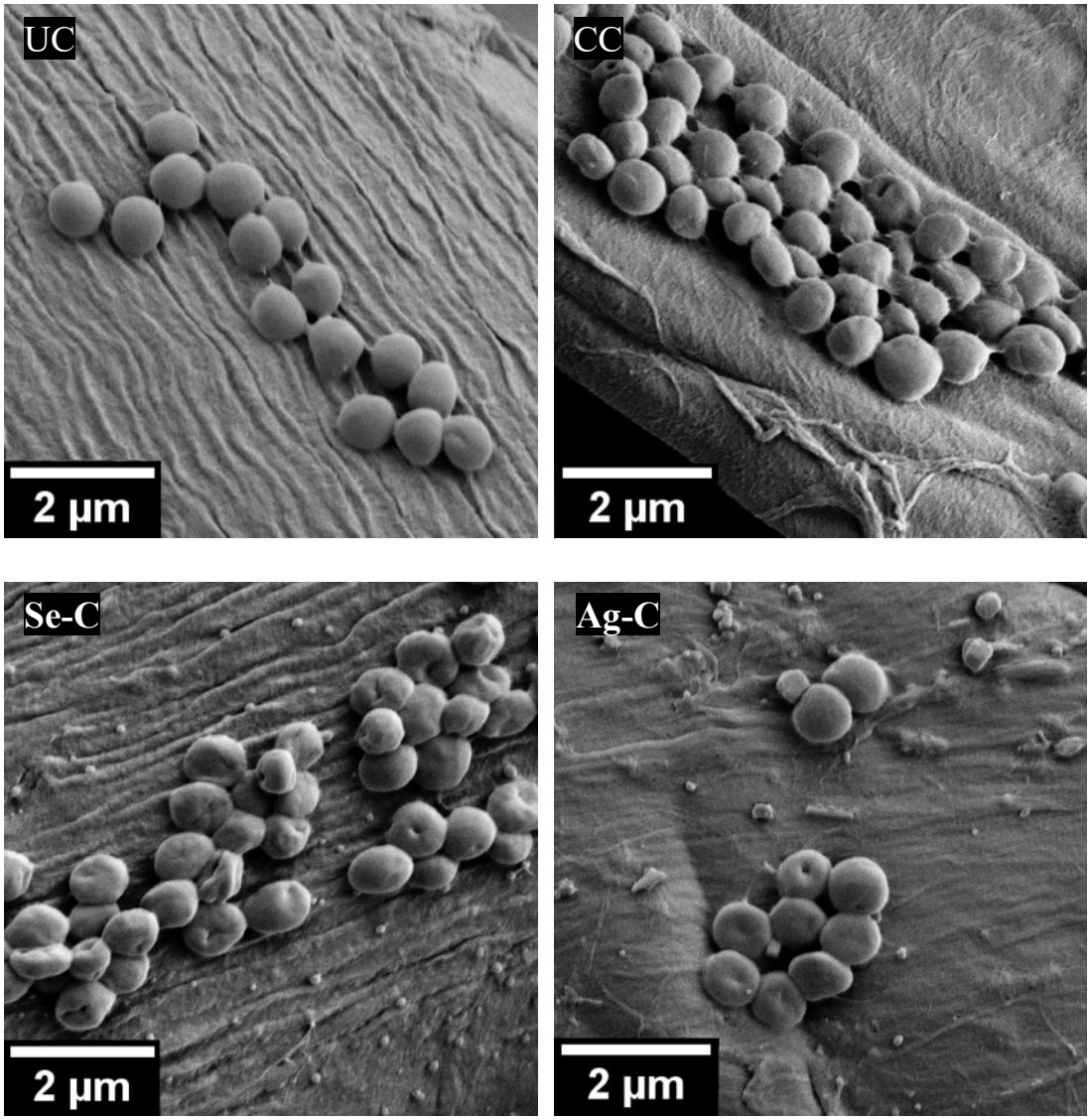

Figure 5.11 SEM images of *S. aureus* cells incubated on the cotton samples for 24 h.

K. pneumoniae

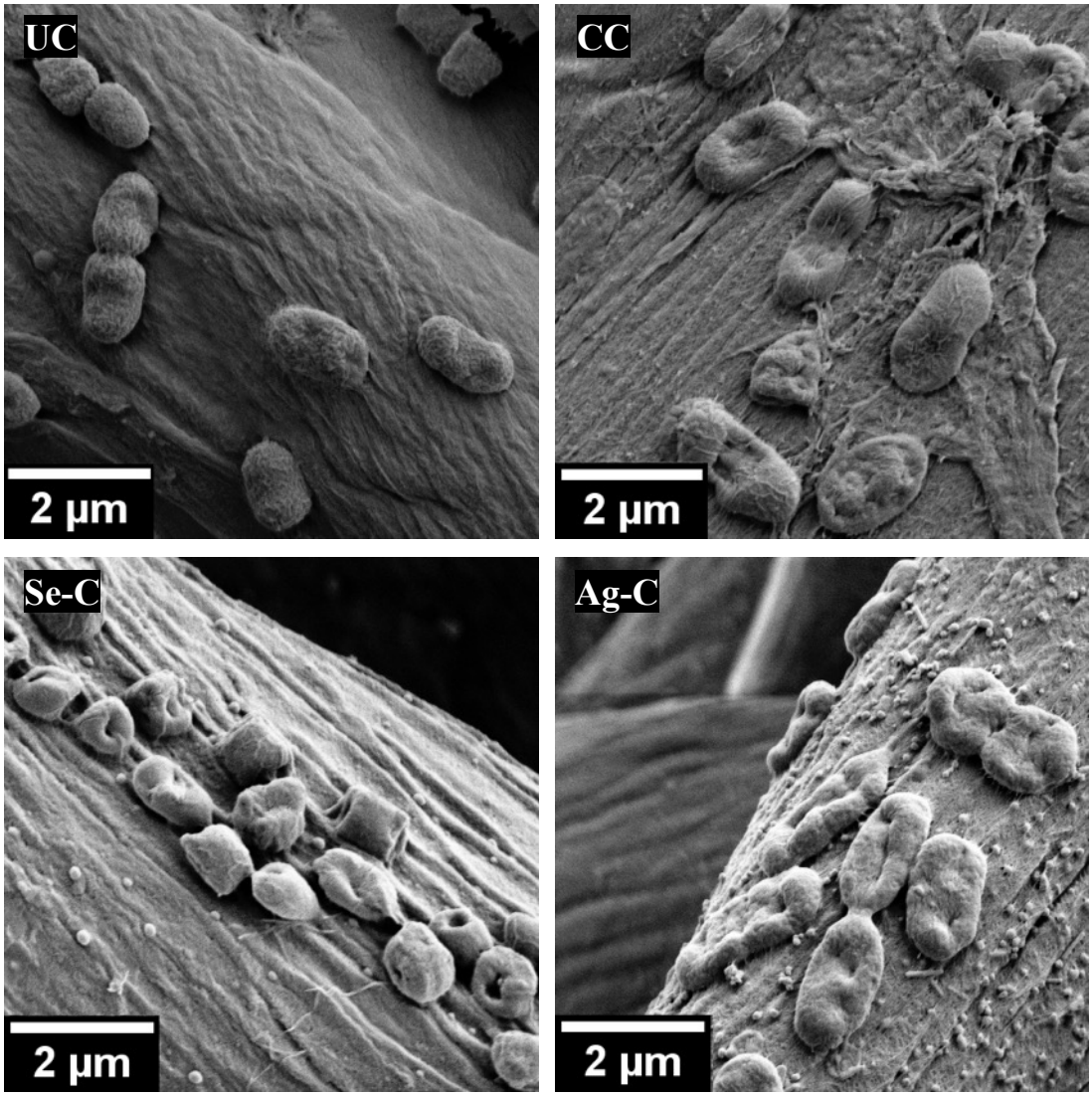

Figure 5.12 SEM images of *K. pneumoniae* cells incubated on the cotton samples for 24 h.

E. coli

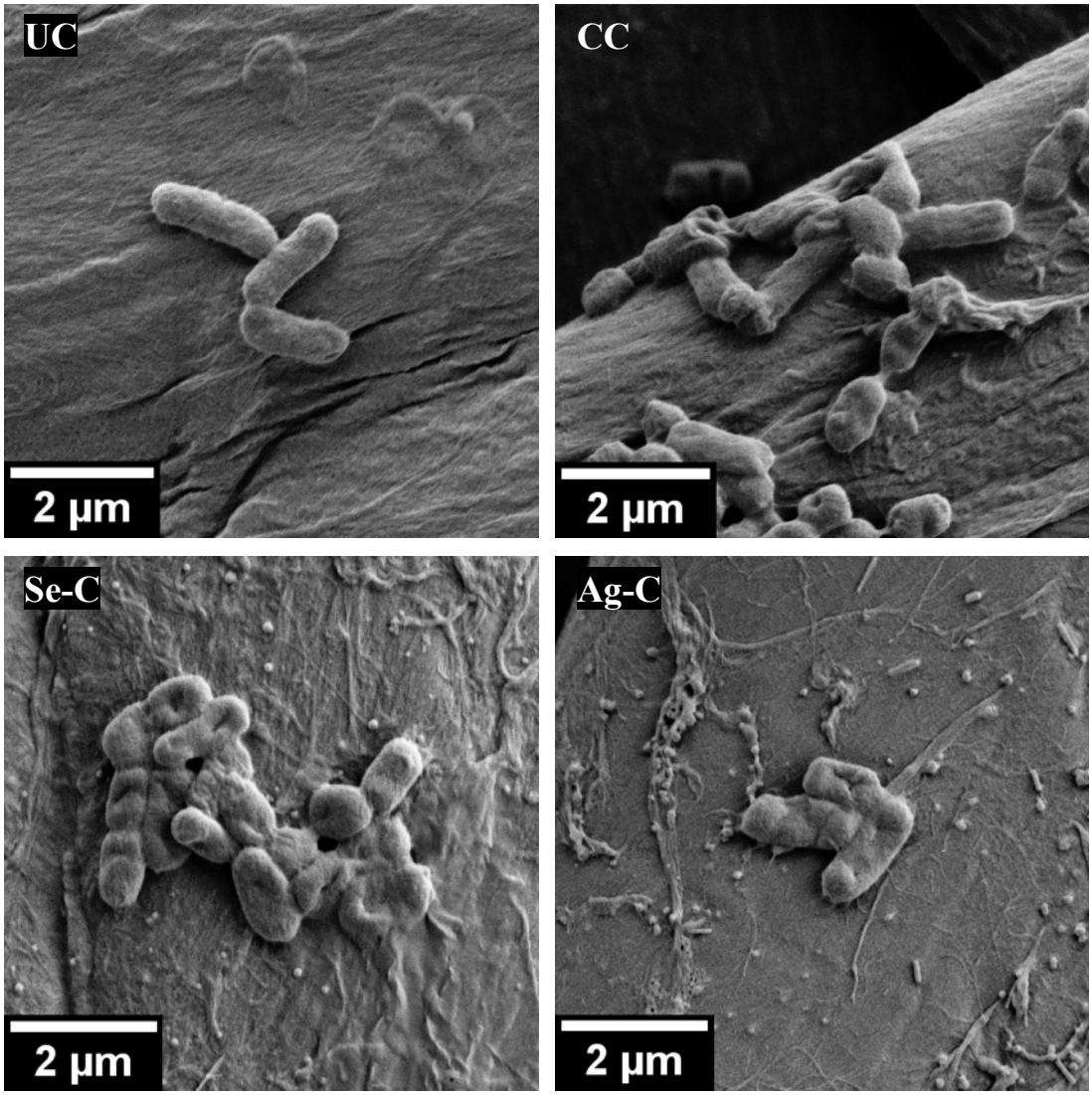

Figure 5.13 SEM images of *E. coli* cells incubated on the cotton samples for 24 h.

In summary, the bacterial cells on the modified cotton fabrics had significant morphological abnormalities, which indicated the damage of cell structures caused by the cationic quaternary ammonium groups and the nanoparticles. The SeNPs seemed to have caused more pronounced effects on the bacterial cells. The SEM analysis is in agreement with the results of the LIVE/DEAD assay.

5.4.5 Laundry durability

In Chapter 4, the laundry durability of the funcitonalised fabrics was determined by analysing the amount of Se or Ag per gram of cotton before and after repeated laundering. The result suggested that all of the samples retained over 80% of the nanoparticles after 4 accelerated laundry cycles (equivalent to 20 home laundry cycles), indicating excellent laundry durability of the NP functionalisation. In order to determine the antibacterial performance after repeated washing, the washed samples were analysed using the challenge test as described in Section 5.3.1.

The antibacterial activity of the modified cotton fabrics before and after being washed for 4 accelerated laundry cycles are summarised in Figure 5.14. As can be seen, the 'A' values of the cationized cotton against all three bacterial species reduced slightly ('A' value reduction<0.5). The reduction of 'A' values may be due to the fact that the detergent contains large amount of anionic surfactants, which may have neutralised some of the cationic groups after repeated washing. For both Se-C and Ag-C, the samples prepared with 0.2 mM precursor salt exhibited lower antibacterial activities after being washed; while the samples prepared with higher concentrations of precursors (0.5 and 1 mM) did not show reduced antibacterial activities. The decreased 'A' values of 0.2 mM Se-C and Ag-C may indicate that concentrations of nanoparticles on these samples were at a critical level for the antibacterial activities that could inactivate all of the bacteria. With the loss of some nanoparticles after repeated washing, the nanoparticle-free areas were increased on the fabric samples treated with 0.2 mM precursor salts. As discussed before, the antibacterial activities were the combined effects of cationic quaternary groups and nanoparticles. The slight decrease in the cationic effects was evidenced by the reduced 'A' values of cationized cotton; and the slight decrease of Se or Ag contents on the 0.2 mM Se-C or Ag-C was evidenced by the MP-AES results. These two factors together led to the decreased 'A' values of 0.2 mM Se-C and Ag-C.

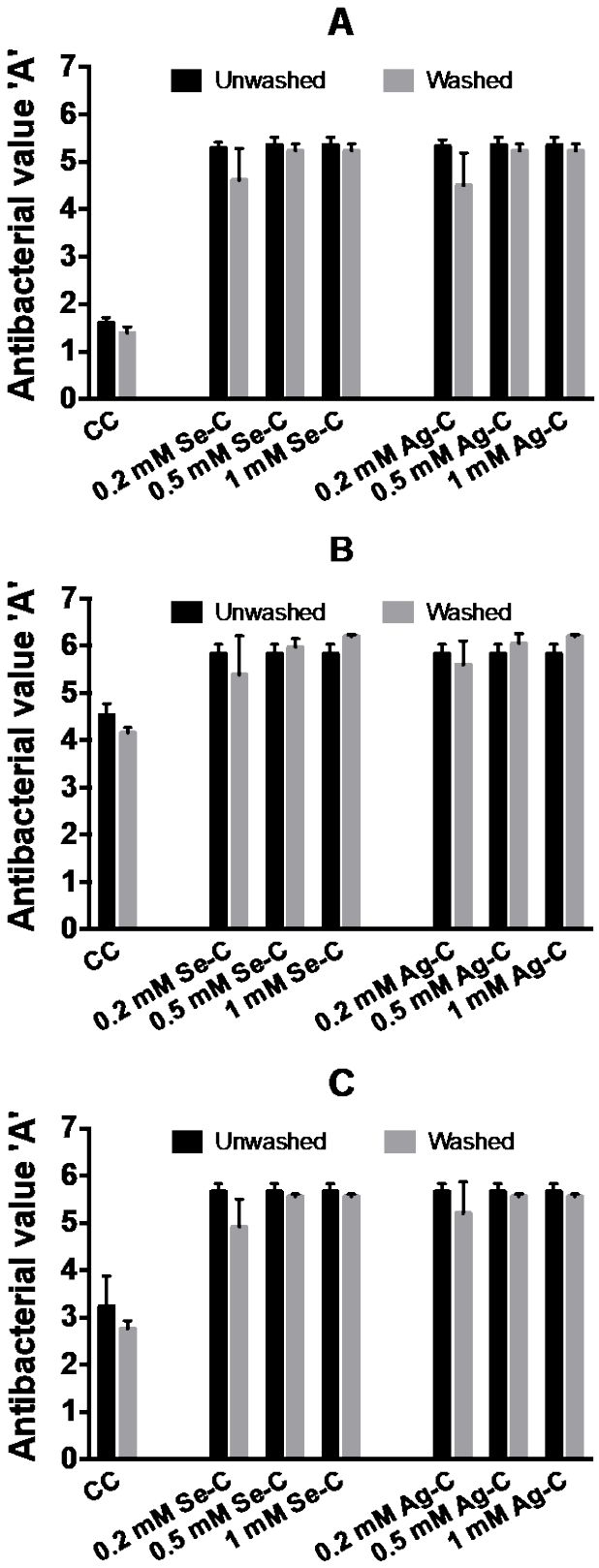

Figure 5.14 Antibacterial value 'A' of the functionalised samples before and after 4 accelerated washing cycles; (A) *S. aureus*, (B) *K. pneumoniae*, and (C) *E. coli.* Data represent the mean ± SD, n=3.

5.5 Chapter summary

In this chapter, the antibacterial performance of the functionalised fabrics was analysed using various methods, and the results indicated excellent antibacterial performance of the functionalised fabrics against both Gram-positive (*S. aureus*) and Gram-negative (*K. pneumoniae* and *E. coli*) bacterial species. It was found that under the test conditions recommended by ISO 20743:2013 (Textiles — Determination of antibacterial activity of textile products), the cationized samples without the addition of nanoparticles showed moderate to strong antibacterial activities, which was more effective against Gram-negative *K. pneumoniae* and *E. coli* than against Gram-positive *S. aureus*; all of the NP-functionalised fabrics showed strong antibacterial efficacy against all of the bacterial strains tested, with the calculated antibacterial value 'A' all above 5. Due to the fact that almost all of the viable count results were lower than the limit of detection, the antibacterial performance between the samples with different concentrations of SeNPs and AgNPs were not able to be differentiated using the challenge test method recommended by ISO 20743:2013. Moreover, the cationic charge on the fabric surfaces made it difficult to remove the bacterial cells and some uncertainty was raised whether the results lower than LOD could be an artefact of failed removal of viable bacteria. Consequently, a supplementary qualitative test based on resazurin chromogenic agar was conducted. With the help of RCA, the colour change of resazurin in contact with the samples was observed *in situ* without the need of removing cells from the samples, which reduced the uncertainty related to the removal precedure. With the RCA tests, results consistent with the challenge test were obtained. CLSM and SEM were used to observe the bacterial cells *in situ* on the surface of the fabric samples. It was found that the bacterial structures appeared to be severely damaged by the cationic quaternary groups and the nanoparticles; many bacterial cells appeared to be orange/yellow on the cationized cotton and were considered to be sub-lethally injured. Overall, different methods were used to evaluate the antibacterial performance of the functionalised fabrics and the results showed excellent antibacterial properties of the fabrics. The samples subjected to 4 accelerated washing cycles were also evaluated using the challenge test method, and it was shown that only the activities of cationized cotton and NP-functionalised cotton prepared with 0.2 mM precursor salts were adversely affected. However, the antibacterial value 'A' of Se-C (0.2 mM) and

Ag-C (0.2 mM) was still higher than 4 against all of the bacterial strains tested, demonstrating strong antibacterial performance.

In conclusion, the functionalised cotton fabrics demonstrated excellent antibacterial performance, even after repeated laundering. The cationized cotton alone already had good antibacterial efficacy, and the presence of SeNPs or AgNPs, even at a low concentration, greatly improved the performance. SeNPs as a novel type of antimicrobial agent showed comparable performance to AgNPs in this study, demonstrating the suitability of SeNPs as antimicrobial agent to functionalise cellulose surface. These results indicated that the cotton fabrics functionalised with quaternary cationic groups and SeNPs or AgNPs have great potential to serve as anti-infective materials.

Chapter 6 Cytotoxicity Evaluation of Functionalised Textile Materials

6.1 Introduction

As discussed in Section 1.4.6, the safety concerns related to the use of nanomaterials need to be considered when developing nanoparticles-based antimicrobial materials. When investigating the effects of a material on a biological system, the first step often involves cell culture studies. Compared to animal studies, cell work is easier to control and reproduce, less expensive, and less ethically complicated.[308] Although the most commonly used *in vitro* cell models are often insufficient to represent or predict the real interactions between the investigated material and the body, cell studies can be an important tool to provide some valuable insights into safety issues.[186] In this chapter, the cytotoxicity of the NP-functionalised fabrics was evaluated to primarily address the safety issues of the selenium and silver nanoparticles.

A wide range of cytotoxicity assays based on different principles can be used for the determination of cytotoxicity towards mammalian cells, as well as antimicrobial activity *in vitro*. An increasing number of studies have reported that nanomaterial toxicity assays conducted with well-established *in vitro* models have generated confounding or even conflicting data.[309] The unique physicochemical properties of nanomaterials may interfere with assay components or detection systems, introducing artefacts into the studies. Monteiro-Riviere *et al.*[233] used a range of different dye-based assays, including calcein AM, Live/Dead, NR, MTT, Celltiter 96® AQueous One, alamar Blue, Celltiter-Blue®, CytoTox One™, and flow cytometry, to determine the cytotoxicity of several carbon-based nanomaterials and quantum dots. The results from different assays varied greatly depending on the interactions of the dye/dye product with the nanomaterials. Therefore, when employing such assays to determine the toxicity of nanomaterials, more than one assay may be required to avoid skewed results. In this chapter, lactate dehydrogenase (LDH) assay and adenosine triphosphate assay (ATP) assay were selected to evaluate the cell activity. LDH is a cytosolic enzyme which will be released into the

cell culture media when the plasma membrane is damaged and therefore can be used to detect cell death. ATP provides energy to drive many processes in living cells, therefore relating to the number of metabolically active cells and as such is used as a cell viability assay.

As discussed in Section 1.4.6, the main risk of exposure of the human body to nanoparticles is via the dermal, respiratory and oral routes. Considering the common usage of textile materials (e.g. beddings, curtains and uniforms), a respiratory epithelial cell line (16HBE14o-) and a dermal cell line (HaCaT) were chosen for the *in vitro* cytotoxicity tests in this study. The 16HBE14o- cell line was originally developed from human bronchial epithelium to study the cystic fibrosis transmembrane conductance regulator and retains many features of differentiated bronchial epithelial cells.[310] The use of the 16HBE14o- cell line to study the cytotoxicity of metal nanoparticles has been reported in several studies.[311–313] For the dermal cells, keratinocytes (HaCaT) were chosen as they are the major component of the epidermis, the outmost skin layer, and one of the first barriers interacting with NPs or NP-functionalised fabrics. The use of HaCaT cell line in nanotoxicology studies has also been widely reported.[314–316]

The studies into the cytotoxicity of NP-functionalised textiles have been discussed in various reports in the literature.[317–319] Most of the studies have used an indirect contact method to evaluate the cytotoxicity. In this method, the textile samples are immersed into a liquid extraction vehicle, which is supplemented with cell culture media in most of the cases, and the extracts are then used to treat the cells. According to ISO 10993-12:2012 (Biological evaluation of medical devices, Part 12: Sample preparation), both polar and non-polar extraction vehicles should be used in this method to maximise the release of different types of substances. The examples of polar extraction vehicles include water, physiological saline, and cell culture media without serum; non-polar extraction vehicles include refined vegetable oil. The use of cell culture medium with serum is preferred because it can support cell growth as well as extract both polar and non-polar substances. However, when studying inorganic nanoparticles such as silver, it is also important to consider the dissolution behaviours of the material in complex media. Biswas *et al*.[142] prepared polymeric porous scaffolds decorated with silver or selenium nanoparticles and studied the extraction of Ag and Se in different media. The NPs were thought to be

embedded in the scaffolds and therefore the release of Ag or Se should be mainly from the soluble species rather than loosely attached NPs. It was found that the amount of silver released into water was over 20 times higher than in cell culture media (Dulbecco's Modified Eagle Medium), and over 100 times higher than in bacterial culture broth (Lysogeny broth). The differences were probably due to the presence of high concentrations of chloride ions in both of the media, which reacted with Ag ions to form AgCl precipitate on the particle surfaces and prevented further release of Ag ions. It was also suggested that some proteins in the media could block the particle surface and prevent the release of silver. On the other hand, the Se released into DMEM and LB broth approximately twice as much as it did in water, indicating that the release of Se was not negatively affected by the complex components present in the media as Ag was. On the contrary, the release was even promoted in the media as elemental Se is not considered to be directly oxidizable and has negligible solubility in water.[320] Based on these findings in the literature, here in this chapter, both water and cell culture media were used as the extraction vehicles to perform indirect contact cytotoxicity studies on Ag-NP and Se-NP functionalised fabrics.

One of the major advantages of SeNPs was assumed to be low cytotoxicity.[122,142,321] Since it has been suggested by some studies that SeNPs have low cytotoxicity to mammalian cells and therefore are potentially suitable for biomedical applications, the research questions of this chapter were:

(1) To determine if the Se-C and Ag-C were toxic to the 16HBE14o- and HaCaT cells *in vitro* using an indirect method with LDH assay and ATP assay; if yes, to determine if Se-C was less toxic than Ag-C as suggested by the literature.
(2) To study the influences of different extraction vehicles (e.g. water and tissue culture media) used for the indirect contact cytotoxicity evaluation method.

6.2 Materials

Human bronchial epithelial cells (16HBE14o-) were purchased from Sigma Aldrich and human keratinocytes (HaCaT) were purchased from AddexBio. Cell culture media, supplements and reagents including Minimum Essential Medium (MEM), Non-essential Amino Acids (NEAA), Dulbecco's Modified Eagle Medium/Nutrient mixture F-12 (DMEM/F-12) and trypsin-EDTA were purchased from Gibco (UK). Fetal bovine serum (FBS) was purchased from Atlanta Biologicals (UK). The samples used in the assays are listed in Table 6.1.

Table 6.1 Fabric samples used in the cytotoxicity tests

Sample	Description
AC	As-purchased cotton without any chemical modification and hand-washed with RO water
UC	Untreated cotton as a non-toxic control: purified AC
CC	Cationised cotton: CHPTAC-treated UC
Se-C	SeNP-modified cotton: prepared with 1 mM Na_2SeO_3 and the CC
Ag-C	AgNP-modified cotton: prepared with 1 mM $AgNO_3$ and the CC

The Se-C and Ag-C prepared with 1 mM precursor salts were used in this chapter for the cytotoxicity analysis. As mentioned in Section 4.3.1, in some preliminary tests it was found that the as-purchased cotton, which was supposed to act as a non-toxic control, was toxic to the 16HBE14o- cells and killed almost all the cells. It was postulated that the as-purchased cotton might retain some toxic chemical residues (e.g. pesticides and surfactants) resulting from the cotton cultivation and manufacturing processes. Consequently, the as-purchased cotton was purified as described in Section 4.3.1 and the functionalised samples were made again using the purified cotton. The as-purchased cotton (AC) was used as a positive control for toxicity in this chapter. Additionally, the NP-modified samples used in the

antibacterial tests were washed with surfactant to remove the insecurely attached nanoparticles, while the samples used here for cytotoxicity tests were only washed with RO water to avoid introducing surfactant as a contaminant which might have an impact on the human cells.

6.3 Methods

6.3.1 Cell culture

The 16HBE14o- cells were maintained in MEM supplemented with 10% FBS and 1% NEAA. The HaCaT cells were maintained in DMEM/F-12 supplemented with 10% FBS. The cells were grown in tissue culture flasks (T75) in a humidified atmosphere at 37 °C with 5% CO_2 and sub-cultured every 2-3 days when the cells reached approximately 80% confluence.

6.3.2 Preparation of fabric sample extracts

The sample preparation method of indirect contact cytotoxicity tests was based on ISO 10993-12:2012. Fabric samples were cut into 2 cm × 2 cm squares (0.1±0.01 g). The samples were placed in sterile glass vials and culture medium, appropriate to the cell line being studied, was added at a material-to-liquid ratio of 0.1g/mL. It was noticed that the fabric samples showed different colours due to the different surface chemistry in the adsorption of components from the cell culture medium. In order to minimise the influence of different nutrient adsorption behaviours of the samples, a pre-treatment step was applied. The samples were first soaked in the cell culture medium for 30 mins at room temperature without shaking to saturate the binding sites on the fabric surfaces, and the medium was discarded after the pre-soaking. Subsequently, fresh medium was added to each vial as the extraction vehicle. Medium only without any fabric sample was also added to a glass vial to be used as a negative control. The glass vials were incubated at 37 °C with 100 rpm agitation for 72 h. After 72 h, the extracts were centrifuged in Eppendorf tubes at 3000 g for 5 mins to remove the short loose fibres from the extracts.

Another group of samples, using RO water as the extraction vehicle, was prepared according to the same method. After 72-h incubation, the extracts were mixed with an equal amount of double strength cell culture medium (double strength MEM supplemented with 20% FBS and 2% NEAA, or double strength DMEM supplemented with 20% FBS) to form single strength media to treat the cells.

6.3.3 Cytotoxicity by indirect contact

The cells were washed with PBS and harvested using 0.05% trypsin-EDTA. After trypsinisation, the cells were counted using a haemocytometer and seeded at a density of 4×10^3 cells/well in 96-well plates. The cells were prepared in two sets of triplicate wells. One set was for each type of the sample extracts or medium-only negative control, and the other set was for total lysis positive control of the treated cells. Cells were allowed to attach the surface for 24 h at 37 °C prior to extract exposure. The culture media for the seeded cells were discarded after 24-h incubation, and 100 µL of the 72-h extracts were then added to the wells. The extracts were also added to empty wells without any cells as cell-free controls. The plates were incubated at 37 °C in a humidified atmosphere with 5% CO_2 for 24 h before the cell activity was assessed.

6.3.4 Lactate Dehydrogenase Assay

Pierce™ LDH Cytotoxicity Assay Kit (Thermo Scientific) was used to measure the LDH release following the 24-h exposure of the cells to the fabric extracts. The LDH Reaction Mixture was prepared according to the manufacturer's instruction. After 24-h incubation, 10 µL of Lysis Buffer (Triton-X 100 solution, included in the kit) was added to the set of total lysis positive control wells to determine the maximum LDH activity of the cells treated with each type of the extracts. The plate was incubated for 45 mins in an incubator (37 °C, 5% CO_2) to allow the lysis of the positive control cells.

After 45 mins, 50 µL of each sample medium or the cell-free extract control was transferred to a new 96-well plate and mixed with 50 µL of the LDH Reaction

Mixture. The reaction mixtures in the plate were mixed by gentle tapping. The plate was incubated at room temperature in the dark for 30 mins, after which 50 µL of Stop Solution was added to each of the wells. Finally, the optical densities at 492 nm and 690 nm were read with a Multiskan Ascent Plate Reader (Thermo Scientific). The results were calculated as percent total cell lysis by the equation 1 below:

Equation 6.1:

$$\text{Cell death (\%)} = \frac{\text{extract treated LDH activity} - \text{extract background}}{\text{extract treated maxinum LDH activity} - \text{extract background}} \times 100$$

Where

extract treated LDH activity is [OD492nm – OD690nm] of the extract treated wells;

extract treated maximum LDH activity is the [OD492nm – OD690nm] of the total lysis positive control of the extract treat wells;

extract background is [OD492nm – OD690nm] of the cell-free media only control wells.

6.3.5 Adenosine Triphosphate Assay

CellTiter-Glo® Luminescent Cell Viability Assay Kit (Promega) was used to determine the cell viability after exposure to the fabric extracts. CellTiter-Glo® is a luminescent cell viability assay to determine the number of viable cells based on quantification of the ATP present. The reagent was prepared according to the manufacturer's instruction. The cells whose media were used to determine the extract-treated LDH activity were also used for the ATP measurement. The 50 µL media left in the wells were discarded and the cells were gently washed with sterile PBS. Fresh media (100 µL) were then added to the cells and 100 µL of the CellTiter-Glo® reagent was added to each of the wells. The plate was gently tapped to mix the reagents well and incubated for 10 mins at room temperature. Subsequently, the mixture was transferred into a white 96-well plate (Costar) and the luminescence was measured by a LUMIstar Microplate Reader (BMG Labtech).

6.3.6 Silver/selenium release into the extracts

The samples were prepared as described above (Section 6.3.2). After centrifugation to remove loose fibres, the samples were digested using concentrated nitric acid. The supernatant (1 mL) was transferred to a capped glass vial and concentrated HNO_3 (1 mL) was added. The vial was kept at 80 °C in an oven for 1 h and left at room temperature overnight. Protein precipitation could be seen in the media-extracts and therefore the solutions were filtered through a syringe filter (0.45 µm) prior to analysis with MP-AES. Moreover, the digested media-extracts were further diluted to 5 mL with RO water (18 mΩ) in order to reduce the salt concentration in the solution to avoid damage to the MP-AES torch.

6.3.7 Protein adsorption to the fabrics

The level of protein remaining in the media-extracts was determined using Coomassie (Bradford) Protein Assay Kit (Thermo Scientific). A 2000 µg/mL bovine serum albumin (BSA) solution included in the kit was used to prepare a range of protein standards (100 – 750 µg/mL) with dilute (1/10) MEM as the diluent. The media-extracts were prepared as described above (Section 6.3.2). After centrifugation, the supernatants of the extracts were diluted to 1/10 with RO water. The dilute extracts and standards (5 µL) were added in triplicate to a 96-well plate with dilute MEM as the blank. The Coomassie Reagent (250 µL) was then added to the wells and the plate was shaken by gentle tapping for 30 s to mix the solutions well. The plate was allowed to stand at room temperature for 5 mins and the absorbance was read at 595 nm using a plate reader (Biotek).

6.2.8 Statistics

All tests were carried out in triplicate and repeated 3 times on different occasions. The statistical analysis was carried out using the analysis tool provided with GraphPad Prism 6. Unpaired Student's t-test was used to compare the different treatments to determine if there was any significant difference from each other.

6.4 Results and discussion

6.4.1 Removal of impurities on as-purchased cotton fabrics

In the preliminary experiments on 16HBE14o- cells, it was found that even the as-purchased cotton (AC), which was supposed to act as a non-toxic control, killed almost all the cells. This was assumed to be due to toxic chemical residues on the as-purchased cotton fabric. Although the cotton was washed repeatedly before and during the functionalisation, it might not have been sufficient to remove the impurities. Many different chemicals used in the cotton growing, processing, and production processes can be harmful for mammalian cells.[322] Examples of such chemicals include pesticides, surfactants, and bleaching agents. The trace amount of chemicals left on the cotton may not be harmful for human in daily use as the body has protective barriers such as skin and mucociliary apparatus to minimise the external stimuli. However, when cultured *in vitro*, the cells are directly exposed to the chemicals and therefore can be very sensitive and vulnerable. Marakova *et al*.[317] also reported similar findings indicating that even untreated cotton control was toxic to the mammalian cells.

The first attempt of purifying the as-purchased cotton was to boil it in a large amount of RO water. It seemed to work well as the cells appeared healthy, as judged by their morphology, and the LDH levels of these cotton samples were similar to the medium-only control (data attached in Appendix B). However, the ATP levels of the cells treated with these cotton samples (extracted in culture media) were still not as high as the medium-only control (data attached in Appendix B). In the meantime, the samples using RO water as the extraction vehicle did not result in lower ATP levels than medium-only control. According to the ISO 10993-12:2012, water is a polar extraction vehicle, while cell culture medium supplemented with serum is an extraction vehicle that can extract both polar and non-polar substances. These results indicated that there might be different types of toxic chemicals left on the as-purchased cotton. Some of the impurities are polar chemicals that can be boiled off in water, while others will only come out in non-polar extraction vehicles. The results indicated that the non-polar impurities were not lethal to the cells at the

concentrations present, but they were still stressing the cells. Consequently, the second attempt of purifying the as-purchased cotton was conducted by soaking the fabric in 50% ethanol. This further step turned out to be efficient in removing the chemical impurities as the difference between the ATP levels of medium-only control and cotton samples were not significant. Therefore, this purification method was applied to the as-purchased cotton and all the samples and tests (including Chapter 4 and 5) were remade and performed again.

6.4.2 Preliminary tests and modifications made thereafter

When the cytotoxicity of biomaterials is evaluated, the cells will be affected by not only substances released into the media from the material, but also by the removal of nutrients by the material.[323] In some preliminary tests, it was noticed that soaking the samples in the media resulted in significantly different colours on the fabrics. As shown in Figure 6.1, both the UC and CC samples were white originally, but after brief soaking in MEM media, the CC sample was significantly pinker than the control cotton, which indicated they had different adsorption capacities for phenol red, and thus potentially for other nutrients too. In order to minimise the influences of the different adsorption abilities, a pre-soaking step was added to the sample preparation method.

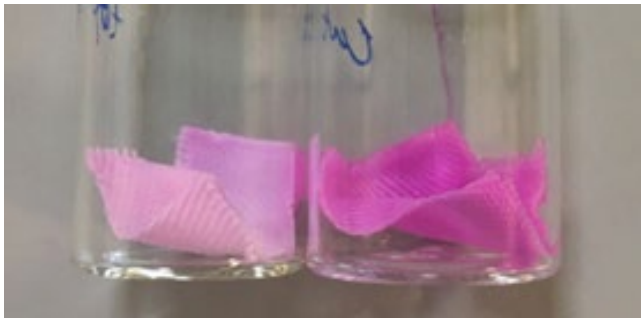

Figure 6.1 Different colours shown on the UC (left) and CC (right) samples after immersion in cell culture media

Original in colour

Moreover, it was found that some short loose fibres were present in the fabric extracts and they were carried over to the cells. Photomicrographs of the control 16HBE14o- cells are shown in Figure 6.2, and cells in the presence of the fibres are shown in Figure 6.3. As can be seen from Figure 6.2, the cells in medium-only control seem elongated and adhered to the tissue culture plastic, while the positive control cells treated with lysis buffer became rounded and shrunken. In Figure 6.3, the carried over fibres are highlighted with red arrows. It can be seen that only cells treated with as-purchased cotton (Figure 6.3 B) became detached from the surface and aggregated, showing even more damaged appearance than the positive control (Figure 6.2 B), indicating the cell death induced by the impurities released from the AC sample. In the other photomicrographs (Figure 6.3 A & C-E), the cells showed similar morphology to the medium-only control (Figure 6.2 A), even under the fibres, which suggested that no significant toxicity was induced by the indirect or direct contact of the cells with the fibres. However, since the fibres were relatively large objects presented in the extracts and their appearance was random between the wells, in order to reduce the potential uncertainty caused by the fibres, a centrifugation step was applied before treating the cells with the extracts to remove the fibres.

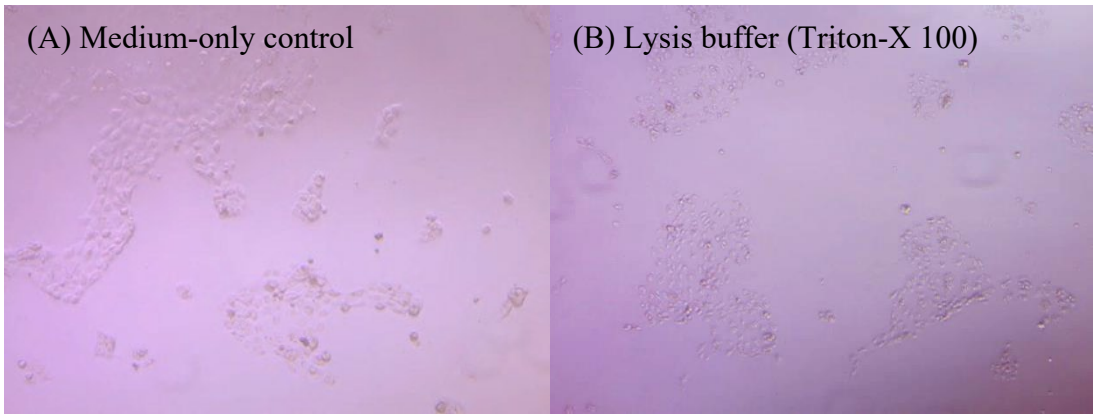

Figure 6.2 Photomicrographs (×100) of 16HBE14o- cells showing different cell morphology; (A) elongated and attached to the plate in medium-only control, (B) shrunken in total lysis positive control.

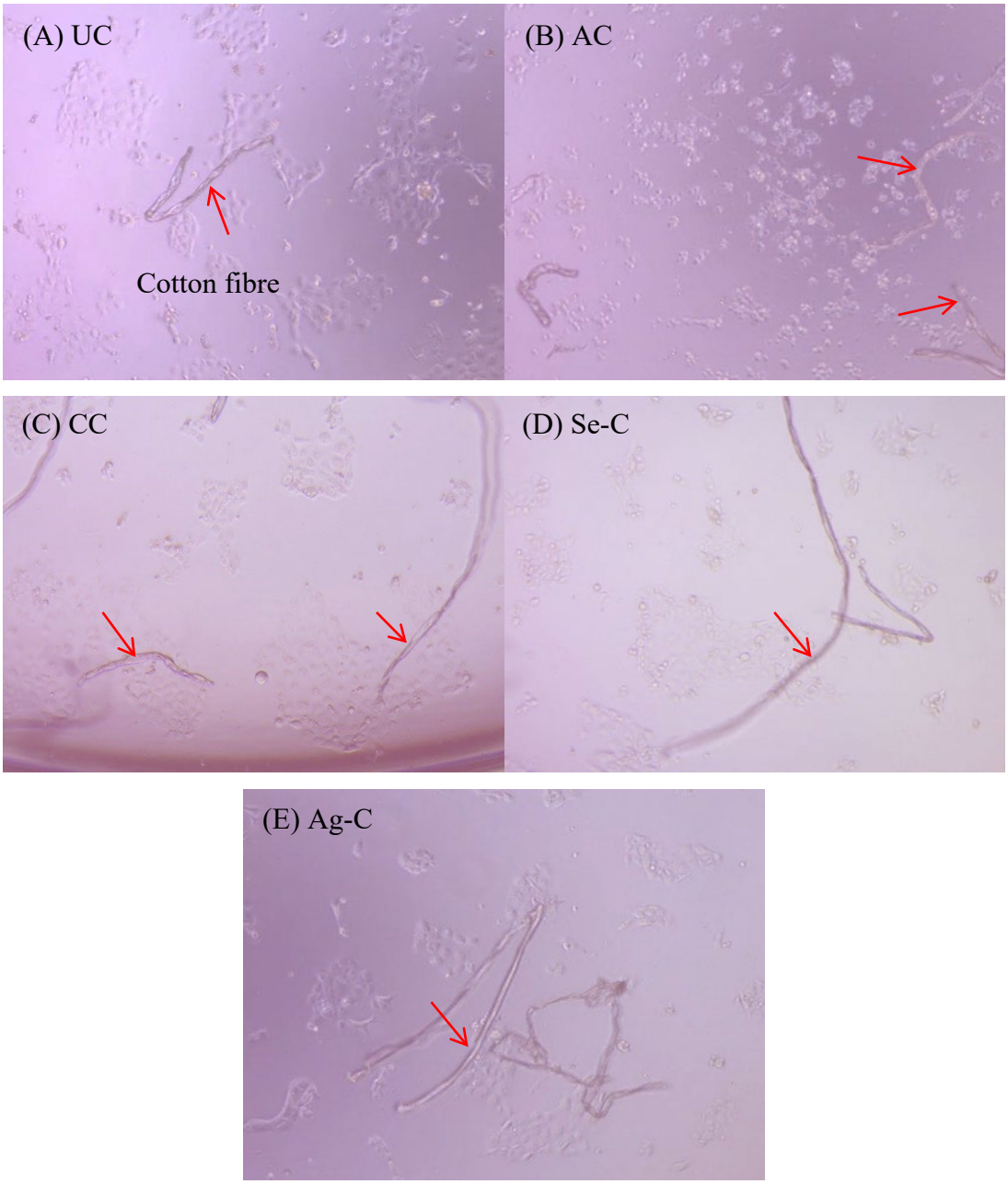

Figure 6.3 Photomicrographs (×100) of 16HBE14o- cells treated with different media extracts with the presence of loose cotton fibres, showing different cell morphology; red arrows highlighting the fibres.

The photomicrographs of the HaCaT cells treated with the extracts containing loose fibres are shown in Figure 6.4. Similar to the findings with 16HBE14o- cells, only the cells treated with the as-purchased cotton showed abnormal cell morphology; in Figure 6.4 (D), some of the cells seem shrunken and clearly detached from the tissue culture plate. Cells treated with the other sample types did not exhibit significantly abnormal cell morphology.

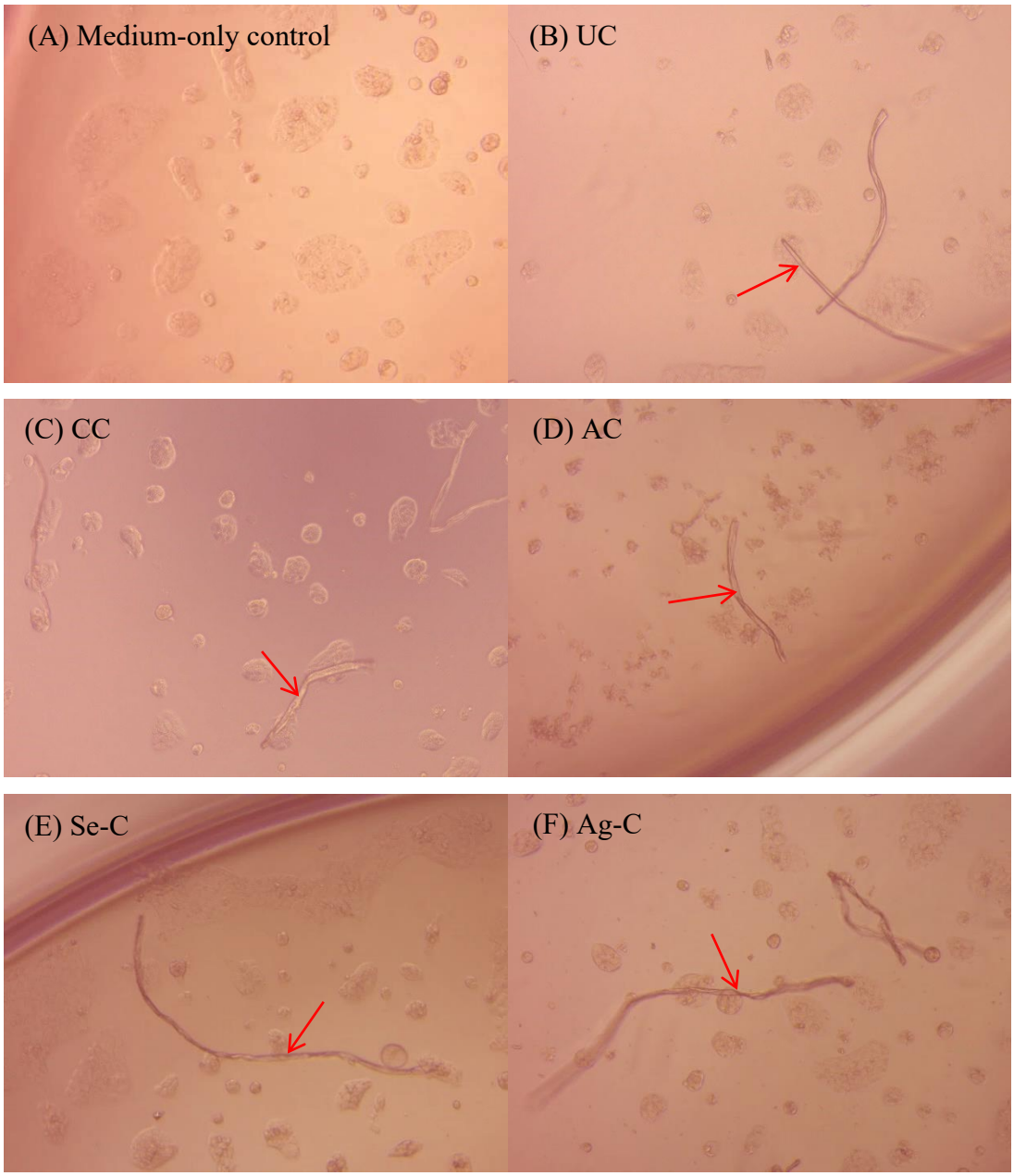

Figure 6.4 Photomicrographs (×100) of HaCaT cells treated with different media extracts with the presence of loose cotton fibres; red arrows highlighting the fibres.

Original in colour

6.4.3 LDH and ATP assays

The results of the LDH assay on 16HBE14o- cells are shown in Figure 6.5. When cell culture medium was used as the extraction vehicle (Figure 6.5 A), all the cell death rates were around 20% except the as-purchased (AC) cotton which had chemical residues on it. Student's *t*-tests indicated that AC was the only sample which resulted in significantly higher cell death rate than the medium only or UC negative controls, with an average cell death rate as high as 79%.

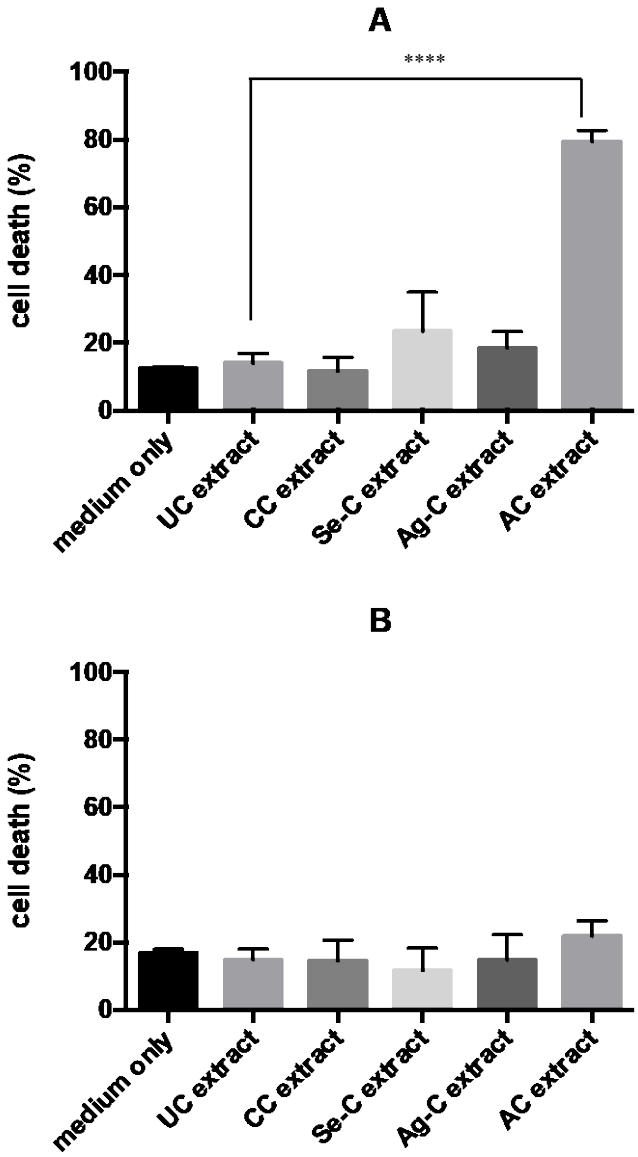

Figure 6.5 Cell death of 16HBE14o- cells after 24-h exposure to the extracts of fabric samples with LDH assay: (A) cell culture medium and (B) DI water as the extraction vehicle. (n=3; data are presented as mean ± SD, **** $p<0.0001$)

With RO water as the extraction vehicle (Figure 6.5 B), no significant difference was found between any of the samples with the medium-only negative control, even the as-purchased cotton sample. This finding is in accordance with the previous observations that the toxic impurities on the as-purchased cotton could only leach out in non-polar extraction vehicles but not in water at low temperature (37 °C and below).

The results of the LDH assay on HaCaT cells are shown in Figure 6.6. The results were similar to the 16HBE14o- cells in terms of the non-toxic effects shown by the cationized and NP-functionalised fabrics as no significant difference was found between the test samples and the medium or UC controls. Interestingly, it was noticeable that the HaCaT cells were not affected by the AC with chemical residues to the extent that the 16HBE14o- cells were. The average cell death rate of AC control (media-extract) was 33%, which was significantly higher than the other cotton samples, with a P value of 0.003 between UC and AC, but not as high as it was for 16HBE14o- cells. Keratinocytes constitute 90% of the cells of the epidermis, which is the outermost layer of the skin that forms a barrier against external insults such as microbes, heat, radiation and chemicals; although in the epidermis there are stratum corneum and a granular cell layer above the spinous layer where the keratinocytes are located, keratinocytes are still good at resisting the environmental stimuli.[324] On the other hand, bronchial epithelial cells are located in the airway inside the body, and therefore are more vulnerable to harmful substances.

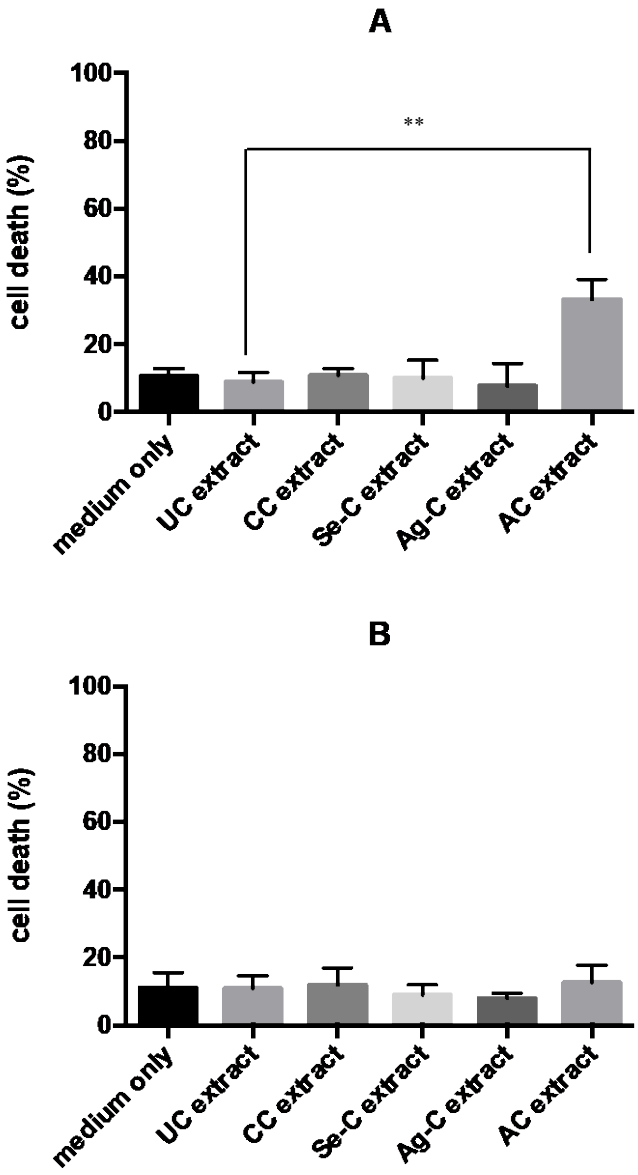

Figure 6.6 Cell death of HaCaT cells after 24-h exposure to the extracts of fabric samples with LHD assay: (A) cell culture medium and (B) DI water as the extraction vehicle. (n=3; data are presented as mean ± SD, ** $p < 0.01$)

Although the NP-functionalised fabrics did not induce significantly higher cell death rate than the controls according to LDH assay, the corresponding ATP levels were significantly lower than the controls. As can be seen from Figure 6.7, when using media as the extraction vehicle, the ATP levels of the 16HBE14o- cells treated with extracts containing Se and Ag were only approximately half of the UC extract, indicating the cells were not as metabolically active as the control cells. This might suggest that the leachates from the fabrics, including AgNPs and silver ions, or SeNPs and selenium ionic species, were causing metabolic stresses to the cells. On the other hand, as mentioned before, Biswas *et al.*[142] reported different releases of silver and selenium in different media. In their study, silver released from AgNP-functionalised polymer scaffold in water was over 100 times more than it was in cell culture media. Although in this chapter the water extracts had to be mixed with double strength cell culture media and therefore were diluted twice, the concentrations of Ag in water extracts should still be higher than the media extracts; however, the media extracts resulted in lower ATP level than the water extracts. Therefore, the lower ATP level might not have resulted solely from the leachable silver. The LDH background reading from the media alone might have provided some hints. According to the manufacturer's instructions, the serum presented in the media also contributes to the LDH signal, and therefore, it is recommended to test the cell-free background signal from each type of the media. As can be seen from Figure 6.8, the background signal from both Se-C and Ag-C extracts were lower than the control UC. Although differences between the Se-C or Ag-C and the control cotton were not statistically significant, the differences between the Se-C or Ag-C and the serum free medium were not significant either. This indicated that the sera concentrations in the Se-C and Ag-C media-extracts were lower than the medium-only and cotton controls, which might have contributed to the lower ATP level of the Se and Ag extracts. Although a pre-soaking step was applied when preparing the extracts, the pre-soaking was performed at room temperature without any agitation and further protein adsorption might have taken place during the 72-h extractions.

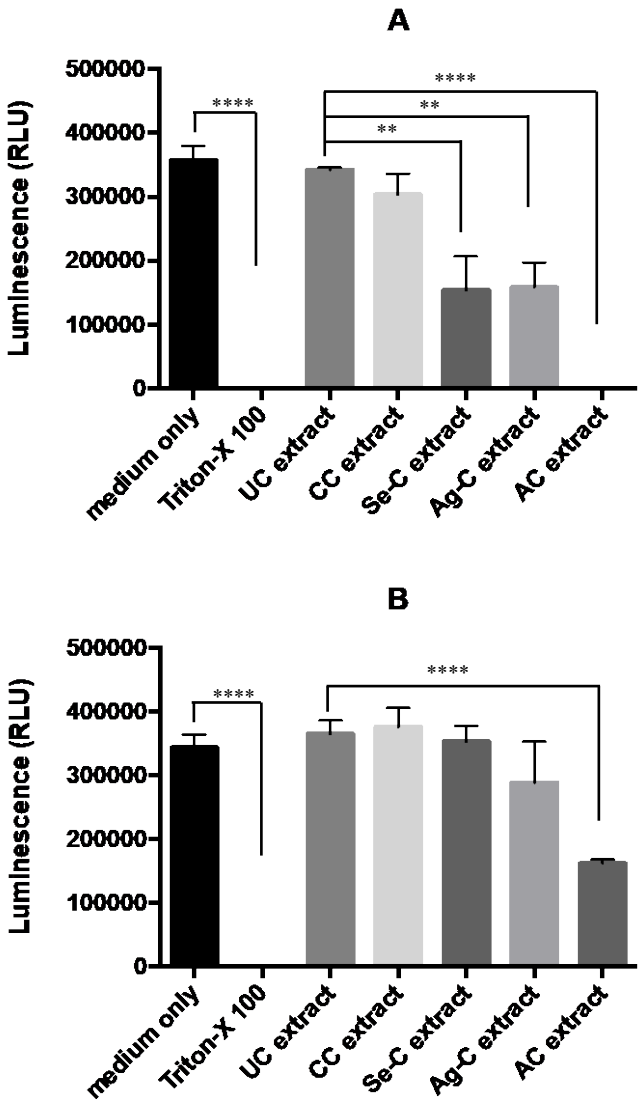

Figure 6.7 ATP levels of 16HBE14o- cells after 24-h exposure to the extracts of fabric samples: (A) cell culture medium and (B) DI water as the extraction vehicle. (n=3; data are presented as mean ± SD; * $p<0.05$, ** $p< 0.01$, *** $p<0.001$, **** $p<0.0001$)

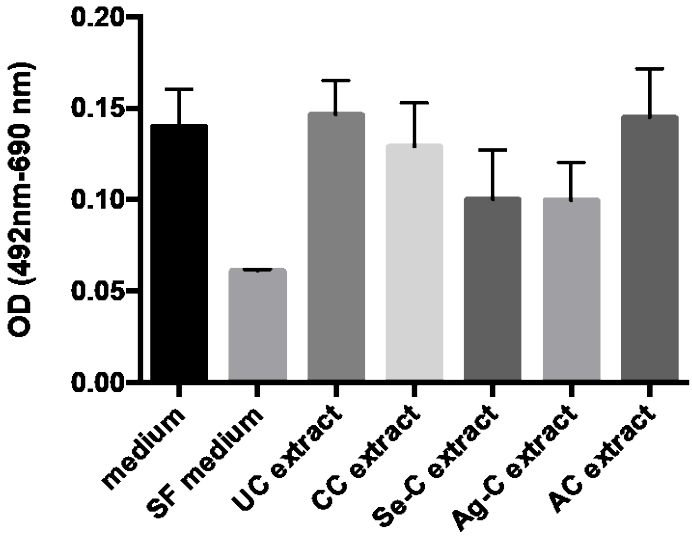

Figure 6.8 LDH background signals from the media-extracts (MEM supplemented with 10% FBS and 1% NEAA); n=3, data are presented as mean ± SD.

The Bradford assay was used to confirm the level of proteins in the media-extracts (Figure 6.9). The proteins remaining in the media-extracts of Se-C and Ag-C were significantly lower than the original medium. Cationised cotton also seemed to have removed some protein from the media (p value=0.0536). These results are in accordance with the LDH background signals, indicating the lower ATP levels of the cells treated with Se-C and Ag-C extracts could partly be due to loss of proteins in the media. When assessing the biocompatibility of some biomaterials, sometimes the abnormal cell activity may be a result of nutrient deficiency as the test materials have removed some components from the tissue culture media, rather than releasing toxic substances into the media. This can happen when the test materials have high surface areas. Barnes *et al.*[323] investigated the cytotoxicity of some activated carbon materials and found that the inhibition of cell growth occurred due to protein and ion adsorption by the carbon materials. Similar effects have also been observed on carbon nanotubes,[325] graphene nanosheet,[326] and metal nanoparticles.[327] In this chapter, the difference in the adsorption ability between different test samples was indicated by the colour change of the samples immersed in tissue culture media (Figure 6.1), and consequently, a pre-soaking step was added as described in Section 6.4.2. It seems that the pre-soaking step has helped to reduce the adsorption potential of the textile materials but did not completely eliminate the difference between

different types of the samples due to the short time. From the application point of view, this is less of a problem for the functionalised textiles reported here as they are not intended for direct contact with human tissue and supporting the cell growth, in comparison to some biomaterials such as wound dressings and tissue scaffolds.

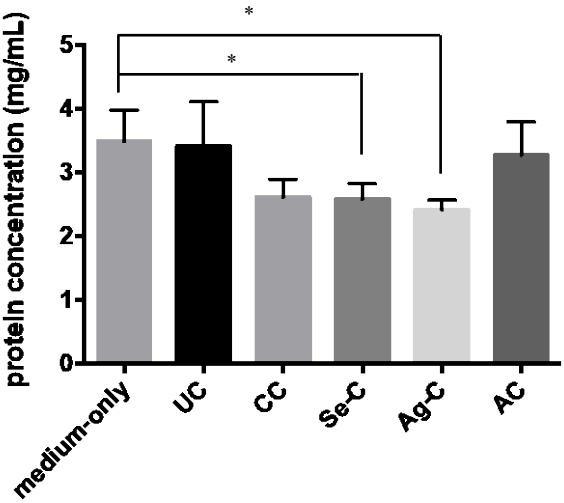

Figure 6.9 Protein concentrations remaining in the media-extracts (MEM supplemented with 10% FBS and 1% NEAA) (n=3; data are presented as mean ± SD; * $p<0.05$)

The results from the ATP assay of HaCaT cells (Figure 6.10) revealed a similar trend to the 16HBE14o- cells. The major difference was with the as-purchased cotton, where HaCaT cells were not affected as much as 14HBE14o- cells, which is in accordance with the results of the LDH assays as discussed above. With media as the extraction vehicle, as can be seen from Figure 6.10 (A), the ATP levels of cells treated with Se-C and Ag-C were lower than that of the UC and CC treated cells, and AC extracts led to the lowest ATP level of HaCaT cells. The p value of cells treated with Se-C, Ag-C and AC was 0.0463, 0.1287, and 0.0133 respectively. The Se-C and AC resulted in significantly lower ATP levels in HaCaT cells, although the p values were lowered compared to the results of 14HBE14o- cells, indicating that HaCaT cells were less sensitive to the fabric extracts. The HaCaT cells were not negatively affected by any of samples with water as the extraction vehicle.

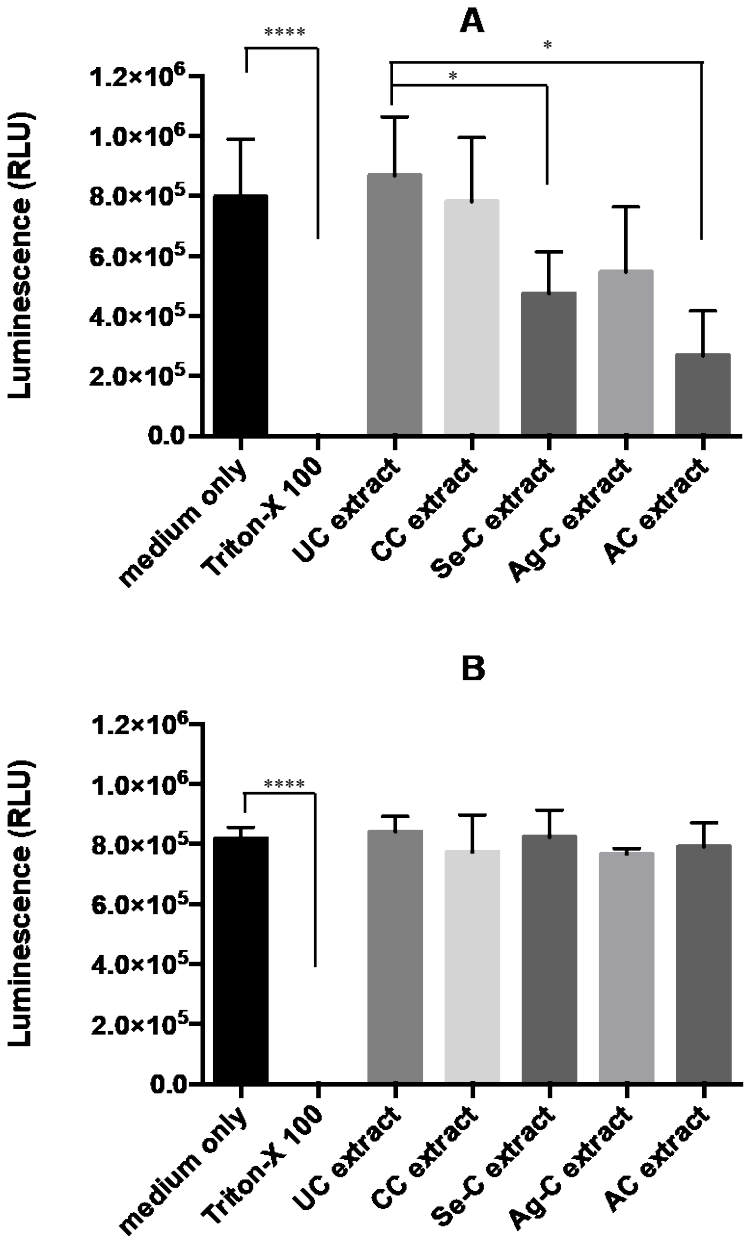

Figure 6.10 ATP level of HaCaT cells after 24-h exposure to the extracts of fabric samples: (A) cell culture medium and (B) DI water as the extraction vehicle. (n=3; data are presented as mean ± SD; * $p<0.05$, **** $p<0.0001$)

6.4.4 Concentrations of Ag or Se in the extracts

The concentrations of Ag or Se in the extracts were measured using MP-AES in order to further investigate the influences of the samples on the cells. It can be seen from Figure 6.11 that the Ag and Se concentrations in the extracts were as low as 0.5 – 1.5 ppm (μg/mL). The significantly higher level of silver released in water than in media reported by Biswas *et al.*[142] was not found here. This is probably due to the fact that the samples they tested had much higher silver contents (up to 178 mg Ag per gram of scaffold prepared with 50 mM $AgNO_3$), and the samples in this chapter only had approximately 1.5 mg Ag per gram of fabric. Moreover, the extraction reported by Biswas *et al.*[142] was performed without agitation and therefore, the Ag detected were probably mainly ionic Ag released from the scaffold. On the contrary, in this chapter, the extraction was performed with constant agitation and consequently, the removal of a small number of loosely attached nanoparticles might have contributed to the Ag or Se content in the extracts rather than solely release of ionic species. The detachment of NPs was probably less influenced by the type of extraction vehicle and therefore the difference between the water and media extraction in this chapter was less pronounced. For the release of Se, Biswas *et al.*[142] also found more Se species in culture media than in water. It is probably because the Se can react with the ingredients of the media (e.g. proteins and amino acids) and become soluble species, whereas Se normally is considered to be insoluble in water.[143,144]

The low concentrations of Ag and Se found in this chapter explained the non-toxic effects of the fabrics. Gliga *et al.*[190] reported that uncoated colloidal AgNPs (50 nm) did not show significant toxicity on BEAS-2B cells (human lung epithelial cells) with concentration of AgNPs as high as 50 μg/mL. Hemlinger *et al.*[167] tested the cytotoxicity of AgNPs (75 nm) on hMSC cells (human mesenchymal stem cells) with a range of concentrations and significant cytotoxicity was found on concentrations of 12.5 μg/mL and above. Various reports have also suggested that the SeNPs were not toxic to mammalian cells at concentrations up to 37.8 μg/mL,[142] 128 μg/mL,[122] and 500 μg/mL.[328] Here in this chapter, the concentrations of Ag and Se were only less than 2 μg/mL (2 ppm), which explained the low cytotoxicity found in this chapter.

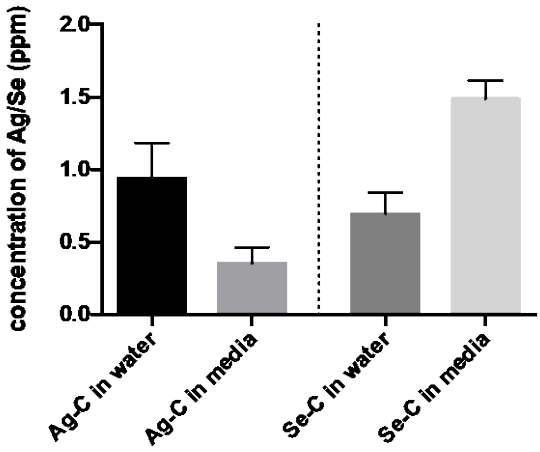

Figure 6.11 Concentrations of Ag or Se in the extracts.

6.5 Chapter summary

In this chapter, the cytotoxicity of the novel functionalised textile samples was tested following the indirect contact sample preparation methods suggested by ISO 10993-12:2012. It was also the first time that the cytotoxicity of AgNP- or SeNP-functionalised cationic cellulose was tested. Only very low levels of Ag or Se were found in the extracts with either water or cell culture media as the extraction vehicle. No significantly higher level of LDH was found from the functionalised samples, with either water or cell culture media as the extraction vehicles, indicating that the samples did not result in significant cell death. When the cells were treated with the media-extracts of the samples, lower ATP levels were found, which might be partly due to the removal of proteins from the media caused by the NP-functionalised fabrics. Other nutrients such as ions and sugar might have also been removed from the media, but this is less of a problem from an application point of view as these functionalised textiles are not expected to directly support the growth of human cells. These results demonstrated the low cytotoxicity of the AgNP- and SeNP-functionalised fabrics and partially addressed the safety concerns associated with the nanomaterials. However, this is only a preliminary study and more comprehensive study is needed if the materials are to be used in healthcare environments.

Chapter 7 Conclusions and Future Work

7.1 Introduction

The use of nanoparticles (NPs) as antimicrobial agents to functionalise biomedical materials has attracted increasing attention in recent years. This study set out to develop antimicrobial textiles based on inorganic nanoparticles in order to reduce the transmission of pathogens, mainly in healthcare settings. Selenium nanoparticles (SeNPs) in this thesis were identified as a novel type of antimicrobial inorganic nanoparticle which show promising antimicrobial performance and low cytotoxicity to mammalian cells. At the early stage of the study, some seemingly conflicting results regarding the antibacterial performance of SeNPs were found from the literature. For example, in some studies, SeNPs were found to be effective against both Gram-positive *S. aureus* and Gram-negative *E. coli*, while in some other studies, the SeNPs did not inhibit the growth of *E. coli*. To develop antimicrobial textiles based on SeNPs, it is important to understand the reasons behind the confounding results and under what conditions SeNPs work more effectively against the bacteria. It was hypothesised by Guisbiers *et al*. that the presence of some surface contamination (e.g. polymer or surfactant as stabilisers) may hinder the antimicrobial activity of SeNPs against some bacterial species. The methods to functionalise textiles with inorganic nanoparticles can be divided into two categories: (i) *ex situ* preparation and immobilisation of the NPs, which enables better control of the characteristics of the NPs, and (ii) *in situ* synthesis of the NPs, which has the advantage of a simpler treatment process. With respect to functionalisation of fabrics with SeNPs, a review of the literature produced very few results. Yip *et al*.[140] functionalised polyester fabrics using SeNPs prepared *ex situ* with the presence of a natural polysaccharide-protein complex as the stabiliser, and the authors only reported the antifungal property of the functionalised textiles. It is of value to investigate whether the presence of stabilisers may have adverse effects on the antimicrobial performance of SeNPs so that the functionalisation process can be better designed. Therefore, the first part of the study focused on colloidal SeNPs prepared with different stabilisers. At the same time, silver nanoparticles (AgNPs) were studied as a comparison since they are probably the most extensively studied

and applied inorganic nanoparticles due to their potent antimicrobial activity and broad antimicrobial spectrum. Based on the findings of this thesis and the results from the literature, in the second half of the study, a new method to functionalise cellulose textiles using quaternary ammonium compounds and *in situ* prepared NPs was developed. This method can be used to prepare both SeNPs and AgNPs *in situ* on the surface of cationized cellulose surface, and it is potentially applicable to other types of inorganic nanoparticles as well. With the assistance of microwave irradiation and the employment of a benign reducing agent (e.g. ascorbic acid), the functionalisation method is simple, rapid, versatile and environmentally friendly. The physicochemical properties, antibacterial performance, and *in vitro* cytotoxicity of the functionalised fabrics were assessed.

7.2 Conclusions

Findings from this study have contributed to the following conclusions:

(1) The stability is a major challenge when employing colloidal SeNPs as antimicrobial agents. The SeNPs require strong steric stabilisation and irreversible agglomeration happens quickly on bare SeNPs with only electrostatic stabilisation. This instability makes the synthesis of bare SeNPs difficult to scale up, which probably explains the rarity of studies on the properties of bare SeNPs in suspensions.

(2) The chemical synthesis of AgNPs is known to be highly sensitive to the reaction parameters including reaction time, temperature, pH, and reactant concentration and volume. There are also other factors that can be critical to the synthesis, for example, the size, shape and material of the reaction vials, as well as the mixing method and speed of the reactants. However, such information is often omitted from the published reports. In this study, the influence of the speed at which $AgNO_3$ was added into the reaction system was studied. It was found that rapid addition of the Ag precursor could result in smaller particle sizes and improved size distribution compared to adding $AgNO_3$ slowly drop by drop. More precise control of the addition and mixing of the reactants is needed for the control of particle sizes and distributions.

(3) There is not single a standard method to evaluate the antibacterial performance of inorganic NPs in suspensions. The unique properties of NPs may introduce artefacts to the tests and, therefore, more than one assay is needed to avoid skewed results. It has been shown that when using an agar diffusion method to assess the antibacterial performance of inorganic NPs, the size and the solubility of the particles play important roles in the process; thus, negative results from the agar diffusion assay do not necessarily mean the NPs have little or no antibacterial activity.

(4) Due to the instability of the bare SeNPs, the hypothesis that polymer or surfactant stabilisers may hinder the antibacterial activity of SeNPs was not able to be tested directly. By studying the antibacterial performance of SeNPs with different stabilising agents, it was found that the interactions between the SeNPs and the bacterial cells were greatly influenced by the bacterial species and the stabiliser. The SeNPs seemed to inhibit the growth of Gram-positive bacteria better than that of Gram-negative bacteria. *S. aureus* was particularly sensitive to SeNPs, regardless of the stabiliser type. The SeNPs stabilised by PVA or polysorbate 20 had no antibacterial effect on *E. coli*. The only type of SeNPs that inhibited the growth of *E. coli* was stabilised by chitosan; the effect might have been due to the positive surface charge introduced by chitosan, which facilitated the interactions between the CS-SeNPs and the bacterial cells; however, the possibility that the antibacterial activity was from chitosan alone could not be eliminated.

(5) The antibacterial performance of AgNPs was dose-, size- and bacterial species-dependent, which is in accordance with the literature: the smaller AgNPs had stronger antibacterial activity than the larger ones, and the AgNPs showed stronger antibacterial activity against the Gram-negative species than the Gram-positive ones. The antibacterial activities of bare TSC-AgNPs and chitosan-coated AgNPs were investigated and compared: due to the different test conditions (i.e. incubation time and contact method), the tests showed different results from the qualitative agar contact assay and from quantitative plate count assay. The qualitative agar contact assay showed that after 24-h contact, the CS-AgNPs showed stronger antibacterial effects than the bare TSC-AgNPs, while the bare TSC-AgNPs demonstrated better antibacterial performance than the CS-AgNPs with 4-h incubation in

the plant count assay, which probably was due to the delayed release of Ag^+ ions in the presence of chitosan coating compared to the bare TSC-AgNPs. These results indicated that when assessing the antimicrobial performance of NPs, the test conditions are very important. Multiple methods may be needed for a better understanding of the activity.

(6) By treating cellulose fabrics with quaternary ammonium compound CHPTAC, the cationic quaternary groups and activated alkali cellulose were introduced to the fabric surface, which enabled both anionic precursor (i.e. $SeNO_3^{2-}$ ions) and cationic metal precursor (i.e. Ag^+ ions) to be adsorbed onto the fabrics and subsequently reduced *in situ* to form nanoparticles. The *in situ* generated NPs were securely attached to the fabric and showed good laundry durability. The NPs had relatively narrow size distributions, with the majority of particle sizes in the range of 40 – 140 nm, and the NPs gave a good coverage to the fabric surface.

(7) The functionalised textile materials showed excellent antibacterial activities against both Gram-positive *S. aureus* and Gram-negative *E. coli* and *K. pneumoniae*. The cationic cellulose alone without the addition of NPs already showed some antibacterial effects, while the presence of NPs greatly increased the antibacterial performance of the functionalised fabrics. SeNPs appeared to be a good alternative to AgNPs as they provided equally excellent antibacterial performance on the functionalised fabrics. The bacterial cells looked severely damaged by the cationic groups and the NPs when examined by SEM and confocal microscopy. The antibacterial activities of all the NP-functionalised fabrics were so high that almost no viable bacterial cells could be detected post-incubation when tested using the challenge test method (absorption method) described by ISO 20734:2013. After repeated washing, the antibacterial performance of the cationic cellulose slightly decreased, probably caused by the anionic surfactant used in the laundry process; the antibacterial efficacies of NP-functionalised fabrics prepared with 0.2 mM precursor salts slightly deteriorated, suggesting that the concentration of precursor salt should be higher than 0.2 mM in order to maintain the excellent antibacterial performance after repeated washing.

(8) The red spherical SeNPs on the fabric grew into grey trigonal selenium when subjected to heat treatment (e.g. washed in hot water or being autoclaved)

even though they were immobilised on the fabric surface. The change of selenium form did not seem to adversely affect the antibacterial performance of the functionalised fabrics.

(9) The functionalised cellulose fabrics did not show significant cytotoxicity towards 16HBE16o- and HaCaT cells when tested using an indirect contact method *in vitro*. The samples functionalised with SeNPs or AgNPs showed different releasing behaviours when using water or cell culture media as the extract vehicles: more Se was detected from cell culture media and more Ag was detected from water as the extraction vehicle. Although, the amounts of Se or Ag released into either type of extraction vehicle were very low (<2 ppm), which probably explained the non-toxicity of the samples and demonstrated the secure attachment of the NPs to the fabrics. When the cells were treated with the media-extracts of the samples, the ATP levels of the cells were found to be lower than the control, which was found to be at least partly due to the removal of nutrients (e.g. proteins) from the cell culture media caused by the fabric samples. This should not be confused with the actual toxicity of a material caused by the release of toxic substances into the surrounding environment.

(10) Due to the attractive properties discussed above, the novel functionalised textiles developed in this study have the potential to serve as anti-infective materials, especially in healthcare environments, to prevent the growth and spread of pathogens.

7.3 Novelty

The work conducted in this study can be described as novel in the following ways:

(1) Conducted systematic comparison of the antibacterial activities of the colloidal SeNPs with different types of stabilisers (i.e. PVA, polysorbate 20 and chitosan).

(2) The antibacterial activity of the SeNPs was tested for the first time against a range of Gram-positive (*S. aureus, E. faecalis* and *S. pyogenes*), and Gram-

negative (*E. coli, P. aeruginosa* and *K. pneumoniae*) bacterial species together in one study for comparison.

(3) Directly compared the antibacterial performance of bare TSC-AgNPs and the corresponding subsequently prepared chitosan-coated AgNPs for the first time.

(4) Developed a new method to prepare inorganic nanoparticles on the surface of cellulose with the presence of cationic quaternary groups. The method employed microwave irradiation and environmentally benign reducing agent ascorbic acid, providing a rapid, simple, versatile and environmentally friendly approach to functionalise cellulose materials with inorganic nanoparticles.

(5) Successfully prepared cellulose fabrics functionalised with cationic groups and *in situ* synthesised SeNPs or AgNPs. The functionalised textile materials had good nanoparticle coverage, narrow particle size distribution, and secure bonding with the nanoparticles which was proven by a laundering test.

(6) The antibacterial property of the novel NP-functionalised cellulose fabrics was studied for the first time, and the results demonstrated excellent antimicrobial performance.

(7) Used Live/dead staining and confocal microscopy to directly observe the bacterial cells attached to the woven fabrics, which has not been reported previously.

(8) The *in vitro* cytotoxicity of the novel NP-functionalised cellulose fabrics was studied for the first time using an indirect contact method; no significant cytotoxicity was found from the test.

7.4 Future work and perspectives

This study explored the feasibility of using SeNPs and AgNPs as antimicrobial agents to functionalise textile materials. Cellulose was chosen as the substrate for the functionalisation, as it is the most abundant renewable polymer on earth which has been used as important textile materials in the form of natural plant fibres for

centuries.[252] In recent years, the development of novel cellulose-based materials using regenerated cellulose has attracted much attention; other applications of cellulose such as wound care, tissue scaffolds, food packaging, and filtration are being explored. A new method was developed in this study to prepare NP-functionalised cellulose fabrics, which can be extended to other forms of cellulose too. The novel functionalised textile materials were found to have excellent antimicrobial performance, low in vitro cytotoxicity and good laundry durability, and therefore, have the potential to be used as anti-infective textiles (e.g. beddings, curtains and uniforms) in healthcare environments to reduce the growth and spread of pathogens.

Due to the limitations of time and resources, there are still some areas requiring further investigation. There are several recommendations for future study:

(1) The novel method to prepare SeNPs and AgNPs *in situ* on the surface of cationic cellulose can potentially be applied to other types of inorganic nanoparticles with anionic precursor (e.g. tellurium) or other metal salt precursors (e.g. copper, gold and palladium). The mix of different types of inorganic nanoparticles may be a potential way to improve the antimicrobial activity and broaden the antimicrobial spectrum of the functionalised textile materials. For example, the combination of silver and copper nanoparticles have been found to show synergistic antimicrobial activity.[329]
(2) Further investigation can be conducted to understand the antimicrobial mechanism of the SeNPs. As a novel type of antimicrobial nanoparticles, SeNPs are still understudied and there are limited data on the antimicrobial mechanism of SeNPs. Possible routes include the investigation on the role of ROS during the process and analysis of organic selenium species involved in the process.
(3) The effect of microwave irradiation on the functionalisation can be explored further by adjusting the microwave time and power and how the samples are presented during the microwave treatment, including the method to scale up. The control of microwave irradiation may offer more precise control of the nanoparticle synthesis.
(4) Various types of benign reducing agent, including plant extracts, can be used. The presence of the natural chemicals may even help to improve the

antimicrobial performance of the functionalised fabrics and introduce other benefits (e.g. better biocompatibility, anti-odour property) to the fabric.

(5) The antimicrobial performance of the functionalised textiles should be tested against a wider range of pathogens, including bacteria, fungi and viruses, as well as clinical isolated strains.

(6) The laundry durability of the functionalised textiles was studied here in terms of the loss of nanoparticles using atomic emission spectroscopy; however, for real life applications, further investigation on the fate of the functionalised textiles subjected to repeated laundering and abrasion is needed regarding the changes in forms and loss of nanoparticles during these processes.

(7) The *in vitro* cytotoxicity study using the indirect contact method was only a preliminary investigation. The toxicity of the functionalised textiles towards humans should be investigated more comprehensively. For example, although the nanoparticles are securely attached to the fabric through *in situ* synthesis, the fabric may be shedding loose fibres containing nanoparticles, in which case direct contact method may be needed for the evaluation.

(8) Apart from general healthcare-textiles, the functionalisation method may also be applied onto other types of cellulose-based materials, for example, tissue engineering scaffolds, wound dressing materials, water/air filtration materials and food packaging.

List of references

(1) Ventola, C. L. The Antibiotic Resistance Crisis. *P T* **2015**, *40* (4), 277–283.

(2) Loftus, R. W.; Koff, M. D.; Burchman, C. C.; Schwartzman, J. D.; Thorum, V.; Read, M. E.; Wood, T. A.; Beach, M. L. Transmission of Pathogenic Bacterial Organisms in the Anesthesia Work Area. *Anesthesiology* **2008**, *109* (3), 399–407. https://doi.org/10.1097/ALN.0b013e318182c855.

(3) World Health Organization. *Report on the Burden of Endemic Health Care-Associated Infection Worldwide*; Geneva, Switzerland, 2011.

(4) Plowman, R. The Socioeconomic Burden of Hospital Acquired Infection. *Eurosurveillance* **2000**, *5* (4), 49–50. https://doi.org/10.2807/esm.05.04.00004-en.

(5) Poolman, J. T.; Anderson, A. S. Escherichia Coli and Staphylococcus Aureus: Leading Bacterial Pathogens of Healthcare Associated Infections and Bacteremia in Older-Age Populations. *Expert Review of Vaccines* **2018**, *17* (7), 607–618. https://doi.org/10.1080/14760584.2018.1488590.

(6) Gastmeier, P.; Stamm-Balderjahn, S.; Hansen, S.; Zuschneid, I.; Sohr, D.; Behnke, M.; Vonberg, R.-P.; Rüden, H. Where Should One Search When Confronted with Outbreaks of Nosocomial Infection? *American Journal of Infection Control* **2006**, *34* (9), 603–605. https://doi.org/10.1016/j.ajic.2006.01.014.

(7) Mitchell, A.; Spencer, M.; Edmiston, C. Role of Healthcare Apparel and Other Healthcare Textiles in the Transmission of Pathogens: A Review of the Literature. *Journal of Hospital Infection* **2015**, *90* (4), 285–292. https://doi.org/10.1016/j.jhin.2015.02.017.

(8) Gupta, D.; Khare, S. K.; Laha, A. Antimicrobial Properties of Natural Dyes against Gram-Negative Bacteria. *Coloration Technology* **2004**, *120* (4), 167–171. https://doi.org/10.1111/j.1478-4408.2004.tb00224.x.

(9) Ohl, M.; Schweizer, M.; Graham, M.; Heilmann, K.; Boyken, L.; Diekema, D. Hospital Privacy Curtains Are Frequently and Rapidly Contaminated with Potentially Pathogenic Bacteria. *American Journal of Infection Control* **2012**, *40* (10), 904–906. https://doi.org/10.1016/j.ajic.2011.12.017.

(10) Wiener-Well, Y.; Galuty, M.; Rudensky, B.; Schlesinger, Y.; Attias, D.; Yinnon, A. M. Nursing and Physician Attire as Possible Source of Nosocomial Infections. *Am J Infect Control* **2011**, *39* (7), 555–559. https://doi.org/10.1016/j.ajic.2010.12.016.

(11) Fijan, S.; Pahor, D.; Šostar Turk, S. Survival of Enterococcus Faecium, Staphylococcus Aureus and Pseudomonas Aeruginosa on Cotton. *Textile Research Journal* **2017**, *87* (14), 1711–1721. https://doi.org/10.1177/0040517516658514.

(12) Fijan, S.; Šostar Turk, S. Hospital Textiles, Are They a Possible Vehicle for Healthcare-Associated Infections? *Int J Environ Res Public Health* **2012**, *9* (9), 3330–3343. https://doi.org/10.3390/ijerph9093330.

(13) Borkow, G.; Gabbay, J. Biocidal Textiles Can Help Fight Nosocomial Infections. *Medical Hypotheses* **2008**, *70* (5), 990–994. https://doi.org/10.1016/j.mehy.2007.08.025.

(14) Marcus, E.-L.; Yosef, H.; Borkow, G.; Caine, Y.; Sasson, A.; Moses, A. E. Reduction of Health Care–Associated Infection Indicators by Copper Oxide–

Impregnated Textiles: Crossover, Double-Blind Controlled Study in Chronic Ventilator-Dependent Patients. *American Journal of Infection Control* **2017**, *45* (4), 401–403. https://doi.org/10.1016/j.ajic.2016.11.022.

(15) Butler, J. P. Effect of Copper-Impregnated Composite Bed Linens and Patient Gowns on Healthcare-Associated Infection Rates in Six Hospitals. *Journal of Hospital Infection* **2018**, *100* (3), e130–e134. https://doi.org/10.1016/j.jhin.2018.05.013.

(16) Hoefer, D.; Hammer, T. R. Antimicrobial Active Clothes Display No Adverse Effects on the Ecological Balance of the Healthy Human Skin Microflora https://www.hindawi.com/journals/isrn/2011/369603/ (accessed 2020 -06 -27). https://doi.org/10.5402/2011/369603.

(17) Coman, D.; Oancea, S.; Vrînceanu, N.; Blaga, L. Biofunctionalization of Textile Materials by Antimicrobial Treatments: A Critical Overview. *Romanian Biotechnological Letters* **2010**, *15* (1), 4913–4921.

(18) Sun, G. Disposable and Reusable Medical Textiles. In *Textiles for Hygiene and Infection Control*; McCarthy, B. J., Ed.; Woodhead Publishing Series in Textiles; Woodhead Publishing, 2011; pp 125–135. https://doi.org/10.1533/9780857093707.2.125.

(19) Zins, H. M.; Howard, M. Reusable Medical Textiles. In *Handbook of Medical Textiles*; Bartels, V. T., Ed.; Woodhead Publishing Series in Textiles; Woodhead Publishing, 2011; pp 80–105. https://doi.org/10.1533/9780857093691.1.80.

(20) Overcash, M. A Comparison of Reusable and Disposable Perioperative Textiles: Sustainability State-of-the-Art 2012. *Anesthesia & Analgesia* **2012**, *114* (5), 1055–1066. https://doi.org/10.1213/ANE.0b013e31824d9cc3.

(21) Hajipour, M. J.; Fromm, K. M.; Akbar Ashkarran, A.; Jimenez de Aberasturi, D.; Larramendi, I. R. de; Rojo, T.; Serpooshan, V.; Parak, W. J.; Mahmoudi, M. Antibacterial Properties of Nanoparticles. *Trends in Biotechnology* **2012**, *30* (10), 499–511. https://doi.org/10.1016/j.tibtech.2012.06.004.

(22) Dastjerdi, R.; Montazer, M. A Review on the Application of Inorganic Nano-Structured Materials in the Modification of Textiles: Focus on Anti-Microbial Properties. *Colloids and Surfaces B: Biointerfaces* **2010**, *79* (1), 5–18. https://doi.org/10.1016/j.colsurfb.2010.03.029.

(23) Auffan, M.; Rose, J.; Bottero, J.-Y.; Lowry, G. V.; Jolivet, J.-P.; Wiesner, M. R. Towards a Definition of Inorganic Nanoparticles from an Environmental, Health and Safety Perspective. *Nature Nanotechnology* **2009**, *4* (10), 634–641. https://doi.org/10.1038/nnano.2009.242.

(24) Jo, Y.-K.; Kim, B. H.; Jung, G. Antifungal Activity of Silver Ions and Nanoparticles on Phytopathogenic Fungi. *Plant Disease* **2009**, *93* (10), 1037–1043. https://doi.org/10.1094/PDIS-93-10-1037.

(25) Pelgrift, R. Y.; Friedman, A. J. Nanotechnology as a Therapeutic Tool to Combat Microbial Resistance. *Advanced Drug Delivery Reviews* **2013**, *65* (13), 1803–1815. https://doi.org/10.1016/j.addr.2013.07.011.

(26) Cantón, R.; Horcajada, J. P.; Oliver, A.; Garbajosa, P. R.; Vila, J. Inappropriate Use of Antibiotics in Hospitals: The Complex Relationship between Antibiotic Use and Antimicrobial Resistance. *Enferm. Infecc. Microbiol. Clin.* **2013**, *31 Suppl 4*, 3–11. https://doi.org/10.1016/S0213-005X(13)70126-5.

(27) Lara, H. H.; Ayala-núñez, N. V.; Ixtepan Turrent, L. D.; Carmen; Rodríguez Padilla, C. Bactericidal Effect of Silver Nanoparticles against Multidrug-

Resistant Bacteria. *World Journal of Microbiology and Biotechnology; Oxford* **2010**, *26* (4), 615–621. http://dx.doi.org/10.1007/s11274-009-0211-3.

(28) Rai, M. K.; Deshmukh, S. D.; Ingle, A. P.; Gade, A. K. Silver Nanoparticles: The Powerful Nanoweapon against Multidrug-Resistant Bacteria. *Journal of Applied Microbiology* **2012**, *112* (5), 841–852. https://doi.org/10.1111/j.1365-2672.2012.05253.x.

(29) Openstax. 3.3 Unique Characteristics of Prokaryotic Cells. In *Microbiology*; American Society for Microbiology Press, 2016.

(30) Ma, B.; Forney, L. J.; Ravel, J. The Vaginal Microbiome: Rethinking Health and Diseases. *Annu Rev Microbiol* **2012**, *66*, 371–389. https://doi.org/10.1146/annurev-micro-092611-150157.

(31) Gram, C. The Differential Staining of Schizomycetes in Tissue Sections and in Dried Preparations. *Fortschitte der Medicin* **1884**, *2*, 185–189.

(32) Ubbink, J.; Schär-Zammaretti, P. Colloidal Properties and Specific Interactions of Bacterial Surfaces. *Current Opinion in Colloid & Interface Science* **2007**, *12* (4), 263–270. https://doi.org/10.1016/j.cocis.2007.08.004.

(33) Neuhaus, F. C.; Baddiley, J. A Continuum of Anionic Charge: Structures and Functions of D-Alanyl-Teichoic Acids in Gram-Positive Bacteria. *Microbiol. Mol. Biol. Rev.* **2003**, *67* (4), 686–723. https://doi.org/10.1128/mmbr.67.4.686-723.2003.

(34) Livermore, D. M. Current Epidemiology and Growing Resistance of Gram-Negative Pathogens. *Korean J Intern Med* **2012**, *27* (2), 128–142. https://doi.org/10.3904/kjim.2012.27.2.128.

(35) Amato, E.; Diaz-Fernandez, Y. A.; Taglietti, A.; Pallavicini, P.; Pasotti, L.; Cucca, L.; Milanese, C.; Grisoli, P.; Dacarro, C.; Fernandez-Hechavarria, J. M.; Necchi, V. Synthesis, Characterization and Antibacterial Activity against Gram Positive and Gram Negative Bacteria of Biomimetically Coated Silver Nanoparticles. *Langmuir* **2011**, *27* (15), 9165–9173. https://doi.org/10.1021/la201200r.

(36) Jung, W. K.; Koo, H. C.; Kim, K. W.; Shin, S.; Kim, S. H.; Park, Y. H. Antibacterial Activity and Mechanism of Action of the Silver Ion in Staphylococcus Aureus and Escherichia Coli. *Appl. Environ. Microbiol.* **2008**, *74* (7), 2171–2178. https://doi.org/10.1128/AEM.02001-07.

(37) Taglietti, A.; Diaz Fernandez, Y. A.; Amato, E.; Cucca, L.; Dacarro, G.; Grisoli, P.; Necchi, V.; Pallavicini, P.; Pasotti, L.; Patrini, M. Antibacterial Activity of Glutathione-Coated Silver Nanoparticles against Gram Positive and Gram Negative Bacteria. *Langmuir* **2012**, *28* (21), 8140–8148. https://doi.org/10.1021/la3003838.

(38) Feng, Q. L.; Wu J.; Chen G. Q.; Cui F. Z.; Kim T. N.; Kim J. O. A Mechanistic Study of the Antibacterial Effect of Silver Ions on Escherichia Coli and Staphylococcus Aureus. *Journal of Biomedical Materials Research* **2000**, *52* (4), 662–668. https://doi.org/10.1002/1097-4636(20001215)52:4<662::AID-JBM10>3.0.CO;2-3.

(39) Núñez-Núñez, M.; Navarro, M. D.; Palomo, V.; Rajendran, N. B.; del Toro, M. D.; Voss, A.; Sharland, M.; Sifakis, F.; Tacconelli, E.; Rodríguez-Baño, J.; Burkert, F.; Carrara, E.; von Cube, M.; Drgona, L.; Gilchrist, K.; Goossens, H.; Harbarth, S.; Hequet, D.; Jafri, H.; Kahlmeter, G.; Kuster, S.; Luxemburger, C.; McCarthy, M.; Niks, M.; Oualim, A.; Poljak, M.; Sandulescu, O.; Schweiger, A.; Vuong, C.; Wiegand, I.; Widmer, A.; Witschi, A. T.; Zanetti, G.; Zingg, W. The Methodology of Surveillance for Antimicrobial Resistance

and Healthcare-Associated Infections in Europe (SUSPIRE): A Systematic Review of Publicly Available Information. *Clinical Microbiology and Infection* **2018**, *24* (2), 105–109. https://doi.org/10.1016/j.cmi.2017.07.014.

(40) Kluytmans, J.; Belkum, A. van; Verbrugh, H. Nasal Carriage of Staphylococcus Aureus: Epidemiology, Underlying Mechanisms, and Associated Risks. *Clin. Microbiol. Rev.* **1997**, *10* (3), 505–520.

(41) Vukušić, S. B.; Grgac, S. F.; Budimir, A.; Kalenić, S. Cotton Textiles Modified with Citric Acid as Efficient Anti-Bacterial Agent for Prevention of Nosocomial Infections. *Croatian Medical Journal* **2011**, *52* (1), 68.

(42) Weinstein, R. A.; Hota, B. Contamination, Disinfection, and Cross-Colonization: Are Hospital Surfaces Reservoirs for Nosocomial Infection? *Clin Infect Dis* **2004**, *39* (8), 1182–1189. https://doi.org/10.1086/424667.

(43) Carroll, K. C. Rapid Diagnostics for Methicillin-Resistant Staphylococcus Aureus. *Mol Diag Ther* **2008**, *12* (1), 15–24. https://doi.org/10.1007/BF03256265.

(44) Davies, J.; Davies, D. Origins and Evolution of Antibiotic Resistance. *Microbiol Mol Biol Rev* **2010**, *74* (3), 417–433. https://doi.org/10.1128/MMBR.00016-10.

(45) Weiser, J. N.; Ferreira, D. M.; Paton, J. C. Streptococcus Pneumoniae: Transmission, Colonization and Invasion. *Nat Rev Microbiol* **2018**, *16* (6), 355–367. https://doi.org/10.1038/s41579-018-0001-8.

(46) Russo, T. A.; Johnson, J. R. Medical and Economic Impact of Extraintestinal Infections Due to Escherichia Coli: Focus on an Increasingly Important Endemic Problem. *Microbes and Infection* **2003**, *5* (5), 449–456. https://doi.org/10.1016/S1286-4579(03)00049-2.

(47) Ko, W.-C.; Paterson, D. L.; Sagnimeni, A. J.; Hansen, D. S.; Von Gottberg, A.; Mohapatra, S.; Casellas, J. M.; Goossens, H.; Mulazimoglu, L.; Trenholme, G.; Klugman, K. P.; McCormack, J. G.; Yu, V. L. Community-Acquired Klebsiella Pneumoniae Bacteremia: Global Differences in Clinical Patterns. *Emerg Infect Dis* **2002**, *8* (2), 160–166. https://doi.org/10.3201/eid0802.010025.

(48) Navon-Venezia, S.; Kondratyeva, K.; Carattoli, A. Klebsiella Pneumoniae: A Major Worldwide Source and Shuttle for Antibiotic Resistance. *FEMS Microbiol Rev* **2017**, *41* (3), 252–275. https://doi.org/10.1093/femsre/fux013.

(49) Chatterjee, M.; Anju, C. P.; Biswas, L.; Anil Kumar, V.; Gopi Mohan, C.; Biswas, R. Antibiotic Resistance in Pseudomonas Aeruginosa and Alternative Therapeutic Options. *International Journal of Medical Microbiology* **2016**, *306* (1), 48–58. https://doi.org/10.1016/j.ijmm.2015.11.004.

(50) Harding, C. M.; Hennon, S. W.; Feldman, M. F. Uncovering the Mechanisms of Acinetobacter Baumannii Virulence. *Nat Rev Microbiol* **2018**, *16* (2), 91–102. https://doi.org/10.1038/nrmicro.2017.148.

(51) Giammanco, A.; Calà, C.; Fasciana, T.; Dowzicky, M. J. Global Assessment of the Activity of Tigecycline against Multidrug-Resistant Gram-Negative Pathogens between 2004 and 2014 as Part of the Tigecycline Evaluation and Surveillance Trial. *mSphere* **2017**, *2* (1). https://doi.org/10.1128/mSphere.00310-16.

(52) McDonnell, G.; Russell, A. D. Antiseptics and Disinfectants: Activity, Action, and Resistance. *Clin Microbiol Rev* **1999**, *12* (1), 147–179.

(53) Davin-Regli, A. Cross-Resistance between Biocides and Antimicrobials: An Emerging Question. *Revue Scientifique et Technique-OIE* **2012**, *31* (1), 16.

(54) Ayukekbong, J. A.; Ntemgwa, M.; Atabe, A. N. The Threat of Antimicrobial Resistance in Developing Countries: Causes and Control Strategies. *Antimicrob Resist Infect Control* **2017**, *6* (1), 47. https://doi.org/10.1186/s13756-017-0208-x.
(55) Gao, Y.; Cranston, R. Recent Advances in Antimicrobial Treatments of Textiles. *Textile Research Journal* **2008**, *78* (1), 60–72. https://doi.org/10.1177/0040517507082332.
(56) Windler, L.; Height, M.; Nowack, B. Comparative Evaluation of Antimicrobials for Textile Applications. *Environment International* **2013**, *53*, 62–73. https://doi.org/10.1016/j.envint.2012.12.010.
(57) Yazdankhah, S. P.; Scheie, A. A.; Høiby, E. A.; Lunestad, B.-T.; Heir, E.; Fotland, T. Ø.; Naterstad, K.; Kruse, H. Triclosan and Antimicrobial Resistance in Bacteria: An Overview. *Microbial Drug Resistance* **2006**, *12* (2), 83–90. https://doi.org/10.1089/mdr.2006.12.83.
(58) Dhillon, G. S.; Kaur, S.; Pulicharla, R.; Brar, S. K.; Cledón, M.; Verma, M.; Surampalli, R. Y. Triclosan: Current Status, Occurrence, Environmental Risks and Bioaccumulation Potential. *International Journal of Environmental Research and Public Health* **2015**, *12* (5), 5657–5684. https://doi.org/10.3390/ijerph120505657.
(59) Latch, D. E.; Packer, J. L.; Arnold, W. A.; McNeill, K. Photochemical Conversion of Triclosan to 2,8-Dichlorodibenzo-p-Dioxin in Aqueous Solution. *Journal of Photochemistry and Photobiology A: Chemistry* **2003**, *158* (1), 63–66. https://doi.org/10.1016/S1010-6030(03)00103-5.
(60) Allen, M. J.; White, G. F.; Morby, A. P. The Response of Escherichia Coli to Exposure to the Biocide Polyhexamethylene Biguanide. *Microbiology,* **2006**, *152* (4), 989–1000. https://doi.org/10.1099/mic.0.28643-0.
(61) Chadeau, E.; Brunon, C.; Degraeve, P.; Leonard, D.; Grossiord, C.; Bessueille, F.; Cottaz, A.; Renaud, F.; Ferreira, I.; Darroux, C.; Simon, F.; Rimbault, F.; Oulahal, N. Evaluation of Antimicrobial Activity of a Polyhexamethylene Biguanide-Coated Textile by Monitoring Both Bacterial Growth (Iso 20743/2005 Standard) and Viability (Live/Dead Baclight Kit). *Journal of Food Safety* **2012**, *32* (2), 141–151. https://doi.org/10.1111/j.1745-4565.2011.00361.x.
(62) Reputex 20 http://vantocil.ru/reputex_20 (accessed 2020 -06 -07).
(63) Morais, D.; Guedes, R.; Lopes, M. Antimicrobial Approaches for Textiles: From Research to Market. *Materials* **2016**, *9* (6), 498. https://doi.org/10.3390/ma9060498.
(64) ÆGIS Microbe Shield UK. AntiMicrobial Environments International - Microbeshield UK http://www.microbeshield.co.uk/ (accessed 2020 -06 -07).
(65) Advanced Agion® Silver Antimicrobial | Sciessent® https://www.sciessent.com/water-repellent-anti-odor-antimicrobial-products/agion-silver-antimicrobial/ (accessed 2020 -06 -07).
(66) 503 Service Temporarily Unavailable http://www.amicorpure.co.uk/ (accessed 2020 -06 -07).
(67) Fiji Chemical Industries. Bactekiller Bactelite | Fuji Chemical Industries https://www.fuji-chem.co.jp/en/ (accessed 2020 -06 -07).
(68) Trevira Bioactive /en/trevira-brands-the-seal-of-quality-for-functional-textiles/trevira-bioactive (accessed 2020 -06 -07).
(69) Antimicrobial Textiles & Fabrics | Antimicrobial Additives | BioCote Ltd. *BioCote*.

(70) BioFresh https://www.textileweb.com/doc/biofresh-0001 (accessed 2020 -06 -07).
(71) PRODUCTS (CHITOPOLY) http://www.denim-kuroki.co.jp/seihin_e.html (accessed 2020 -06 -07).
(72) Beda Ricklin, S. A. Crabyon fibers for anti-bacteria textile products http://old.swicofil.com/crabyon.html (accessed 2020 -06 -07).
(73) Cupron | Copper Based Antimicrobial Technology https://cupron.com/ (accessed 2020 -06 -07).
(74) FEELFRESH フィールフレッシュ https://www.toyobo.co.jp/seihin/jg/feelfresh/ (accessed 2020 -06 -07).
(75) Statex | Metallized Technical Textiles, Made in Germany https://statex.de/en/ (accessed 2020 -06 -07).
(76) Fibre Specific Auxiliaries - L. N. Chemical Industries https://www.lnchemicals.com/cotton-products2.html (accessed 2020 -06 -07).
(77) Silvadur™ http://silvadur.dupont.com/ (accessed 2020 -06 -07).
(78) Microban. Zinc Antimicrobial Protection for Textiles https://www.microban.com/odor-control/technologies/zptech (accessed 2020 -06 -07).
(79) SwicoSilver - Plasma Silver Coated Yarns providing flexibility, high conductivity, longevity https://www.swicofil.com/commerce/brands/swicosilver (accessed 2020 -09 -17).
(80) Gilbert, P.; Moore, L. E. Cationic Antiseptics: Diversity of Action under a Common Epithet. *J. Appl. Microbiol.* **2005**, *99* (4), 703–715. https://doi.org/10.1111/j.1365-2672.2005.02664.x.
(81) Simoncic, B.; Tomsic, B. Structures of Novel Antimicrobial Agents for Textiles - A Review. *Textile Research Journal* **2010**, *80* (16), 1721–1737. https://doi.org/10.1177/0040517510363193.
(82) Marini, M.; Bondi, M.; Iseppi, R.; Toselli, M.; Pilati, F. Preparation and Antibacterial Activity of Hybrid Materials Containing Quaternary Ammonium Salts via Sol–Gel Process. *European Polymer Journal* **2007**, *43* (8), 3621–3628. https://doi.org/10.1016/j.eurpolymj.2007.06.002.
(83) Wang, X.; Wang, C. The Antibacterial Finish of Cotton via Sols Containing Quaternary Ammonium Salts. *J Sol-Gel Sci Technol* **2009**, *50* (1), 15–21. https://doi.org/10.1007/s10971-009-1914-5.
(84) Bragg, R.; Jansen, A.; Coetzee, M.; van der Westhuizen, W.; Boucher, C. Bacterial Resistance to Quaternary Ammonium Compounds (QAC) Disinfectants. In *Infectious Diseases and Nanomedicine II*; Adhikari, R., Thapa, S., Eds.; Advances in Experimental Medicine and Biology; Springer India: New Delhi, 2014; pp 1–13. https://doi.org/10.1007/978-81-322-1774-9_1.
(85) Jennings, M. C.; Minbiole, K. P. C.; Wuest, W. M. Quaternary Ammonium Compounds: An Antimicrobial Mainstay and Platform for Innovation to Address Bacterial Resistance. *ACS Infect. Dis.* **2015**, *1* (7), 288–303. https://doi.org/10.1021/acsinfecdis.5b00047.
(86) Berger, J.; Reist, M.; Mayer, J. M.; Felt, O.; Peppas, N. A.; Gurny, R. Structure and Interactions in Covalently and Ionically Crosslinked Chitosan Hydrogels for Biomedical Applications. *European Journal of Pharmaceutics and Biopharmaceutics* **2004**, *57* (1), 19–34. https://doi.org/10.1016/S0939-6411(03)00161-9.

(87) Kong, M.; Chen, X. G.; Xing, K.; Park, H. J. Antimicrobial Properties of Chitosan and Mode of Action: A State of the Art Review. *International Journal of Food Microbiology* **2010**, *144* (1), 51–63. https://doi.org/10.1016/j.ijfoodmicro.2010.09.012.

(88) Goy, R. C.; Britto, D. de; Assis, O. B. G. A Review of the Antimicrobial Activity of Chitosan. *Polímeros* **2009**, *19* (3), 241–247. https://doi.org/10.1590/S0104-14282009000300013.

(89) No, H. K.; Kim, S. H.; Lee, S. H.; Park, N. Y.; Prinyawiwatkul, W. Stability and Antibacterial Activity of Chitosan Solutions Affected by Storage Temperature and Time. *Carbohydrate Polymers* **2006**, *65* (2), 174–178. https://doi.org/10.1016/j.carbpol.2005.12.036.

(90) Gadd, G. M.; Griffiths, A. J. Microorganisms and Heavy Metal Toxicity. *Microb Ecol* **1977**, *4* (4), 303–317. https://doi.org/10.1007/BF02013274.

(91) Silver, S.; Phung, L. T.; Silver, G. Silver as Biocides in Burn and Wound Dressings and Bacterial Resistance to Silver Compounds. *J IND MICROBIOL BIOTECHNOL* **2006**, *33* (7), 627–634. https://doi.org/10.1007/s10295-006-0139-7.

(92) Durán, N.; Durán, M.; de Jesus, M. B.; Seabra, A. B.; Fávaro, W. J.; Nakazato, G. Silver Nanoparticles: A New View on Mechanistic Aspects on Antimicrobial Activity. *Nanomedicine: Nanotechnology, Biology and Medicine* **2016**, *12* (3), 789–799. https://doi.org/10.1016/j.nano.2015.11.016.

(93) Jelenko 3rd, C. Silver Nitrate Resistant E. Coli: Report of Case. *Annals of surgery* **1969**, *170* (2), 296.

(94) Kremer, A. N.; Hoffmann, H. Subtractive Hybridization Yields a Silver Resistance Determinant Unique to Nosocomial Pathogens in the Enterobacter Cloacae Complex. *J Clin Microbiol* **2012**, *50* (10), 3249–3257. https://doi.org/10.1128/JCM.00885-12.

(95) Davis, I. J.; Richards, H.; Mullany, P. Isolation of Silver- and Antibiotic-Resistant Enterobacter Cloacae from Teeth. *Oral Microbiology and Immunology* **2005**, *20* (3), 191–194. https://doi.org/10.1111/j.1399-302X.2005.00218.x.

(96) Percival, S. L.; Bowler, P. G.; Russell, D. Bacterial Resistance to Silver in Wound Care. *Journal of Hospital Infection* **2005**, *60* (1), 1–7. https://doi.org/10.1016/j.jhin.2004.11.014.

(97) Yazdanshenas, M. E.; Shateri-Khalilabad, M. In Situ Synthesis of Silver Nanoparticles on Alkali-Treated Cotton Fabrics. *Journal of Industrial Textiles* **2013**, *42* (4), 459–474. https://doi.org/10.1177/1528083712444297.

(98) Nakashima, T.; Sakagami, Y.; Ito, H.; Matsuo, M. Antibacterial Activity of Cellulose Fabrics Modified with Metallic Salts. *Textile Research Journal* **2001**, *71* (8), 688–694. https://doi.org/10.1177/004051750107100807.

(99) Yuranova, T.; Rincon, A. G.; Bozzi, A.; Parra, S.; Pulgarin, C.; Albers, P.; Kiwi, J. Antibacterial Textiles Prepared by RF-Plasma and Vacuum-UV Mediated Deposition of Silver. *Journal of Photochemistry and Photobiology A: Chemistry* **2003**, *161* (1), 27–34. https://doi.org/10.1016/S1010-6030(03)00204-1.

(100) Feynman, R. P. There's Plenty of Room at the Bottom. *California Institute of Technology, Engineering and Science magazine* **1960**.

(101) Morones, J. R.; Elechiguerra, J. L.; Camacho, A.; Holt, K.; Kouri, J. B.; Ramírez, J. T.; Yacaman, M. J. The Bactericidal Effect of Silver Nanoparticles.

Nanotechnology **2005**, *16* (10), 2346–2353. https://doi.org/10.1088/0957-4484/16/10/059.

(102) Salata, O. Applications of Nanoparticles in Biology and Medicine. *J Nanobiotechnology* **2004**, *2*, 3. https://doi.org/10.1186/1477-3155-2-3.

(103) Parak, W.; Gerion, D.; Pellegrino, T.; Zanchet, D.; Micheel, C.; Williams, S.; Boudreau, R.; Gros, M.; Larabell, C.; Alivisatos, A. Biological Applications of Colloidal Nanocrystals. *Nanotechnology* **2003**, *14*, R15. https://doi.org/10.1088/0957-4484/14/7/201.

(104) Panáček, A.; Kvítek, L.; Prucek, R.; Kolář, M.; Večeřová, R.; Pizúrová, N.; Sharma, V. K.; Nevěčná, T.; Zbořil, R. Silver Colloid Nanoparticles: Synthesis, Characterization, and Their Antibacterial Activity. *J. Phys. Chem. B* **2006**, *110* (33), 16248–16253. https://doi.org/10.1021/jp063826h.

(105) Sondi, I.; Salopek-Sondi, B. Silver Nanoparticles as Antimicrobial Agent: A Case Study on E. Coli as a Model for Gram-Negative Bacteria. *Journal of Colloid and Interface Science* **2004**, *275* (1), 177–182. https://doi.org/10.1016/j.jcis.2004.02.012.

(106) Lara, H. H.; Ayala-Nuñez, N. V.; Ixtepan-Turrent, L.; Rodriguez-Padilla, C. Mode of Antiviral Action of Silver Nanoparticles against HIV-1. *Journal of Nanobiotechnology* **2010**, *8*, 1. https://doi.org/10.1186/1477-3155-8-1.

(107) Marambio-Jones, C.; Hoek, E. M. V. A Review of the Antibacterial Effects of Silver Nanomaterials and Potential Implications for Human Health and the Environment. *J Nanopart Res* **2010**, *12* (5), 1531–1551. https://doi.org/10.1007/s11051-010-9900-y.

(108) Ruparelia, J. P.; Chatterjee, A. K.; Duttagupta, S. P.; Mukherji, S. Strain Specificity in Antimicrobial Activity of Silver and Copper Nanoparticles. *Acta Biomaterialia* **2008**, *4* (3), 707–716. https://doi.org/10.1016/j.actbio.2007.11.006.

(109) Lok, C.-N.; Ho, C.-M.; Chen, R.; He, Q.-Y.; Yu, W.-Y.; Sun, H.; Tam, P. K.-H.; Chiu, J.-F.; Che, C.-M. Proteomic Analysis of the Mode of Antibacterial Action of Silver Nanoparticles. *Journal of Proteome Research* **2006**, *5* (4), 916–924. https://doi.org/10.1021/pr0504079.

(110) Carlson, C.; Hussain, S. M.; Schrand, A. M.; K. Braydich-Stolle, L.; Hess, K. L.; Jones, R. L.; Schlager, J. J. Unique Cellular Interaction of Silver Nanoparticles: Size-Dependent Generation of Reactive Oxygen Species. *J. Phys. Chem. B* **2008**, *112* (43), 13608–13619. https://doi.org/10.1021/jp712087m.

(111) Ninganagouda, S.; Rathod, V.; Singh, D.; Hiremath, J.; Singh, A. K.; Mathew, J.; ul-Haq, M. Growth Kinetics and Mechanistic Action of Reactive Oxygen Species Released by Silver Nanoparticles from Aspergillus Niger on Escherichia Coli. *Biomed Res Int* **2014**, *2014*, 753419. https://doi.org/10.1155/2014/753419.

(112) Hoseinnejad, M.; Jafari, S. M.; Katouzian, I. Inorganic and Metal Nanoparticles and Their Antimicrobial Activity in Food Packaging Applications. *Critical Reviews in Microbiology* **2018**, *44* (2), 161–181. https://doi.org/10.1080/1040841X.2017.1332001.

(113) Espitia, P. J. P.; Soares, N. de F. F.; Coimbra, J. S. dos R.; de Andrade, N. J.; Cruz, R. S.; Medeiros, E. A. A. Zinc Oxide Nanoparticles: Synthesis, Antimicrobial Activity and Food Packaging Applications. *Food and Bioprocess Technology* **2012**, *5* (5), 1447–1464. https://doi.org/10.1007/s11947-012-0797-6.

(114) Li, Y.; Zhang, W.; Niu, J.; Chen, Y. Mechanism of Photogenerated Reactive Oxygen Species and Correlation with the Antibacterial Properties of Engineered Metal-Oxide Nanoparticles. *ACS Nano* **2012**, *6* (6), 5164–5173. https://doi.org/10.1021/nn300934k.

(115) Li, Q.; Xie, R.; Li, Y. W.; Mintz, E. A.; Shang, J. K. Enhanced Visible-Light-Induced Photocatalytic Disinfection of E. Coli by Carbon-Sensitized Nitrogen-Doped Titanium Oxide. *Environ. Sci. Technol.* **2007**, *41* (14), 5050–5056. https://doi.org/10.1021/es062753c.

(116) Dakal, T. C.; Kumar, A.; Majumdar, R. S.; Yadav, V. Mechanistic Basis of Antimicrobial Actions of Silver Nanoparticles. *Front Microbiol* **2016**, *7*. https://doi.org/10.3389/fmicb.2016.01831.

(117) Meghana, S.; Kabra, P.; Chakraborty, S.; Padmavathy, N. Understanding the Pathway of Antibacterial Activity of Copper Oxide Nanoparticles. *RSC Adv.* **2015**, *5* (16), 12293–12299. https://doi.org/10.1039/C4RA12163E.

(118) Pan, X.; Redding, J. E.; Wiley, P. A.; Wen, L.; McConnell, J. S.; Zhang, B. Mutagenicity Evaluation of Metal Oxide Nanoparticles by the Bacterial Reverse Mutation Assay. *Chemosphere* **2010**, *79* (1), 113–116. https://doi.org/10.1016/j.chemosphere.2009.12.056.

(119) Wang, S.; Lawson, R.; Ray, P. C.; Yu, H. Toxic Effects of Gold Nanoparticles on Salmonella Typhimurium Bacteria. *Toxicol Ind Health* **2011**, *27* (6), 547–554. https://doi.org/10.1177/0748233710393395.

(120) Graves, J. L. J.; Tajkarimi, M.; Cunningham, Q.; Campbell, A.; Nonga, H.; Harrison, S. H.; Barrick, J. E. Rapid Evolution of Silver Nanoparticle Resistance in Escherichia Coli. *Front. Genet.* **2015**, *6*. https://doi.org/10.3389/fgene.2015.00042.

(121) Zhang, J.; Wang, H.; Bao, Y.; Zhang, L. Nano Red Elemental Selenium Has No Size Effect in the Induction of Seleno-Enzymes in Both Cultured Cells and Mice. *Life Sciences* **2004**, *75* (2), 237–244. https://doi.org/10.1016/j.lfs.2004.02.004.

(122) Tran, P. A.; O'Brien-Simpson, N.; Reynolds, E. C.; Pantarat, N.; Biswas, D. P.; O'Connor, A. J. Low Cytotoxic Trace Element Selenium Nanoparticles and Their Differential Antimicrobial Properties against S . Aureus and E. Coli. *Nanotechnology* **2016**, *27* (4), 045101. https://doi.org/10.1088/0957-4484/27/4/045101.

(123) Estevam, E. C.; Griffin, S.; Nasim, M. J.; Denezhkin, P.; Schneider, R.; Lilischkis, R.; Dominguez-Alvarez, E.; Witek, K.; Latacz, G.; Keck, C.; Schäfer, K.-H.; Kieć-Kononowicz, K.; Handzlik, J.; Jacob, C. Natural Selenium Particles from Staphylococcus Carnosus: Hazards or Particles with Particular Promise? *Journal of Hazardous Materials* **2017**, *324*, 22–30. https://doi.org/10.1016/j.jhazmat.2016.02.001.

(124) Navarro-Alarcon, M.; Cabrera-Vique, C. Selenium in Food and the Human Body: A Review. *Science of The Total Environment* **2008**, *400* (1), 115–141. https://doi.org/10.1016/j.scitotenv.2008.06.024.

(125) MacFarquhar, J. K.; Broussard, D. L.; Melstrom, P.; Hutchinson, R.; Wolkin, A.; Martin, C.; Burk, R. F.; Dunn, J. R.; Green, A. L.; Hammond, R.; Schaffner, W.; Jones, T. F. Acute Selenium Toxicity Associated With a Dietary Supplement. *Arch Intern Med* **2010**, *170* (3), 256–261. https://doi.org/10.1001/archinternmed.2009.495.

(126) Brown, K. M.; Arthur, J. R. Selenium, Selenoproteins and Human Health: A Review. *Public Health Nutrition* **2001**, *4* (2b), 593–599. https://doi.org/10.1079/PHN2001143.
(127) Chen, W.; Li, Y.; Yang, S.; Yue, L.; Jiang, Q.; Xia, W. Synthesis and Antioxidant Properties of Chitosan and Carboxymethyl Chitosan-Stabilized Selenium Nanoparticles. *Carbohydrate Polymers* **2015**, *132*, 574–581. https://doi.org/10.1016/j.carbpol.2015.06.064.
(128) Yu, B.; You, P.; Song, M.; Zhou, Y.; Yu, F.; Zheng, W. A Facile and Fast Synthetic Approach to Create Selenium Nanoparticles with Diverse Shapes and Their Antioxidation Ability. *New Journal of Chemistry* **2016**, *40* (2), 1118–1123. https://doi.org/10.1039/C5NJ02519B.
(129) Zimmerman, M. T.; Bayse, C. A.; Ramoutar, R. R.; Brumaghim, J. L. Sulfur and Selenium Antioxidants: Challenging Radical Scavenging Mechanisms and Developing Structure–Activity Relationships Based on Metal Binding. *Journal of Inorganic Biochemistry* **2015**, *145*, 30–40. https://doi.org/10.1016/j.jinorgbio.2014.12.020.
(130) Yang, F.; Tang, Q.; Zhong, X.; Bai, Y.; Chen, T.; Zhang, Y.; Li, Y.; Zheng, W. Surface Decoration by Spirulina Polysaccharide Enhances the Cellular Uptake and Anticancer Efficacy of Selenium Nanoparticles. *Int J Nanomedicine* **2012**, *7*, 835–844. https://doi.org/10.2147/IJN.S28278.
(131) Yu, B.; Zhang, Y.; Zheng, W.; Fan, C.; Chen, T. Positive Surface Charge Enhances Selective Cellular Uptake and Anticancer Efficacy of Selenium Nanoparticles. *Inorg. Chem.* **2012**, *51* (16), 8956–8963. https://doi.org/10.1021/ic301050v.
(132) Tran, P. A.; Webster, T. J. Selenium Nanoparticles Inhibit Staphylococcus Aureus Growth. *International Journal of Nanomedicine* **2011**, 1553. https://doi.org/10.2147/IJN.S21729.
(133) Bartůněk, V.; Junková, J.; Šuman, J.; Kolářová, K.; Rimpelová, S.; Ulbrich, P.; Sofer, Z. Preparation of Amorphous Antimicrobial Selenium Nanoparticles Stabilized by Odor Suppressing Surfactant Polysorbate 20. *Materials Letters* **2015**, *152*, 207–209. https://doi.org/10.1016/j.matlet.2015.03.092.
(134) Piacenza, E.; Presentato, A.; Zonaro, E.; Lemire, J. A.; Demeter, M.; Vallini, G.; Turner, R. J.; Lampis, S. Antimicrobial Activity of Biogenically Produced Spherical Se-Nanomaterials Embedded in Organic Material against Pseudomonas Aeruginosa and Staphylococcus Aureus Strains on Hydroxyapatite-Coated Surfaces. *Microbial Biotechnology* **2017**, *10* (4), 804–818. https://doi.org/10.1111/1751-7915.12700.
(135) Shakibaie, M.; Forootanfar, H.; Golkari, Y.; Mohammadi-Khorsand, T.; Shakibaie, M. R. Anti-Biofilm Activity of Biogenic Selenium Nanoparticles and Selenium Dioxide against Clinical Isolates of Staphylococcus Aureus, Pseudomonas Aeruginosa, and Proteus Mirabilis. *Journal of Trace Elements in Medicine and Biology* **2015**, *29*, 235–241. https://doi.org/10.1016/j.jtemb.2014.07.020.
(136) Srivastava, N.; Mukhopadhyay, M. Green Synthesis and Structural Characterization of Selenium Nanoparticles and Assessment of Their Antimicrobial Property. *Bioprocess Biosyst Eng* **2015**, *38* (9), 1723–1730. https://doi.org/10.1007/s00449-015-1413-8.
(137) Wang, Q.; Larese-Casanova, P.; Webster, T. J. Inhibition of Various Gram-Positive and Gram- Negative Bacteria Growth on Selenium Nanoparticle

Coated Paper Towels. *Int J Nanomedicine* **2015**, *10*, 2885–2894. https://doi.org/10.2147/IJN.S78466.

(138) Tran, P. A.; Webster, T. J. Antimicrobial Selenium Nanoparticle Coatings on Polymeric Medical Devices. *Nanotechnology* **2013**, *24* (15), 155101. https://doi.org/10.1088/0957-4484/24/15/155101.

(139) Wang, Q.; Webster, T. J. Short Communication: Inhibiting Biofilm Formation on Paper Towels through the Use of Selenium Nanoparticles Coatings. *Int J Nanomedicine* **2013**, *8*, 407–411. https://doi.org/10.2147/IJN.S38777.

(140) Yip, J.; Liu, L.; Wong, K.-H.; Leung, P. H. M.; Yuen, C.-W. M.; Cheung, M.-C. Investigation of Antifungal and Antibacterial Effects of Fabric Padded with Highly Stable Selenium Nanoparticles. *J. Appl. Polym. Sci.* **2014**, *131* (17). https://doi.org/10.1002/app.40728.

(141) Nguyen, T. H. D.; Vardhanabhuti, B.; Lin, M.; Mustapha, A. Antibacterial Properties of Selenium Nanoparticles and Their Toxicity to Caco-2 Cells. *Food Control* **2017**, *77*, 17–24. https://doi.org/10.1016/j.foodcont.2017.01.018.

(142) Biswas, D. P.; O'Brien-Simpson, N. M.; Reynolds, E. C.; O'Connor, A. J.; Tran, P. A. Comparative Study of Novel in Situ Decorated Porous Chitosan-Selenium Scaffolds and Porous Chitosan-Silver Scaffolds towards Antimicrobial Wound Dressing Application. *Journal of Colloid and Interface Science* **2018**, *515*, 78–91. https://doi.org/10.1016/j.jcis.2018.01.007.

(143) Skalickova, S.; Milosavljevic, V.; Cihalova, K.; Horky, P.; Richtera, L.; Adam, V. Selenium Nanoparticles as a Nutritional Supplement. *Nutrition* **2017**, *33*, 83–90. https://doi.org/10.1016/j.nut.2016.05.001.

(144) Palomo-Siguero, M.; Gutiérrez, A. M.; Pérez-Conde, C.; Madrid, Y. Effect of Selenite and Selenium Nanoparticles on Lactic Bacteria: A Multi-Analytical Study. *Microchemical Journal* **2016**, *126*, 488–495. https://doi.org/10.1016/j.microc.2016.01.010.

(145) Kieliszek, M.; Błażejak, S.; Gientka, I.; Bzducha-Wróbel, A. Accumulation and Metabolism of Selenium by Yeast Cells. *Appl. Microbiol. Biotechnol.* **2015**, *99* (13), 5373–5382. https://doi.org/10.1007/s00253-015-6650-x.

(146) Letavayová, L.; Vlasáková, D.; Spallholz, J. E.; Brozmanová, J.; Chovanec, M. Toxicity and Mutagenicity of Selenium Compounds in Saccharomyces Cerevisiae. *Mutation Research/Fundamental and Molecular Mechanisms of Mutagenesis* **2008**, *638* (1), 1–10. https://doi.org/10.1016/j.mrfmmm.2007.08.009.

(147) Stolzoff, M.; Wang, S. Q.; Webster, T. J. Frontiers | Efficacy and Mechanism of Selenium Nanoparticles as Antibacterial Agents.

(148) Huang, T.; A. Holden, J.; E. Heath, D.; M. O'Brien-Simpson, N.; J. O'Connor, A. Engineering Highly Effective Antimicrobial Selenium Nanoparticles through Control of Particle Size. *Nanoscale* **2019**, *11* (31), 14937–14951. https://doi.org/10.1039/C9NR04424H.

(149) Ahmad, A.; Mukherjee, P.; Senapati, S.; Mandal, D.; Khan, M. I.; Kumar, R.; Sastry, M. Extracellular Biosynthesis of Silver Nanoparticles Using the Fungus Fusarium Oxysporum. *Colloids and Surfaces B: Biointerfaces* **2003**, *28* (4), 313–318. https://doi.org/10.1016/S0927-7765(02)00174-1.

(150) Mafuné, Fumitaka; Kohno, J.; Takeda, Y.; Kondow, T.; Sawabe, H. Formation and Size Control of Silver Nanoparticles by Laser Ablation in Aqueous Solution. *J. Phys. Chem. B* **2000**, *104* (39), 9111–9117. https://doi.org/10.1021/jp001336y.

(151) Salkar, R. A.; Jeevanandam, P.; Aruna, S. T.; Koltypin, Y.; Gedanken, A. The Sonochemical Preparation of Amorphous Silver Nanoparticles. *Journal of Materials Chemistry* **1999**, *9* (6), 1333–1335. https://doi.org/10.1039/A900568D.
(152) Sharma, V. K.; Yngard, R. A.; Lin, Y. Silver Nanoparticles: Green Synthesis and Their Antimicrobial Activities. *Advances in Colloid and Interface Science* **2009**, *145* (1–2), 83–96. https://doi.org/10.1016/j.cis.2008.09.002.
(153) Song, J. Y.; Kim, B. S. Rapid Biological Synthesis of Silver Nanoparticles Using Plant Leaf Extracts. *Bioprocess and Biosystems Engineering* **2009**, *32* (1), 79–84. https://doi.org/10.1007/s00449-008-0224-6.
(154) Pillai, Z. S.; Kamat, P. V. What Factors Control the Size and Shape of Silver Nanoparticles in the Citrate Ion Reduction Method? *J. Phys. Chem. B* **2004**, *108* (3), 945–951. https://doi.org/10.1021/jp037018r.
(155) Zhang, Y.; Wang, J.; Zhang, L. Creation of Highly Stable Selenium Nanoparticles Capped with Hyperbranched Polysaccharide in Water. *Langmuir* **2010**, *26* (22), 17617–17623. https://doi.org/10.1021/la1033959.
(156) Li, Q.; Chen, T.; Yang, F.; Liu, J.; Zheng, W. Facile and Controllable One-Step Fabrication of Selenium Nanoparticles Assisted by l-Cysteine. *Materials Letters* **2010**, *64* (5), 614–617. https://doi.org/10.1016/j.matlet.2009.12.019.
(157) Baruwati, B.; Polshettiwar, V.; S. Varma, R. Glutathione Promoted Expeditious Green Synthesis of Silver Nanoparticles in Water Using Microwaves. *Green Chemistry* **2009**, *11* (7), 926–930. https://doi.org/10.1039/B902184A.
(158) Lim, I.-I. S.; Mott, D.; Ip, W.; Njoki, P. N.; Pan, Y.; Zhou, S.; Zhong, C.-J. Interparticle Interactions in Glutathione Mediated Assembly of Gold Nanoparticles. *Langmuir* **2008**, *24* (16), 8857–8863. https://doi.org/10.1021/la800970p.
(159) Asmathunisha, N.; Kathiresan, K. A Review on Biosynthesis of Nanoparticles by Marine Organisms. *Colloids and Surfaces B: Biointerfaces* **2013**, *103*, 283–287. https://doi.org/10.1016/j.colsurfb.2012.10.030.
(160) Iravani, S. Green Synthesis of Metal Nanoparticles Using Plants. *Green Chem.* **2011**, *13* (10), 2638–2650. https://doi.org/10.1039/C1GC15386B.
(161) Mittal, A. K.; Chisti, Y.; Banerjee, U. C. Synthesis of Metallic Nanoparticles Using Plant Extracts. *Biotechnology Advances* **2013**, *31* (2), 346–356. https://doi.org/10.1016/j.biotechadv.2013.01.003.
(162) Narayanan, K. B.; Sakthivel, N. Biological Synthesis of Metal Nanoparticles by Microbes. *Advances in Colloid and Interface Science* **2010**, *156* (1), 1–13. https://doi.org/10.1016/j.cis.2010.02.001.
(163) Agnihotri, S.; Mukherji, S.; Mukherji, S. Size-Controlled Silver Nanoparticles Synthesized over the Range 5–100 Nm Using the Same Protocol and Their Antibacterial Efficacy. *RSC Advances* **2014**, *4* (8), 3974–3983. https://doi.org/10.1039/C3RA44507K.
(164) Martínez-Castañón, G. A.; Niño-Martínez, N.; Martínez-Gutierrez, F.; Martínez-Mendoza, J. R.; Ruiz, F. Synthesis and Antibacterial Activity of Silver Nanoparticles with Different Sizes. *Journal of Nanoparticle Research* **2008**, *10* (8), 1343–1348. https://doi.org/10.1007/s11051-008-9428-6.
(165) Dwivedi, S.; Wahab, R.; Khan, F.; Mishra, Y. K.; Musarrat, J.; Al-Khedhairy, A. A. Reactive Oxygen Species Mediated Bacterial Biofilm Inhibition via Zinc Oxide Nanoparticles and Their Statistical Determination. *PLOS ONE* **2014**, *9* (11), e111289. https://doi.org/10.1371/journal.pone.0111289.

(166) Heng, B. C.; Zhao, X.; Tan, E. C.; Khamis, N.; Assodani, A.; Xiong, S.; Ruedl, C.; Ng, K. W.; Loo, J. S. Evaluation of the Cytotoxic and Inflammatory Potential of Differentially Shaped Zinc Oxide Nanoparticles. *Archives of Toxicology. Archiv für Toxikologie* **2011**, *85* (12), 1517–1528. http://dx.doi.org/10.1007/s00204-011-0722-1.

(167) Helmlinger, J.; Sengstock, C.; Groß-Heitfeld, C.; Mayer, C.; A. Schildhauer, T.; Köller, M.; Epple, M. Silver Nanoparticles with Different Size and Shape: Equal Cytotoxicity, but Different Antibacterial Effects. *RSC Advances* **2016**, *6* (22), 18490–18501. https://doi.org/10.1039/C5RA27836H.

(168) Pal, S.; Tak, Y. K.; Song, J. M. Does the Antibacterial Activity of Silver Nanoparticles Depend on the Shape of the Nanoparticle? A Study of the Gram-Negative Bacterium Escherichia Coli. *Appl. Environ. Microbiol.* **2007**, *73* (6), 1712–1720. https://doi.org/10.1128/AEM.02218-06.

(169) Abbaszadegan, A.; Ghahramani, Y.; Gholami, A.; Hemmateenejad, B.; Dorostkar, S.; Nabavizadeh, M.; Sharghi, H. The Effect of Charge at the Surface of Silver Nanoparticles on Antimicrobial Activity against Gram-Positive and Gram-Negative Bacteria: A Preliminary Study https://www.hindawi.com/journals/jnm/2015/720654/ (accessed 2018 -06 -19). https://doi.org/10.1155/2015/720654.

(170) El Badawy, A. M.; Silva, R. G.; Morris, B.; Scheckel, K. G.; Suidan, M. T.; Tolaymat, T. M. Surface Charge-Dependent Toxicity of Silver Nanoparticles. *Environ. Sci. Technol.* **2011**, *45* (1), 283–287. https://doi.org/10.1021/es1034188.

(171) Guisbiers, G.; Wang, Q.; Khachatryan, E.; Mimun, L. C.; Mendoza-Cruz, R.; Larese-Casanova, P.; Webster, T. J.; Nash, K. L. Inhibition of E. Coli and S. Aureus with Selenium Nanoparticles Synthesized by Pulsed Laser Ablation in Deionized Water. *INT J NANOMED* **2016**. https://doi.org/10.2147/IJN.S106289.

(172) Hebeish, A.; El-Naggar, M. E.; Fouda, M. M. G.; Ramadan, M. A.; Al-Deyab, S. S.; El-Rafie, M. H. Highly Effective Antibacterial Textiles Containing Green Synthesized Silver Nanoparticles. *Carbohydrate Polymers* **2011**, *86* (2), 936–940. https://doi.org/10.1016/j.carbpol.2011.05.048.

(173) Khalil-Abad, M. S.; Yazdanshenas, M. E.; Nateghi, M. R. Effect of Cationization on Adsorption of Silver Nanoparticles on Cotton Surfaces and Its Antibacterial Activity. *Cellulose* **2009**, *16* (6), 1147. https://doi.org/10.1007/s10570-009-9351-8.

(174) Tang, B.; Li, J.; Hou, X.; Afrin, T.; Sun, L.; Wang, X. Colorful and Antibacterial Silk Fiber from Anisotropic Silver Nanoparticles. *Ind. Eng. Chem. Res.* **2013**, *52* (12), 4556–4563. https://doi.org/10.1021/ie3033872.

(175) Li, Y.; Hou, Y.; Zou, Y. Microwave Assisted Fabrication of Nano-ZnO Assembled Cotton Fibers with Excellent UV Blocking Property and Water-Wash Durability. *Fibers Polym* **2012**, *13* (2), 185–190. https://doi.org/10.1007/s12221-012-0185-x.

(176) Montazer, M.; Amiri, M. M.; Malek, R. M. A. In Situ Synthesis and Characterization of Nano ZnO on Wool: Influence of Nano Photo Reactor on Wool Properties. *Photochemistry and Photobiology* **2013**, *89* (5), 1057–1063. https://doi.org/10.1111/php.12090.

(177) Perera, S.; Bhushan, B.; Bandara, R.; Rajapakse, G.; Rajapakse, S.; Bandara, C. Morphological, Antimicrobial, Durability, and Physical Properties of Untreated and Treated Textiles Using Silver-Nanoparticles. *Colloids and*

Surfaces A: Physicochemical and Engineering Aspects **2013**, *436*, 975–989. https://doi.org/10.1016/j.colsurfa.2013.08.038.

(178) Vance, M. E.; Kuiken, T.; Vejerano, E. P.; McGinnis, S. P.; Jr, M. F. H.; Rejeski, D.; Hull, M. S. Nanotechnology in the Real World: Redeveloping the Nanomaterial Consumer Products Inventory. *Beilstein J. Nanotechnol.* **2015**, *6* (1), 1769–1780. https://doi.org/10.3762/bjnano.6.181.

(179) Ellis, L.-J. A.; Baalousha, M.; Valsami-Jones, E.; Lead, J. R. Seasonal Variability of Natural Water Chemistry Affects the Fate and Behaviour of Silver Nanoparticles. *Chemosphere* **2018**, *191*, 616–625. https://doi.org/10.1016/j.chemosphere.2017.10.006.

(180) Li, X.; Lenhart, J. J. Aggregation and Dissolution of Silver Nanoparticles in Natural Surface Water. *Environ. Sci. Technol.* **2012**, *46* (10), 5378–5386. https://doi.org/10.1021/es204531y.

(181) Johnston, H. J.; Hutchison, G.; Christensen, F. M.; Peters, S.; Hankin, S.; Stone, V. A Review of the in Vivo and in Vitro Toxicity of Silver and Gold Particulates: Particle Attributes and Biological Mechanisms Responsible for the Observed Toxicity. *Crit. Rev. Toxicol.* **2010**, *40* (4), 328–346. https://doi.org/10.3109/10408440903453074.

(182) Larese Filon, F.; Bello, D.; Cherrie, J. W.; Sleeuwenhoek, A.; Spaan, S.; Brouwer, D. H. Occupational Dermal Exposure to Nanoparticles and Nano-Enabled Products: Part I—Factors Affecting Skin Absorption. *International Journal of Hygiene and Environmental Health* **2016**, *219* (6), 536–544. https://doi.org/10.1016/j.ijheh.2016.05.009.

(183) Larese, F. F.; D'Agostin, F.; Crosera, M.; Adami, G.; Renzi, N.; Bovenzi, M.; Maina, G. Human Skin Penetration of Silver Nanoparticles through Intact and Damaged Skin. *Toxicology* **2009**, *255* (1), 33–37. https://doi.org/10.1016/j.tox.2008.09.025.

(184) Wu, J.; Liu, W.; Xue, C.; Zhou, S.; Lan, F.; Bi, L.; Xu, H.; Yang, X.; Zeng, F.-D. Toxicity and Penetration of TiO2 Nanoparticles in Hairless Mice and Porcine Skin after Subchronic Dermal Exposure. *Toxicology Letters* **2009**, *191* (1), 1–8. https://doi.org/10.1016/j.toxlet.2009.05.020.

(185) Larese Filon, F.; Mauro, M.; Adami, G.; Bovenzi, M.; Crosera, M. Nanoparticles Skin Absorption: New Aspects for a Safety Profile Evaluation. *Regulatory Toxicology and Pharmacology* **2015**, *72* (2), 310–322. https://doi.org/10.1016/j.yrtph.2015.05.005.

(186) Rothen-Rutishauser, B.; Blank, F.; Mühlfeld, C.; Gehr, P. In Vitro Models of the Human Epithelial Airway Barrier to Study the Toxic Potential of Particulate Matter. *Expert Opin Drug Metab Toxicol* **2008**, *4* (8), 1075–1089. https://doi.org/10.1517/17425255.4.8.1075.

(187) Bakand, S.; Hayes, A.; Dechsakulthorn, F. Nanoparticles: A Review of Particle Toxicology Following Inhalation Exposure. *Inhal Toxicol* **2012**, *24* (2), 125–135. https://doi.org/10.3109/08958378.2010.642021.

(188) Quadros, M. E.; Marr, L. C. Environmental and Human Health Risks of Aerosolized Silver Nanoparticles. *Journal of the Air & Waste Management Association* **2010**, *60* (7), 770–781. https://doi.org/10.3155/1047-3289.60.7.770.

(189) Oberdörster Günter; Oberdörster Eva; Oberdörster Jan. Nanotoxicology: An Emerging Discipline Evolving from Studies of Ultrafine Particles. *Environmental Health Perspectives* **2005**, *113* (7), 823–839. https://doi.org/10.1289/ehp.7339.

(190) Gliga, A. R.; Skoglund, S.; Odnevall Wallinder, I.; Fadeel, B.; Karlsson, H. L. Size-Dependent Cytotoxicity of Silver Nanoparticles in Human Lung Cells: The Role of Cellular Uptake, Agglomeration and Ag Release. *Particle and Fibre Toxicology* **2014**, *11* (1), 11. https://doi.org/10.1186/1743-8977-11-11.
(191) Geranio, L.; Heuberger, M.; Nowack, B. The Behavior of Silver Nanotextiles during Washing. *Environ. Sci. Technol.* **2009**, *43* (21), 8113–8118. https://doi.org/10.1021/es9018332.
(192) Moore, M. N. Do Nanoparticles Present Ecotoxicological Risks for the Health of the Aquatic Environment? *Environment International* **2006**, *32* (8), 967–976. https://doi.org/10.1016/j.envint.2006.06.014.
(193) Griffitt, R. J.; Luo, J.; Gao, J.; Bonzongo, J.-C.; Barber, D. S. Effects of Particle Composition and Species on Toxicity of Metallic Nanomaterials in Aquatic Organisms. *Environmental Toxicology and Chemistry* **2008**, *27* (9), 1972–1978. https://doi.org/10.1897/08-002.1.
(194) Reed, R. B.; Zaikova, T.; Barber, A.; Simonich, M.; Lankone, R.; Marco, M.; Hristovski, K.; Herckes, P.; Passantino, L.; Fairbrother, D. H.; Tanguay, R.; Ranville, J. F.; Hutchison, J. E.; Westerhoff, P. K. Potential Environmental Impacts and Antimicrobial Efficacy of Silver- and Nanosilver-Containing Textiles. *Environ. Sci. Technol.* **2016**, *50* (7), 4018–4026. https://doi.org/10.1021/acs.est.5b06043.
(195) Silva, L. P.; Reis, I. G.; Bonatto, C. C. Green Synthesis of Metal Nanoparticles by Plants: Current Trends and Challenges. In *Green Processes for Nanotechnology: From Inorganic to Bioinspired Nanomaterials*; Basiuk, V. A., Basiuk, E. V., Eds.; Springer International Publishing: Cham, 2015; pp 259–275. https://doi.org/10.1007/978-3-319-15461-9_9.
(196) Zhang, S.-Y.; Zhang, J.; Wang, H.-Y.; Chen, H.-Y. Synthesis of Selenium Nanoparticles in the Presence of Polysaccharides. *Materials Letters* **2004**, *58* (21), 2590–2594. https://doi.org/10.1016/j.matlet.2004.03.031.
(197) Kong, H.; Yang, J.; Zhang, Y.; Fang, Y.; Nishinari, K.; Phillips, G. O. Synthesis and Antioxidant Properties of Gum Arabic-Stabilized Selenium Nanoparticles. *International Journal of Biological Macromolecules* **2014**, *65*, 155–162. https://doi.org/10.1016/j.ijbiomac.2014.01.011.
(198) Bai, K.; Hong, B.; He, J.; Hong, Z.; Tan, R. Preparation and Antioxidant Properties of Selenium Nanoparticles-Loaded Chitosan Microspheres. *Int J Nanomedicine* **2017**, *12*, 4527–4539. https://doi.org/10.2147/IJN.S129958.
(199) Lin, Z.-H.; Chris Wang, C. R. Evidence on the Size-Dependent Absorption Spectral Evolution of Selenium Nanoparticles. *Materials Chemistry and Physics* **2005**, *92* (2), 591–594. https://doi.org/10.1016/j.matchemphys.2005.02.023.
(200) Shah, C. P.; Kumar, M.; Bajaj, P. N. Acid-Induced Synthesis of Polyvinyl Alcohol-Stabilized Selenium Nanoparticles. *Nanotechnology* **2007**, *18* (38), 385607. https://doi.org/10.1088/0957-4484/18/38/385607.
(201) Bindhu, M. R.; Umadevi, M. Synthesis of Monodispersed Silver Nanoparticles Using Hibiscus Cannabinus Leaf Extract and Its Antimicrobial Activity. *Spectrochimica Acta Part A: Molecular and Biomolecular Spectroscopy* **2013**, *101*, 184–190. https://doi.org/10.1016/j.saa.2012.09.031.
(202) Mohan Kumar, K.; Mandal, B. K.; Kiran Kumar, H. A.; Maddinedi, S. B. Green Synthesis of Size Controllable Gold Nanoparticles. *Spectrochimica Acta Part A: Molecular and Biomolecular Spectroscopy* **2013**, *116*, 539–545. https://doi.org/10.1016/j.saa.2013.07.077.

(203) Xiong, J.; Wang, Y.; Xue, Q.; Wu, X. Synthesis of Highly Stable Dispersions of Nanosized Copper Particles Using L-Ascorbic Acid. *Green Chemistry* **2011**, *13* (4), 900. https://doi.org/10.1039/c0gc00772b.
(204) Zonaro, E.; Lampis, S.; Turner, R. J.; Qazi, S. J. S.; Vallini, G. Biogenic Selenium and Tellurium Nanoparticles Synthesized by Environmental Microbial Isolates Efficaciously Inhibit Bacterial Planktonic Cultures and Biofilms. *Front Microbiol* **2015**, *6*. https://doi.org/10.3389/fmicb.2015.00584.
(205) Zhang, C.; Zhai, X.; Zhao, G.; Ren, F.; Leng, X. Synthesis, Characterization, and Controlled Release of Selenium Nanoparticles Stabilized by Chitosan of Different Molecular Weights. *Carbohydrate Polymers* **2015**, *134*, 158–166. https://doi.org/10.1016/j.carbpol.2015.07.065.
(206) Qin, Y.; Ji, X.; Jing, J.; Liu, H.; Wu, H.; Yang, W. Size Control over Spherical Silver Nanoparticles by Ascorbic Acid Reduction. *Colloids and Surfaces A: Physicochemical and Engineering Aspects* **2010**, *372* (1), 172–176. https://doi.org/10.1016/j.colsurfa.2010.10.013.
(207) Zhang, J.; Wang, H.; Yan, X.; Zhang, L. Comparison of Short-Term Toxicity between Nano-Se and Selenite in Mice. *Life Sciences* **2005**, *76* (10), 1099–1109. https://doi.org/10.1016/j.lfs.2004.08.015.
(208) Ng, C. H. B.; Fan, W. Y. Colloidal Beading: Sonication-Induced Stringing of Selenium Particles. *Langmuir* **2014**, *30* (25), 7313–7318. https://doi.org/10.1021/la5012617.
(209) Chen, Z.; Shen, Y.; Xie, A.; Zhu, J.; Wu, Z.; Huang, F. L-Cysteine-Assisted Controlled Synthesis of Selenium Nanospheres and Nanorods. *Crystal Growth & Design* **2009**, *9* (3), 1327–1333. https://doi.org/10.1021/cg800398b.
(210) Gates, B.; Mayers, B.; Grossman, A.; Xia, Y. A Sonochemical Approach to the Synthesis of Crystalline Selenium Nanowires in Solutions and on Solid Supports. *Adv. Mater.* **2002**, *14* (23), 1749–1752. https://doi.org/10.1002/1521-4095(20021203)14:23<1749::AID-ADMA1749>3.0.CO;2-Z.
(211) Liu, L.; Peng, Q.; Li, Y. Preparation of Monodisperse Se Colloid Spheres and Se Nanowires Using Na2SeSO3 as Precursor. *Nano Res.* **2008**, *1* (5), 403–411. https://doi.org/10.1007/s12274-008-8040-5.
(212) Prozorov, T.; Prozorov, R.; Suslick, K. S. High Velocity Interparticle Collisions Driven by Ultrasound. *J. Am. Chem. Soc.* **2004**, *126* (43), 13890–13891. https://doi.org/10.1021/ja049493o.
(213) Bhattacharjee, S. DLS and Zeta Potential – What They Are and What They Are Not? *Journal of Controlled Release* **2016**, *235*, 337–351. https://doi.org/10.1016/j.jconrel.2016.06.017.
(214) Patel, V. R.; Agrawal, Y. K. Nanosuspension: An Approach to Enhance Solubility of Drugs. *J Adv Pharm Technol Res* **2011**, *2* (2), 81–87. https://doi.org/10.4103/2231-4040.82950.
(215) Kvítek, L.; Panáček, A.; Soukupová, J.; Kolář, M.; Večeřová, R.; Prucek, R.; Holecová, M.; Zbořil, R. Effect of Surfactants and Polymers on Stability and Antibacterial Activity of Silver Nanoparticles (NPs). *J. Phys. Chem. C* **2008**, *112* (15), 5825–5834. https://doi.org/10.1021/jp711616v.
(216) Claes, N.; Asapu, R.; Blommaerts, N.; Verbruggen, S. W.; Lenaerts, S.; Bals, S. Characterization of Silver-Polymer Core–Shell Nanoparticles Using Electron Microscopy. *Nanoscale* **2018**, *10* (19), 9186–9191. https://doi.org/10.1039/C7NR09517A.

(217) International Organization for Standardization. *Particle Size Analysis — Dynamic Light Scattering (DLS) (ISO 22412:2017)*; 2017.
(218) Hackley, V. A.; Clogston, J. D. Measuring the Size of Nanoparticles in Aqueous Media Using Batch-Mode Dynamic Light Scattering. **2015**.
(219) Gaumet, M.; Vargas, A.; Gurny, R.; Delie, F. Nanoparticles for Drug Delivery: The Need for Precision in Reporting Particle Size Parameters. *European Journal of Pharmaceutics and Biopharmaceutics* **2008**, *69* (1), 1–9. https://doi.org/10.1016/j.ejpb.2007.08.001.
(220) Bartůněk, V.; Junková, J.; Babuněk, M.; Ulbrich, P.; Kuchař, M.; Sofer, Z. Synthesis of Spherical Amorphous Selenium Nano and Microparticles with Tunable Sizes. *Micro & Nano Letters* **2016**, *11* (2), 91–93. https://doi.org/10.1049/mnl.2015.0353.
(221) Van Phu, D.; Quoc, L. A.; Duy, N. N.; Lan, N. T. K.; Du, B. D.; Luan, L. Q.; Hien, N. Q. Study on Antibacterial Activity of Silver Nanoparticles Synthesized by Gamma Irradiation Method Using Different Stabilizers. *Nanoscale Research Letters* **2014**, *9* (1), 162. https://doi.org/10.1186/1556-276X-9-162.
(222) Skrabalak, S. E.; Au, L.; Li, X.; Xia, Y. Facile Synthesis of Ag Nanocubes and Au Nanocages. *Nat. Protocols* **2007**, *2* (9), 2182–2190. https://doi.org/10.1038/nprot.2007.326.
(223) Li, H.; Xia, H.; Wang, D.; Tao, X. Simple Synthesis of Monodisperse, Quasi-Spherical, Citrate-Stabilized Silver Nanocrystals in Water. *Langmuir* **2013**, *29* (16), 5074–5079. https://doi.org/10.1021/la400214x.
(224) Seil, J. T.; Webster, T. J. Antimicrobial Applications of Nanotechnology: Methods and Literature. *Int J Nanomedicine* **2012**, *7*, 2767–2781. https://doi.org/10.2147/IJN.S24805.
(225) The European Committee on Antimicrobial Susceptibility Testing. *Antimicrobial Susceptibility Testing EUCAST Disk Diffusion Method*; 2020.
(226) Dong, P. V.; Ha, C. H.; Binh, L. T.; Kasbohm, J. Chemical Synthesis and Antibacterial Activity of Novel-Shaped Silver Nanoparticles. *Int Nano Lett* **2012**, *2* (1), 9. https://doi.org/10.1186/2228-5326-2-9.
(227) Jain, D.; Daima, H. K.; Kachhwaha, S.; Kothari, S. L. Synthesis of Plant-Mediated Silver Nanoparticles Using Papaya Fruit Extract and Evaluation of Their Anti Microbial Activities. *Digest journal of nanomaterials and biostructures* **2009**, *4* (3), 557–563.
(228) Li, W.-R.; Xie, X.-B.; Shi, Q.-S.; Zeng, H.-Y.; OU-Yang, Y.-S.; Chen, Y.-B. Antibacterial Activity and Mechanism of Silver Nanoparticles on Escherichia Coli. *Applied Microbiology and Biotechnology* **2010**, *85* (4), 1115–1122. https://doi.org/10.1007/s00253-009-2159-5.
(229) Dasari, T. P.; Pathakoti, K.; Hwang, H.-M. Determination of the Mechanism of Photoinduced Toxicity of Selected Metal Oxide Nanoparticles (ZnO, CuO, Co3O4 and TiO2) to E. Coli Bacteria. *Journal of Environmental Sciences* **2013**, *25* (5), 882–888. https://doi.org/10.1016/S1001-0742(12)60152-1.
(230) Hu, X.; Cook, S.; Wang, P.; Hwang, H. In Vitro Evaluation of Cytotoxicity of Engineered Metal Oxide Nanoparticles. *Science of The Total Environment* **2009**, *407* (8), 3070–3072. https://doi.org/10.1016/j.scitotenv.2009.01.033.
(231) Rasool, K.; Helal, M.; Ali, A.; Ren, C. E.; Gogotsi, Y.; Mahmoud, K. A. Antibacterial Activity of Ti3C2Tx MXene. *ACS Nano* **2016**, *10* (3), 3674–3684. https://doi.org/10.1021/acsnano.6b00181.

(232) Beheshti, N.; Soflaei, S.; Shakibaie, M.; Yazdi, M. H.; Ghaffarifar, F.; Dalimi, A.; Shahverdi, A. R. Efficacy of Biogenic Selenium Nanoparticles against Leishmania Major: In Vitro and in Vivo Studies. *Journal of Trace Elements in Medicine and Biology* **2013**, *27* (3), 203–207. https://doi.org/10.1016/j.jtemb.2012.11.002.

(233) Monteiro-Riviere, N. A.; Inman, A. O.; Zhang, L. W. Limitations and Relative Utility of Screening Assays to Assess Engineered Nanoparticle Toxicity in a Human Cell Line. *Toxicology and Applied Pharmacology* **2009**, *234* (2), 222–235. https://doi.org/10.1016/j.taap.2008.09.030.

(234) Bankier, C.; Cheong, Y.; Mahalingam, S.; Edirisinghe, M.; Ren, G.; Cloutman-Green, E.; Ciric, L. A Comparison of Methods to Assess the Antimicrobial Activity of Nanoparticle Combinations on Bacterial Cells. *PLOS ONE* **2018**, *13* (2), e0192093. https://doi.org/10.1371/journal.pone.0192093.

(235) Xiu, Z.; Zhang, Q.; Puppala, H. L.; Colvin, V. L.; Alvarez, P. J. J. Negligible Particle-Specific Antibacterial Activity of Silver Nanoparticles https://pubs.acs.org/doi/suppl/10.1021/nl301934w (accessed 2018 -05 -20). https://doi.org/10.1021/nl301934w.

(236) Li, L.; Mendis, N.; Trigui, H.; Oliver, J. D.; Faucher, S. P. The Importance of the Viable but Non-Culturable State in Human Bacterial Pathogens. *Front. Microbiol.* **2014**, *5*. https://doi.org/10.3389/fmicb.2014.00258.

(237) Stewart, P. S. Diffusion in Biofilms. *Journal of Bacteriology* **2003**, *185* (5), 1485–1491. https://doi.org/10.1128/JB.185.5.1485-1491.2003.

(238) Lara, H. H.; Guisbiers, G.; Mendoza, J.; Mimun, L. C.; Vincent, B. A.; Lopez-Ribot, J. L.; Nash, K. L. Synergistic Antifungal Effect of Chitosan-Stabilized Selenium Nanoparticles Synthesized by Pulsed Laser Ablation in Liquids against Candida Albicans Biofilms. *Int J Nanomedicine* **2018**, *13*, 2697–2708. https://doi.org/10.2147/IJN.S151285.

(239) British Standards Institution. *Chemical Disinfectants and Antiseptics — Quantitative Suspension Test for the Evaluation of Basic Bactericidal Activity of Chemical Disinfectants and Antiseptics — Test Method and Requirements (Phase 1)*; 2005.

(240) Sanpui, P.; Murugadoss, A.; Prasad, P. V. D.; Ghosh, S. S.; Chattopadhyay, A. The Antibacterial Properties of a Novel Chitosan–Ag-Nanoparticle Composite. *International Journal of Food Microbiology* **2008**, *124* (2), 142–146. https://doi.org/10.1016/j.ijfoodmicro.2008.03.004.

(241) Slavin, Y. N.; Asnis, J.; Häfeli, U. O.; Bach, H. Metal Nanoparticles: Understanding the Mechanisms behind Antibacterial Activity. *J Nanobiotechnology* **2017**, *15*. https://doi.org/10.1186/s12951-017-0308-z.

(242) Boroumand, S.; Safari, M.; Shaabani, E.; Shirzad, M.; Faridi-Majidi, R. Selenium Nanoparticles: Synthesis, Characterization and Study of Their Cytotoxicity, Antioxidant and Antibacterial Activity. *Mater. Res. Express* **2019**, *6* (8), 0850d8. https://doi.org/10.1088/2053-1591/ab2558.

(243) Hegerova, D.; Vesely, R.; Cihalova, K.; Kopel, P.; Milosavljevic, V.; Heger, Z.; Hynek, D.; Guran, R.; Vaculovicova, M.; Sedlacek, P.; Adam, V. Antimicrobial Agent Based on Selenium Nanoparticles and Carboxymethyl Cellulose for the Treatment of Bacterial Infections. *Journal of Biomedical Nanotechnology* **2017**, *13* (7), 767–777. https://doi.org/10.1166/jbn.2017.2384.

(244) Arakawa, Y.; Shibata, N.; Shibayama, K.; Kurokawa, H.; Yagi, T.; Fujiwara, H.; Goto, M. Convenient Test for Screening Metallo-β-Lactamase-Producing Gram-Negative Bacteria by Using Thiol Compounds. *J Clin Microbiol* **2000**, *38* (1), 40–43.
(245) Zhang, R.; Qin, X.; Kong, F.; Chen, P.; Pan, G. Improving Cellular Uptake of Therapeutic Entities through Interaction with Components of Cell Membrane. *Drug Delivery* **2019**, *26* (1), 328–342. https://doi.org/10.1080/10717544.2019.1582730.
(246) Jena, P.; Mohanty, S.; Mallick, R.; Jacob, B.; Sonawane, A. Toxicity and Antibacterial Assessment of Chitosancoated Silver Nanoparticles on Human Pathogens and Macrophage Cells. *Int J Nanomedicine* **2012**, *7*, 1805–1818. https://doi.org/10.2147/IJN.S28077.
(247) Wu, F.; J. Harper, B.; L. Harper, S. Differential Dissolution and Toxicity of Surface Functionalized Silver Nanoparticles in Small-Scale Microcosms: Impacts of Community Complexity. *Environmental Science: Nano* **2017**, *4* (2), 359–372. https://doi.org/10.1039/C6EN00324A.
(248) Chaudhary, S.; Chauhan, P.; Kumar, R.; Bhasin, K. K. Toxicological Responses of Surfactant Functionalized Selenium Nanoparticles: A Quantitative Multi-Assay Approach. *Science of The Total Environment* **2018**, *643*, 1265–1277. https://doi.org/10.1016/j.scitotenv.2018.06.296.
(249) Ionin, A. A.; Ivanova, A. K.; Khmel'nitskii, R. A.; Klevkov, Y. V.; Kudryashov, S. I.; Levchenko, A. O.; Nastulyavichus, A. A.; Rudenko, A. A.; Saraeva, I. N.; Smirnov, N. A.; Zayarny, D. A.; Gonchukov, S. A.; Tolordava, E. R. Antibacterial Effect of the Laser-Generated Se Nanocoatings on Staphylococcus Aureus and Pseudomonas Aeruginosa Biofilms. *Laser Phys. Lett.* **2017**, *15* (1), 015604. https://doi.org/10.1088/1612-202X/aa897f.
(250) Elmaaty, T. A.; Raouf, S.; Sayed-Ahmed, K. Novel One Step Printing and Functional Finishing of Wool Fabric Using Selenium Nanoparticles. *Fibers Polym* **2020**, *21* (9), 1983–1991. https://doi.org/10.1007/s12221-020-9461-3.
(251) Reddy, K. O.; Maheswari, C. U.; Dhlamini, M. S.; Mothudi, B. M.; Kommula, V. P.; Zhang, J.; Zhang, J.; Rajulu, A. V. Extraction and Characterization of Cellulose Single Fibers from Native African Napier Grass. *Carbohydrate Polymers* **2018**, *188*, 85–91. https://doi.org/10.1016/j.carbpol.2018.01.110.
(252) Klemm, D.; Heublein, B.; Fink, H.-P.; Bohn, A. Cellulose: Fascinating Biopolymer and Sustainable Raw Material. *Angewandte Chemie International Edition* **2005**, *44* (22), 3358–3393. https://doi.org/10.1002/anie.200460587.
(253) Helmy, S. A.; Abd El-Motagali, H. A. Studies of the Alkaline Degradation of Cellulose: Part 1. Changes in the Characteristics of Cellulose with Time and Temperature. *Polymer Degradation and Stability* **1992**, *38* (3), 235–238. https://doi.org/10.1016/0141-3910(92)90118-O.
(254) Lewin, M.; Pearce, E. M. *Handbook of Fiber Chemistry, Second Edition, Revised and Expanded*; CRC Press, 1998.
(255) Farrell, M. J. Sustainable Cotton Dyeing. Ph.D, North Carolina State University, Raleigh, North Carolina, 2012.
(256) Farrell, M. J. Cationic Cotton, Reservations to Reality. *2012 Proceedings of AATCC International Conference, Hilton University Place, Charlotte, NC, USA, March 21-23, 2012* **2012**, 29–38.
(257) Acharya, S.; Abidi, N.; Rajbhandari, R.; Meulewaeter, F. Chemical Cationization of Cotton Fabric for Improved Dye Uptake. *Cellulose* **2014**, *21* (6), 4693–4706. https://doi.org/10.1007/s10570-014-0457-2.

(258) European Commission. *European Union Risk Assessment Report (3-CHLORO-2-HYDROXYPROPYL)TRIMETHYLAMMONIUM CHLORIDE (CHPTAC)*; 2008.
(259) Hu, D.; Wang, L. Physical and Antibacterial Properties of Polyvinyl Alcohol Films Reinforced with Quaternized Cellulose. *Journal of Applied Polymer Science* **2016**, *133* (25). https://doi.org/10.1002/app.43552.
(260) Fei, P.; Liao, L.; Meng, J.; Cheng, B.; Hu, X.; Song, J. Non-Leaching Antibacterial Cellulose Triacetate Reverse Osmosis Membrane via Covalent Immobilization of Quaternary Ammonium Cations. *Carbohydrate Polymers* **2018**, *181*, 1102–1111. https://doi.org/10.1016/j.carbpol.2017.11.036.
(261) Littunen, K.; Snoei de Castro, J.; Samoylenko, A.; Xu, Q.; Quaggin, S.; Vainio, S.; Seppälä, J. Synthesis of Cationized Nanofibrillated Cellulose and Its Antimicrobial Properties. *European Polymer Journal* **2016**, *75*, 116–124. https://doi.org/10.1016/j.eurpolymj.2015.12.008.
(262) Farouk, A.; Sharaf, S.; Abd El-Hady, M. M. Preparation of Multifunctional Cationized Cotton Fabric Based on TiO2 Nanomaterials. *International Journal of Biological Macromolecules* **2013**, *61*, 230–237. https://doi.org/10.1016/j.ijbiomac.2013.06.022.
(263) Uğur, Ş. S.; Sarıışık, M.; Aktaş, A. H.; Uçar, M. Ç.; Erden, E. Modifying of Cotton Fabric Surface with Nano-ZnO Multilayer Films by Layer-by-Layer Deposition Method. *Nanoscale Res Lett* **2010**, *5* (7), 1204–1210. https://doi.org/10.1007/s11671-010-9627-9.
(264) Dong, B. H.; Hinestroza, J. P. Metal Nanoparticles on Natural Cellulose Fibers: Electrostatic Assembly and In Situ Synthesis. *ACS Appl. Mater. Interfaces* **2009**, *1* (4), 797–803. https://doi.org/10.1021/am800225j.
(265) Valodkar, M.; Modi, S.; Pal, A.; Thakore, S. Synthesis and Anti-Bacterial Activity of Cu, Ag and Cu–Ag Alloy Nanoparticles: A Green Approach. *Materials Research Bulletin* **2011**, *46* (3), 384–389. https://doi.org/10.1016/j.materresbull.2010.12.001.
(266) Raspolli Galletti, A. M.; Antonetti, C.; Marracci, M.; Piccinelli, F.; Tellini, B. Novel Microwave-Synthesis of Cu Nanoparticles in the Absence of Any Stabilizing Agent and Their Antibacterial and Antistatic Applications. *Applied Surface Science* **2013**, *280*, 610–618. https://doi.org/10.1016/j.apsusc.2013.05.035.
(267) Zain, N. M.; Stapley, A. G. F.; Shama, G. Green Synthesis of Silver and Copper Nanoparticles Using Ascorbic Acid and Chitosan for Antimicrobial Applications. *Carbohydrate Polymers* **2014**, *112*, 195–202. https://doi.org/10.1016/j.carbpol.2014.05.081.
(268) Zhao, T.; Fan, J.-B.; Cui, J.; Liu, J.-H.; Xu, X.-B.; Zhu, M.-Q. Microwave-Controlled Ultrafast Synthesis of Uniform Silver Nanocubes and Nanowires. *Chemical Physics Letters* **2011**, *501* (4–6), 414–418. https://doi.org/10.1016/j.cplett.2010.11.031.
(269) Sun, H.; Lin, L.; Jiang, X.; Bai, X. The Improvement of Dyeability of Flax Fibre by Microwave Treatment. *Pigment & Resin Technology* **2005**, *34* (4), 190–196. https://doi.org/10.1108/03699420510609079.
(270) Budimir, A.; Bischof Vukusic, S.; Grgac Flincec, S. Study of Antimicrobial Properties of Cotton Medical Textiles Treated with Citric Acid and Dried/Cured by Microwaves. *Cellulose* **2012**, *19* (1), 289–296. https://doi.org/10.1007/s10570-011-9614-z.

(271) Zhang, F.; Chen, Y.; Lin, H.; Lu, Y. Synthesis of an Amino-Terminated Hyperbranched Polymer and Its Application in Reactive Dyeing on Cotton as a Salt-Free Dyeing Auxiliary. *Coloration Technology* **2007**, *123* (6), 351–357. https://doi.org/10.1111/j.1478-4408.2007.00108.x.
(272) Rashidi, A.; Shahidi, S.; Ghoranneviss, M.; Dalalsharifi, S.; Wiener, J. Effect of Plasma on the Zeta Potential of Cotton Fabrics. *Plasma Sci. Technol.* **2013**, *15* (5), 455–458. https://doi.org/10.1088/1009-0630/15/5/12.
(273) American Association of Textile Chemists and Colorists. *AATCC Test 61-2013 (Colorfastness to Laundering: Accelerated)*; 2013.
(274) Department of Health. *Health Technical Memorandum 01-04: Decontamination of Linen for Health and Social Care*; 2016.
(275) Hashem, M.; Hauser, P.; Smith, B. Reaction Efficiency for Cellulose Cationization Using 3-Chloro-2- Hydroxypropyl Trimethyl Ammonium Chloride. *Textile Research Journal* **2003**, *73* (11), 1017–1023. https://doi.org/10.1177/004051750307301113.
(276) Bastús, N. G.; Merkoçi, F.; Piella, J.; Puntes, V. Synthesis of Highly Monodisperse Citrate-Stabilized Silver Nanoparticles of up to 200 Nm: Kinetic Control and Catalytic Properties. *Chem. Mater.* **2014**, *26* (9), 2836–2846. https://doi.org/10.1021/cm500316k.
(277) Tarbuk, A.; Grancaric, A. M.; Leskovac, M. Novel Cotton Cellulose by Cationisation during the Mercerisation Process—Part 1: Chemical and Morphological Changes. *Cellulose* **2014**, *21* (3), 2167–2179. https://doi.org/10.1007/s10570-014-0245-z.
(278) Wang, L.; Ma, W.; Zhang, S.; Teng, X.; Yang, J. Preparation of Cationic Cotton with Two-Bath Pad-Bake Process and Its Application in Salt-Free Dyeing. *Carbohydrate Polymers* **2009**, *78* (3), 602–608. https://doi.org/10.1016/j.carbpol.2009.05.022.
(279) Li, M.; Zhang, L.; Qiu, M.; Zhang, Y.; Fu, S. Dyeing Property of Fluorescent Pigment Latex on Cationic Knitted Cotton Fabrics. *Textile Research Journal* **2019**, *89* (3), 422–433. https://doi.org/10.1177/0040517517748494.
(280) Wan, X.; Guo, C.; Feng, J.; Yu, T.; Chai, X.-S.; Chen, G.; Xie, W.-Q. Determination of the Degree of Substitution of Cationic Guar Gum by Headspace-Based Gas Chromatography during Its Synthesis. *J. Agric. Food Chem.* **2017**, *65* (32), 7012–7016. https://doi.org/10.1021/acs.jafc.7b03144.
(281) Ferraria, A. M.; Carapeto, A. P.; do Rego, A. M. B. X-Ray Photoelectron Spectroscopy: Silver Salts Revisited. *Vacuum* **2012**, *86* (12), 1988–1991. https://doi.org/10.1016/j.vacuum.2012.05.031.
(282) Moulder, J. F.; Stickle, W. F.; Sobol, P. E.; Bomben, K. D. *Handbook of X-Ray Photoelectron Spectroscopy*; Perkin-Elmer Corporation, 1995.
(283) Wang, Q.; Mejía Jaramillo, A.; Pavon, J. J.; Webster, T. J. Red Selenium Nanoparticles and Gray Selenium Nanorods as Antibacterial Coatings for PEEK Medical Devices. *J. Biomed. Mater. Res.* **2016**, *104* (7), 1352–1358. https://doi.org/10.1002/jbm.b.33479.
(284) Pinho, E.; Magalhães, L.; Henriques, M.; Oliveira, R. Antimicrobial Activity Assessment of Textiles: Standard Methods Comparison. *Ann Microbiol* **2011**, *61* (3), 493–498. https://doi.org/10.1007/s13213-010-0163-8.
(285) American Association of Textile Chemists and Colorists. *AATCC TM147-Antibacterial Activity of Textile Materials: Parallel Streak*; 2016.

(286) International Organization for Standardization. *Textile Fabrics — Determination of Antibacterial Activity — Agar Diffusion Plate Test (ISO 20645:2004)*; 2004.
(287) Japanese Standards Association. *Textiles -- Determination of Antibacterial Activity and Efficacy of Textile Products (JIS L 1902:2015)*; 2015.
(288) American Association of Textile Chemists and Colorists. *TM100-Test Method for Antibacterial Finishes on Textile Materials: Assess*; 2019.
(289) International Organization for Standardization. *Textiles — Determination of Antibacterial Activity of Textile Products (ISO 20743:2013)*; 2013.
(290) American Society of Testing and Materials. *Standard Test Method for Determining the Antimicrobial Activity of Immobilized Antimicrobial Agents Under Dynamic Contact Conditions (E2149-13)*; 2013.
(291) International Bureau for Standardisation of Man-made Fibres. *International Bureau for Standardisation of Man-Made Fibres Booklet*; 2002.
(292) Haase, H.; Jordan, L.; Keitel, L.; Keil, C.; Mahltig, B. Comparison of Methods for Determining the Effectiveness of Antibacterial Functionalized Textiles. *PLoS One* **2017**, *12* (11). https://doi.org/10.1371/journal.pone.0188304.
(293) Sener, S.; Acuner, I. C.; Bek, Y.; Durupinar, B. Colorimetric-Plate Method for Rapid Disk Diffusion Susceptibility Testing of Escherichia Coli. *Journal of Clinical Microbiology* **2011**, *49* (3), 1124–1127. https://doi.org/10.1128/JCM.02104-10.
(294) Molecular Probes. *LIVE/DEAD® BacLight™ Bacterial Viability Kits Product Information*; 2004.
(295) Cooper, I. R.; Pollini, M.; Paladini, F. The Potential of Photo-Deposited Silver Coatings on Foley Catheters to Prevent Urinary Tract Infections. *Materials Science and Engineering: C* **2016**, *69*, 414–420. https://doi.org/10.1016/j.msec.2016.07.004.
(296) Cen, L.; Neoh, K. G.; Kang, E. T. Surface Functionalization Technique for Conferring Antibacterial Properties to Polymeric and Cellulosic Surfaces. *Langmuir* **2003**, *19* (24), 10295–10303. https://doi.org/10.1021/la035104c.
(297) Roy, D.; Knapp, J. S.; Guthrie, J. T.; Perrier, S. Antibacterial Cellulose Fiber via RAFT Surface Graft Polymerization. *Biomacromolecules* **2008**, *9* (1), 91–99. https://doi.org/10.1021/bm700849j.
(298) Tiller, J. C.; Liao, C.-J.; Lewis, K.; Klibanov, A. M. Designing Surfaces That Kill Bacteria on Contact. *PNAS* **2001**, *98* (11), 5981–5985. https://doi.org/10.1073/pnas.111143098.
(299) Yang, Y.-F.; Hu, H.-Q.; Li, Y.; Wan, L.-S.; Xu, Z.-K. Membrane Surface with Antibacterial Property by Grafting Polycation. *Journal of Membrane Science* **2011**, *376* (1), 132–141. https://doi.org/10.1016/j.memsci.2011.04.012.
(300) Gottenbos, B.; Grijpma, D. W.; van der Mei, H. C.; Feijen, J.; Busscher, H. J. Antimicrobial Effects of Positively Charged Surfaces on Adhering Gram-Positive and Gram-Negative Bacteria. *J Antimicrob Chemother* **2001**, *48* (1), 7–13. https://doi.org/10.1093/jac/48.1.7.
(301) Vivian Feng, Z.; L. Gunsolus, I.; A. Qiu, T.; R. Hurley, K.; H. Nyberg, L.; Frew, H.; P. Johnson, K.; M. Vartanian, A.; M. Jacob, L.; E. Lohse, S.; D. Torelli, M.; J. Hamers, R.; J. Murphy, C.; L. Haynes, C. Impacts of Gold Nanoparticle Charge and Ligand Type on Surface Binding and Toxicity to Gram-Negative and Gram-Positive Bacteria. *Chemical Science* **2015**, *6* (9), 5186–5196. https://doi.org/10.1039/C5SC00792E.

(302) Boulos, L.; Prévost, M.; Barbeau, B.; Coallier, J.; Desjardins, R. LIVE/DEAD® BacLight™: Application of a New Rapid Staining Method for Direct Enumeration of Viable and Total Bacteria in Drinking Water. *Journal of Microbiological Methods* **1999**, *37* (1), 77–86. https://doi.org/10.1016/S0167-7012(99)00048-2.

(303) Hu, W.; Murata, K.; Zhang, D. Applicability of LIVE/DEAD BacLight Stain with Glutaraldehyde Fixation for the Measurement of Bacterial Abundance and Viability in Rainwater. *Journal of Environmental Sciences* **2017**, *51*, 202–213. https://doi.org/10.1016/j.jes.2016.05.030.

(304) Zawadzka, K.; Kisielewska, A.; Piwoński, I.; Kądzioła, K.; Felczak, A.; Różalska, S.; Wrońska, N.; Lisowska, K. Mechanisms of Antibacterial Activity and Stability of Silver Nanoparticles Grown on Magnetron Sputtered TiO2 Coatings. *Bull Mater Sci* **2016**, *39* (1), 57–68. https://doi.org/10.1007/s12034-015-1137-z.

(305) Liu, W.; H. Golshan, N.; Deng, X.; J. Hickey, D.; Zeimer, K.; Li, H.; J. Webster, T. Selenium Nanoparticles Incorporated into Titania Nanotubes Inhibit Bacterial Growth and Macrophage Proliferation. *Nanoscale* **2016**, *8* (34), 15783–15794. https://doi.org/10.1039/C6NR04461A.

(306) Raffi, M.; Mehrwan, S.; Bhatti, T. M.; Akhter, J. I.; Hameed, A.; Yawar, W.; ul Hasan, M. M. Investigations into the Antibacterial Behavior of Copper Nanoparticles against Escherichia Coli. *Ann Microbiol* **2010**, *60* (1), 75–80. https://doi.org/10.1007/s13213-010-0015-6.

(307) Hartmann, M.; Berditsch, M.; Hawecker, J.; Ardakani, M. F.; Gerthsen, D.; Ulrich, A. S. Damage of the Bacterial Cell Envelope by Antimicrobial Peptides Gramicidin S and PGLa as Revealed by Transmission and Scanning Electron Microscopy. *Antimicrob. Agents Chemother.* **2010**, *54* (8), 3132–3142. https://doi.org/10.1128/AAC.00124-10.

(308) Lewinski, N.; Colvin, V.; Drezek, R. Cytotoxicity of Nanoparticles. *Small* **2008**, *4* (1), 26–49. https://doi.org/10.1002/smll.200700595.

(309) Kroll, A.; Pillukat, M. H.; Hahn, D.; Schnekenburger, J. Current in Vitro Methods in Nanoparticle Risk Assessment: Limitations and Challenges. *European Journal of Pharmaceutics and Biopharmaceutics* **2009**, *72* (2), 370–377. https://doi.org/10.1016/j.ejpb.2008.08.009.

(310) Forbes, B.; Shah, A.; Martin, G. P.; Lansley, A. B. The Human Bronchial Epithelial Cell Line 16HBE14o− as a Model System of the Airways for Studying Drug Transport. *International Journal of Pharmaceutics* **2003**, *257* (1), 161–167. https://doi.org/10.1016/S0378-5173(03)00129-7.

(311) Cho, W.-S.; Duffin, R.; Bradley, M.; Megson, I. L.; MacNee, W.; Lee, J. K.; Jeong, J.; Donaldson, K. Predictive Value of in Vitro Assays Depends on the Mechanism of Toxicity of Metal Oxide Nanoparticles. *Particle and Fibre Toxicology* **2013**, *10* (1), 55. https://doi.org/10.1186/1743-8977-10-55.

(312) Guadagnini, R.; Moreau, K.; Hussain, S.; Marano, F.; Boland, S. Toxicity Evaluation of Engineered Nanoparticles for Medical Applications Using Pulmonary Epithelial Cells. *Nanotoxicology* **2015**, *9* (sup1), 25–32. https://doi.org/10.3109/17435390.2013.855830.

(313) Ma, Y.; Guo, Y.; Wu, S.; Lv, Z.; Zhang, Q.; Ke, Y. Titanium Dioxide Nanoparticles Induce Size-Dependent Cytotoxicity and Genomic DNA Hypomethylation in Human Respiratory Cells. *RSC Advances* **2017**, *7* (38), 23560–23572. https://doi.org/10.1039/C6RA28272E.

(314) Lopes, V. R.; Loitto, V.; Audinot, J.-N.; Bayat, N.; Gutleb, A. C.; Cristobal, S. Dose-Dependent Autophagic Effect of Titanium Dioxide Nanoparticles in Human HaCaT Cells at Non-Cytotoxic Levels. *J Nanobiotechnol* **2016**, *14* (1), 22. https://doi.org/10.1186/s12951-016-0174-0.

(315) Yang, X.; Liu, J.; He, H.; Zhou, L.; Gong, C.; Wang, X.; Yang, L.; Yuan, J.; Huang, H.; He, L.; Zhang, B.; Zhuang, Z. SiO2 Nanoparticles Induce Cytotoxicity and Protein Expression Alteration in HaCaT Cells. *Particle and Fibre Toxicology* **2010**, *7* (1), 1. https://doi.org/10.1186/1743-8977-7-1.

(316) Gong, C.; Tao, G.; Yang, L.; Liu, J.; He, H.; Zhuang, Z. The Role of Reactive Oxygen Species in Silicon Dioxide Nanoparticle-Induced Cytotoxicity and DNA Damage in HaCaT Cells. *Mol Biol Rep* **2012**, *39* (4), 4915–4925. https://doi.org/10.1007/s11033-011-1287-z.

(317) Maráková, N.; Humpolíček, P.; Kašpárková, V.; Capáková, Z.; Martinková, L.; Bober, P.; Trchová, M.; Stejskal, J. Antimicrobial Activity and Cytotoxicity of Cotton Fabric Coated with Conducting Polymers, Polyaniline or Polypyrrole, and with Deposited Silver Nanoparticles. *Applied Surface Science* **2017**, *396*, 169–176. https://doi.org/10.1016/j.apsusc.2016.11.024.

(318) Petkova, P.; Francesko, A.; Fernandes, M. M.; Mendoza, E.; Perelshtein, I.; Gedanken, A.; Tzanov, T. Sonochemical Coating of Textiles with Hybrid ZnO/Chitosan Antimicrobial Nanoparticles. *ACS Appl. Mater. Interfaces* **2014**, *6* (2), 1164–1172. https://doi.org/10.1021/am404852d.

(319) Singh, G.; Beddow, J.; Mee, C.; Maryniak, L.; Joyce, E. M.; Mason, T. J. Cytotoxicity Study of Textile Fabrics Impregnated With CuO Nanoparticles in Mammalian Cells. *Int J Toxicol* **2017**, *36* (6), 478–484. https://doi.org/10.1177/1091581817736712.

(320) Zawislanski, P. T.; Benson, S. M.; TerBerg, R.; Borglin, S. E. Selenium Speciation, Solubility, and Mobility in Land-Disposed Dredged Sediments. *Environ. Sci. Technol.* **2003**, *37* (11), 2415–2420. https://doi.org/10.1021/es020977z.

(321) Forootanfar, H.; Adeli-Sardou, M.; Nikkhoo, M.; Mehrabani, M.; Amir-Heidari, B.; Shahverdi, A. R.; Shakibaie, M. Antioxidant and Cytotoxic Effect of Biologically Synthesized Selenium Nanoparticles in Comparison to Selenium Dioxide. *Journal of Trace Elements in Medicine and Biology* **2014**, *28* (1), 75–79. https://doi.org/10.1016/j.jtemb.2013.07.005.

(322) Zhang, X.; Liao, Q.; Zhang, Y. Simultaneous determination of nine organochlorine pesticide residues in textile by high performance liquid chromatography. *Se Pu* **2007**, *25* (3), 380–383.

(323) Barnes, L.-M.; Phillips, G. J.; Davies, J. G.; Lloyd, A. W.; Cheek, E.; Tennison, S. R.; Rawlinson, A. P.; Kozynchenko, O. P.; Mikhalovsky, S. V. The Cytotoxicity of Highly Porous Medical Carbon Adsorbents. *Carbon* **2009**, *47* (8), 1887–1895. https://doi.org/10.1016/j.carbon.2009.01.047.

(324) Heenen, M.; Galand, P. The Growth Fraction of Normal Human Epidermis. *Dermatology* **1997**, *194* (4), 313–317. https://doi.org/10.1159/000246122.

(325) Casey, A.; Herzog, E.; Lyng, F. M.; Byrne, H. J.; Chambers, G.; Davoren, M. Single Walled Carbon Nanotubes Induce Indirect Cytotoxicity by Medium Depletion in A549 Lung Cells. *Toxicology Letters* **2008**, *179* (2), 78–84. https://doi.org/10.1016/j.toxlet.2008.04.006.

(326) Qiang, S.; Wang, M.; Liang, J.; Zhao, X.; Fan, Q.; Geng, R.; Luo, D.; Li, Z.; Zhang, L. Effects of Morphology Regulated by Pb2+ on Graphene Oxide Cytotoxicity: Spectroscopic and in Vitro Investigations. *Materials Chemistry*

and Physics **2020**, *239*, 122016. https://doi.org/10.1016/j.matchemphys.2019.122016.

(327) Wei, Z.; Chen, L.; Thompson, D. M.; Montoya, L. D. Effect of Particle Size on in Vitro Cytotoxicity of Titania and Alumina Nanoparticles. *Journal of Experimental Nanoscience* **2014**, *9* (6), 625–638. https://doi.org/10.1080/17458080.2012.683534.

(328) Cremonini, E.; Zonaro, E.; Lampis, S.; Boaretti, M.; Dusi, S.; Melotti, P.; Lleo, M. M.; Vallini, G. Biogenic Selenium Nanoparticles: Characterization, Antimicrobial Activity and Effects on Human Dendritic Cells and Fibroblasts. *Microbial Biotechnology* **2016**, *9* (6), 758–771. https://doi.org/10.1111/1751-7915.12374.

(329) Biswas, P.; Bandyopadhyaya, R. Synergistic Antibacterial Activity of a Combination of Silver and Copper Nanoparticle Impregnated Activated Carbon for Water Disinfection. *Environmental Science: Nano* **2017**, *4* (12), 2405–2417. https://doi.org/10.1039/C7EN00427C.

Appendices

Appendix A Preparation and characterisation of shaped silver nanoparticles

As mentioned in Section 2.4.2, at the initial stage of the project, investigating the antimicrobial activity of shaped AgNPs and the potential of applying the shaped AgNPs with superior antimicrobial performance onto fabric surface was chosen as one of the research objectives. However, the reproducibility of the shaped AgNPs (including silver nanoplates and silver nanocubes) was poor, and the special shape was easily lost due to the sensitivity of the nano-silver to environmental changes, which indicated the unsuitability of shaped AgNPs for textile treatment. The main objective of the thesis later switched to the investigation of SeNPs as a novel antimicrobial agent. Consequently, similar synthetic methods that can be used for both AgNPs and SeNPs were desired for easy comparison, and ascorbic acid was chosen as the mild reducing agent. The originally used methods and results are presented here in this appendix.

Materials and Methods

Silver nitrate ($AgNO_3$, 99.99%), trisodium citrate dehydrate ($C_6H_5O_7Na_3.2H_2O$, 99.99%), sodium borohydride ($NaBH_4$, 99.99%), hydrogen peroxide (H_2O_2, 30%), D-glucose, polyvinylpyrrolidone (PVP; Mw= 40,000), NaOH, ethylene glycol (EG) and sodium sulfide (Na_2S, 99.99%) were purchased from Sigma Aldrich. Ammonium hydroxide ($NH_3.H_2O$, 35%) was purchased from Fisher Scientific. RO water with resistance of 18 MΩ cm was used in all the experiments. All the glassware was cleaned by aqua regia ($HCl:HNO_3$ in a 3:1 ratio by volume) and rinsed with RO water prior to the experiments. A commercial quasi-spherical silver nanoparticle colloid of particle size at 20 nm was purchased from Sigma Aldrich as a reference to validate the techniques, named *commercial AgNPs*.

Preparation of quasi-spherical silver nanoparticles

Two different methods were used to prepared quasi-spherical silver nanoparticles. In the first method,[1] AgNPs were prepared by reducing aqueous silver nitrate by strong reducing agent sodium borohydride ($NaBH_4$). An aqueous solution of $AgNO_3$ (0.25 mM, 100 mL) was rapidly mixed with sodium citrate (30 mM, 1 mL). A 3 mL ice-cooled aqueous solution of $NaBH_4$ (10 mM) was then added under vigorous stirring. Upon the injection of $NaBH_4$, the solution became yellow immediately, indicating the formation of AgNPs. After 30 s, the stirring was stopped. Particles produced by this method were called *borohydride-AgNPs*.

In the second method, colloidal silver particles were synthesized by the reduction of $[Ag(NH_3)_2]+$ complex with glucose following a method reported by Panacek *et al*.[2] In an aqueous solution of 20 mL, silver nitrate (0.1 mM), ammonium hydroxide (0.01 M) and D-glucose (1 mM) were combined. The pH value of the solution was adjusted to 11.5 using NaOH (1 M) to initialise the reaction. In around 15 min, the solution turned yellow, indicating the formation of silver nanoparticles. Particles produced by this method were called *Glucose-AgNPs*.

Preparation of silver nanoplates

Triangular silver nanoplates were synthesised by using a method reported by Metraux and Mirkin.[3] In a typical procedure, an aqueous solution of silver nitrate (0.1 mL), trisodium citrate (30 mM, 1.5 mL), polyvinylpyrrolidone (PVP, 0.7 mM, 1.5 mL), and hydrogen peroxide (30wt%, 60µl) were combined and vigorously stirred at room temperature (22 °C) in the presence of air. To this mixture, sodium borohydride (100 mM, 100 µl) was rapidly injected, generating a colloid that was pale yellow in colour, indicating the formation of small silver nanoparticles. After around 20 min, the solution turned into pink, purple or blue within minutes, indicating the formation of silver nanoplates.

Preparation of silver nanocubes

Silver nanocubes were prepared by reducing silver nitrate in ethylene glycol in the presence of PVP and sodium sulfide with the assistance of microwave heat.[4] Typically,

PVP (0.1 mM), $AgNO_3$ (25 mM) and Na_2S (0.2 mM) were dissolved in 10 ml EG with vigorous stirring. When the solution was well mixed and turned light yellow, the solution was microwaved at 800 w for 5 s and cooled for 30 s, and the process was repeated for 3 times and allowed to cool down to room temperature. During the process, the colour of the solution changed from light yellow, to ruby-red, and finally green-ochre.

Results

The formation of colloidal suspensions of AgNPs was evident by visual inspection of the solution colour change as well as UV-vis spectrophotometer. Images of the AgNPs suspensions are shown in Figure 1. Quasi-spherical AgNPs have previously been reported to be of yellowish colour in aqueous solution. An intense adsorption peak is seen at 390 nm on the spectra of *borohydride-AgNPs*, 400 nm on the spectra of *commercial AgNPs*, and at 405 nm on the spectra of *glucose-AgNPs* (Figure 2). As these peaks are close to one another, the suspensions all appeared to be bright yellow colour in Figure 1. It has been reported that the adsorption peak of spherical silver nanoparticles range from around 380 nm to 460 nm corresponds to the size of particles range from 4nm to 100nm.[3] The adsorption peak of AgNPs shifts to longer wavelength with increase in size. According to the literature and the comparison with commercial AgNPs, the sizes of *borohydride-AgNPs* and *glucose-AgNPs* were estimated to be around 5 nm and 30 nm.

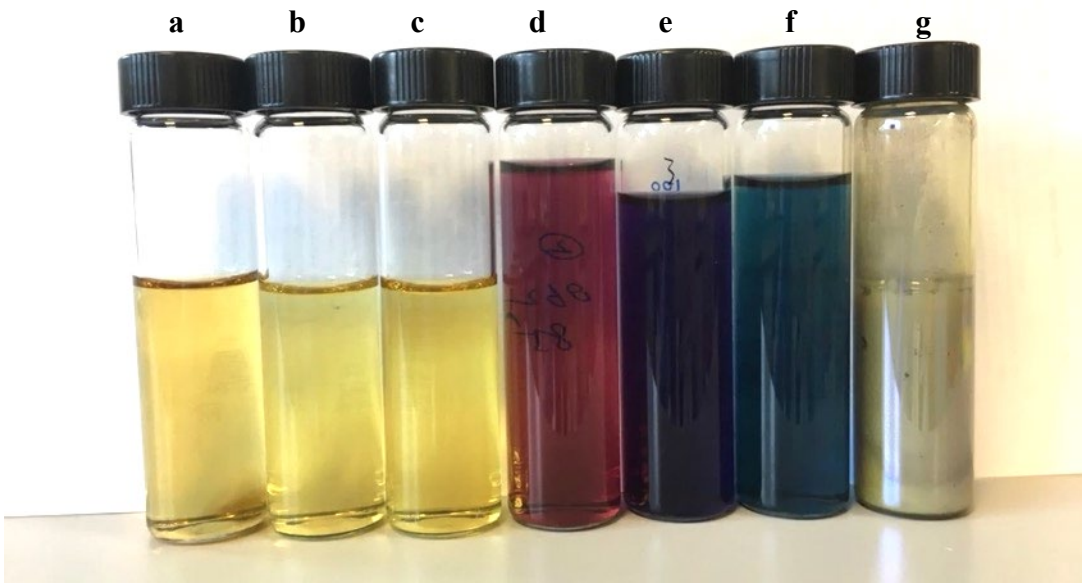

Figure 1. Photographic image of AgNPs suspensions of (a) borohydride-AgNPs, (b) glucose-AgNPs, (c) commercial AgNPs, (d) silver nanoplates—pink, (e) silver nanoplates—purple, (f) silver nanoplates—blue, (g) silver nanocubes

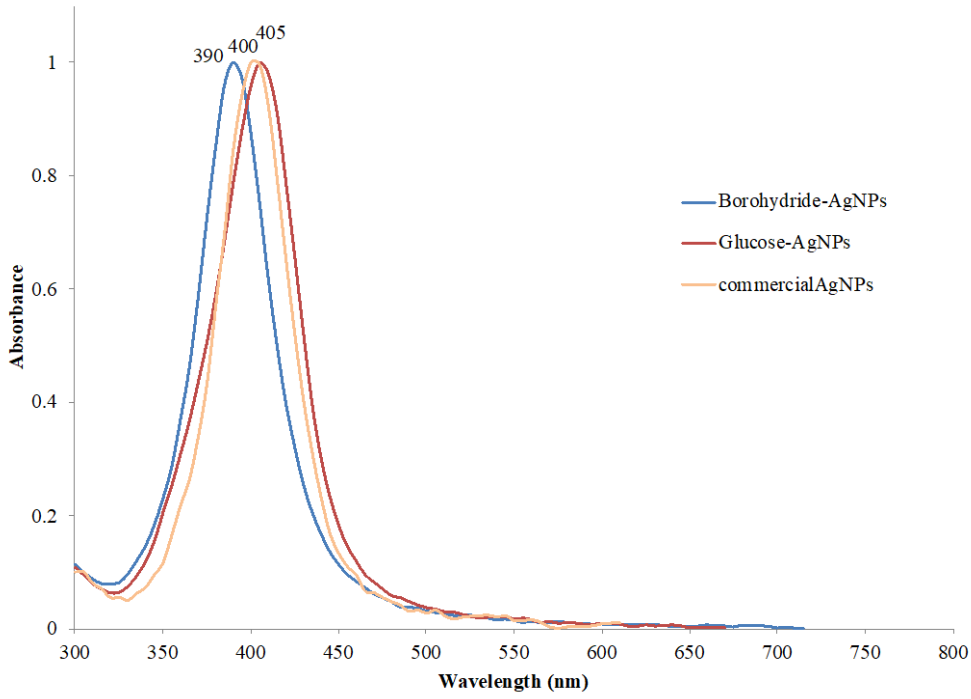

Figure 2. UV-vis spectra of quasi-spherical AgNPs colloids.

Dynamic light scattering technique was only used on quasi-spherical nanoparticles since the distinct shapes are not suitable for this technique and the quality of reports are poor. Figure 3 shows the DLS report of *glucose-AgNPs* and *commercial AgNPs* respectively. TEM images of silver nanoparticles and the average sizes obtained from the images are shown in Figure 4. When comparing DLS and TEM analysis results of *glucose-AgNPs* and *commercial AgNPs*, it can be seen that the results obtained from DLS technique are slightly larger than the results got from TEM particle analysis as DLS determines the hydrodynamic sizes of the particles.

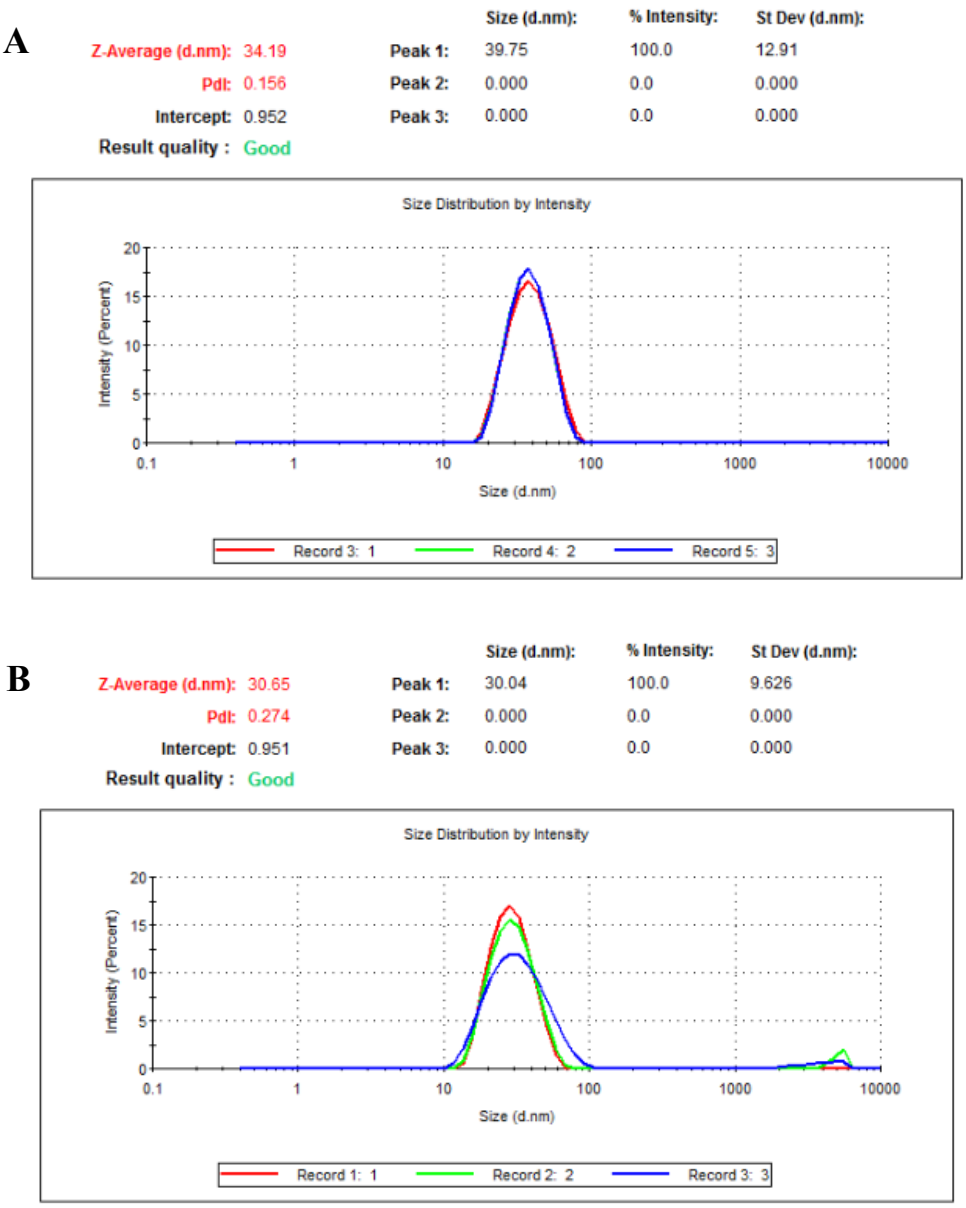

Figure 3. DLS reports of (A) *glucose-AgNPs* and (B) *commercial AgNPs*

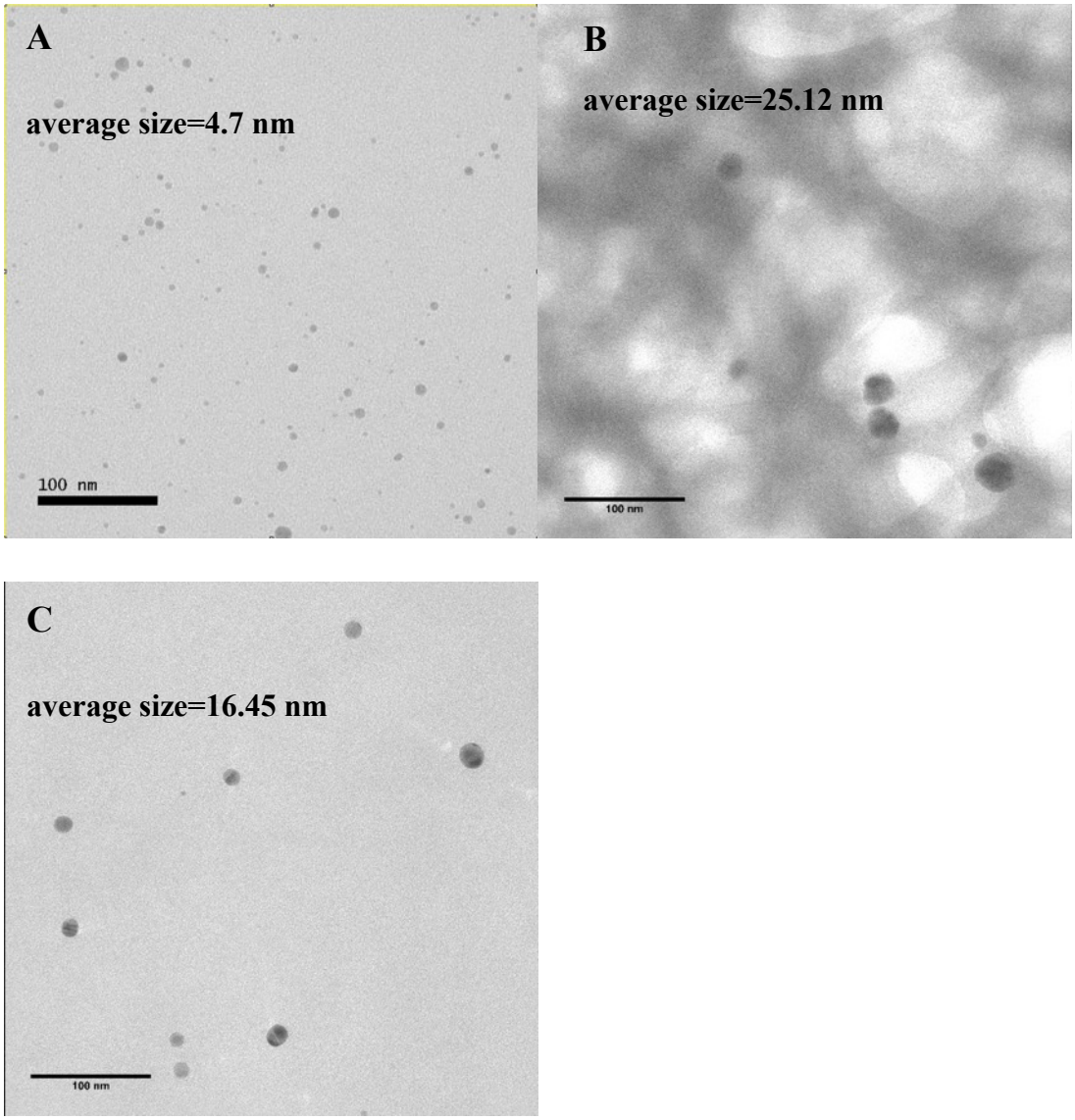

Figure 4. TEM images of (A) *borohydride-AgNPs*; (B) *glucose-AgNPs*; (C) *commercial-AgNPs*

Unlike quasi-spherical AgNPs which are measured in diameter, the nanoplates have many dimensional measurements, including plate shape (e.g. with pointy or round corners), edge length, and plate thickness. These properties determine the optical property of the colloid, and therefore they show different colours as the demensional measurements alter. The colour of silver nanoplate colloids can range from pink, red, purple, blue, and turquoise (examples shown in Figure 1). It was first noticed that the reproducibility of the Ag nanoplates were poor as the colour of the suspension altered between different batches. It has been reported that the UV-vis spectra of silver nanoplates have diagonistic surface plasmon resonance (SPR) bands at 335nm, 380-460 nm, and 520-725 nm.[3] The UV-vis spectra of triangular Ag nanoplates prepared

in different batches using the same method are presented in Figure 5. It can be seen that the reproduciability was poor. TEM images of the nanoplates are shown in Figure 6. It was noticed that the edge length, corner sharpness and the thickness of the nanoplates were different from batch to batch. Similar observation was made for silver nanocubes. The edge length and the presence of other spherical or irregular shaped AgNPs in the synthesis products varied between different batches (Figure 6). Silver nanoparticles in Figure 6 (A) are mostly triangular shaped, while in (B) there are many round disks, and in (C) some undesired large silver nanoparticles can be seen.

More importantly, the Ag nanoplates suspension was sensitive to external stimuli (e.g. heat, light and eletrostatic disturbance). It was noticed that elevated temperature led to quick change of the suspension colour, indicating dimensional changes of the Ag nanoplates, possibily through aggregation of the plates or quick dissolution of the sharp edges. When fixed onto fabric surfaces, the nano-silver will be subjected to environment changes, for example, raised temperature during laundering and being in contact with human body which may cause the Ag nanoplates to lost the special shapes. Attempts were also made to use eletrostatic assembly to fix the Ag nanoplates onto fabric surfaces. However, the charged fabric immediately disturbed the equilibirium of the Ag nanoplate suspension, resulting in an instant colour change (e.g. from pink or blue to grey). The nano-silver needs to be stable and not to lose the unique features during the preparation and usage of the functionalised fabrics. Therefore, the experiment on these shaped nano-silver was terminated.

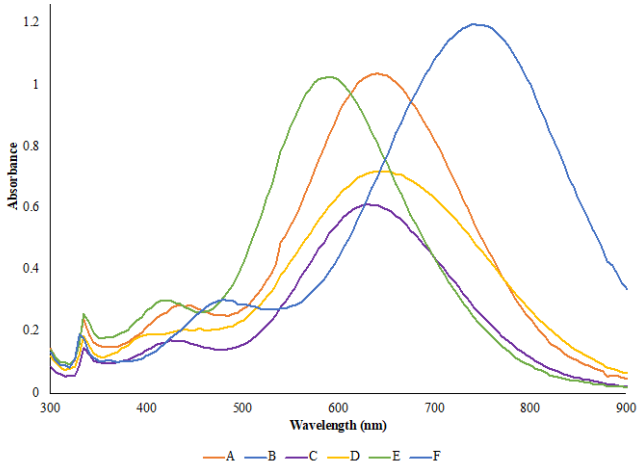

Figure 5. UV-vis spectra of colloidal silver nanoplates, sample A-F were prepared on different occasions using the same method.

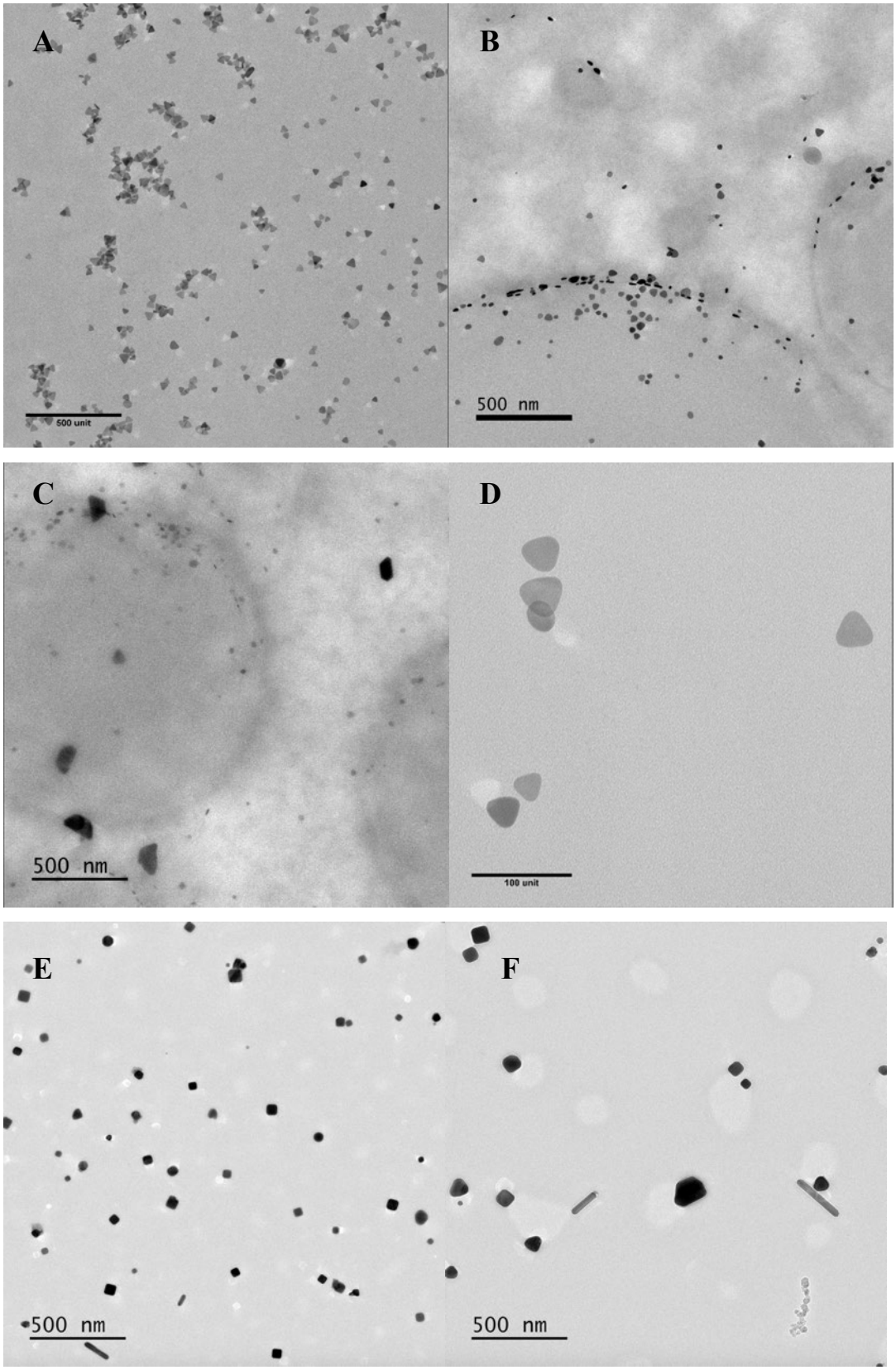

Figure 6. TEM images of (A-C) silver nanopalates from different batches with the same magnification; (D) sample A with higher magnification to show details of the nanoplates; (E-F) silver nanocubes from different batches with different irregular shaped particles and rods.

References

(1) Li, H.; Xia, H.; Wang, D.; Tao, X. Simple Synthesis of Monodisperse, Quasi-Spherical, Citrate-Stabilized Silver Nanocrystals in Water. Langmuir 2013, 29 (16), 5074–5079. https://doi.org/10.1021/la400214x.

(2) Panáček, A.; Kvítek, L.; Prucek, R.; Kolář, M.; Večeřová, R.; Pizúrová, N.; Sharma, V. K.; Nevěčná, T.; Zbořil, R. Silver Colloid Nanoparticles: Synthesis, Characterization, and Their Antibacterial Activity. J. Phys. Chem. B 2006, 110 (33), 16248–16253. https://doi.org/10.1021/jp063826h.

(3) Métraux, G. S.; Mirkin, C. A. Rapid Thermal Synthesis of Silver Nanoprisms with Chemically Tailorable Thickness. Adv. Mater. 2005, 17 (4), 412–415. https://doi.org/10.1002/adma.200401086.

(4) Chen, D.; Qiao, X.; Qiu, X.; Chen, J.; Jiang, R. Convenient, Rapid Synthesis of Silver Nanocubes and Nanowires via a Microwave-Assisted Polyol Method. Nanotechnology 2010, 21 (2), 025607. https://doi.org/10.1088/0957-4484/21/2/025607.

Appendix B

Chapter 3

Optical density – bacterial cell concentration standard curve of *S. aureus* and *E. coli* as described in Section 3.3.2.

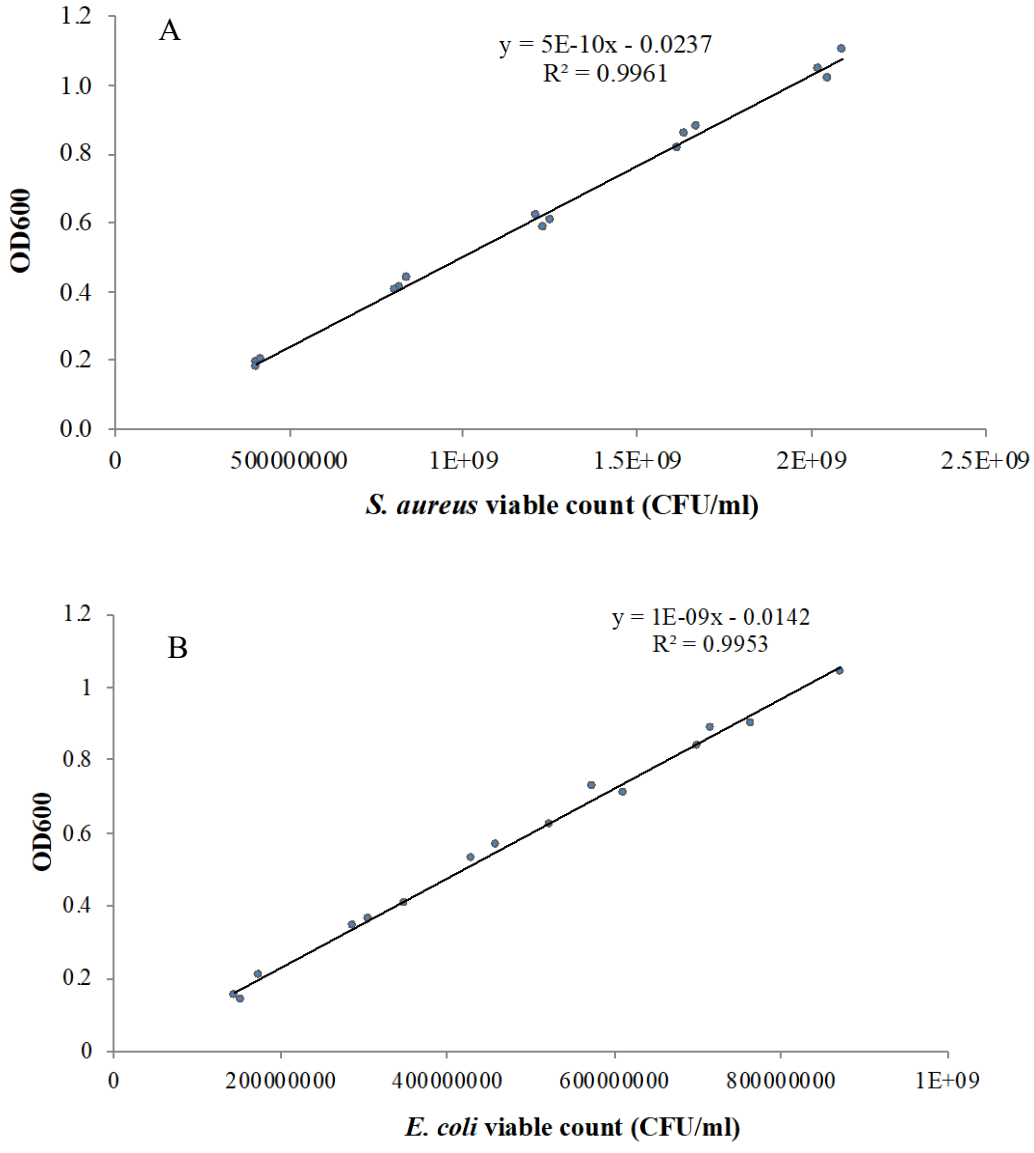

Figure 1. Standard curves of (A) *S. aureus* and (B) *E. coli*: viable colony count against OD600.

The as-purchased cotton fabrics were purified with boiling water only in the first attempt, which resulted in reduced ATP levels in 16HBE14o- cells treated with the media-extracts but did not cause significantly higher cell death (shown in Figure 2 and Figure 3 below). Subsequently, ethanol was employed to further remove non-polar impurities which interfered with the test, as described in Section 4.3.1 and Chapter 6 (Table 6.1). UC = untreated cotton, CC = cationised cotton, Se-C = SeNP-functionalised CC, Ag-C = AgNP-functionalised CC.

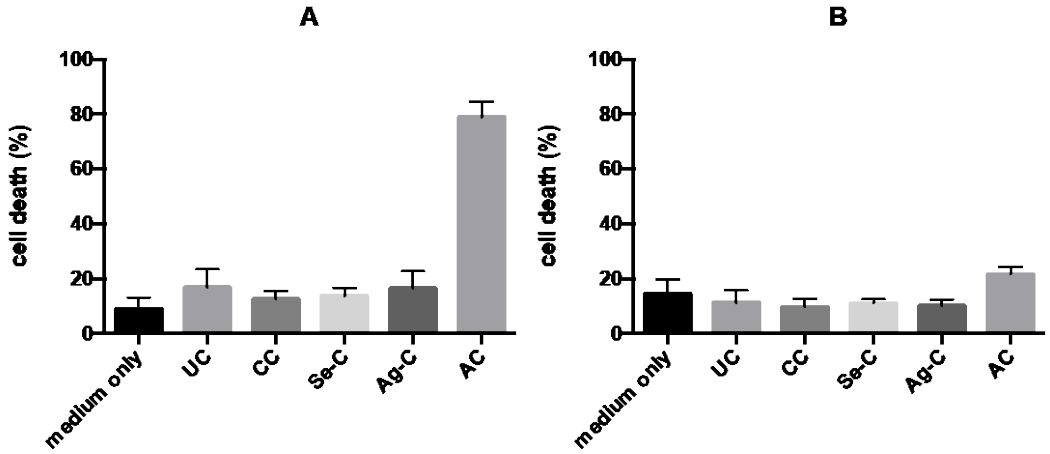

Figure 2. Cell death rate of 16HBE14o- cells after 24-h exposure to the extracts of fabric samples (prepared with boiled cotton but not cleaned with ethanol): (A) cell culture medium and (B) DI water as the extraction vehicle.

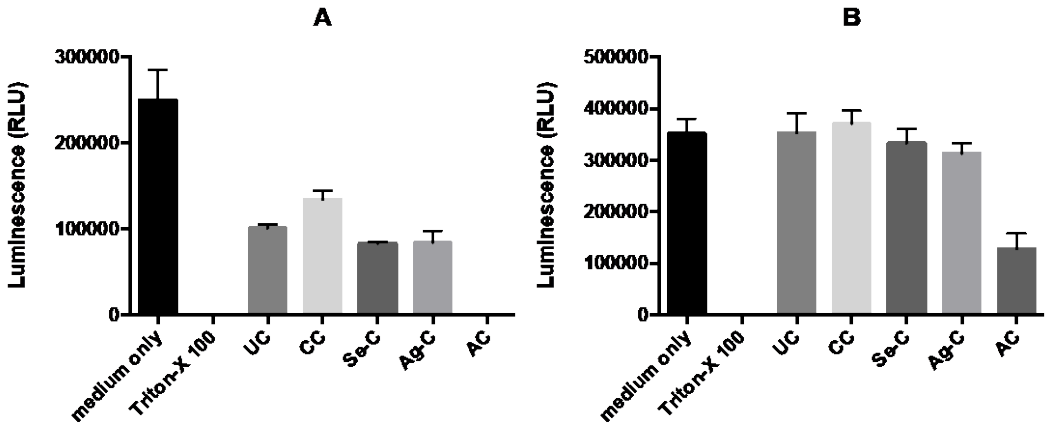

Figure 3. ATP level of 16HBE14o- cells after 24-h exposure to the extracts of fabric samples (prepared with boiled cotton without washing with ethanol): (A) cell culture medium and (B) DI water as the extraction vehicle.

Appendix C

Work contained within Chapter 4, 5 and 6 has been published in the following paper:

Wang, Q., Barnes, L.M., Maslakov, K.I., Howell, C.A., Illsley, M.J., Dyer, P. and Savina, I.N. In situ synthesis of silver or selenium nanoparticles on cationized cellulose fabrics for antimicrobial application. *Materials Science and Engineering: C* **2021**, 121, 111859. https://doi.org/10.1016/j.msec.2020.111859

Materials Science & Engineering C 121 (2021) 111859

Contents lists available at ScienceDirect

Materials Science & Engineering C

journal homepage: www.elsevier.com/locate/msec

In situ synthesis of silver or selenium nanoparticles on cationized cellulose fabrics for antimicrobial application

Qiaoyi Wang [a], Lara-Marie Barnes [a], Konstantin I. Maslakov [b], Carol A. Howell [a,e], Matthew J. Illsley [a,d], Patricia Dyer [c], Irina N. Savina [a,*]

[a] School of Pharmacy and Biomolecular Sciences, University of Brighton, Huxley Building, Lewes Road, Brighton BN2 4GJ, United Kingdom
[b] Department of Chemistry, Lomonosov Moscow State University, Leninskie Gory 1–3, Moscow 119991, Russia
[c] School of Art, University of Brighton, 58-67 Grand Parade, Brighton BN2 0JY, United Kingdom
[d] Anamad Ltd., Sussex Innovation Centre, Science Park Square, Brighton, BN1 9SB, United Kingdom
[e] Enteromed Ltd., 85 Great Portland St, First floor, London, W1W 7LT, United Kingdom

ARTICLE INFO

Keywords:
Silver
Selenium
Nanoparticles
Cellulose
Cationization
Antimicrobial textiles

ABSTRACT

In this study, we developed a method to prepare inorganic nanoparticles *in situ* on the surface of cationized cellulose using a rapid microwave-assisted synthesis. Selenium nanoparticles (SeNPs) were employed as a novel type of antimicrobial agent and, using the same method, silver nanoparticles (AgNPs) were also prepared. The results demonstrated that both SeNPs and AgNPs of about 100 nm in size were generated on the cationized cellulose fabrics. The antibacterial tests revealed that the presence of SeNPs clearly improved the antibacterial performance of cationized cellulose in a similar way as AgNPs. The functionalised fabrics demonstrated strong antibacterial activity when assessed using the challenge test method, even after repeated washing. Microscopic investigations revealed that the bacterial cells were visually damaged through contact with the functionalised fabrics. Furthermore, the functionalised fabrics showed low cytotoxicity towards human cells when tested *in vitro* using an indirect contact method. In conclusion, this study provides a new approach to prepare cationic cellulose fabrics functionalised with Se or Ag nanoparticles, which exhibit excellent antimicrobial performance, low cytotoxicity and good laundry durability. We have demonstrated that SeNPs can be a good alternative to AgNPs and the functionalised fabrics have great potential to serve as an anti-infective material.

1. Introduction

From beddings, drapes and uniforms, to bandaging materials and wound dressings, textiles play vital roles in healthcare facilities. Due to the large surface areas, textiles have superior abilities to retain warmth, moisture, and nutrients from spillages and exudates, making them ideal substrates for microorganisms to grow on [1]. Some studies have suggested that healthcare textiles can act as reservoirs and vehicles for the spread of microorganisms in hospitals [2–4]. Healthcare-associated infections (HAIs) have become a serious threat to patients' health and result in significant economic burdens to healthcare systems [5]. It is estimated that in Europe, approximately 4.1 million patients acquire at least one HAI each year, causing 37,000 deaths directly and contributing to an additional 110,000 deaths each year [6]. Furthermore, the emergence of antibiotic resistance is increasing the urgency with which we must find alternative ways to control the growth and transmission of pathogens in hospitals. With the development of nanotechnology, some inorganic nanoparticles (NPs) such as silver, copper and zinc, have been identified as promising candidates in combatting pathogenic microorganisms, including antibiotic-resistant strains [7]. Although the exact antimicrobial mechanisms of the NPs remain unclear, it is believed that they act differently from conventional antibiotics. NPs may exhibit multiple modes of action simultaneously, including physical damage of the microbial cell structures, release of toxic ions, and catalysed formation of reactive oxygen species (ROS) which can cause severe damage to the cell components [8,9], whereas antibiotics normally have only one mechanism of action, for example, the inhibition of either cell wall synthesis, protein synthesis, or DNA replication [10]. The multiple modes of action by NPs are believed to make it more difficult for the bacteria to develop resistance because simultaneous mutations in the bacterial cells will be needed [11]. Antimicrobial nanoparticles have been studied to functionalise different surfaces such as textiles [12,13],

* Corresponding author.
E-mail address: i.n.savina@brighton.ac.uk (I.N. Savina).

https://doi.org/10.1016/j.msec.2020.111859
Received 4 October 2020; Received in revised form 28 November 2020; Accepted 28 December 2020
Available online 6 January 2021
0928-4931/